CRANFIELD UNIVERSITY

Hisham Al Baroudi

DEVELOPMENT OF SAFE AND RELIABLE OPERATIONS IN LARGE-SCALE CO_2 SHIPPING: AN EXPERIMENTAL APPROACH

SCHOOL OF WATER, ENERGY AND ENVIRONMENT
Ph.D In Energy And Power

PhD
Academic Year: 2020 - 2021

Supervisor: Dr Kumar Patchigolla
Associate Supervisor: Prof John Oakey
January 2021

CRANFIELD UNIVERSITY

SCHOOL OF WATER, ENERGY AND ENVIRONMENT
Ph.D In Energy And Power

PhD

Academic Year 2020 - 2021

Hisham Al Baroudi

DEVELOPMENT OF SAFE AND RELIABLE OPERATIONS IN LARGE-SCALE CO_2 SHIPPING: AN EXPERIMENTAL APPROACH

Supervisor: Dr Kumar Patchigolla
Associate Supervisor: Prof John Oakey
January 2021

This thesis is submitted in partial fulfilment of the requirements for the degree of PhD

ABSTRACT

A successful worldwide implementation of Carbon Capture, Utilisation and Storage largely relies on the establishment of a safe and reliable CO_2 transmission network. CO_2 shipping hereby represents a promising transport option, characterised by a high degree of flexibility in sink-source matching. This study addressed some key knowledge gaps that currently pose a limitation on large-scale commercialisation of this technology by providing information on operational and maintenance challenges in the chain.

Firstly, an extensive review of technological advancements and future projections in large scale CO_2 shipping drew the attention to the fact that key technical challenges still need to be addressed in both pipeline and sea vessel systems in order to establish a worldwide network of CO_2 transport infrastructure. In particular, significant dearth concerns the adoption of appropriate safety protocols during accidental scenarios and selection of suitable materials to ensure integrity of transport infrastructure throughout real operations.

Thus, an experimental lab scale rig was built and commissioned, capable of handling refrigerated carbon dioxide batches (up to 2.25 L) at conditions typical of sea vessel transport (~0.7 - 2.7 MPa, 223 - 259 K); the facility was designed to permit investigation of accidental leakage behaviour and to determine the qualification assessment of elastomer materials exposed under real shipping conditions.

A technical qualification of elastomer materials for CO_2 transport systems was then performed with the aim of assessing their suitability in the intended systems and propensity for degradation. Such elastomers are used as seals in pressure-relief valves, providing elastomer-to-metal shutoff and eliminating leakage around stem during relief mode. Samples previously tested under pipeline conditions (9.5 MPa, 318 K) at exposure times of 50 – 400 h were characterised for a visual inspection, mechanical and thermo-analytical properties. Based on the suitable performance of the elastomers under such pipeline conditions, Ethylene Propylene Diene Monomer was selected for testing under operations typical of

CO_2 shipping; constrained (25% compression) samples thereby underwent 20 – 100 CO_2 loading and offloading cycles at average decompression rates of 1.6 MPa/min; tested materials were then qualified through the aforementioned characterisation methodology, demonstrating a satisfactory resistance to rapid gas decompression and mechanical stability.

A detailed experimental campaign was considered to assess the accidental leakage behaviour of CO_2 under shipping conditions; the main risks associated with CO_2 are asphyxiation due to displacement of oxygen to critically low levels, and exposure to concentrations of 15% or above in air are deemed life threating due to toxicological impacts on humans. The study highlighted that selection of initial fluid conditions significantly affects the propensity for solid formation in the vessel and blockages in the pipe section, thus resulting in significantly diverse leakage behaviours. Low-pressure decompression tests (0.7 – 0.94 MPa) resulted in the highest amount of inventory solidification (36 – 39 wt%) while high-pressure decompression scenarios (1.8 – 2.65 MPa) demonstrated the lowest (17 – 22 wt%).

Lastly, a real-scale investigation on liquid CO_2 discharge from the coupler of an emergency release system was undertaken in order to scrutinise the applicability of such spillage containment measure to CO_2 shipping operations. The study focused on two refrigerated states, namely low- (0.87 – 0.94 MPa, 227 – 231 K) and medium-pressure conditions (1.62 – 1.65 MPa, 239 – 240 K) typical of shipping transport; findings demonstrated the presence of an abrupt outflow behaviour, characterised by full inventory discharge form the coupler in less than 1 s and achievement of peak depressurisation rates of 6 MPa/s. Moreover, the discharge behaviour showed considerable variations in relation to the selected initial conditions.

Keywords: CO_2 transport; CO_2 shipping; leakage behaviour; emergency release system; material selection; refrigerated fluid

This page is intentionally left blank

In the Name of God, the Compassionate, the Merciful

I thank God for guiding me through this journey.

This is dedicated to my wife for being my light in the dark, my safe haven.

To my beloved parents, for their unconditional support and love

To my sisters, the best gifts I could receive from my parents

To my family and friends, for always being there on my side

ACKNOWLEDGEMENTS

I would like to express my gratitude to Dr Kumar Patchigolla for providing me with the opportunity to undertake this research and for his patient and concise supervision throughout these years. This work would not have materialised without your efforts.

I am immensely grateful to Professor Masahiko Ozaki and Professor Ryota Wada from the University of Tokyo for hosting me in their research group at the Department of Ocean Technology, Policy and Environment and making me feel at home during my stay in Japan.

I would also like to thank the technical staff in building 43a for the invaluable support provided: Euan, Howard, Adriana, Andrew, Peter. Your professional expertise added immense value to my research experience and kept me going throughout my experimental work. I am indebted to the academic, research, and administrative staff at the university for the advice and guidance dispensed during these years: Prof John Oakey, Prof Ben Anthony, Dr Kranthi Jonnalagadda, Dr Stefano Mori, Dr David Ayre, Dr Joy Sumner, Prof Nigel Simms, Mrs Sam Skears to name a few.

I am much obliged to the Tokyo Boeki Engineering team in Nagaoka, Japan: I learnt a lot from your invaluable expertise and it was a privilege to be able to work with you. I also extend my gratitude to the UK CCS Research Centre, for providing a network of professional development and granting funds for international collaboration. Special thanks to my friends and colleagues at Cranfield University and University of Tokyo for the friendly environment and for always being there to lend a hand.

To my wife Sara: your love and unconditional support are the blessings that make the difference in my life. To my beloved parents, for teaching me the values of hard work and gratitude in life, and for always believing in me.

To my family and friends, for their immense support and wonderful memories shared together that grace every day of my life with happiness.

TABLE OF CONTENTS

LIST OF FIGURES

LIST OF TABLES

LIST OF ABBREVIATIONS

ANOVA	Analysis of Variance
BES	Department for Business, Energy and Industrial Strategy
BLEVE	Boiling Liquid Expanding Vapour Explosion
BOG	Boil-Off Gas
ACN	Acrylonitrile
CAPEX	Capital Expenditure
COP21	Paris Climate Conference
CCUS	Carbon Capture Utilisation and Storage
DPS	Dynamic Positioning System
DSC	Differential Scanning Calorimetry
EP	Ethylene Propylene
EPDM	Ethylene Propylene Diene Monomer
ERS	Emergency Release System
ESD	Emergency Shutdown
ESDV	Emergency Shutdown Valve
ETS	Emissions Trading System
FBMA	Fully Balanced Marine Arm
FKM	Fluoroelastomer
GCCSI	Global Carbon Capture and Storage Institute
HFO	Heavy Fuel Oil
HNBR	Hydrogenated Nitrile Butadiene Rubber
IEAGHG	International Energy Agency Greenhouse Gas programme
IGCC	Integrated Gasification Combined Cycle
IMO	International Maritime Organisation
IPCC	Intergovernmental Panel on Climate Change
JT	Joule Thomson
LCC	Life-Cycle Costs
LNG	Liquefied Natural Gas
LOC	Loss Of Containment
LPG	Liquefied Petroleum Gas
NBR	Nitrile Rubber
NETL	National Energy Technology Laboratory
PHA	Preliminary Hazard Analysis

PCI	Project of Common Interest
PTFE	Polytetrafluoroethylene
RGD	Rapid Gas Decompression
SIGTTO	Society of International Gas Tankers and Terminal Operators
TEG	Triethylene Glycol
T_G	Glass transition temperature
VLE	Vapour Liquid Equilibrium
ZEP	Zero Emission Platform

1 INTRODUCTION

1.1 Background

According to the IPCC Special Report in 2018 [1], human activity is considered to have prompted an estimated 1 °C of global warming above pre-industrial thresholds, and a projection for this value to reach 1.5 °C between 2030 and 2050 is considered if the increment progresses at such rate. Risks for natural and human systems are dramatically increased in the 1.5 °C scenario, with land and sea already displaying signs of changes induced by global warming in the form of alterations to the ecosystem. For example, the mean sea levels are undergoing augment worldwide and the frequency and intensity of precipitations in several regions of the world are noticeably growing. Such occurrences are primarily credited to the increased concentration of greenhouse gases in the atmosphere, to which carbon dioxide is the prime component [2,3] given its remarkable concentration increase from 280 ppmv prior to industrial era to over 400 ppmv as of 2013 [2]. Under this framework, achieving and maintaining net zero anthropogenic CO_2 emissions worldwide is imperative to stop the adverse effects of anthropogenic global warming over the next few decades. As summarised in Figure 1-1, the control of cumulative CO_2 emissions is determinant, as different scaled responses and selected paths play a crucial role in reducing the likelihood of warming to 1.5°C.

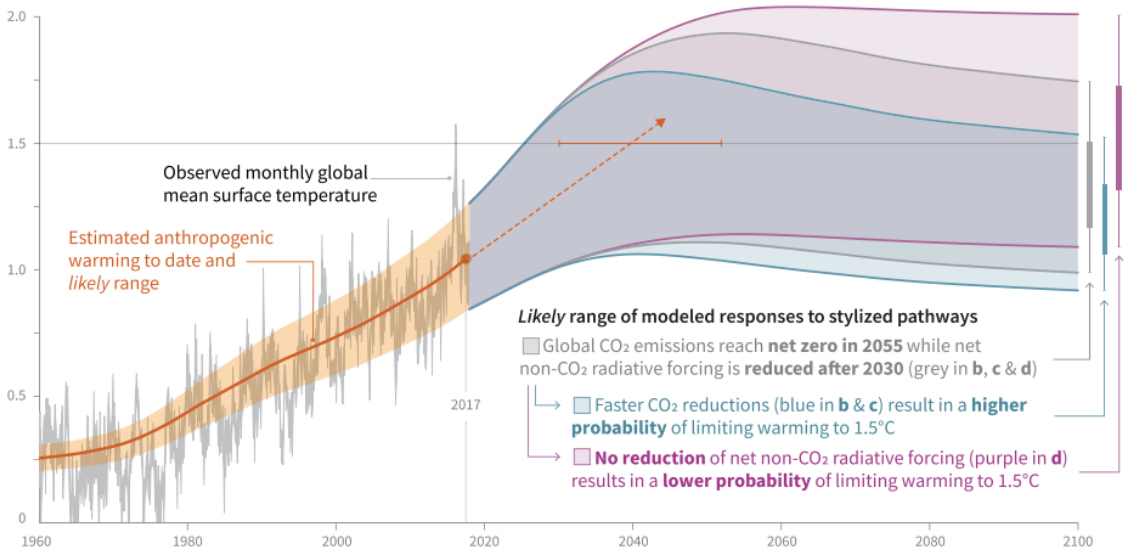

Figure 1-1: Observed global temperature change and responses scenarios to anthropogenic emissions [1]

Implementation of effective measures to reduce the global concentration CO_2 is essential, given that 80% of the world's energy was still being produced form fossil fuels as of 2016 [4]. Therefore, it is essential to consider extensive decarbonisation of power and industrial sectors in order to limit the increasing concentration of greenhouse gases. As such, Carbon Capture, Utilisation and Storage (CCUS) could provide a feasible mitigation technology that is showing promising signs of implementation in recent years [5]. CCUS is largely considered a "bridging" mitigation technology in the portfolio of required actions to mitigate and contain global warming and its impact [4,6] with other key mitigation strategies including improved energy efficiency, switching to low-carbon fuels, renewable energies and direct air capture [5]. The process consists in the separation of carbon dioxide from flue gases of power and industrial emitters and transmission to suitable storage location for long-term storage via a transmission network of pipelines or sea vessels. Alongside permanent storage of carbon dioxide, in recent years the concept of Carbon Utilisation is demonstrating to be an attractive option to increase the global use of CO_2 and thus enhance the business model of CCUS. To date, the use of carbon dioxide amounts to 230 Mt/year [7], primarily as fertiliser, and in the oil and gas and food and beverage applications. However, in practice, it appears that future projections for CO_2 utilisation will be significantly lower that the amounts required to mitigate emission reductions. Thus, storage of CO_2 for permanent storage remains the primary focus of CCUS. The ZEP report [4] found that CCUS is a currently available technology that plays an indispensable and feasible role to successfully decarbonise the energy and industrial sectors. Lack of implementation of CCUS could raise the risk of industrial disinvestment and relocation away from Europe due to an increased climate pressure. CCUS thereby represents a transitional measure that can preserve these sectors and the investments made to create additional jobs, leading to further economic growth. The industrialised regions in Europe could see their emissions reduced by up to 95% in 2050 through connection of their emitting clusters to the abundant storage locations of the continent via a CO_2 transportation networks, creating a sustainable economic model [4].

It is widely agreed that a successful global implementation of CCUS is subject to the establishment of a suitable CO_2 transportation network that can reliably and cost-effectively interconnect carbon emitters with storage sites [8]. Pipelines and sea

vessels thereby represent the main transmission options available for future CCUS projects, each exhibiting distinct feasibility in relation to techno-economic, geographical and logistical considerations [9]. Pipeline infrastructure is characterised by high capital investments, relatively low operational costs and remarkable sensitivity to transportation distance, making it an optimum option to transport relatively large amounts over short distances. Conversely, sea vessel transportation implies relatively lower upfront capital investment but require high conditioning and operating costs, making this option suitable to transport relatively small volumes over long distances [10]. Overall, a global decarbonisation of power and industrial sectors will most likely require the implementation of a complex transmission network that includes both pipelines and sea vessels. CO_2 shipping represents a highly flexible sink-source matching transportation alternative for CCUS that exhibits lower capital costs, as opposed to pipelines which consist of fixed and costly investments. It is noteworthy that this technology represents the only CO_2 transmission alternative to countries such as Japan and Korea, where emitters are dislocated, and lack of hydrocarbon activity and high propensity for natural calamity preclude implementation of an extensive pipeline network is infeasible [11,12]. Moreover, the UK is also scrutinising a thorough implementation of CO_2 shipping as part of its decarbonisation strategies, particularly given the location of storage sites in the North Sea, and the opportunity to import captured carbon from neighbouring countries [13].

Under sea vessel transport, CO_2 will need to be liquefied; conditions that future CO_2 shipping project should adopt are still under debate: a state near the triple point (~0.7 MPa, 223 K) enhances density and reduces the cost requirements of the tanks, but its proximity to the triple point may pose a hazard in the formation of solids during real operation [13–15]. Conversely, higher liquid pressures (~1.5 – 2.7 MPa, 243 - 265 K) have a higher safety margin from the triple point but an increased cost of the vessels due to higher thickness requirements [15]. Overall, the optimal shipping conditions are expected to be a trade-off between costs and safety of operations, with several key factors such as disposal amount, distance and geographical location of emitters and sinks affecting the choice. To date, no consensus has been achieved in the selection of transport conditions that future CO_2 shipping projects should adopt. Despite CO_2 shipping already being established in the food and brewery industries to transport relatively small volumes [16] at medium pressure conditions (~1.5 MPa and 243 K),

considerable uncertainties are still associated with the continuity of large scale shipping operations typical of CCUS projects [17], and particularly at conditions near the triple point where an appropriate margin from the triple point needs to be determined and maintained throughout operations. Moreover, a lack of demonstrational projects imply a lack of critical understanding of the safety and reliability of the shipping chain, particularly when handling CO_2 during real operations. Deployment of CO_2 shipping at a large scale for CCUS therefore comes with a considerable set of technical and operational challenges that still need to be addressed to allow commercialisation of this technology [18].

1.2 Hazards and risks associated with carbon dioxide

Carbon dioxide is largely used in different commercial and residential applications, and thus, the use of this substance is highly regulated by legislative codes and standards to minimise and control the risks and hazards associated [19]. In the past, several industrial releases of carbon dioxide have resulted in injuries and deaths caused by ingestion and asphyxiation [19]. The US Environmental Protection Agency (EPA) recorded a total number of 51 incidents involving CO_2 in the period going from 1975 to 2000. These accidents have led to 72 deaths and 145 injuries from accidental release of CO_2 from fire extinguishing systems alone [19]. In 2008, an accident involving the release of carbon dioxide from a fire extinguishing installation in Mönchengladbach, Germany, caused 107 people to be intoxicated, 19 of whom were hospitalised. Such incidents emphasize that the potential consequences that carbon dioxide can have on humans, when released in high-concentration clouds, can be catastrophic. Therefore, the growing interest in Carbon Capture, Utilisation and Storage technologies implies that the current uncertainties concerning safe handling and reliability of industrial CO_2 systems need to be thoroughly addressed. Considerations of engineering aspects when handling high-pressure CO_2 in a large-scale release scenarios has highlighted that critical risks include emergency response and temporary refuge issues and structural integrity issues. The latter are related to prolonged exposure to subliming solids, brittle to ductile transitions and fast cooling of structural components [19].

1.3 Motivation for this research

As highlighted in the previous paragraph, a dearth of both demonstrational and commercially focused CO_2 shipping projects implies that a number of technical uncertainties are still present in relation to this technology implementation. Some of the key highlighted technical gaps include:

- Lack of understanding on the advantages and challenges inherent to operations closer to the triple point of CO_2 (~0.7 MPa, 223 K) as opposed to higher pressure liquid conditions (~1.8 – 2.7 MPa and 240- 265 K) [14,15].
- Thorough investigation of the leakage behaviours resulting from accidental loss of containment of transport infrastructure is extensively explored in relation to supercritical CO_2 typical of pipeline transport [20,21]. However, a significant dearth of knowledge is present in relation to the discharge behaviour exhibited by liquid, refrigerated CO_2 under shipping conditions. In particular, experimental demonstrations under refrigerated liquid conditions are still reportedly scarce [19] and propensity for solid formation during release is not well understood [22].
- The wide range of operating conditions – from refrigerated CO_2 during sea vessel transport to supercritical state during offloading and injection to storage site [23] – imply a high-performance requirement in relation to selected materials and their performance during real operations. There is particular reference to lack of understanding on the performance of polymers and elastomers [24] that are considered to be at high risk of rapid decompression damage and degradation from the thermal and CO_2 pressure cycling typical of the batch-wise, intermittent nature of sea vessel transport.
- Lack of demonstrational projects means lack of understanding on potential hazardous events occurring during real CO_2 shipping operations. Several works emphasised the importance of highlighting hazardous occurrences that can compromise the integrity of the CO_2 shipping terminal during real operations and pose risks to surrounding people or environment [22,25,26]. In particular, there appears to be an indisputable requirement for robust engineering control measures to be implemented when the risk of a hazard occurring is inacceptable [27]. Under this framework, the implementation of an emergency release system to mitigate the impact of spillages from the marine arm during emergency shutdown is

suggested as a necessary engineering measure by several sources [17,22,25,26] although its application to CO_2 carriers is not well established.

1.4 Project Aim and Objectives

Aim

In response to the highlighted gaps and technical challenges, the aim of this research is to address the increasing need to decarbonise the power and industrial sectors by providing invaluable information on how to assist in the safe and reliable operations of this intermediate CO_2 shipping chain. In order to accomplish this aim, several objectives are formulated:

Objective 1

- Conduct a critical review on the technological status, challenges and future developments of large-scale CO_2 shipping for CCUS.

Objective 2

- Design and commission an experimental facility capable of handling refrigerated liquid CO_2 (0.7 - 2.7 MPa, 223 - 259 K) to investigate accidental leakage behaviour and evaluate the performance of elastomer materials.

Objective 3a

- Technically qualify the performance and degradation of elastomer materials under real CO_2 transport conditions.

Objective 3b

- Experimentally investigate the accidental leakage behaviour of liquid carbon dioxide under CO_2 shipping conditions (0.7 – 2.7 MPa, 223 - 259 K).

Objective 4

- Undertake a real-scale investigation of the instantaneous discharge behaviour of liquid CO_2 from the of emergency release system’s coupler of a marine loading arm.

1.5 Novelty and linkage of project outputs

Figure 1-2 presents a summary of connection between the different outputs generated from this PhD. An extensive literature review is undertaken as part of this work to provide the basis of the workflow of this thesis; developments in large-scale CO_2 shipping for CCUS were presented and the current technological gaps that require addressing to facilitate commercialisation of this technology were highlighted (Objective 1). The study was presented in the form of a review paper (Paper 1).

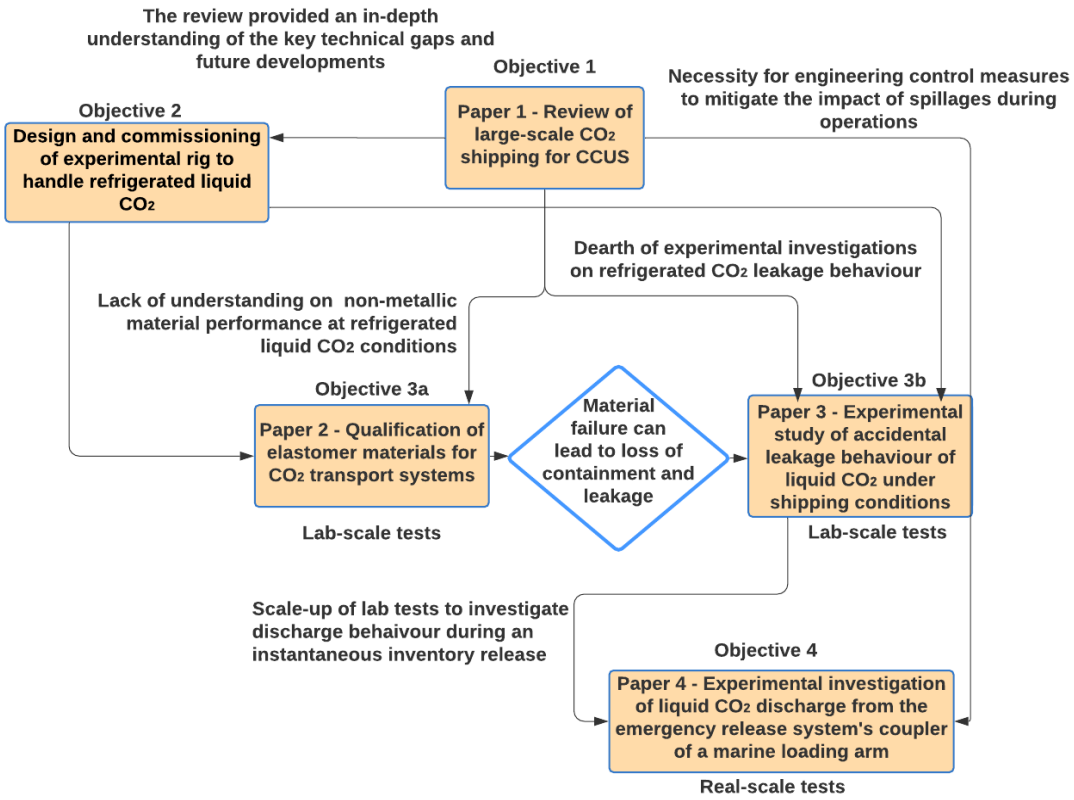

Figure 1-2: Connection between the different outputs generated from this PhD

Therefore, in order to respond to the highlighted technological gaps, an experimental facility capable of handling liquid, refrigerated CO_2 was designed and commissioned in this PhD. The facility was conceived with a versatile mind set to allow a wide range of testing capability (Objective 2). The developed facility enabled to engage in an experimental campaign aimed at addressing two key technological gaps identified in Objective 1, namely qualification of elastomer seals performance under CO_2 shipping conditions (Objective 3a) and the investigation of accidental leakage behaviour of liquid CO_2 under shipping conditions (objective 3b). Outputs of these objectives were

compiled in the form of two papers, respectively Paper 2 and Paper 3. A scale-up endeavour was considered to investigate the discharge behaviour of instantaneous liquid CO_2 release as opposed to the transient leakage scrutiny undertaken under Objective 3b. This led to the formulation and achievement of Objective 4, which was presented under Paper 4.

1.6 Thesis outline

- **Chapter 1** gives an introduction and background knowledge on the topic, providing a rationale behind this work and formulating the project's aim and objectives. Moreover, it provides information on the novelty of this thesis and the linkage among the project's outputs
- **Chapter 2** presents an in-depth review that highlights the key developments and technological gaps concerning CO_2 shipping for CCUS. The chapter critically scrutinises the wider literature on sea vessel transportation for CCUS, summarising technical findings on conditioning and preparation for shipping, and debating the relevant transport properties and conditions in order to explore the future role of this technology as part of global CO_2 transport networks. The review is presented in a paper titled "A Review of Large-scale CO_2 Shipping and Marine Emissions Management for Carbon Capture, Utilisation and Storage."
- **Chapter 3** presents the qualification of elastomers materials with the potential to be considered in CO_2 transport systems. Namely, it applies a methodology to characterise four types of materials previously aged under CO_2 pipeline conditions; the chapter also presents testing of one selected material under CO_2 shipping conditions and relative qualification using the previously developed methodology. It should be noted that testing of elastomers under pipeline conditions was not performed by the author of this thesis, as it is part of a previous project. The author however developed and implemented the characterisation methodology.
- **Chapter 4** presents an experimental campaign that investigates accidental leakage behaviour of refrigerated liquid CO_2. Namely, the chapter considers different conditions typical of CO_2 shipping for CCUS to scrutinise the

propensity for phase transitions, leakage duration and solidification of inventory.

- **Chapter 5** presents a real-scale study on the implementation of a marine loading arm emergency release system to observe the discharge behaviour of liquefied CO_2 and its impact on the surroundings at two distinct carbon dioxide refrigerated conditions.
- **Chapter 6** discusses some general considerations on the implementation of this research that links all the chapters together.
- **Chapter 7** presents the key conclusions, contributions to knowledge from this PhD and suggestions for future work.

Due to the nature of this thesis in "paper format", some key concepts may be repeated throughout the chapters of this work.

1.7 Dissemination from the PhD

1. **Al Baroudi H**, Awoyomi A, Patchigolla K, Jonnalagadda K, Anthony EJ. A Review of Large-scale CO_2 Shipping and Marine Emissions Management for Carbon Capture, Utilisation and Storage (paper accepted in 'Applied Energy')
2. **Al Baroudi H**, Patchigolla K, Mori S, Oakey JE. Technical qualification of elastomer materials for CO_2 transport systems (paper drafted – accepted for poster presentation at GHGT-15).
3. **Al Baroudi H**, Patchigolla K, Thanganadar D, Jonnalagadda K. Experimental study of accidental leakage behaviour of liquid CO_2 under shipping conditions (paper accepted in 'Process Safety and Environmental Protection').
4. **Al Baroudi H**, Wada R, Ozaki M, Patchigolla K, Iwatomi M, Murayama K, Otaki T. Experimental investigation of liquid CO_2 discharge from the emergency release system's coupler of a marine loading arm (paper under review in 'International Journal of Greenhouse Gas Control').

References

[1] IPCC. Summary for Policymakers: Global warming of 1.5°C. An IPCC Special Report on the impacts of global warming. 2018; https://www.ipcc.ch/2018/10/08/summary-for-policymakers-of-ipcc-special-report-on-global-warming-of-1-5c-approved-by-governments/

[2] IEA. Redrawing the Energy-Climate Map – World Energy Outlook Special Report. 2013; https://webstore.iea.org/download/direct/480

[3] IPCC. Climate Change 2007 - Synthesis report. 2007. https://www.ipcc.ch/report/ar4/syr/

[4] ZEP. Role of CCUS in a below 2 degrees scenario 2018:1–30. https://zeroemissionsplatform.eu/wp-content/uploads/ZEP-Role-of-CCUS-in-below-2c-report.pdf

[5] Bui M, Adjiman CS, Anthony EJ, Boston A, Brown S, Fennell PS, et al. Carbon capture and storage (CCS): the way forward. Eenergy Environ Sci 2018:1062–176.

[6] Metz B, Davidson O, de Coninck H, Loos M, Meyer L. Carbon dioxide capture and storage. 2012.

[7] IEA. Energy Technology Perspectives 2020 - Special Report on Carbon Capture Utilisation and Storage, CCUS in clean energy transitions, OECD Publishing, Paris, France: 2020. https://doi.org/10.1787/208b66f4-en. International Energy Agency.

[8] Doctor R, Palmer A, Coleman D, Davison J, Hendriks C, Kaarstad O, et al. Chapter 4: Transport of CO_2. IPCC Spec. Rep. Carbon dioxide Capture Storage, 2005, p. 179–94.

[9] ZEP. The Costs of CO_2 Transport Post-demonstration CCS in the EU; 2011. European Technology Platform for Zero Emission Fossil Fuel Power Plants, Zero Emissions Platform. Available at https://www.globalccsinstitute.com/resources/publications-reports-research/the-costs-of-co2-transport-post-demonstration-ccs-in-the-eu/

[10] Knoope MMJ, Ramírez A, Faaij APC. Investing in CO_2 transport infrastructure under uncertainty: A comparison between ships and pipelines. Int J Greenh Gas Control 2015; 41:174–93.

[11] Ozaki M, Ohsumi T, Kajiyama R. Ship-based offshore CCS featuring CO_2 shuttle ships equipped with injection facilities. Energy Procedia 2013; 37:3184–90.

[12] Nam H, Lee T, Lee J, Lee J, Chung H. Design of carrier-based offshore CCS system: Plant location and fleet assignment. Int J Greenh Gas Control 2013; 12:220–30.

[13] IEAGHG. The Status and Challenges of CO_2 Shipping Infrastructures. 2020; IEAGHG Technical Report 2020-10.

[14] Element Energy. CCS deployment at dispersed industrial sites; 2020. Department for Business Energy and Industrial Strategy; Research paper number 2020/030.

[15] Ministry of Petroleum and Energy, Gassco, Gassnova. Feasibility study for full-scale CCS in Norway. 2016; https://www.cslforum.org/cslf/Publications/NorwayCCSFeasibility

[16] Brownsort P. Ship transport of CO_2 for Enhanced Oil Recovery – Literature Survey 2015;44. http://www.sccs.org.uk/images/expertise/reports/co2-eor-jip/SCCS-CO2-EOR-JIP-WP15-Shipping.pdf

[17] Element Energy, TNO, Engineering Brevik, SINTEF, Polarkonsult. Shipping UK Cost Estimation Study; 2018. Available at: https://assets.publishing.service.gov.uk/government/uploads/system/uploads/attachment_data/file/761762/BEIS_Shipping_CO2.pdf

[18] Han SH, Chang D, Kim J, Chang W. Experimental investigation of the flow characteristics of jettisoning in a CO_2 carrier. Process Saf Environ Prot 2013; 92:60–9.

[19] Harper P, Wilday J, Bilio M. Assessment of the major hazard potential of carbon dioxide (CO_2). Health and Safety Executive. 2015.

[20] Li K, Zhou X, Tu R, Yi J, Xie Q, Jiang X. Experimental Investigation of CO_2 Accidental Release from a Pressurised Pipeline. Energy Procedia 2015; 75:2221–6.

[21] Ahmad M, Lowesmith B, De Koeijer G, Nilsen S, Tonda H, Spinelli C, et al. COSHER joint industry project: Large scale pipeline rupture tests to study CO_2 release and dispersion. Int J Greenh Gas Control 2015; 37:340–53.

[22] Koers P, Looij M de. Final Public Report Safety Study for Liquid Logistics Shipping Concept. 2011; https://www.globalccsinstitute.com/archive/hub/publications/19011/co2-liquid-logistics-shipping-concept-llsc-overall-supply-chain-optimization.pdf

[23] Seo Y, Huh C, Lee S, Chang D. Comparison of CO_2 liquefaction pressures for ship-based carbon capture and storage (CCS) chain. Int J Greenh Gas Control 2016; 52:1–12.

[24] Ansaloni L, Alcock B, Peters TA. Effects of CO_2 on polymeric materials in the CO_2 transport chain : A review. Int J Greenh Gas Control 2020; 94:102930.

[25] Noh H, Kang K, Huh C, Kang SG, Seo Y. Identification of potential hazardous events of unloading system and CO_2 storage tanks of an intermediate storage terminal for the Korea clean carbon storage project 2025. Int J Saf Secur Eng 2018;8:258–65.

[26] Vermeulen TN. Knowledge sharing report – CO_2 Liquid Logistics Shipping Concept (LLSC): Overall Supply Chain Optimization 2011:143. Available at: https://www.globalccsinstitute.com/resources/publications-reports-research/knowledge-sharing-report-co2-liquid-logistics-shipping-concept-business-model/

[27] Energy Institute. Hazard analysis for offshore carbon capture platforms and offshore pipelines. 2013; https://www.globalccsinstitute.com/archive/hub/publications/115563/hazard-analysis-offshore-platforms-offshore-pipelines.pdf

2 A REVIEW OF LARGE-SCALE CO_2 SHIPPING FOR CARBON CAPTURE, UTILISATION AND STORAGE.

Hisham Al Baroudi[1], Adeola Awoyomi[1], Kumar Patchigolla[1]*, Kranthi Jonnalagadda[1], E.J. Anthony[1]

1. Centre for Thermal Energy and Materials (CTEM), School of Water, Energy and Environment (SWEE), Cranfield University, Cranfield, Bedfordshire, MK43 0AL, U.K.

This has been accepted in Applied Energy

Statement of contributions of joint authorship

Hisham Al Baroudi and Adeola Awoyomi conducted the literature review and wrote this manuscript, titled "***A Review of Large-scale CO_2 Shipping and Marine Emissions Management for Carbon Capture, Utilisation and Storage.***" Kumar Patchigolla and E.J Anthony critically commented on the manuscript before submission to Applied Energy. The part of the article covering marine emission management was written by the colleague Adeola Awoyomi and therefore it has not been included as part of this thesis.

Abstract

Carbon Capture, Utilisation and Storage (CCUS) can reduce greenhouse gas emissions for a range of technologies which capture CO_2 from a variety of sources and transport it to permanent storage locations such as depleted oil fields or saline aquifers or supply it for use. CO_2 transport is the intermediate step in the CCUS chain and can use pipeline systems or sea carriers depending on the geographical location and the size of the emitter. In this paper, CO_2 shipping is critically reviewed in order to explore its techno-economic feasibility in comparison to other transportation options. This review provides an overview of CO_2 shipping for CCUS and scrutinise its potential role for global CO_2 transport. It also provides insights into the technological advances in marine carrier CO_2 transportation for CCUS, including preparation for shipping, and in addition investigates existing experience and discusses relevant transport properties and optimum conditions. Thus far, liquefied CO_2 transportation by ship has been mainly used in the food and brewery industries for capacities varying between 800 m^3 and 1000 m^3. However, CCUS requires much greater capacities and only

limited work is available on the large-scale transportation needs for the marine environment. Despite most literature suggesting conditions near the triple-point, in-depth analysis shows optimal transport conditions to be case sensitive and related to project variables. Ship-based transport of CO_2 is a better option to decarbonise dislocated emitters over long distances and for relatively smaller quantities in comparison to offshore pipeline, as pipelines require a continuous flow of compressed gas and have a high cost-dependency on distance. Finally, this work explores the potential environmental footprint of marine chains, with particular reference to the energy implications and emissions from ships and their management. A careful scrutiny of potential future developments highlights the fact, that despite some existing challenges, implementation of CO_2 shipping is crucial to support CCUS both in the UK and worldwide.

2.1 Introduction

Global CO_2 emissions from fossil fuel combustion in 2018, were estimated to be 37.1 Gt, which is a 2.7% increase over 2017 [1]. This is worrisome as a global average temperature rise of 1.5°C will easily be exceeded if such increases continue. Deployment of renewable energy and energy efficiency are often considered by the general public as the priority for greenhouse gas (GHG) mitigations, however the potential of reducing emissions, via such routes, over the short term will not prevent serious impacts from climate change [2]. Carbon capture, utilisation and storage (CCUS) is considered to be a technical and economically viable method to lower GHG emissions. CCUS consists of a number of technologies which capture CO_2 from power generation and industrial sectors such as cement, iron and steel making [3]. These technologies vary from chemical absorption (Boundary Dam in Canada and PetraNova in the United States), physical separation (the Great Plains Synfuels Plant in North Dakota and the Terrell Natural Gas Processing Plant in Texas), membrane separation (Petrobas in Brazil, France's Air Liquide and Membrane Technology and Research Institute), calcium looping, chemical looping (CLEANKER pilot and pre-commercial scale project), direct separation (Low Emissions Intensity Lime and Cement pilot plant in Belgium) and oxy-fuel separation (Callide project in Australia and Heidelberg Cement's Colleferro plant in Italy) [4]. Most of the aforementioned technologies have been adopted globally in different sectors but their use is generally dependent on cost

of installation, flue gas composition and properties, desired purity of the flue gas and integration with existing facility [4].

According to the IPCC Fifth Assessment Report, CCUS is essential to keep CO_2 concentrations in the atmosphere below 450 ppm by 2100. Current lack of implementation of CCUS will magnify the costs of future CCUS implementations by 138% or more [5,6]. Presently, there are sixty-five commercial CCS facilities with twenty-six in operation; the total capacity of the facilities can capture and store about 40 Mt of CO_2 per year [7]. A number of them are in advanced and early development ranging from pilot and demonstration scale projects. Some of the projects seek a commercial return from the captured carbon dioxide by either selling it for enhanced oil recovery (EOR) or by utilising it as chemical feed stock [8,9].

The concentration of CO_2 in the atmosphere is currently about 411 ppm, and future increases will cause catastrophic climate change issues if storage and utilisation methods are not considered [10]. The International Energy Agency (IEA) Blue Scenario Map which aims to halve global energy-related emissions by 2050, emphasises that CCUS could reduce emissions by 19% [11]. To date, the global use of CO_2 is estimated to be 230 Mt CO_2/year, mainly in the fertiliser, oil and gas and food and beverage industries [4]. New routes to carbon utilisation, including fuels, chemicals and building materials are currently being explored, with a high-level projection showing that potential use of CO_2 could reach 5 GtCO_2/year in the future [4] However, in practice, it is unlikely that these estimations will be achievable in the near future, particularly given the economic costs of developing these products and technologies. Therefore, it is clear that the market demand for CO_2 in the forthcoming decades will still be significantly lower than that required for GHG emissions reduction. This necessitates disposal of captured CO_2 in geological formations or marine aquifers and, hence, the transmissions of captured CO_2 remain a critical aspect of CO_2 mitigation. Despite receiving less attention than other components of this chain, CO_2 transport poses both technical and operational challenges and must involve cooperation between multiple stakeholders and industries [12,13].

The transport options for captured CO_2 from power and industrial emitters includes pipelines, ships, railways and motor carriers. Pipeline systems are appropriate for transmitting large quantities of carbon dioxide over relatively short distances but are

associated with high initial capital cost and limited versatility. Conversely, carbon dioxide shipping can discharge lower quantities over relatively longer distances given its low capital expenditure and high flexibility. Figure 2-1 shows the whole chain of CO_2 shipping, which represents a promising alternative to pipelines for smaller and scattered sources [14].

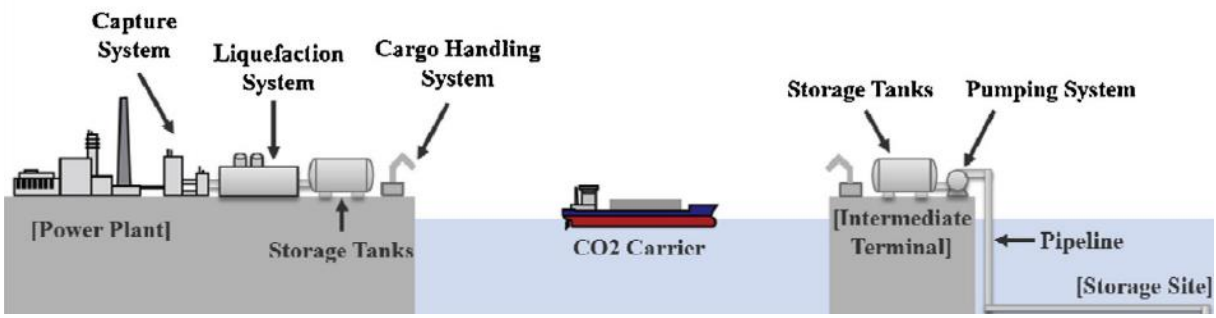

Figure 2-1: Carbon dioxide shipping chain [14]

Furthermore, there is a compelling commercial requirement to reduce emissions as climate impact is now a criterion that determines bank loans to shipping companies [15]. Lending and investing decisions will now be screened for environmental consequences, thus encouraging an industrial transition to cleaner energy technology. According to the third International Maritime Organisation (IMO) GHG study, maritime shipping represents approximately 3% of CO_2 emissions along with 13% and 15% of SO_X and NO_X emissions from anthropogenic sources, respectively [16,17]. Shipping emissions generation arises from fossil fuel consumption for on-board propulsion and electrical generation. Currently, dedicated on-board power plants using diesel engines are standard in marine applications [18].

The aquatic environment must also not be ignored, given that more than 70% of our planet is covered by water. Early marine activities were mostly for food harvesting and trading, but as a result of the industrial revolution, a vast increase in shipping has occurred. For instance, from 1992-2012, worldwide ship traffic increased by 300% [19]. These developments have led to oil spills, waste deposition, and noise pollution in the marine environment. Several techniques have been studied for controlling emissions on-board ships [20], but only limited studies have been done on reducing emissions using CCUS technologies. Onshore projects can use CCUS for power plants and other industrial processes, but these are not currently installed on-board ships [21–23]. CO_2 and SO_2 emissions are a major concern in any combustion

process, especially when residual fuels are used. A world cap has been placed by the IMO on sulphur emissions from ships, which is effective as of 2020 [24]. The EU plans to reduce GHG emissions by at least 20% in 2020 in comparison to the 1990 levels [25]. A lack of up-to-date commercial applications of shipping with CCUS indicates that more R&D aimed at reducing operational costs of the chain is desirable, particularly due to the fact that carbon dioxide is perceived as a waste product rather than a valuable commodity. The following reviews the current technological status and investigate the potential role of CO_2 shipping for the future of CCUS both in Europe and worldwide. In addition to exploring the literature on CCUS as it relates to shipping, the present work also focuses on the use of CCUS technologies to reduce CO_2 and SO_2 emissions, examining potential solvents that can serve for these dual purposes; thus, embracing the concept of a near zero-emission CO_2 shipping chain.

2.2 Comparison of CO_2 transport systems

Transport of CO_2 for sequestration requires the implementation of both a coordinated and efficient transportation network. As such pipelines are the most obvious solution, particularly where a constant flow from the CO_2 capture sites is required. Where economies of scale do not justify pipelines as the transportation method in a CCUS project, other possibilities include ships, railway and motor carriers. These are economically viable when emitters do not have direct access to a suitable pipeline or when the captured quantities are insufficient to justify pipeline construction. Access to adequate seaport facilities or proximity to the sea or railway system are some of the factors that impact decision makers. Pipeline and carrier transport of CO_2 are found to be comparable in cost for similar capacities when distances of 250 km or more are considered, as shown in Figure 2 [26].

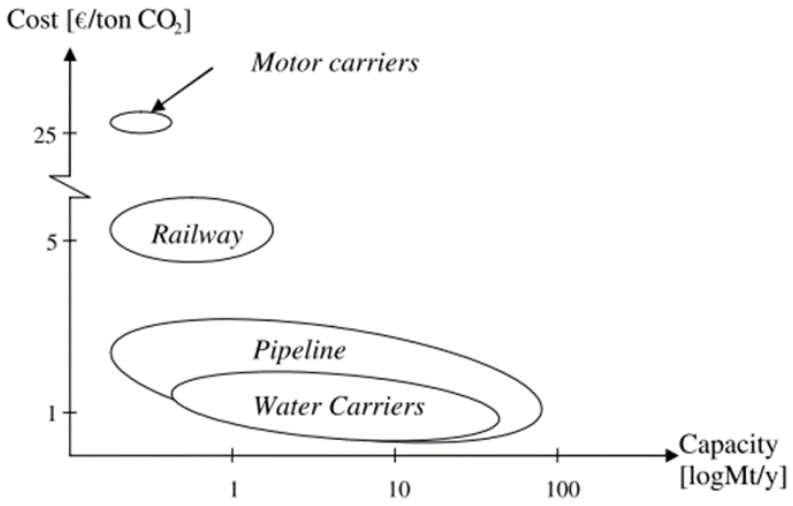

Figure 2-2: Cost and capacity for transportation alternatives at 250km [26]

Despite being an early-stage study, this comparison has proved useful in identifying pipeline and water carriers as the main transportation solutions for CCUS.

The potential of railway CO_2 transport has been evaluated by Roussanaly et al. [27] who compared costs of conditioning and transport of pipeline and railway transport in relation to the distance for different project scenarios periods. Unlike the work of Svensson et al. [26], this study showed that, where there is an existing infrastructure in place, transport by means of railway system could represent a viable option to pipelines for long-range distances, mainly due to the lower financial risks. However, it should be noted, that in practise railway and motor carriers have seldom been considered for CCUS projects, and have limitations in route choice due to dangerous substance transport and potential disturbance to local populations being some of the key constraints [13,28–30].

A summary of CO_2 transportation solutions based on estimated transport capacities and conditions highlight the key issues associated with each system (see Table 2-1). Thus, Roussanaly et al. [31] performed a comprehensive multi-criteria analysis of pipeline and shipping as transport technologies for 10 Mt CO_2/year from an industrial cluster to identify the most appropriate transport solutions. Pipeline technology showed the best performance indicators with regard to operational costs and consumption of utilities, with shipping being more advantageous only in relation to the required capital expenditure. For this reason, shipping was deemed as a temporary solution for the first CCUS deployments in order to contain upfront costs and

investment risk, before transitioning to pipeline infrastructure when larger capture quantities become available. The authors also put emphasis on the fact that pipelines show better performance compared to shipping with regards to fuel, electricity and water consumption in the chain, generating a transportation system with overall lower greenhouse gas emission footprint. The value of this study to decision makers stretches beyond economic considerations, by recognising the importance of life cycle assessment in selecting the best transport alternatives.

Knoope et al. [32] suggested that the flexibility of the shipping chain does not necessarily shift the investment decision from pipeline to ships, even when options such as abandoning the project, halting the capture process temporarily and switching to a different storage reservoir are considered. The reason is that components such as the liquefaction plant and intermediate storage represent 80% of the costs and are considered as fixed costs similar to pipelines. The COCATE Project found that the cost of transporting 13.1 Mt CO_2/year over 450 - 600 km to an offshore storage site in the North Sea is marginally higher by onshore pipeline in comparison to ships, with the latter resulting in 5% lower costs [12]. Fimbres Weihs et al. [33] suggested that CO_2 shipment is economically advantageous over pipelines for distances higher than 700 km and quantities of the order of 6 Mt CO_2 /year. The Zero Emission Platform [34] explored the cost of CO_2 transport in point-to-point connections for CCUS demonstration projects with typical transmission capacity of 2.5 Mt CO_2/year; the report found transport cost per ton of CO_2 to be 45% lower in offshore pipelines compared to shipping on the basis of 180 km distance. The trend however reverses when transport distances of 500 – 1500 km are considered, where shipping cost per ton of CO_2 becomes 27% - 62% lower than that of offshore pipelines.

Table 2-1: Carbon Dioxide transportation alternatives

Transportation method	Conditions	Phase	Capacity	Remarks
Pipelines	4.8-20 MPa, 283-307 K [35–37]	Vapour, dense phase	~100 Mt CO_2/year [26] 6500 km of pipeline transport in operation [27]	• Higher capital costs, lower operating costs • low-pressure pipeline system is 20% more expensive than dense phase transmission. • Well-established for EOR USE.
Ships	0.65-4.5 MPa 221-283 K [38–41]	Liquid	> 70 Mt CO_2/year [26]	• Higher operating costs, lower capital costs • Currently applied in food and brewery industry for smaller quantities and different conditions. • Enhanced sink-source matching
Motor carriers	1.7-2 MPa, 243-253 K [42,43]	Liquid	> 1 Mt CO_2/year [26]	• 2-30 tonnes per batch • Not economical for large-scale CCUS projects • Boil-off gas emitted 10% of the load [42]
Railway	0.65-2.6 MPa, 223-253 K [27,42,43]	Liquid	> 3 Mt CO_2/year [26]	• No large-scale systems in place • Loading/unloading and storage infrastructure required • Only feasible with existing rail line (Wong, 2005) • More advantageous over medium and long distances

The IEAGHG investigated the unit cost of pipeline and ship transport for different flow rates of 0.5 – 10 MtCO_2/year and a transport distance of 1000 km. Findings show shipping to be 64% less expensive in discharging 0.5 MtCO_2/year, with this economic gap progressively narrowing with increase of flow rates; here 2 MtCO_2/year sea vessel transport is only 10% cheaper than pipeline, and at 5 MtCO_2/year pipeline transport is 24% economically advantageous. Overall, larger disposal amounts generally shift breakeven distances towards larger distances for ship transport making this option

advantageous [37,44]. Several more project variables such as geographical location, security, layout of port-terminals and seabed stability affect breakeven distances after which ships becomes more economic than pipelines.

Roussanaly et al. [45,46] performed detailed economic, technical and climate impact assessment comparisons between pipeline and shipping when considering transportation connecting both two onshore and two offshore areas. Unlike previous studies, these authors consider a range of distances and amounts. In line with other studies, they found that for a fixed throughput, a pipeline is preferred to discharge CO_2 over shorter distances. However, the study also emphasised that factors such as geographical location, regional fluctuations of pipelines costs, first-of-a-kind challenges and ownership arrangements can significantly affect the choice of transportation system. Conversely, project variables such as fluctuation of electricity and shipping fuel price do not appear to have a profound impact. However, complex transportation networks as opposed to single-system infrastructure are expected to show different trends and will require additional work to assess them.

Table 2-2 summarises the factors relevant to the practicality of pipelines and shipping systems in relation to economic aspects of the projects and Figure 2-3 provides a graphical representation of the breakeven distances between ships and pipelines in the literature. Disagreements on trends for the cross-over point between pipelines and ships can also be attributed to the different economic methodology and assumptions. However, shipping compares favourably with offshore pipelines compared to onshore pipelines, due to the higher costs involved in putting offshore installations in place and the constraint on drop of system pressure for offshore transport [46]. However, despite being more economically viable, onshore pipeline systems can better meet stringent health and safety operations due to the hazard of CO_2 exposure in inhabited areas [47].

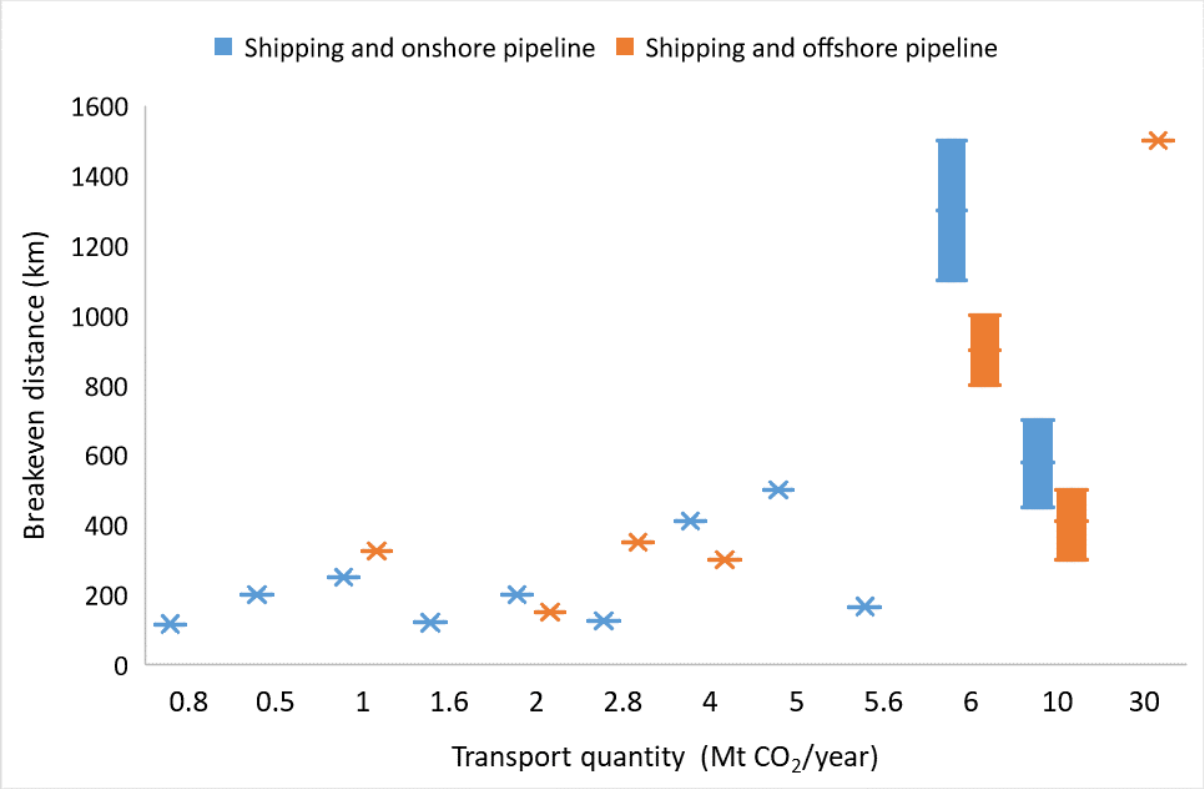

Figure 2-3: Box and Whisker representation of breakeven distances between ships and pipelines in the literature

In summary, the practicality of carrier transport is subject to a number of techno-economic and geographic considerations; it is generally agreed that pipelines are advantageous to transport larger amounts of CO_2 due to the high capital expenditure associated with onshore and offshore infrastructure in light of lower operational costs [37,41,45,48,49]; transport by ships has relatively higher operational costs and displays nonlinear dependency with distance, making it an attractive option to transport smaller volumes over longer distances [34,50,51]. Throughout this review, the role of carbon dioxide shipping in global CCUS transportation network will be investigated beyond simply considering the techno-economic aspects.

Table 2-2: Breakeven distance comparison of shipping transportation with offshore and onshore pipeline options.

Source	Quantity	Methodology	Breakeven distance with shipping transport		Remarks
			Onshore pipeline	Offshore pipeline	
Mitsubishi Heavy Industries [52]	6.2 Mt CO_2/year 30 Mt CO_2/year	Corporate economic model	1,500 km	600 km 1,500 km	Economies of scale can be considerable
Doctor et al. [37]	6 Mt CO_2/year	Cost estimation developed by authors	1,500 km	1,000 km	Higher amounts will favour long distances Full-scale considered
Decarre et al. [44]	0.8 Mt CO_2/year 1.6 Mt CO_2/year 2.8 Mt CO_2/year 5.6 Mt CO_2/year	Economic model by French Environment and Energy Management Agency	115 km 120 km 125 km 165 km	300 km	Comprehensive economic model on full transport chain Vessel transportation is the most cost-intensive part of the chain .
ZEP [34]	10 Mt CO_2/year		700 km	500 km	
Fimbres Weihs et al. [33]	6 Mt CO_2/year	Integrated techno-economic model	1,100 km	Shallow pipeline: 900 km Deep pipeline: 700 km	Cost model was validated from wider literature Electricity and ship fuel are the main costs
Yoo et al. [53]	10 Mt CO_2/year	Techno-economic model developed by shipping company	450 km	300 km	
Vermeulen [39]	1 – 4 Mt CO_2/year		200 km	150 km	Based on CO_2 Liquid Logistics Shipping report by engineering consultancies and shipbuilders
Knoope et a. [32]	1 Mt CO_2/year 2.5 Mt CO_2/year 10 Mt CO_2/year	Real Option Approach (ROA) based on standard Net Present Value (NPV)	N/A	250 km <500 km < 250 km	Assess the value of flexibility on investment decision of CCUS transport network Flexibility does not necessarily favour shipping systems
Element Energy et al. [41]	1 Mt CO_2/year	In-house techno-economic model based on 20-year lifetime project and 0% discount rate	250 km	N/A	Report commissioned by the UK's Business, Energy and Industrial Strategy Department
Roussanaly et al. [45,46]	4 Mt CO_2/year 10 Mt CO_2/year	Scenario-range approach based on standard Net Present Value (NPV)	410 km 580 km	300 km 410 km	Impact and sensitivity of a range of project variables (utility costs, geographical location etc.) is considered into this work

2.3 Overview of CO_2 shipping

The first serious investigation into liquid CO_2 shipping began in the early 2000s with studies by Mitsubishi Heavy Industries [52] and Doctor et al [37]. Subsequently, the technological studies carried out on CO_2 shipping [8,39,40,54–56] have identified its potential and relevance for applications in CCUS and EOR applications. Table 2-3 provides a summary of the key literature published on CO_2 shipping for CCUS from the early stages up to date. Figure 2-4 represents a graphical representation of the indicated shipping conditions in the literature.

Table 2-3: Summary of the literature on CO_2 shipping for CCUS

Sources	Remarks
Mitsubishi Heavy Industries [52]	• Detailed report completed for IEAGHG R&D Programme based on a previous patent from Mitsubishi Heavy Industries • It explored feasibility of ship transport for CO_2 and sensitivity to several project variables by comparing costs with pipelines • Additional CO_2 emissions due to long distances and high energy requirements for liquefaction were found to be limiting factors
Svensson et al. [26]	• Comparison of costs of transporting CO_2 by pipeline, ships and railway within Europe • It was concluded that for offshore transport of large amounts of CO_2, both pipelines and ships will have a significant role in a pan-European transportation network • Lack of techno-economic analyses of stream liquefaction and conditioning
Hegerland et al. [9]	• Conference paper specifically focused on integration of CO_2 shipping for EOR • CO_2 shipping technology was deemed ready for implementation • Full-chain was found to be easily adaptable to allow handling quantities relevant to CCS and EOR
IPCC [37]	• Book chapter on CO_2 transport mainly based on the Mitsubishi Heavy Industries Report (2004) and corporate information from STATOIL • Techno-economic comparison between pipelines and ships with highlights of risks and process safety considerations • CO_2 shipping was found to be feasible and competitive with pipelines transport when small amounts or long distances are considered

Sources	Remarks
Aspelund et al. [57]	• Technical peer-reviewed paper presenting the challenges encountered in large-scale CO_2 shipping to that date. • Concept of open- and close-cycle liquefaction is explained, and internal refrigeration system was deemed to be favourable, though no clear justification was provided • Energy and cost estimates highlighted that CO_2 liquefaction is the most-energy intensive part of the shipping chain • Considerable technical details area provided despite some limited assumptions (e.g. no clear transport distance)
ZEP [34]	• Technically detailed report based on real data; it compared costs of transport by pipelines and shipping by taking into account several project sensitivities. Despite covering several technical issues, its simplistic assumptions may result in an underestimation of costs.
Vermeulen [39]	• Detailed report from Rotterdam CCS Network covering all aspects of CO_2 shipping including stream conditioning, ship design, loading and offloading • Comprehensive transport network (including pipelines) was considered • Uncertainties associated with selection of materials, carbon emissions and process safety are clearly highlighted • Provided information on absolute costs are subject to commercial sensitivity
Omata and Kajiyama [58]	• Detailed techno-economic analysis of feasibility of CO_2 shipping with direct injection from ship to sub-sea wellhead • Suitability of carrier transport in Eastern Asia was identified in relation to geographical factors • Unusual transport conditions are indicated though no clear justification was provided
Jung et al. [55]	• Publication on CO_2 transport scenarios and techno-economic analysis for offshore CCUS in South Korea • Transportation costs of shipping found to be higher than those of pipeline systems • Extensive optimisation of CO_2 transport networks was deemed incomplete yet essential to establish optimum CCUS transport alternatives suited for South Korea
Nam et al. [59]	• Analysis of an offshore, ship based CCUS system in South Korea combined with the transport of crude oil • Focuses on the optimal layout of the chain including location of the industrial units, appointment of the fleet, and the favourable cargo conditions for CO_2 transport • Unlike previous literature, optimum operating conditions are found to be case-sensitive and potentially not at the triple point

Sources	Remarks
Yoo et al. [53]	• Work focused on the establishment of a CCUS infrastructure for future commercial projects showing the key role of shipping in discharging large amounts of carbon dioxide • Detailed technological and economic analysis is performed by exploring different disposal amounts, liquefaction cycles and ship carriers • Established that carbon dioxide shipping can play a key role in scenarios where short-distances and large-quantities are considered
Ozaki and Ohsumi; Ozaki et al. [40,60]	• Conference papers at GHGT-10 and GHGT-11 • Focuses on ship based offshore CCUS featuring shuttle ships and amongst the first studies to consider the concept of direct injection form ships • Shuttle transport is deemed more suitable than large CO_2 carriers in mitigating the risk of matching large-scale sink to large-scale sources • Indicated cargo conditions are considerably far from the triple point
Skagestad et al. [56]	• Technically detailed report on the status of CO_2 shipping, highlighted its role in discharging small volumes over longer distances • Challenges related to conditioning, loading, transport and offloading are highlighted but not found to be critical to the feasibility of carrier transport • Further and highly prioritised research is found to be required on injection of carbon dioxide to the storage site
Brownsort [54]	• Technical report by the Scottish Carbon Capture and Storage focusing on the implementation of CO_2 for Enhanced Oil Recovery with a shipping transportation system • Shipping found to be relevant to execute EOR projects in the North Sea • Detailed review of the available literature on carbon dioxide shipping emphasised the high-level of understanding of the chain despite limited projects running
Seo et al. [14]	• Study focusing on ship based CCUS chain with different CO_2 liquefaction pressures to determine the optimal pressure • One of limited number of studies performing techno-economic analysis on different shipping conditions with sensitivity studies • Optimum transport pressure found to be 1.5 MPa regardless of disposal amount and distance
Ministry of Energy and Petroleum [38]	• Technical and economic study on the implementation of a CCUS chain in Norway, assigned by the Ministry of Petroleum and Energy and focusing on incentives and regulation framework • Different transport conditions – low-, medium- or high-pressure – are investigated with their technical and safety considerations • Future demonstration projects availing of CO_2 ships have been considered.

Sources	Remarks
De Kler et al. [61]	• Highly technical report commissioned by the Dutch National R&D programme for CCUS (CATO) on transportation and unloading of CO_2 by ship • Focus on North Sea storage sites by providing cost estimations with 50% margin with regards to different offloading options • Completion of studies focusing on realistic storage options in the North Sea is suggested
Neele et al. [8,48]	• Conference proceeding from GHGT-13 in Lausanne, Switzerland, here ship transport is found to be the most advantageous option to match sources with storage sites in the first phase of CCUS. • Costs associated with shipping projects are developed and validated with existing literature
ZEP [62]	• Broader report on the role of CCUS in a below 2 degrees' scenario, covering a range of case studies • Cooperation between industries and countries is deemed crucial with CCUS being considered responsibility of multiple stakeholders • Shipping is deemed to be fully implemented by 2050 by employing 600 vessels and 10,000 jobs; though no rationale is provided
Element Energy et al. [41]	• Study assigned by the UK's Department for Business, Energy and Industrial Strategy (BEIS) to explore the role of CO_2 shipping as part of CCUS strategies • A good summary of the existing literature is provided, and particularly in relation to economic assumptions; aspects relating to emissions from ships are explored • Overall outline of international opportunities and current barriers highlight that carrier-based transport can well be a key part of the UK decarbonisation. • Detailed techno-economic models are produced for a range of project sensitivities.
Element Energy [30]	• Report commissioned by BEIS to identify dispersed emitters in the UK and the challenges they exhibit to deployment of CCS infrastructure • For the majority of the cluster groups – including South Wales and clusters close to big ports - a combination of pipelines and shipping represent the most advantageous transportation option • Infrastructural limitations of some ports to accommodate CO_2 ships, lack of experience in sea vessel transport and viable business models represent the main drawbacks to implementation

Sources	Remarks
IEAGHG [63]	• The report demonstrated that long-distance, low-volume (<2 $MtCO_2$/year) transport of CO_2 by shipping vessels from different cluster emitters represents a viable decarbonisation option • Based on a shipping distance of 1,000 km, minimal cost advantage or penalty is found in relation to increasing/decreasing the ship size from the standard 10,000 tons CO_2 capacity • Direct injection is found to be the most cost-effective offloading solution with transfer to floating storage injection unit being the least cost-effective one

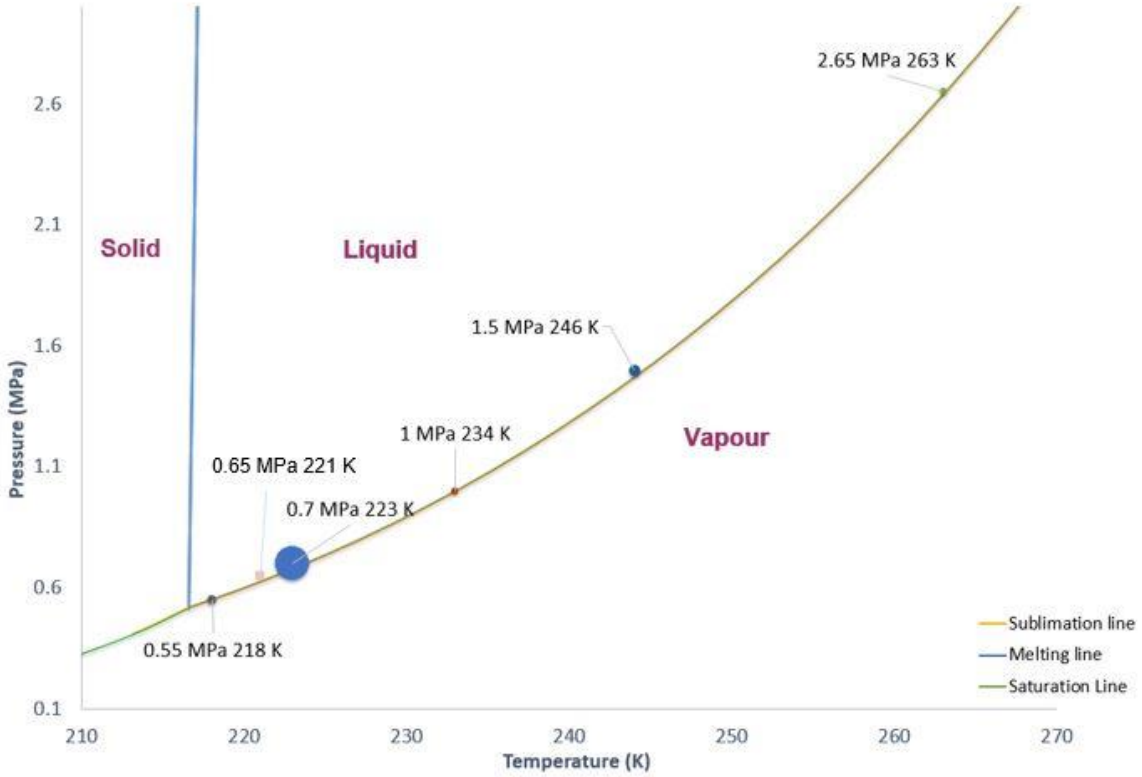

Figure 2-4: Graphical representation of proposed shipping conditions in the literature on the CO_2 phase diagram. Size of the bubble represents the proportional representation of shipping conditions in the literature.

The Netherlands and Norway, and in particular SINTEF and STATOIL [64], have started projects in Europe, while in the Far East – mostly Japan and Korea –a series of projects has meant that these countries have become key players in R&D on large-scale carbon dioxide shipment [52,57,65]. As of 2015, 60% of the literature relating to CO_2 shipping was published in Europe, whilst 35% of the literature came from the Far East [54]. Carrier-based transport of CO_2 has however generated differing opinions by decision makers in recent years. As of 2012, ship-based transport of CO_2 was deemed by the then 'Department of Energy and Climate Change' in the UK to require short-

term research and development in order to optimise transport [66]. However, more recently, the 'Role of CCUS in the below 2 degrees scenario' report [62] suggested that the near-future implementation of CCUS will require up to 600 marine vessels and create up to 10,000 jobs, with Norwegian firms being the most likely to benefit from such opportunities. Similarly, the British government found that CO_2 transport infrastructure, which includes shipping, is essential to support the deployment of CCUS in the UK [41].

A contrasting pattern is seen in North America, where the extensive network of pipelines and the presence of onshore EOR sites limit the focus of R&D on CO_2 shipping thus favouring pipeline implementation [37]. Shipping has been utilised in the last decade to transport relatively small quantities of food grade liquid CO_2 at 1.5-2 MPa and 243 K [8,39,41,56,61]. However, in order to become an option for transporting larger volumes, the literature suggests actual conditions should be as near to the triple point as possible (~ 0.7 MPa and 223 K) [32,39,41,49,56,67–70]. Shipping has the potential to introduce significant decarbonisation for a wider number of small industries due to its high flexibility in source-sink matching [13], and extend the benefits of CCUS to those countries where implementation of a pipeline-based transport network is essentially infeasible due to the propensity for natural calamities (e.g., earthquakes) such as Korea and Japan [40,59]. Moreover, CO_2 carriers are found to be particularly suitable due to the increased use of offshore sink sites, such as saline aquifers or depleted hydrocarbon sites [59]. In Norway, a significant number of sources are located on or near the coast and an already established maritime tradition has created a suitable environment for CO_2 shipping [56]; in the UK, the Department for Business, Energy and Industrial strategy is actively exploring the implementation of this technology in relation to sites isolated from CO_2 transport and storage infrastructure in the British North Sea [30].

In summary, with CCUS being perceived as a risk due to financial uncertainty, ship transport offers flexibility in terms of sources and destinations to implement capture, variations in the routes of CO_2 transported, the possibility to reutilise the ships and also short set-up times [48]. By contrast, the high capital investment of pipelines represents a sunk cost with few opportunities to reuse such infrastructure. Despite this, there are currently no demonstration projects that use shipping for the transport of CO_2 [61], although a full-scale CCUS demonstration project deploying carriers as

carbon dioxide transport launched by Norway is expected to enter the realisation stage sometime in 2020 [71].

2.4 Existing experience

Large-scale CO_2 shipping can significantly benefit from knowledge developed by the more established LNG and LPG industries, especially regarding early-stage implementations. Despite the difference in pressure and temperature requirements, liquid carbon dioxide near the triple point has a comparable liquid/gas density ratio to LNG, making comparisons more appropriate (Table 2-4). Moreover, the design and operation strategy of CO_2 terminals can greatly benefit from LNG and LPG experience, especially in relation to process safety and liquid cargo handling procedures [72]. The design of tank arrangements on the carrier for low and medium pressure liquid CO_2 can largely be based on existing LPG ship designs due to their similar operating conditions [63]. The largest LNG ships have capacities of 120,000 m^3 up to 270,000 m^3 [52,56] which would potentially be relevant for large-scale carbon dioxide shipping projects.

Table 2-4: Typical conditions and properties across the shipping chain [29]

Properties	Units	Typical LNG	Typical CO_2 Buffer Storage and Transport by Ship	Typical CO_2 Buffer Storage and Transport by Road	Typical CO_2 Transport by Pipelines	Typical CO_2 Injection and Storage (sequestration)
Fluid	-	Liquid	Semi-refrigerated liquid	Semi-refrigerated liquid	Semi-refrigerated fluid (dense phase)	Supercritical fluid (dense phase)
Density	kg/m^3	450	1163	1078	838	702
Density ratio (liquid/gas)	-	600	568	545	424	355
Pressure	MPa (gauge)	0.05	0.65	2	7.3-15	10
Temperature	K	113	221	243	293	308

However, shipbuilding companies emphasise that retrofitting of LNG ships for liquid CO_2 purposes will involve significant efforts and challenges in the face of modest added value given that a ship's capital expenditure constituting only 14% of the project cost [41]. Conversely, the IEAGHG [63] reports that the conversion between cargo inventories is deemed practically feasible for single conversion only, thus providing an option to reduce risks to project feasibility. Some of the technical drawbacks are that

only up to 60% of the tank capacity of LPG carriers can be utilised for CO_2 transport due to the difference in density between liquid CO_2 and LPG (550 – 700 kg/m^3 for LPG and 1050-1200 kg/m^3 for liquid CO_2) and the limit to the maximum storage pressures due to the fact that large LPG and ethylene carriers have maximum design pressures lower than 0.8 MPa. An exception is made for smaller LPG carriers, designed to operate between 1.1 – 1.9 MPa, that could potentially accommodate 2,000 – 3,000 tons of CO_2 at medium pressures. The report also provides a list of 26 potential LPG carriers with capacities ranging from 5,000 – 30,000 m^3 from several companies that could be repurposed for CO_2 transport [63]. The established experience in hydrocarbon carriers can also be beneficial in the design of equipment for onshore loading and offloading, with articulated loading arms developed in such industries also being deemed suitable for CO_2 carriers [63].

There are 3 types of tanks suitable for the transport of liquid gases [37,49];

- pressure type, manufactured to limit boiling of the content under ambient conditions;
- low-temperature type which are suitable for large-scale transport and designed to operate at low temperatures; and
- semi-refrigerated type which combines both the pressure and low temperature type and is pressurised and cooled.

Currently, semi-refrigerated type C tanks are identified as the only applicable solution due to the trade-off between pressure and temperature requirements; and the largest existing pressurised refrigerated gas transport ship has a capacity of 30,000 m^3 [52]. Six LPG/ethylene semi-refrigerated carriers of 8-10,000 m^3, owned by IM Skaugen, have been approved for transport of carbon dioxide in bulk quantities [41]. Furthermore, TGE Marine has focused on building 30,000 m^3 ships implementing Type C tanks and has operated a 7,500 m^3 carrier [28]. Doctor et al. [37] stated that carrier vessels for carbon dioxide transport with a size of 22,000 m^3, capable of transporting up to 24,000 t, are feasible and do not pose significant new technical challenges. Accordingly, large ships of 40,000 m^3 and 100,000 m^3 with pressurised on-board tanks have been proposed [60,73]. In summary, it appears that the existing shipbuilding experience derived from LNG and LPG can greatly assist in the construction of large CO_2 carriers and that no major technical challenges have been identified. Designs can integrate a variety of concepts such as close packing of vertical

tanks and X-bow design - insulation and double-walled cargo options [65]. Potential arrangements of the carrier have been extensively explored in the literature with the aim of finding the optimum solutions [37–39]; a potential carrier arrangement is shown in Figure 2-5. It is found that vessels for transportation of CO_2 at low pressure would have designs similar to those of LPG boats [38,39], and could avail themselves of cylindrical tanks. These ships will transport carbon dioxide at the highest density, requiring the smallest vessels size. Transport of carbon dioxide at medium pressures however permit designs typical of carriers currently used in the commercial transport of CO_2 for the food and brewery industries; conversely, high-pressure solutions would require small cylindrical bottles similar to those used in pipe transport of natural gas. In such a case, a ship would typically require 700-900 cylinders, thus creating challenges in terms of available space [38]. Neele et al. [48] suggested that the shipping design should consider the required wellhead conditions at the storage site rather than the conditions of the stream during capture, thus recommending medium- or high-pressure conditions. Implementation of a Dynamic Positioning system (DPS) is suggested to track the location of the carrier at the offshore site [41,64]. Existing and scheduled CO_2 carrier projects are summarised in Table 2-5.

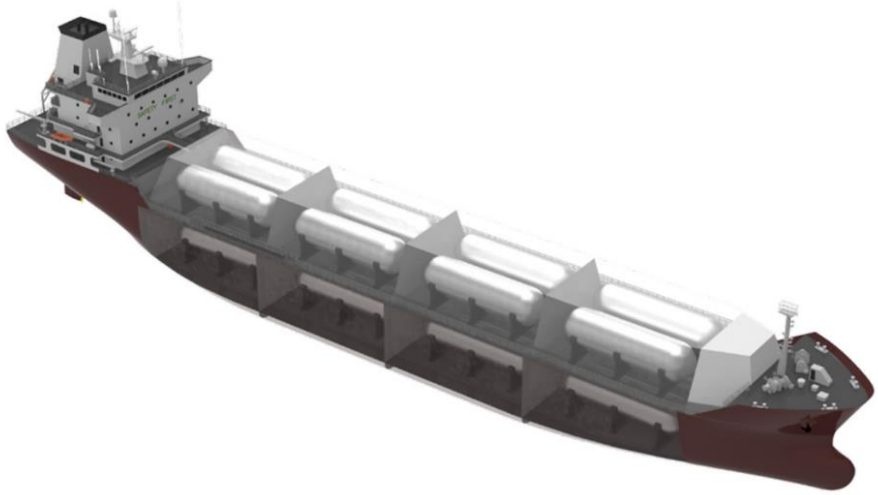

Figure 2-5: Conceptual design of CO_2 carrier [14]

Table 2-5: Existing and scheduled CO_2 carrier projects

Developer	Application	Location	System	Status	Remarks	Source
IM Skaugen	Unspecified	Unspecified	6 x 8,000-10,000 m^3 semi-refrigerated ships	Approved for transport of CO_2 (2010)	2-3 Mt CO_2/year; 480 km	[74]
Anthony Veder – Coral Carbonic	Food and beverage	Port-to-port - Northern Europe	1,250 m^3 – 600 t cargo capacity	In operation	1.8 MPa, 233 K; LNG/CO_2 dual purpose	[54]
Yara	Food and beverage	Port-to-port - unspecified	4 x 1,250 m^3	In operation	Disposal capacity 400,000 t CO_2/year	[13]
Larvik Shipping	Food and beverage	Port-to-port - Europe	2 x 900 tons capacity ships 1 x 1,200 tons capacity ship	In operation	2 MPa, 243 K,	[54]
Yara & Larvik Shipping	Food and beverage	Port-to-port - Europe	1-4 1,850 m^3 ships; 1.776 t – 7,104 tons capacity	Planned	1.6 MPa, 248 K	[64]
Yara Embla and Yara Froya	Food and beverage	Port-to-port - Europe	1,800 tons capacity	Reconditioned	Reconditioned LPG tanker, 1.5 MPa, 243 K	[54]
Praxair/ Larvik Shipping	Food and beverage	Port-to-port - Europe	1,200 - 1,800 tons capacity	Reconditioned	Reconditioned from cargo carriage, 1.6-2.1 MPa, 243 K	[41]
Vermeulen	CCUS (storage)	Offshore storage sites, NL	6 x 3,833 m^3 tanks; 26,450 t	Proposed	0.7 MPa, 223 K	[39]
Yoo et al.	CCUS (storage)	Unspecified offshore storage	6 x 5,000 m^3 tanks; 34,500 tons	Proposed	0.7 MPa, 223 K	[53]
Brevik	CCUS (storage)	Offshore storage sites, Norway	2,315 tons – 9,787 tons	Proposed	1.4 – 1.9 MPa; 0.2 – 0.8 Mt CO_2/year	[41]
Polarkonsult, Praxair, Larvik Shipping			2,400-9,400 tons capacity ships	Proposed	1.4 – 2 MPa, 233 – 243 K	[75]
Nippon Gases Europe AS	Food and beverage	Port-to-port – unspecified	3 x ships with 1,770 tons capacity	In operation	2 MPa 243 K	[63]
Nippon Gases Europe AS	Food and beverage	Port-to-port – unspecified	1,200 tons capacity ship	In operation	2.1 MPa, 243 K	[63]

It is worth noting that CO_2 shipment has been exploited for over 30 years on a significantly smaller scale in the brewery and food industries at conditions of 1.4 - 1.7 MPa and 238 - 243 K. However, the cumulative transport across Europe amounts to 3 Mt CO_2/year [54]; such quantities are significantly lower than those intended for CCUS- projects [41]. Three projects have selected ship transport: two are located in Korea and are known as Korea–CCUS 1 and Korea–CCUS 2. The third project was implemented in China, the Dongguan Taiyangzhou IGCC with CCUS Project that switched from pipeline to ships in 2003 [29,43]. The first ship built with the purpose of transporting CO_2 is the 'Coral Carbonic' with a 1,250 m^3 capacity, which translates to a cargo capacity of 600 t; design transport limits are 1.9 MPa and 233 K; finally four additional CO_2 carriers (1,250 m3) are currently being built [34] by Yara Gerda in projects with cumulative disposal capacity of 400,000 t CO_2/year, approximately half the amount of a CCUS demonstration project. Larvik shipping operates three food-grade CO_2 shipping carriers – two of which have a capacity of 900 t and one of 1,200 t - from the Yara fertiliser plant in Larvik to various destinations in Europe at 243 K and 2 MPa. However, all of the above-mentioned quantities and, therefore, specifications are not suitable to transport large-scale CCUS-related CO_2 cargoes, due to lower pressures required in larger vessels [60].

2.5 Role of shipping in global CO_2 transport

Industrial and power emitters are seldom found in close proximity to geological storage sites and relocation in order to reduce transportation distances is usually unrealistic. Therefore, designing an optimum transport network that integrates pipelines and ships can lead to a flexible and sustainable infrastructure and facilitate the implementation of CCUS worldwide [8,13,39,49,55,67,76]. The European Commission's GATEWAY report found that CCUS technology could have been applied to the power generation and industrial sectors for several years, though no full chain has in fact yet been established in Europe due to the uncertainties in the financial framework of CCUS [77]. Svensson et al. [26] indicated that coordinated pan-European transport networks can contribute to reducing transportation costs to as low as $2.3/t when a long-term infrastructure capable of handling 40-300 Mt CO_2 per year is considered.

From a wider prospective, the Global CCS Institute [78] highlighted that global underground storage resources are certainly sufficient to meet the Paris climate targets. As shown in Figure 2-6, countries such as the US, Canada, China, Brazil and

Australia all have significant onshore storage capacity and will probably not require significant implementation of carrier-based transport as part of their CCUS strategies, thus favouring a pipeline-based approach. Conversely, scenarios such as Europe, where storage sites are dislocated in the North Sea, or Japan where CO_2 emitters are mainly concentrated in proximity to the coast, suggest that carrier-based transport can facilitate sink-source matching and enhance flexibility of a transport network. In 2011, Morbee et al. [79] suggested that carrier transport of carbon dioxide will not likely be implemented during early-stage CCUS projects due the inadequate maturity of shipping technology; and as such only four large-scale integrated projects between Europe and Asia proposed CO_2 shipping as the selected transportation method [13]. However, significant technological progress has been made since this work was published, indicating that large-scale CO_2 shipping indeed can and will be a key part of global decarbonisation strategies [62].

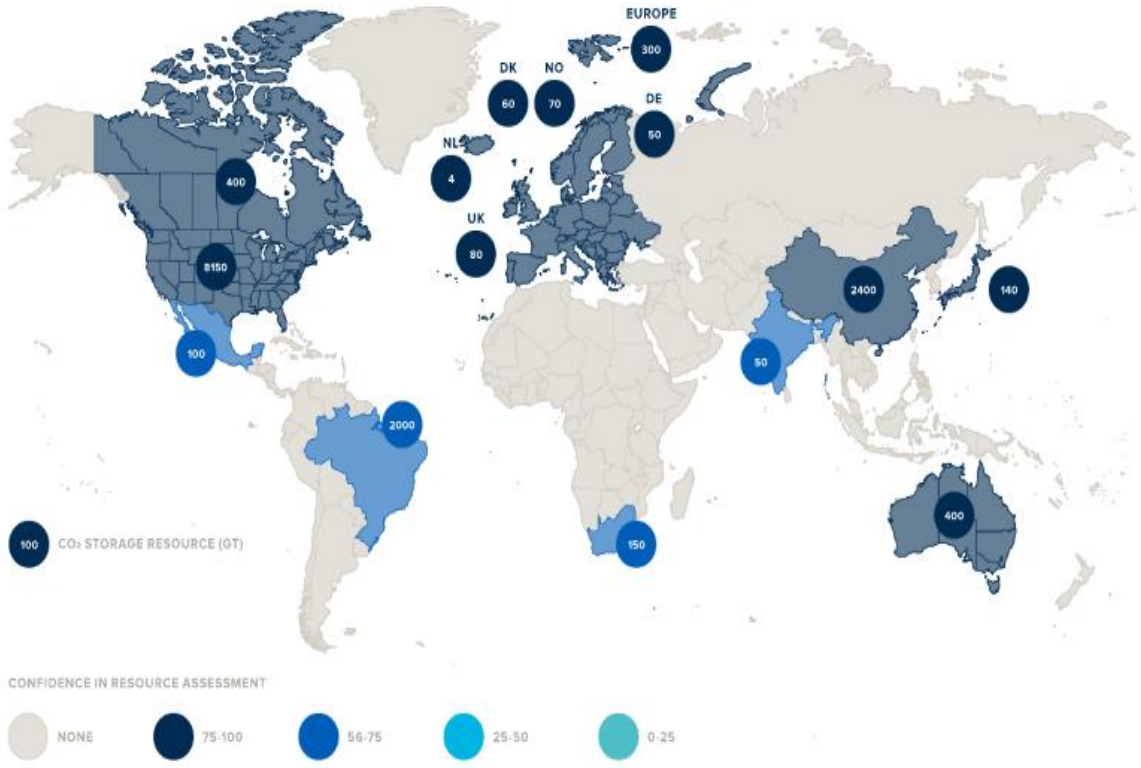

Figure 2-6: Global storage resource potential [78]

Potential storage assets in the North Sea can be deployed by implementing shipping in the early stage and potentially on a longer term (2030-2040) for CCUS across Europe (Table 2-6). Ships can extend the feasibility of CCUS to smaller emitters where implementation of a pipeline is economically infeasible, and they can exploit relatively

smaller storage sites without incurring high sunk costs. Several potential shipping routes to decarbonise the Netherland's emitters clusters have been explored in the 2013 GCCSI report [80] with the intention of diversifying CCUS transportations solutions and reducing costs. Demonstration projects such as in the Port of Antwerp with relatively low emissions (<1 Mt CO_2/year) were found to favour shipping for distances of approximately 400 km, with offshore pipeline being preferred when higher amounts of 5 Mt CO_2/year are considered [80]. Conversely, when longer transport distances of 1,000 km were considered for the same discharge amounts in the Skagerrak-Kattegat region in Scandinavia, transport by ship was only deemed to be a transitional approach until a full-scale pipeline system was implemented, despite dislocated distribution of emitters favouring a flexible shipping solution [81].

Table 2-6: Potential CCUS Transport Networks implementing shipping transport [41,55,80].

Storage	Type/Capacity	Offshore Transport	CO_2 Sources	Remarks
P18/P15(NL)	Dep. Gas Field ~79 Mt CO_2	Pipeline	Rotterdam	Selected by the ROAD and Green Hydrogen projects in The Netherlands
Q1(Netherland)	Aquifer ~200 Mt CO_2	Pipeline Shipping	Rotterdam Eemshaven	Suitable for the Dutch Continental Shelf
Dan Oilfield EOR (D)	Dep. Oil Field	Shipping	Rotterdam Eemshaven	Selected for the Green Hydrogen project in The Netherlands
Q1 (Netherlands)	Aquifer ~200 Mt CO_2	Pipeline Shipping	Rotterdam FS Eemshaven Antwerp	Suitable for the Dutch Continental Shelf
South North Sea Aquifer (UK)	Aquifer [>2000 Mt CO_2]	Pipeline Shipping	Rotterdam FS Antwerp	Potential sink site for CCUS projects in the UK
Captain Aquifer (UK)	Aquifer [>360 Mt CO_2]	Shipping Pipeline	Rotterdam FS Antwerp Eemshaven FS	Potential CO_2 storage site for Scotland in the North Sea.
Captain Aquifer (UK)	Aquifer [>360 Mt CO_2]	Pipeline, Shipping	St Fergus, Teesside clusters	Potential future transport scenario for the UK
Bunter Aquifer (UK)	Aquifer	Pipeline	St Fergus	Potential future transport scenario for the UK
Utsira Sandstone (Norway)	Aquifer [> Gt]	Shipping	Eemshaven FS	CO_2 storage site in place for Sleipner project in the North Sea
Ulleung Basin, Korea	5.1 Gt CO_2	Pipeline, Shipping	Hadong and Boryeong Power Plant,	Transport strategy implies offshore pipelines or shipping [55]

During the ramp-up phase of the project, as more clusters become decarbonised, a combination of ship and pipeline transport was deemed advantageous. Kjärstad et al.

[82] however suggests that due to the modest size and geographical coastal dislocation of Norwegian emitters, shipping will be viable to integrate additional cluster combinations around the region as well. Interestingly, poor injectivity in reservoirs in the Baltic Sea can make transportation of emissions captured from Finnish sources more economically viable than injection into unsuitable storage sites, despite additional distances of 800 – 1,300 km being required to reach the aquifers in the Skagerrak region of the North Sea. As a general consideration, CO_2 pipelines an connect the major sources or collection hubs to the storage site, while discharges from minor sources are more suitable for transportation by ship to a hub. Recently, a demonstration project has been developed and pursued by the Norwegian government with the intention of making themselves one of the early movers in CCUS. The 'Northern Lights' project [83] – currently undergoing feasibility scrutiny, is forecasted to capture 800,000 tons of CO_2 per year from three Norwegian emitters situated on the east coast – including a cement plant and an ammonia plant – and ship them to a collection hub in the west coast of the country prior to permanent storage in the North Sea. Participating entities include Gassco, Total, Equinor, Larvik Shipping AS and Knutsen OA. The shipping options has been selected in order to facilitate ramp-up to higher transport amounts from multiple sources and hence allow expansion and involvement of neighbouring countries by importing up to 4 Mt CO_2/year from other European countries. This approach can facilitate the implementation CCUS projects from an early stage.

In the UK, the Acorn CO_2 SAPLING project has synergies with the Norwegian Northern Lights project; and aims to establish a strategic transportation infrastructure capable of delivering over 12 Mt CO_2/year from emitters in the North Sea for permanent storage in the Central North Sea, and provide a model for similar hubs in Europe and elsewhere [84]. As illustrated in Figure 2-7, large shipping vessels can be accommodated within Peterhead Port and import 6 Mt CO_2/year from neighbouring European countries. The Acorn project is currently expected to reach its final investment decision in 2020/21. The recent report by Element Energy et al. [41] highlighted the potential of carrier transport to connect the ports in the UK with other emerging CCUS projects from Norway and The Netherlands, and relevant industrial sites that exhibit modest storage potential, for countries such as France and Germany. Within the UK, shipping can allow transport of emissions from South Wales CCUS clusters to Hamilton storage site as well as decarbonisation from several clusters on

the east coast – Teesside, Humber, Thames and Grangemouth – thus collecting up to 5 Mt CO_2/year to supply the St. Fergus offshore pipeline and storage at Captain Aquifer in the North Sea [41]. A further study on the deployment of CCS at dispersed industrial sites in the UK [30], could serve as the first step to the establishment of a European transportation network.

The Far East will also likely exploit shipping as part of its decarbonisation efforts. In Japan and South Korea, where CO_2 emitters are concentrated at coastal locations and an offshore pipeline network is not in place due to minimal activities of oil and gas industries and the high probability of earthquakes, implementation of a pipeline network would be impractical according to Ozaki and Ohsumi and Nam et al. [59,60].

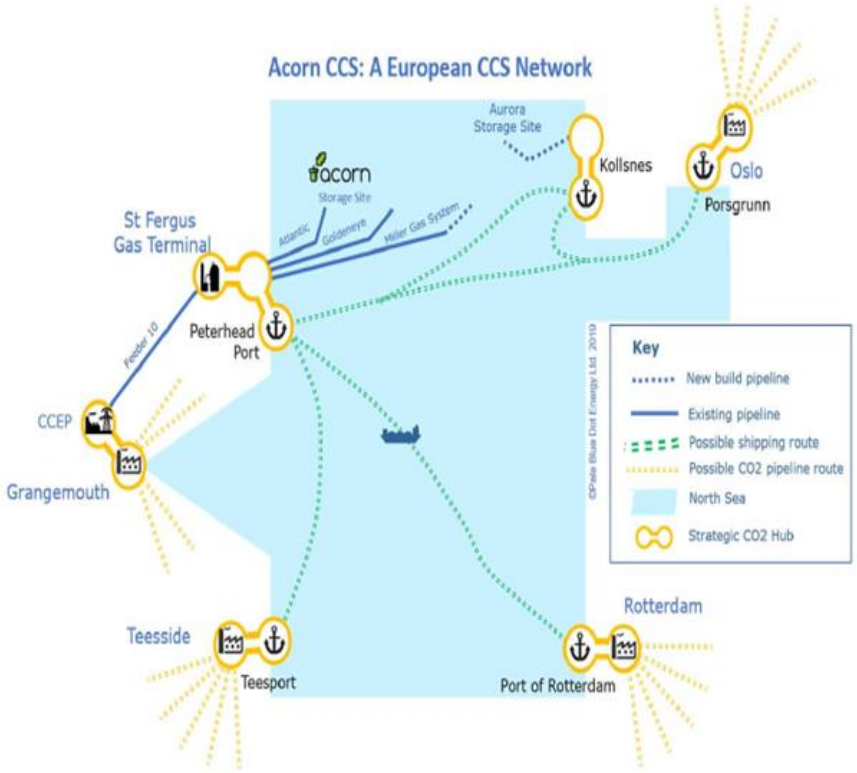

Figure 2-7: Representation of the CO_2 SAPLING project of common interest (PCI) ambition and transnational connectivity [84]

Moreover, the presence of offshore storage capacity located in proximity of Japan's coast (Figure 2-6) suggests that CO_2 shipping is a suitable solution to mitigate the sink-source matching conditions and facilitate implementation of CCUS in East Asia. Specifically, the concept of short-range shuttle ships transporting relatively low amounts of CO_2 at high-pressures is identified by Ozaki et al. [40] as the best approach for Japan due to the limited capacity of individual storage sites. Conversely, Jung et

al. [55] suggests that a CO_2 transportation approach based on pipelines will be more economical than a ship-based approach for CCUS in Korea when amounts of 1 – 6 Mt CO_2/year are considered. These authors however emphasised that future efforts are needed to shape the CCUS vision and provide costing data on both demonstration and commercial stages, with carrier transport expected to become considerably more economically competitive in future.

Chiyoda Corporation [58] and Kokubun et al. [85] investigated the applicability of gas carriers to transport liquid CO_2 on coastal locations of Japan and found that discharging a few million tons of carbon dioxide per year over 200 km and 400-800 km is feasible and necessities the implementation of three 3,000 m^3 ships. Direct injection from ship to offshore storage site was explored in order to eliminate offshore storage platforms, and particularly in relation for the high propensity for earthquakes and tsunamis; however, further work is required to make this option techno-economically feasible.

In summary, in a realistic scenario where no prior infrastructure is in place, the preferred transport solutions between shipping and pipeline will be subject to considerations of transport distances, and the quantities and location of emitters. Geographical and environmental factors are key and can significantly influence the selection and design of transportation networks. Lower discharge amounts and early CCUS implementations favour shipping solutions due to low capital investment, with a transition to offshore pipelines indicated when demonstration projects develop and must handle significant capture amounts; there is an exception to such scenarios where emitters are dislocated and a pipeline installation is, therefore, impractical, whereas carrier transport can provide the required flexibility. Unfortunately, the literature is not in agreement in assessing the role of shipping in future CCUS projects; some work suggests it is only a temporary solution [80], while more recently, several studies suggest that it will have a crucial part in long-term CCUS infrastructure too [41,62]. The development of complex transportation systems that can interconnect a substantial number of emitters in any given region should involve multiple stakeholders and industries cooperating in the region [12,13]. As such cross-border transport of carbon dioxide emissions can successfully avail itself of the flexible shipping option and potentially create a market for countries whose storage capacity are significantly higher than their expected emissions. Currently, some crucial impediments to the

implementation of CO_2 shipping exist. The first one is the London Protocol - a regulating agreement which forbids cross-border transport of CO_2 as part of its scope to prevent the export of “waste to other countries for dumping” within Convention on the Prevention of Marine Pollution by Dumping of Wastes [41]. Another significant limitation is represented by the EU ETS Directive, which precluded CO_2 shipping from being part of the greenhouse gas emission trading scheme thus preventing it from availing itself of financial incentives for CCUS [63]. While the former is currently under amendment through a resolution in October 2019, that effectively enables rectifying Contracting Parties to temporarily adopt cross-country transport within CCUS applications until enough ratifications for this permanent amendment of the Protocol become effective, the latter remains a major barrier. The IEAGHG [63] recommends active participation of parties in addressing such regulatory limitations, including a revision of the ETS Directive to extend to CO_2 shipping and acceleration of the amendment of the London Protocol by promoting an increasing number of Contracting Parties to sign in the near future.

2.6 Properties relevant to carbon dioxide shipping

A detailed understanding of thermo-physical properties of CO_2 is essential to enable efficient, safe and cost-effective operations in the transport chain, including CO_2 shipping. Table 2-7 summarises physical and thermodynamic properties relevant to CO_2 shipping systems.

2.6.1 Density

Density is a major factor influencing utilisation of available cargo capacity and, therefore, transportation schedule and shipping chain costs; it also affects the voyage and vessel stability during sea transport [95]. From an operational point of view, a high-density state, i.e., near triple-point conditions, is desirable to maximise the utilisation of cargo capacity. Therefore, a thorough understanding of the density of carbon dioxide related to shipping conditions is essential. The Energy Institute [73] and Al-Siyabi [86] note that change in pressure (0.5-5 MPa) has a moderate effect on density when sub-zero temperatures of 228-243 K are considered (Figure 2-8). The presence of soluble impurities, however, has a major impact on density; non-condensable contaminants reduce the density of the carbon dioxide mixture [87], thus decreasing the storage capacity and increasing the injection pressure required. The standard molar volume of most impurities is higher than that of CO_2 resulting in impurities

occupying a higher volume even though their percentage concentrations are low. Seo et al. [14] reported the density of liquefied CO_2 is inversely proportional to the storage pressure, ranging from 1159 kg/m^3 at 0.6 MPa and 221 K to as low as 649 kg/m^3 at 6.5 MPa and 298 K.

Table 2-7: Physical and thermodynamic properties and their relevance to CO_2 shipping [86 – 94]

Property	Relevance	Remarks	Impurities	Sources
Density	Vessel dimensioning, compressor and pump design, carrier stability	Highest near the triple point	N_2, Ar, H_2S	[86–88]
Solubility of water	Risk of corrosion and hydrate formation	Limited experimental data covering shipping conditions	CH_4, N_2, NO_2, SO_2, O_2	[89–91]
Viscosity	Estimation of pressure drop in the system Design of process equipment	Liquid viscosity data is limited to CO_2-H_2O systems	H_2O	[88]
Phase Equilibria	Water solubility Phase boundaries Liquid loading/unloading Temperature-pressure characteristics	Minimal presence of impurities can alter phase equilibria significantly	H_2, SO_2, N_2	[92–94]

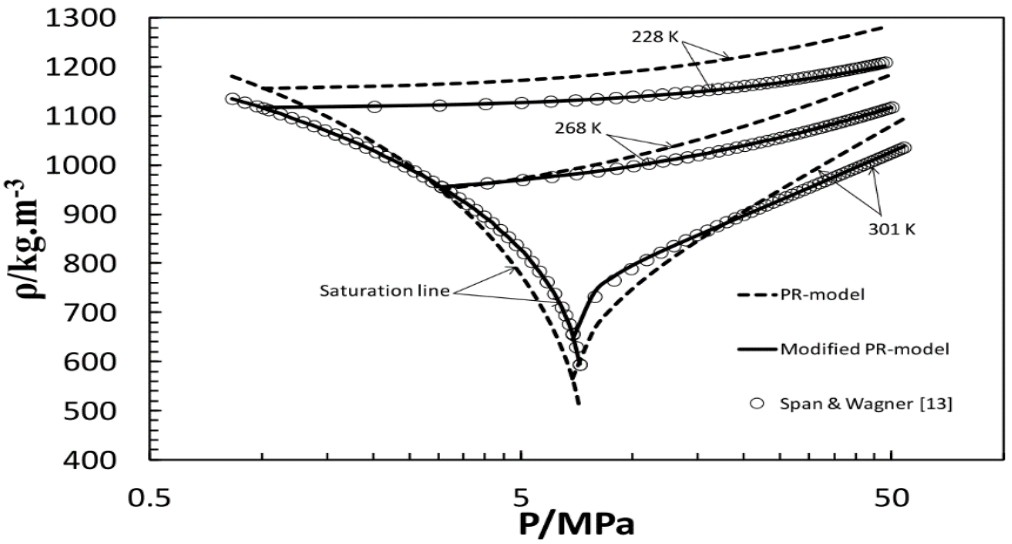

Figure 2-8: Liquid and saturation liquid densities of carbon dioxide [86]

The authors [14] investigated the cargo tank volume required to discharge the same amount of CO_2 to be 78% higher at the low-density state of 6.5 MPa compared to the high-density condition of 0.6 MPa. This will result in a significantly higher number of storage and cargo tanks required, which will in turn increase the required capital investment of any given project. Additionally, and beyond simple density considerations on storage capacity, the maximum size of a single storage vessel decreases with increase of pressure due to limitations in wall thickness; this consideration poses a further cost penalty the storage capacity for high-pressure, low-density states.

Studies and experimental work on the supercritical phase, and evaluations for the liquid phase near the triple point are relatively scarce [87]. Moreover, only a few studies focus on the densities of binary mixtures [88] such as the CO_2 – H_2S system [96–98]. Some work focuses on the presence of SO_2 and O_2 but only for a limited concentration range [88]. There is also a dearth of experimental findings on CO_2-H_2O mixtures at temperatures below 273 K and for binary mixtures of other impurities like as CO, NO, NO_2 N_2O_4 and NH_3 [93]. When considering real composition scenarios encountered in CCUS, Engel and Kather [95] found that liquid densities of pure, post-combustion, pre-combustion and oxy-fuel composition scenarios are similar at conditions typical of CO_2 shipping (218-225 K and bubble-point pressure).

2.6.2 Solubility of water

Free water is an unwanted impurity capable of producing operational and technical challenges such as corrosion and hydrate formation. Therefore, numerous models to determine the solubility of water in carbon dioxide have been made and several validations of those models have been reviewed by Austegard et al. [89]. Empirical results are generally limited to the gas phase or conditions related to pipeline transport [99] with limited data available in low-temperature, liquid phase; unfortunately, the available empirical data does not necessarily focus on CCUS projects [89,100]. As highlighted in Figure 2-9, the solubility tends to increase with pressure and, more strongly with higher temperatures [89,99]. The solubility of pure H_2O in low-temperature, liquid carbon dioxide decreases from 1000 ppm at 283 K to 180 ppm at 233 K. Liquid CO_2 exhibits higher water-carrying capacity than gas-phase CO_2 and, hence, water solubility in CO_2 increases significantly during the transition from gaseous to liquid state [101].

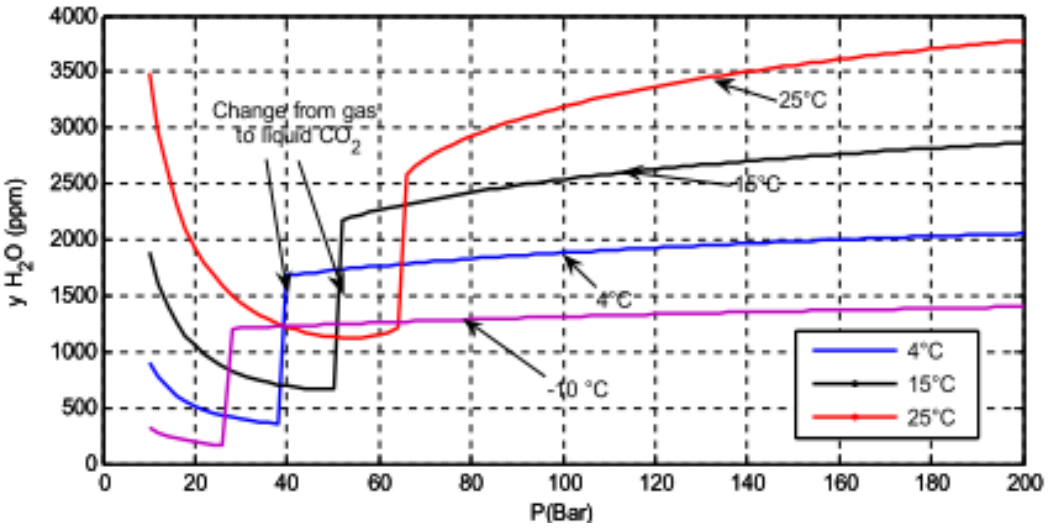

Figure 2-9: Solubility of water in pure carbon dioxide [107]

In streams which also contain impurities such as CH_4, N_2 or O_2, the solubility of water in CO_2 is further reduced [89,102,103]. Minimal amounts of NO_2 and SO_2 (500 ppm) are found to reduce water solubility significantly more, in comparison to the other impurities mentioned above. By contrast, H_2S at concentrations as low as 200 ppm can result in increased water solubility [99].

Finally, in order to investigate the interaction between impurities in realistic capture scenarios, a study by Pereira et al. [104] covering a composition of 89.83% CO_2, 5.05% N_2, 3.07% O_2 and 2.05% Ar, (typical of oxy-fuel capture scenarios) found that at 15 MPa the presence of these impurities results in the solubility of water being reduced by 20% in comparison to a pure CO_2 stream at the same conditions. However, it should be noted that the published data relating to the absolute effects of impurities on realistic capture compositions remains very limited, especially with regards to liquid, cryogenic scenarios [91].

In summary, more empirical results and better thermodynamic models are required to cover cryogenic shipping conditions typical of shipping transport for realistic complex composition scenarios as opposed to simple binary and tertiary mixtures. Results available in the gaseous and supercritical phase can provide an indication of the effect of certain impurities on solubility of water, although they are not directly relevant to shipping and are therefore unreliable for planning real operations.

2.6.3 Phase equilibria

Extensive understanding of pressure-temperature-composition mechanisms is essential to develop appropriate conditioning, transport and storage procedures as CO_2 will need to be processed in liquid forms at all times throughout the chain. Overall, there is a lack of vapour-liquid equilibrium (VLE) data relevant to shipping conditions for binary systems such as CO_2–COS, CO_2–NO, or CO_2–amines, CO_2–SO_2 and, even more remarkably for tertiary systems, as highlighted by Munkejord et al. [88] in Table 2-8.

Table 2-8: VLE data for CCUS-relevant systems at shipping conditions [88]

System	# sources	#points	T(K) range	P(MPa) range	Impurity Concentration (mol%)
CO_2 – N_2	34	>700	208-303	0.6-21.4	0.15-0.99
CO_2 – O_2	8	>292	218-298	0.9-14.7	0.15-0.99
CO_2 – Ar	4	~200	233-299	1.5-14	0.25-0.99
CO_2 – H_2S	8	>270	248-365	1-8.9	0.01-0.97
CO_2 – CO	3	106	223-293	0.8-14.2	0.2-0.99
CO_2 – H_2	8	>400	218-303	0.9-172	0.07-0.99
CO_2 – N_2 - O_2	3	80	218-273	5.1-13	0-0.93
CO_2 – CO - H_2	1	36	233-283	2-20	0.17-0.98
CO_2 – CH_4- N_2	2	>100	220-293	6-10	0.27-0.99
CO_2 - CH_4 - H_2S	1	16	222-239	2.1-4.8	0.024-0.78
CO_2 - CH_4 - H_2O	5	>132	243-423	0.1-100	0.001-0.83

Upon liquefaction, the supplied CO_2 will be stored and transported as a liquid. The presence of relatively small amounts of impurities can significantly alter pressure-temperature phase equilibria and two-phase regions at conditions relevant to carbon dioxide shipping as showed in Figure 2-10. Even a minimal presence of H_2 and N_2 (<0.5 mol%) can increase vapour pressure by 30% thus making carrier transport infeasible due to the elevated bubble-point pressures at cryogenic temperatures as summarised in Table 2-9; such impurities, and particularly N_2, also widen the two-phase envelope in the stream, thus increasing the risk of operational issues throughout the chain.

Table 2-9: Effect of impurities on equilibrium pressure of carbon dioxide at 223 K [39]

Mixture	Vapour pressure	Mixture	Vapour pressure
100% CO_2	0.67 MPa	CO_2 mixture – 0.05 mol% O_2	0.69 MPa
CO_2 mixture – 0.05 mol% N_2	0.7 MPa	CO_2 mixture – 0.05 mol% H_2	1.03 MPa
CO_2 mixture – 0.1 mol% N_2	0.73 MPa	CO_2 mixture – 0.05 mol% CO	0.7 MPa
CO_2 mixture – 0.5 mol% N_2	0.97 MPa	CO_2 mixture – 0.05 mol% Ar	0.68 MPa

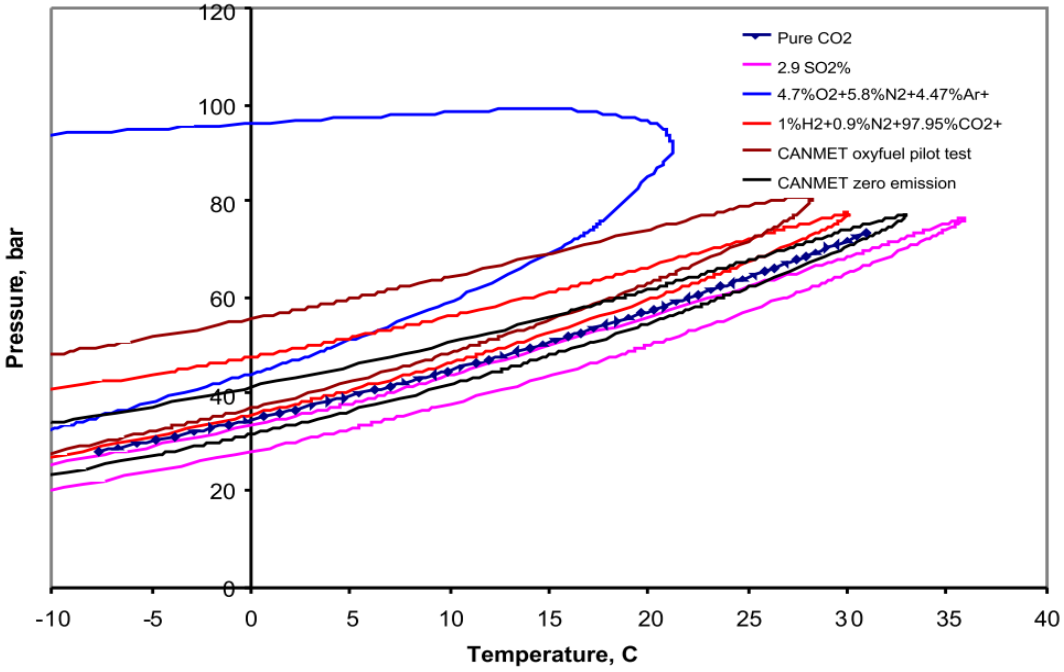

Figure 2-10: Calculated phase boundaries for mixtures of carbon dioxide [87]

In contrast, the presence of SO_2 is found to reduce the bubble pressure, although other process safety considerations exist in relation to the presence of SO_2 in the mixture. Chapoy et al. [90] developed commercial software predictions for 98 mol% CO_2 and 2 mol% H_2 mixtures at 253 K and 263 K, which showed bubble-point pressures of 6.12 MPa and 6.24 MPa, respectively. These values are moderately higher than pure CO_2 scenarios. When considering real CCUS capture compositions, Wetenhall et al. [91] (Table 2-10) and Engel and Kather [95] assessed bubble-point curves and phase envelopes for the worst-case impurity scenarios; and despite some discrepancies between the two studies, their work was in line with the trend for binary and tertiary systems, it appears that marine transport of such streams would not be feasible under most capture options due to the high liquefaction pressures exhibited even at cryogenic temperatures. Purification of such streams thus becomes necessary

to implement carrier transport. Conversely, compression power does not appear to be highly affected by impurities.

Table 2-10: Summary of electrical consumption of four-stage compressions from 0.18 MPa to 11 MPa for several capture scenarios [91]

	vol% content								Power (MW)
	CO_2	O_2	N_2	Ar	H_2	CO	H_2S	CH_4	
Pure	100								48
Adsorption 1	90	1	9						51.25
Adsorption 2	95		5						49.67
Oxyfuel 1	90	6	3	1					50.78
Oxyfuel 2	96.5	.5	2.5	0.5					49.07
Pre-combustion	98				2				49.34
CO_2 membrane 1	93		7						50.33
CO_2 membrane 2	97	3							48.81
Calcium looping	95	1	2	2					49.33
H_2 membrane	96		1		1	0.5	1.5		49.33
Methane-rich	98							2	48.82
Blast furnace	96		0.5			3.5			49.33

2.6.4 Stream composition and presence of impurities

Despite the lack of significant technical limitations to achieving high-purity CO_2 streams captured from industrial plants, the composition of discharge streams is mainly dictated by process safety and techno-economic considerations throughout the CCUS chain. A thorough understanding of the impact of contaminants is of critical importance in the shipping chain for several reasons. From a process safety prospective, minimal amounts of H_2S or SO_2 greatly increases the risk associated with the transport of the stream due to their toxicity. Their presence therefore implies rigorous scrutiny of regulations during real operations, particularly in scenarios involving loss of containment and leaks [105]. Understanding the impact of impurities on materials is also crucial to preserve the integrity of vessels and components; for instance the performance and degradation of metallic and polymeric and elastomer materials alike [106] at conditions typical of shipping projects is particularly important, with H_2S generating a risk of embrittlement and SOx, NOx and O_2 enhancing corrosion hazards [105].

Table 2-11: Impurity range scenarios. Adapted from [88]

Impurity	Content range (mol%)
CO_2	75-99
N_2	0.02-10
O_2	0.04-5
Ar	0.005-3.5
SO_2	$<10^{-3}$-1.5
H_2S/COS	0.01-1.5
NO_X	<0.002-0.3
CO	$<10^{-3}$-0.3
H_2	0.06-4
CH_4	0.7-4
H_2O	0.005-6.5
Amines	$<10^{-3}$-0.01
NH_3	$<10^{-3}$-3

Impurities also affect the vapour-liquid and phase equilibria of CO_2, with non-condensable contaminates such as N_2 or O_2 in particular increasing the saturation pressure of liquid CO_2 thus impacting on the selection of potential conditions of shipping projects and liquefaction processes. Additionally, the density for different composition scenarios is greatly affected by the presence of impurities, and this aspect needs to be considered to ensure the stability of the sea vessel during voyage and to evaluate the cargo capacity of the ship for economic reasons [91]. Lack of operational data implies rather conservative limitations in relation to the presence of impurities [39,51,94]. Potential reactivity between impurities and construction material results in an enhanced risk of corrosion and formations of acids in the presence of free water [105]. A number of projects, including ENCAP, DYNAMIS, IMPACT, CO2QUEST and CO2Mix have helped establish appropriate CO_2 quality recommendations in order to guarantee the durability and integrity of the transport infrastructure [93,107–109]. Their focus was largely focused on the effect of contaminants on transportation by pipelines thus these studies are somewhat lacking in data relevant to CO_2 shipping systems. However, capture compositions and impurity content ranges have been investigated in the literature and details are provided in Table 2-11.

The tolerance to the presence of impurities can vary in relation to the expected transport and storage conditions, as well as destination of the stream (EOR or storage). Findings from the DYNAMIS project [107] are summarised in Table 2-12 and

compared to investigations from the United States National Energy Technology Laboratory (NETL) [110]; however, NETL's specifications are more stringent. Conservative allowances in both projects are attributed to the lack of experimental results assessing the effects of oxygen underground [107]. Moreover, there is a significant shortage of empirical findings covering the effect of impurities such as O_2, Ar, SO_2, CO, H_2 despite their relevance to CCUS [94]. High concentrations of H_2S and SO_x can react to form elemental sulphur, which may result in blockages at temperatures above 673 K; this consideration is particularly relevant to the liquefaction process, where compressor discharge can approach such temperatures [39]. Finally, there is a dearth of data directly applicable to shipping conditions, as thermo-physical properties of carbon dioxide under liquid, cryogenic conditions are expected to differ significantly from those typical of pipelines under gaseous or supercritical state.

Table 2-12: Quality recommendations from the DYNAMIS project and NETL allowance [107,110]

Component	Concentration	Limitation
H_2O	500 ppm	Lower than solubility range of H_2O in CO_2
H_2S	100-200 ppm	Health and Safety evaluation
CO	1200-2000 ppm	Health and Safety evaluation
O_2	Aquifer < 4 vol% E.O.R. 100-1,000 ppm	Due to absence of experimental findings on effect of oxygen underground
CH_4	Aquifer < 4 vol% E.O.R. < 2 vol%	Based on previous project
N_2	< 4 vol%	Based on previous project
Ar	< 4 vol%	Based on previous project
H_2	< 4 vol%	Limits the energy requirement in the chain
SOx	100 ppm	Health and Safety evaluation
NOx	100-200 ppm	Health and Safety evaluation
CO_2	>95.5%	

2.7 Selection of transport conditions and economic aspects

2.7.1 Choice of shipping conditions

The literature generally indicates 0.65 MPa and 221 K is the preferred condition for CO_2 shipping for CCUS, though this choice is often simply attributed to the high-density state and lower capital cost of the vessels near the triple point rather than a comprehensive techno-economic analysis of the transport chain [8,39,54,56,57]. It is expected that operations near the triple point will require additional measures to mitigate the risk of freezing during operations, thus resulting in more stringent safety protocols and higher costs [64]. Table 2-13 summarises shipping conditions highlighted in several projects. As can be seen, conditions near the triple point, often indicated in the literature, tend to be based on generic assumptions and corporate preference. Some work actively investigates case-specific scenarios [14,38,59] and suggests that optimal shipping conditions can move away from the triple point when complex transportation infrastructure is considered.

Table 2-13: Summary of conditions indicated for CO_2 shipping projects.

Source	Conditions	Remarks
Skagestad et al. [56,81]	0.7-0.8 MPa, 223 K	Deemed optimum for CCUS-related quantities
Hagerland et al. [9]	Close to 0.52 MPa, 217 K	To reduce investment costs of tanks and ship
Engel and Kather [111]	0.7-0.8 MPa, 223 K	Low pressure is desirable from an economic point of view
Seo et al. [14]	1.5 MPa, 246 K	Based on the full shipping chain's energetic and economic analysis for pressures 0.6-6.5 MPa
Nam et al. [59]	1 MPa, 234 K	Based on system configuration and economic analysis of a realistic CO_2 transport chain in Korea
Mitsubishi Heavy Industries [52]	0.7 MPa, 223 K	Deemed advantageous for large scale projects due to enhanced density and relatively lower pressure.
Wong [42]	0.7-0.8 MPa, 223 K	Lower pressure results in vessels with lower cost
Worley Parsons [29]	0.75 MPa, 223 K	Density is enhanced under liquid conditions

Source	Conditions	Remarks
Omata [58], Ozaki et al. [40]	2.65-2.8 MPa, 263 K	Adaptable to small ship-shuttle concept; reduced liquefaction cost; no heat treating on tank is required this temperature
Yoo et al. [53]	0.7-0.8 MPa, 223 K	Enhanced cargo capacity for large vessels
Zahid et al. [72]	0.7 MPa, 223 K	Higher pressures - 0.8 MPa and 0.9 MPa – are considered; their liquefaction capital investment is lower, but storage and ship investment are higher. Overall capital expenditure is higher in both cases
Scottish Development International and Scottish Enterprise [112]	0.7-0.9 MPa, 218 K	Similar cargo condition to semi-refrigerated LPG carriers currently in operation
Aspelund et al. [57,70]	0.55 MPa, 218 K	Enhanced density at such conditions
Ministry of Petroleum and Energy et al. [38]	i. 0.7-0.8 MPa, 223 K ii. 1.5 MPa, 248 K iii. 4.5 MPa, 283 K	i. High density, LPG experience ii. Technically ready to be implemented iii. Lowest energy demand
Kang et al. [113]	0.7 MPa, 223 K	Lower costs associated with low-temperature carrier
Jakobsen et al [114]	0.65 MPa, 223 K	Relevant to large-scale projects
Engel and Kather [95]	0.68 MPa, 223 K	Pipeline-shipping system; lower pressure results in lower capital expenditure for the vessels
Vermeulen [39]	0.7 MPa, 223 K	Based on economic analysis
Koers and Looji [67]	0.7 MPa, 223 K	No remarks made
ZEP [34]	0.7 MPa, 223 K	Based on enhanced density and lower pressures for large projects
Roussanaly et al. [31,68]	0.65 MPa, 223 K	Appropriate for large CCUS projects
Knoope et al. [32]	0.7 MPa, 223 K	Conditions near the triple point
Yoo et al. [115]	0.7 MPa, 223 K	Enhanced density at these conditions
Neele et al. [48]	0.7-0.9 MPa, 218 K	Appropriate for large volumes
Svensson et al. [49]	0.7 MPa, 223 K	Enhanced density; low pressure
Brownsort et al. [54]	0.65 MPa, 221 K	Shipping is more cost-effective at lower pressures
Element Energy et al. [41]	I. 0.7 MPa, 223 K	Different conditions are indicated but transport near the triple point is deemed

Source	Conditions	Remarks
	II. 1.5 MPa, 248 K III. 4.5 MPa, 283 K	most appropriate as per wider literature conclusions

As summarised in Table 2-14, the Norwegian Ministry of Petroleum assesses vessel transportation of CO_2 at three different conditions; although all the solutions are reported to be technologically feasible, however different considerations must be carefully evaluated. Low-pressure conditions, although associated with higher propensity for dry-ice formation due to the proximity to the triple point, enhances cargo efficiency due to its high-density state. Conversely, a high-pressure state implies lower energy-intensive processes but results in more challenging and costly tank design and unfavourable cargo efficiency. Finally, medium-pressure conditions around 1.5 – 2 MPa in pressure represent a mature concept that is already extensively applied for transporting CO2 for the food and brewery industries but poses several techno-economic disadvantages such as complicated tank design which may not be economically viable for large CCUS projects.

Table 2-14: General assessment of alternative transport conditions for carbon dioxide shipping [38]

Condition	Low-pressure (0.7-0.8 MPa, 223 K)	Medium pressure (1.5 MPa, 248 K)	High-pressure (4.5 MPa, 283 K)
Advantages	- High density. - Established know-how on LPG experience. - Scalable tank size and ships	Commercially mature concept in the food and brewery industries	- Low conditioning costs - Most appropriate condition for direct-injection from ship.
Challenges	- Proximity to solid phase - High conditioning costs - Complex insulation	- Relatively high volume of steel in the tank - Technically challenging tank structure	- Complex design of tanks - Low TRL - Low density - Risk for cold boiling liquid expanding vapour explosion (BLEVE)

Some of the literature that has highlighted the selection of appropriate conditions in the shipping chain as part of the wider transportation infrastructure is case-sensitive and related to numerous project variables; according to this approach, selection of appropriate conditions should not be based simply on corporate experience and

assumptions [14,59]. As such, Seo et al. [14] explored a different approach and developed a comprehensive comparison of different carbon dioxide shipping conditions. These authors considered seven pressure conditions – 0.6 MPa, 1.5 MPa, 2.5 MPa, 3.5 MPa, 4.5 MPa, 5.5 MPa and 6.5 MPa for conditioning, preparation and shipping components of the chain and found life-cycle costs (LCC) of the overall chain to be the lowest at 1.5 MPa and 245 K, which contrasts with the majority of the literature on CCUS shipping summarised in Table 2-13.

In order to consolidate their findings, sensitivity analyses that took into account discharge amounts, distances, uncertainties of CAPEX estimations and electricity costs were made to evaluate the impact of such variables on LCC of the chain [14]. Despite the fact that a lack of reliable data at such an early stage of shipping implementation can affect the reliability of findings, this study [14] is a useful starting point for decision-makers in the field. Furthermore, a techno-economic analysis of the overall CO_2 shipping chain for CCUS projects in South Korea investigated the discharge of 6 Mt CO_2/year using southeast Asian offshore oil wells as storage locations; here Nam et al. [59] found that the most favourable cargo transport condition in a scenario that integrated shipping with pipeline to be 1 MPa and 234 K. This study represents a rare and valuable investigation of plant location and fleet assignment for specific CCUS clusters and projects and it clearly highlights the fact that development of a viable transportation network for CCUS is case-sensitive and dependent on various factors. As such, selection of optimum shipping conditions must carefully consider long-term decarbonisation strategies. Limited studies are available on case-specific approaches and planning of shipping projects for the future of CCUS [39,41,59,60]. More work is required to explore ad-hoc techno-economic optimisation of wider CCUS clusters and transportation networks both in Europe and Asia, as these findings will strongly affect the conditions at which shipping projects will operate.

Nonetheless, several economic assumptions made in the literature are still associated with a high level of potential inaccuracy due to lack of commercial applications [38], thus strengthening the need for CO_2 shipping demonstration projects worldwide. Beyond mere economic considerations, optimal transportation conditions can also vary in relation to climate and geographical location; the phenomenon of boil-off gas generation within the cargo tank during voyage, due to heat leak from the atmosphere [116,117], is expected to be more significant in the warmer regions of the planet.

Therefore, it is suggested that shipping projects covering such routes should explore the implementation of higher liquefaction pressures and temperatures to reduce the extent of heat ingress from the atmosphere and thus limit the pressurisation of the tank during transport.

2.7.2 Economic and financial aspects of CO_2 shipping

The determination of costs of carrier transport projects is complex and subject to several financial and logistical factors. Economic considerations for transport systems are not known in detail due to lack of implementation of CCUS projects. Economies of scale are anticipated to be key in reducing the costs of carrier-based transport [37], as larger ships are found to be relatively cheaper to construct than smaller ones. Costs related to shipping projects have been extensively assessed in the relevant literature – as summarised in Table 2-15 and graphically represented in Figure 2-11 - covering a range of geographical locations, distances, and disposal amounts [39,45,56–58]. The literature consistently indicates that carbon dioxide shipping will require significantly lower capital expenditure in comparison to pipeline transportation [34,37,39,49].

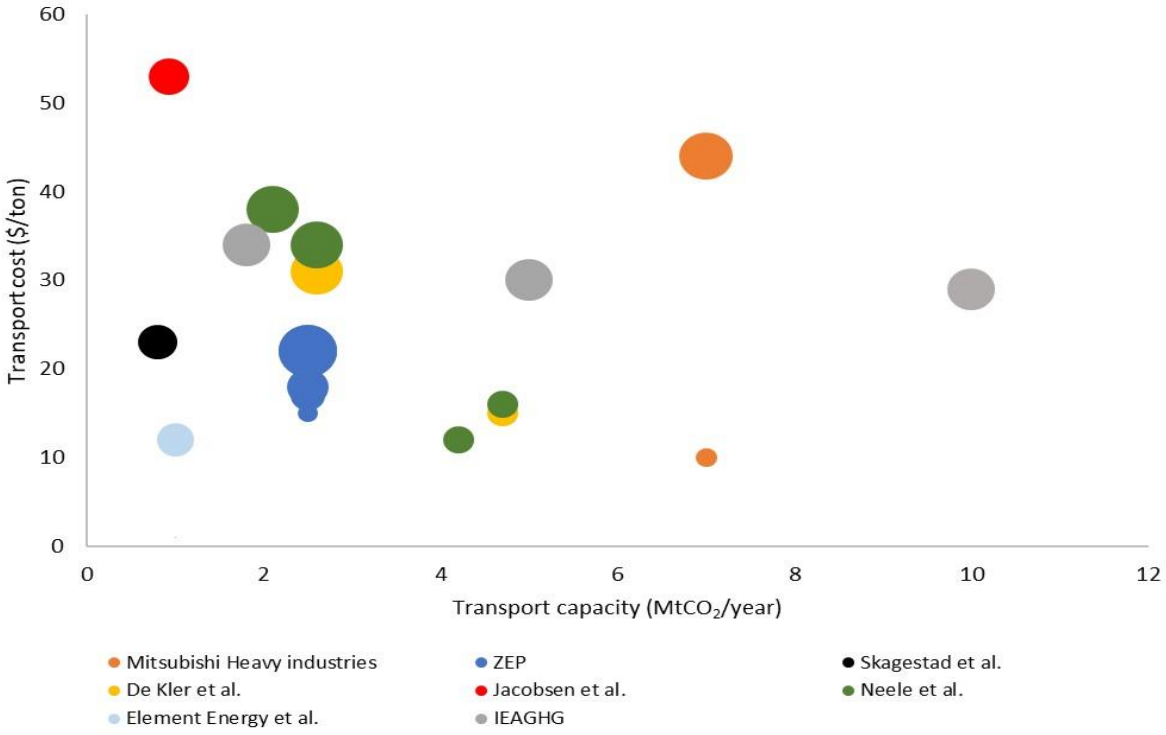

Figure 2-11: Graphical representation of cost comparison in CO_2 shipping projects with respect to transport capacity; bubble areas are the relative representation of the transport distance

Table 2-15: Summary and cost comparison of CO_2 shipping projects

Source	Year	Shipping system	Conditions	Transport capacity	Location	Storage	Transport Cost	Capital Expenditure	Distance
Mitsubishi Heavy industries [52]	2004	50,000 tons ship (5 tanks)	0.7 MPa, 223 K	7 $MtCO_2$/year	Japan	Saline formation or gas field	a. \$10/t CO_2 b. \$44/t CO_2	M\$ 150	a. 200 km b. 1,200 km
Aspelund et al. [57]	2006	20,000 m^3 ship	0.65 MPa, 221 K	2 $MtCO_2$/year	Northern Europe	Depleted oil field	\$20-30/t CO_2	N/A	North Sea distances
ZEP [34]	2010	40,000 m^3 ship	0.7 MPa, 223 K	2.5 $MtCO_2$/year	North Sea	Saline formation	a. \$15/t CO_2 b. \$17/t CO_2 c. \$18/t CO_2 d. \$22/t CO_2	a. M\$ 153 b. M\$ 174 c. M\$ 193 d. M\$ 237	a. 180 km b. 500 km c. 750 km d. 1,500 km
Kokubun et al. [85]	2011	a. 2 x 1,500 m^3 tankers shuttle carrier b. 4 x 1,500 m^3 tankers shuttle carrier	2.65 MPa, 263 K	1 $MtCO_2$/year	Japan	Sub-seabed geological formation	a. \$106/t CO_2 b. \$167/t CO_2	a. M\$ 91 b. M\$ 142	a. 200 km b. 400 – 800 km
Skagestad et al. [56]	2014	13,000 m^3 ship	0.7 MPa, 223 K	800 $ktCO_2$/year	Norway	Johansen formation – saline aquifer	\$23/t CO_2	M\$ 81	670 km
De Kler et al. [61]	2016	a. 2 x 50,000 tons ships b. 3 x 30,000 tons ships	0.7 – 0.9 MPa, 218 K	a. 4.7 $MtCO_2$/year b. 2.6 $MtCO_2$/year	North West Europe	Saline formation	a. \$15/t CO_2 b. \$31/t CO_2	a. M\$ 358 b. M\$ 394	a. 400 km b. 1,200 km

Jacobsen et al. [114]	2017	a. 25,000 tons ship b. 35,000 tons ship c. 45,000 tons ship	0.65 MPa, 223 K	925 $ktCO_2$/year	Norway	Depleted gas field or saline formation	$53/t CO_2	M$ 44 (ship) M$ 52 (ship) M$ 60 (ship)	300 – 730 km
Neele et al. [48]	2017	a. 5 x 10,000 tons ships b. 4 x 30,000 tons ships c. 6 x 10,000 tons ships d. 4 x 30,000 tons ships	0.7 MPa, 218 K	a. 4.2 $MtCO_2$/year b. 2.1 $MtCO_2$/year c. 4.7 $MtCO_2$/year d. 2.6 $MtCO_2$/year	North Sea	Depleted gas field or saline formation	a. $12/t CO_2 b. $38/t CO_2 c. $16/t CO_2 d. $34/t CO_2	a. M$ 348 b. M$ 461 c. M$ 393 d. M$ 465	a. 400 km b. 1,200 km c. 400 km d. 1,200 km
Element Energy et al.[41]	2018	10,000 t ship	0.65 MPa, 223 K	1 $MtCO_2$/year	North Sea	Depleted gas field or saline formation	$12/t CO_2	N/A	600 km
IEAGHG [63]	2020	3 x 10,000 tons ship	0.8 MPa, 223 K	a. 1.8 $MtCO_2$/year b. 5 $MtCO_2$/year c. 10 $MtCO_2$/year	North Sea	Medium depth offshore site	a. 34/ t CO_2 b. 30/ t CO_2 c. 29/ t CO_2	M$ 124 (ships + onshore buffer)	1,000 km

Accordingly, Aspelund et al. [57] and Element Energy et al [41] found that in a scenario where up to 3 Mt CO_2/year is to be transported over 600-1,500 km, ship and liquefaction alone can constitute 73 - 83% of the specific costs of the chain, with operational expenditure contributing to 54% of the total costs. Specific operating and capital costs involved in the shipping chain are therefore found to be strongly dependent on project variables including discharge amount and distance. The Mitsibushi Heavy Industry report [52], Fimbres Weihs et al. [33] and Ozaki et al. [40] suggest that when long shipping distances are considered, costs relating to conditioning, storage and harbour fees are relatively low in comparison to the added economic value of sea transportation over pipelines thus making shipping more viable for long routes. Unlike pipeline transport, shipping costs for CO_2 exhibit a non-linear dependency with transport distances [14,34] and for this reason, Knoope et al. [32] suggested that carrier transport is economically advantageous over pipeline for greater distances and lower amounts of carbon dioxide; while at constant, high-capture throughput, higher transportation distances are required to justify the choice of vessel transport over pipelines.

The choice of appropriate shipping conditions is essential to minimise expenditures and create a cost-effective transportation system; unfortunately, no consensus is available in the literature due to the high sensitivity to project variables such as transport distance, quantity and size of emitters and storage sites. Ozaki et al. [40] found that for Japan's situation, where emitters are scattered and near the coast and storage sites are of medium capacity, the concept of shuttle carriers including a direct injection system is more economically viable than large-scale ships. Optimal conditions are found to be 2.65 MPa and 263 K due to the reduced energy requirement for both onshore liquefaction and offshore heating near the injection site. An additional consideration from these authors is that at temperatures above 263 K no heat treatment procedure after welding is required, thus facilitating the cargo tank design. Conversely, transportation routes in Europe would imply large carriers operated in conjunction with collection hubs that interconnect major clusters to port terminals at lower pressures, as indicated by several preliminary studies [39,48]. A comparative study based in South Korea indicated that optimum global shipping pressure should be 1.5 MPa [14] for distances of 300 – 700 km, with LCC increasing with conditioning pressure. This gap widens when the considered amounts increase from 1 to 3 Mt CO_2/year. This analysis covers all parts of the chain, starting from stream conditioning to the pumping system.

Cumulative costs are related to the shipping schedule and can be reduced by selecting the appropriate ship size for each distance and disposal amount. Low disposal amounts favour smaller ships, while higher amounts imply the selection of larger ships at constant transport distance. Moreover, smaller ships are indicated for shorter distances and larger ships are required for longer distances when constant amounts are considered [115]; overall costs decrease significantly when the ship size increases, though this trend is expected to reach a limit [52]. By contrast, the IEAGHG [63] report emphasises that little economic advantages or penalties arise from the implementation of ships with capacities larger than 10,000 tons , when transportation routes in Europe and distances of 1,000 km are considered, highlighting the fact that optimal ship size is strongly related to flowrates. In line with this analysis, Roussanaly et al. [68] found that choice of different ship size lead to similar costs for transportation of 13.1 Mt CO_2/year over 480 km from Le Havre to Rotterdam were considered. Higher utilisation rate for medium size ships however makes them marginally more economically advantageous than small vessels. Beyond mere economic considerations, it is found that larger ships will generally spend a higher proportion of the project time offloading rather than transporting the captured carbon dioxide, particularly due to the fact that maximum unloading rates in case of direct injection from the vessel are limited by the capacity of the reservoir [63]. This consideration will also affect the shipping schedule and discharge capacity. Moreover, larger sea vessels are more likely to encounter constraints at the receiving port,and can potentially require modifications of existing infrastructure. These factors are therefore expected to have a significant impact on selection of ship size in CCUS projects, meaning that bigger ships are not necessarily expected to dominate in all circumstances, despite the economic benefits.

Given the current uncertainties over CCUS, minimisation of financial demand and investment risks is essential. Overall, implementation strategy can significantly reduce capital expenditure and uncertainties related to the future CO_2 projects. As CCUS-related infrastructure would be deployed gradually, CO_2 shipping can prove to be particularly advantageous in the early stage, prior to the deployment of pipeline networks [68]. For small-scale, short-duration (10 years) projects, the value of potential sunk costs is found to be significantly lower for shipping in comparison to pipelines. This is because the lack of high up-front CAPEX required to implement carrier-based CO_2 transport, coupled with short lead time represent an advantage over offshore pipeline, particularly due to the fact

that feasibility of construction of the latter relies on constant volumes throughput during the entire project life [39,119,120]. Although large scale carbon dioxide shipping is deemed technologically feasible, demonstrational projects are still required to generate confidence in the economic investment, demonstrating validity of cost estimation made in the literature and the effect of the economy of scale on reduction of project costs. [30] Under this framework, the full-scale CCUS project in Norway aims to generate a pan-European storage infrastructure and provide this economic demonstration. The Norwegian project will start-off by collecting emissions from two sites, progressively ramping to 1.5 $MtCO_2$/year capacity in Phase 1 to up to 5 $MtCO_2$/year in Phase 2. [63]

Potential cost reduction by re-utilisation of existing infrastructure is found to be negligible for carrier transportation in comparison to pipeline [41], due to the fact that the capital expenditure of the ship only representing 14% of total costs; conversely Aspelund et al. [57] found that cost of the ship accounts for 30% of the specific costs when 3 Mt CO_2/year are to be transported over 1,500 km thus, thus adding value to the concept of ship re-utilisation. The IEAGHG [63] emphasizes that the repurposing process of LPG and ethylene ships between different gases – although only feasible for a single conversion - is an attractive option to reduce capital expenditure of the projects thus de-risking investments of early stage CO_2 shipping projects.

The flexibility of the shipping option for collection from several European CCUS clusters such as Norway, the Netherlands and, potentially, France and Germany to serve several storage sites is particularly beneficial in creating a dynamic architectural system and consequently increasing transport capacity in while maintaining relatively low capital investments. As such, there is potential for the UK to import CO_2 emissions from other European countries in the future by availing itself of a flexible and efficient transport and storage infrastructure and, thus, create a new market to contribute to the economic growth of the United Kingdom. As previously noted, there are several CCUS clusters in Norway and the Netherlands, but also in France and Germany that can be connected to British North Sea storage sites via shipping. Nonetheless, there is a lack of a suitable framework of business models in relation to CO_2 shipping for CCUS, due to the fact that existing LPG and LNG financial arrangements are not found to be adaptable to carbon dioxide shipping [30]. Despite this, the IEAGHG proposes that standard conceptual models – namely voyage charter, time charter and bareboat charter – that specify contractual arrangements for the specific cargo to be discharged between given ports and ships -

could be deemed relevant for CO_2 transport. On this basis, the exclusion of ship transportation from the EU framework of emissions trading of the ETS directive – as discussed earlier in this work - effectively makes any CCUS value chain looking to implement sea vessel as transportation option unable to access relevant financial incentives that could otherwise generate an advantageous business model for the commercialisation of this technology, and implementation of CCUS as a whole. This in turn has the repercussion of creating an environment of unpredictability for stake holders willing to make CO_2 shipping part of their value chain, although this burden should not be perceived as absolute and can be reviewed by the ETS Directive under the initiative of EU member states [63].

2.8 Components of the CO_2 shipping chain

In the shipping chain, carbon dioxide is liquefied upon arriving from the capture plant in the form of pressurised or non-pressurised gas [41]. It is then stored in appropriate tanks prior to being loaded onto the ship by means of a cargo handling system; the carrier then completes its journey by reaching the final storage destination or port terminal (Figure 2-12). In the case of shipping to a port, the carbon dioxide is unloaded to intermediate storage tanks before being pumped and heated to conditions suitable for pipeline transmission to its final destination. Transport to offshore storage is also an option for shipping projects, whereby the two unloading alternatives are direct injection from ship or onto a platform with storage. In the case of direct injection, the fluid is pumped and conditioned on board the ship and transmitted to the injection well of an offshore storage site. The second offshore unloading option is to transfer the CO_2 in liquid form to an offshore platform, where it is stored prior to injection to the storage site. Accurate planning of the shipping chain, from liquefaction to offshore unloading, is essential to enhance the commercial feasibility of CO_2 shipping projects [59,60] as inaccurate schedules will inevitably result in project delays. Such delays can thus lead to requirement of more ships to discharge a fixed amount of carbon dioxide, hence inevitably producing higher costs. Throughout this section, technical insights of the shipping chain's operations provided in the literature are summarised and critically reviewed with the aim of elucidating the key challenges and level of consistency of the literature.

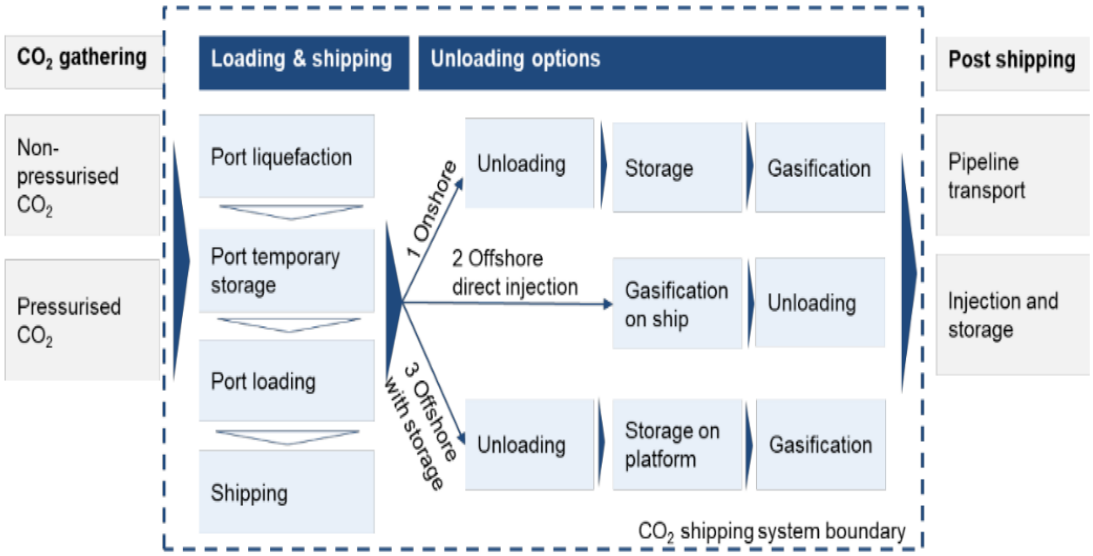

Figure 2-12: Components of the CO_2 shipping chain [41]

2.8.1 Conditioning

2.8.1.1 Dehydration

Dehydrating the carbon dioxide stream is a necessary step to preserve integrity of the system, including the loading of pipelines and vessels in order to reduce the potential for corrosion, hydrate formation and freezing. Unfortunately, there is no uniform consensus in terms of quantifying the acceptable moisture level, albeit that the ultimate objective is the minimisation or elimination of free water. As previously noted, the solubility of water varies in relation to the stream conditions and presence of impurities and, therefore, a detailed understanding of phase behaviour specific to CO_2 shipping conditions is essential. The maximum allowable water content in the system is often regarded to be 10-50 ppmv or, otherwise less than 60% of the dew point, in order to avoid operational issues when handling liquid, cryogenic carbon dioxide [39,51,121].

However, the DYNAMIS project [107] conclusions suggest that these specifications are too rigid. Also, technical challenges are still being addressed to achieve full-scale implementations of dehydration plants for such low moisture contents. As shown in Figure 2-13, several dehydration methods are available depending on required stream specifications; but data disclosed by vendors are limited due to commercial sensitivity, hence, technical and economic information available in the literature is also limited and associated with some degree of uncertainty. Some solutions, such as refrigerant drier and compression and cooling, do not achieve themoisture levels required for CO_2

shipping, but they can be implemented as a preliminary step to reduce the duty required from the main dehydration unit, thus leading to less costly dehydration processes.

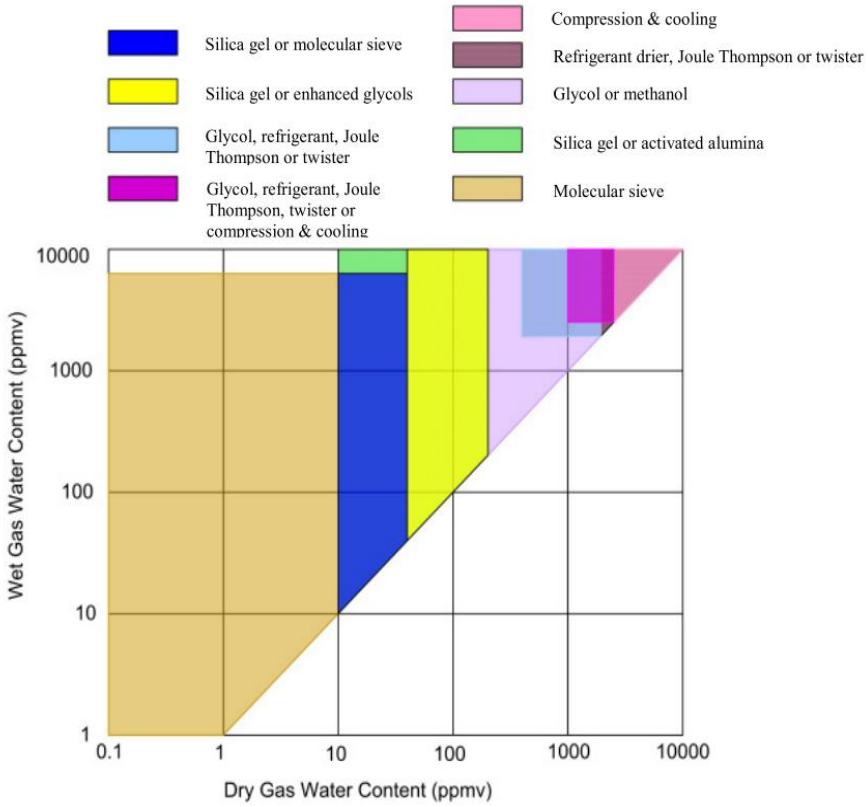

Figure 2-13: Comparison of different dehydration technologies [121]

In some circumstances, the presence of some impurities is unacceptable due to their potential for system damage or impairment of the stringent dehydration requirements associated with their presence; in such cases, their removal in an alternative process becomes a requirement, as summarised in Table 2-16. Impurities such as amines, glycols, SO_x and NO_X can be significant for both the triethylene glycol (TEG) system and molecular sieve dehydration, but their impacts are still not well-understood and further research is required to assess their impact on these processes.

Absorption by TEG followed by desorption is an established gas dehydration method that can achieve 30-150 ppmv moisture levels in CO_2 systems depending on intensity of the process and glycol concentrations [80,121]; however, when very low water content (~1 ppmv) is required, the use of solid adsorbents is the most appropriate choice [122]. A comparison between the two technologies highlighted that capital expenditure and energy consumption of molecular sieve are 20% and

80% higher than TEG respectively [39]. One of the current limitations remains the lack of empirical validations on the effect of impurities on solubility of water at liquid cryogenic conditions [80].

Table 2-16: Effect of contaminants on TEG and molecular sieve systems [121]

Impurity	Effect on TEG system	Max. limit	Effect on molecular sieve	Max. limit
H_2O	Formation of liquid droplets can weaken absorption capacity	N/A	Degradation of the sieve or reaction with the binder; damage to the system	N/A
Inert gases (N_2, Ar, H_2, CH_4)	No impact	N/A	No impact reported	No limit
O_2	Oxidative degradation of TEG	N/A	If hydrocarbon present: coke formation, pore blockage; if sulphur present: blockages	15-50 ppm
H_2S	N/A	3000 ppm	Degradation of the sieve, corrosion caused by the generation of free sulphur	Up to 1000 ppmv none if oxygen is present
NO_X, SO_X	N/A	N/A	Damage to sieve system and life-span	N/A
HCl	Lower pH causes corrosion	200-300 ppm, Chlorides pH 6-9	De-alumination of zeolite framework, causing dust formation	1 ppmv
CO	N/A	N/A	No impact	No limit
COS	N/A	N/A	Corrosion	N/A
Amines	Foaming	N/A	Dust and damage to the system	N/A

Impurity	Effect on TEG system	Max. limit	Effect on molecular sieve	Max. limit
Aldehydes	Change in pH, corrosion, foaming	N/A	Polymerisation and generation of toxic materials	200 ppmv
Methanol	Column flooding	N/A	Hydrogen formation	513K maximum stream temperature
NH_3	N/A	N/A	Damage to sieve system	5-10 ppmv
Glycols	N/A	N/A	Premature damage to the system	N/A
NaCl	Corrosion	N/A	Blockages and damage to materials	N/A

2.8.1.2 Liquefaction

Appropriate conditioning of CO_2 is required to conveniently transport it in liquid form via cargo vessels, hence, several studies have focused on liquefaction of carbon dioxide streams for transportation by ship [51,123–126]. According to Aspelund et al. [57] liquefaction takes 77% of the energetic requirement of the transmission chain, or 10% of the total consumption for the entire CCUS chain according to Lee et al. [127]; here the duties and costs of compressors dominate energy requirements and capital expenditure of the process, respectively. This is 11-14% more energy than comparable purification and pipeline conditioning [128]. As shown in Figure 2-14, liquefaction can be achieved using either open- or closed-cycle refrigeration processes, the choice depending on temperature/availability of cooling water and refrigerants [125,128]. Open-cycles, also known as internal refrigeration systems, involve the compression of the stream to a pressure higher than the intended conditions prior to single or multi-stage expansion to achieve the desired condition; the first authors to explore such liquefaction solutions

applied to carbon dioxide are Aspelund et al. [51], although further extensive optimisation studies were subsequently performed by Lee et al. [127].

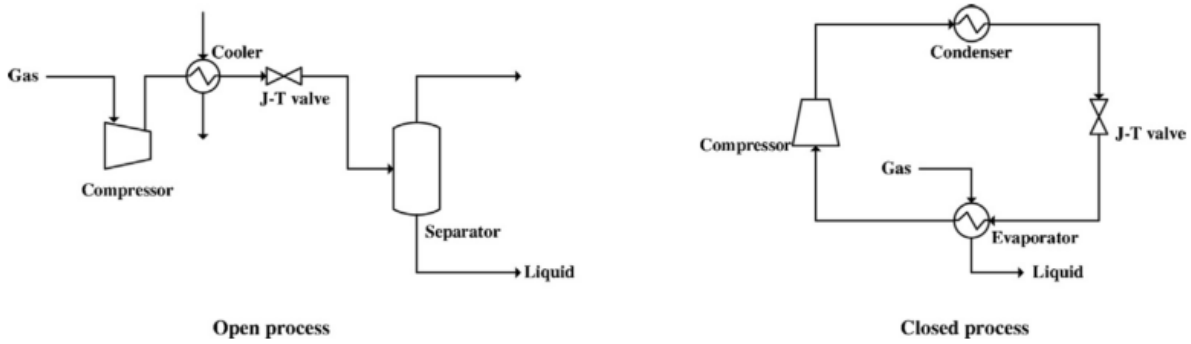

Figure 2-14: Open- and closed-cycle liquefaction systems [123]

Closed cycles, or external refrigeration systems, involve the compression of the stream to the liquefaction pressure and refrigeration using external coolants such as ammonia, propane, R134a, or combinations of these. Seo et al. [14] suggests propane and ethane as refrigerant for closed systems at 0.6 MPa, propane at 1.5 – 3.5 MPa and ammonia when the target liquefaction pressure is 4.5 – 6.5 MPa Generally, there appears to be little effort to compare liquefaction systems and most work focuses on a single process based on local cooling service availability or corporate experience, although some detailed comparative evaluations are available [123]. Some work actively investigate the effect of delivery pressure and presence of impurities on liquefaction costs and the selection of appropriate processes [126,129], though further study is required to integrate findings related to the liquefaction cycles within the wider chain.

As shown in Table 2-17, most of the literature recommends conditions near the triple point for shipping of liquid CO_2, owing to the lower storage costs and enhanced density [34,39,51,57]. However, Nam et al. [59] and Seo et al. [14] found liquefaction to be most energy efficient at 6 MPa and 295 K, although the optimum's chain conditions differ when a pipeline infrastructure is also considered. This consideration indicates that choice of appropriate liquefaction must not be based simply on energetic and economic performance of the process, but also consider the wider chain and project variables. Overall, the energy requirement of the liquefaction process can vary significantly in relation to disposal amount, desired conditions and type of process.

Table 2-17: Summary of carbon dioxide liquefaction projects

Type of system and refrigerant	Inlet stream condition	Liquefaction conditions	Inlet composition (mass%)	Quantity	Energy consumption	End use	Remarks	Author
Open cycle, CO_2 as refrigerant	0.1-2 MPa	0.6-0.7 MPa, 221 K	97.62% CO_2 2.38% H_2O	Unspecified	144-378 kJ/kg depending on inlet pressure	EOR, storage	0.2-0.5 mol% volatiles 50 ppm water dehydration	Aspelund and Jordal ([51]
Open cycle, CO_2 as refrigerant – multi-stage expansion – optimised	0.1 MPa, 298 K	0.65 MPa, 221 K	97.62% CO_2 2.38% H_2O	2.8 Mt CO_2/year	353-356 kJ/kg	Offshore storage	90% of a 600 MW coal plant $9.95-10.51/t 4-stage compression and 3-stage expansion 2 multi-stream heat exchangers	Lee et al. [127]
Open cycle, CO_2 as refrigerant	0.1 MPa	0.8 MPa, 228 K	89.98% CO_2 9.99% H_2O 0.016% N_2	700,000 t CO_2/year	327-366 kJ/kg with optimisation	Storage		Alabdulkarem et al. [125]
External refrigeration using different coolants a. NH_3 b. NH_3-CO_2 c. C_3H_8-NH_3 d. C_3H_8-CO_2 e. R134a-NH_3	0.1 MPa	0.8 MPa, 228 K	89.98% CO_2 9.99% H_2O 0.016% N_2	700,000 t CO_2/year	a. 387 kJ/kg b. 409 kJ/kg c. 371 kJ/kg d. 432 kJ/kg e. 377 kJ/kg	Storage		Alabdulkarem et al. [125]
External refrigeration process with multi-stage compression and expansion	a. 0.13M Pa 313K b. 10.3M Pa 293K	a. 0.7 MPa, 223 K b. 0.7 MPa, 227 K	a. 97.55% CO_2 2.39% H_2O 0.05% N_2 b. 99.93% CO_2	7.3 Mt CO_2/year	a. 442 kJ/kg b. 52 kJ/kg	Storage	R22 utilised as coolant. Molecular sieve dehydration system included	Mitsubishi Heavy Industries [52]

			0.07% N_2					
a. Single-stage ammonia refrigeration cycle b. Two-stage ammonia refrigeration cycle c. Simple internal refrigeration process d. Multi-stage internal refrigeration process	0.2 MPa, 293 K	0.7 MPa, 223 K	97.62% CO_2 2.38% H_2O	1.1 Mt CO_2/year	a. 299 kJ/kg b. 296 kJ/kg c. 515 kJ/kg d. 313 kJ/kg	Storage	CAPEX 25.2 – 30.9 M$ depending on the process	Øi et al. [124]
External refrigeration processes	0.18 MPa, 313 K	a. 0.6 MPa, 221 K b. 1.5 MPa, 245 K c. 2.5 MPa, 262 K d. 3.5 MPa, 274 K e. 4.5 MPa, 283 K f. 5.5 MPa, 291 K g. 6.5 MPa, 299 K	98.26% CO_2 1.72% H_2O 0.012% N_2	1 Mt CO_2/year	a. 473 kJ/kg b. 378 kJ/kg c. 331 kJ/kg d. 331 kJ/kg e. 315 kJ/kg f. 331 kJ/kg	Offshore storage		Seo et al. [14]
a. Linde Hampson b. Linde dual-pressure system c. Precooled Linde-Hampson system d. Closed liquefaction system	0.1 MPa, 308 K	1.5 MPa, 245 K	100% CO_2	1 Mt CO_2/year	a. 485.9 kJ/kg b. 472.5 kJ/kg c. 381.9 kJ/kg d. 2,376 kJ/kg	Storage site	Seawater temperature 303 K, Compressor adiabatic efficiency 75% CAPEX 34 - 43 M$ depending on the process	Seo et al. [123]

The work of Aspelund and Jordal [51] and Alabdulkarem et al. [125] suggested that internal CO_2 systems are preferred when large amounts of CO_2 are considered, due to stringent expenditure related to the implementation of heat exchangers and external refrigerants. In addition, external refrigeration processes are deemed to be economically advantageous only when low pressures are considered (0.6 MPa), as higher pressures (1.5 MPa, 2.5 MPa, 3.5 MPa, 4.5 MPa, 5.5 MPa and 6.5 MPa) facilitate implementation of internal refrigeration systems instead [123]. LCCs of both open and closed systems provide a comparable trend in relation to liquefaction pressures. As far as internal liquefaction systems are considered, variation of intercooling seawater temperature due to seasonal and locational variations can have a remarkable effect on plant layout and energy consumption; for a seawater temperature range of 278-303 K the total compressor power can vary from 90 to 140 kWh/t CO_2; temperatures of the seawater also appears to affect the layout of the liquefaction plant [130]. On the other hand, the impact of seawater conditions on external refrigeration systems is modest. Zahid et al. [72] suggests that operational costs of closed-cycle liquefaction processes increase with higher liquefied pressures, unlike Seo et al. [14] who concluded that liquefaction power decreases with higher pressures when conditions of 0.6 to 6.5 MPa and corresponding saturation temperatures are considered. The trend is attributed to the fact that the resulting reduction in refrigeration power at higher pressures is more significant than the increase of compression power, making 6.5 MPa and 298 K the optimal liquefaction condition in terms of energy intensity. The authors however found 4.5 MPa and 283 K to be the most cost effective liquefaction condition in terms of life-cycle cost due to the fact that compression to 5.5 – 6.5 MPa requires equipment that demands higher capital expenditure [14]. Overall, and despite the profound impact of the liquefaction process on the chain's economic aspects, it was found that optimal project conditions with regards to costing to be 1.5 MPa and 245 K [14], demonstrating that optimisation of liquefaction processes is not necessarily the key aspect within the full-chain. Both Engel and Kather [95] and Øi et al. [124] found that energy efficiency in the external refrigeration system can be improved by adding a series of refrigeration stages at variable temperatures; and propene, ammonia-propane and ammonia

are found to be the most energy optimal refrigerants in the 1-stage, 2-stage and 3-stage closed cycles, respectively [95]. The effect of the working fluid is also important in the 1-stage closed-cycle system but less important in both the 2-stage and 3-stage cycles. In a subsequent study, these authors moreover identified measures of process optimisation by energy recovery from the stream – including liquid expanders and phase separators instead of conventional cascade heat exchangers – and found that energy intensity of the processes can be reduced by 30-40% [131]. Although such studies are relevant in providing an overview of the energy consumption of different liquefaction cycles, they do not take into account cost analyses and the effect of the discharge amount on choice of the appropriate cycle. Increasing the inlet pressure to the liquefaction system reduces energy requirements and costs for both types of liquefaction systems, although the impact is more significant for internal cooling systems and, in general, with higher pressures; an inlet pressure of 1 MPa results in five times the total cost in comparison with an inlet pressure of 10 MPa [52,57,95].

The location of the liquefaction plant has been extensively investigated in order to establish the ideal location of the infrastructure to minimise transmission costs. Nam et al. [59] developed a modelling tool with the aim of maximising efficiency of the chain, which shows that when an industrial or power emission cluster is considered, it is convenient to establish a liquefaction plant in the high emitting regions and connect it to low emitting regions via pipelines, thus promoting a transportation infrastructure. As previously noted, contaminants directly impact the phase boundaries of CO_2-rich streams and, hence, the choice of liquefaction conditions and processes. Most realistic capture scenarios are found to require high purification to facilitate the CO_2 being transported as liquid. Wetenhall et al. [91] summarised the power required to compress twelve realistic capture scenarios, from 0.18 MPa to 11 MPa to assess the effect of impurities; they found the additional power requirements to be 1.5% to 7% higher than the pure CO_2 reference state, with adsorption capture (90 vol% CO_2, 1 vol% O_2 and 9 vol% N_2) being the most intensive and CO_2 membrane (97 vol% CO_2, 3 vol% O_2) the least demanding. This analysis is particularly relevant to open-cycle liquefaction systems where streams are compressed above the critical point prior to

expansion. The pure CO_2 stream requires the lowest electrical consumption whilst the absorption and oxy-fuel scenarios, containing nitrogen and oxygen, respectively, are the most power intensive [51]. Overall, the extra power required does not exceed 7% for the worst-case scenarios. This work found, for example, that energy consumption of an oxy-fuel scenario is 10% higher than for a pre-combustion capture scenario. Such energy assessment does not address the consumption related to refrigeration of carbon dioxide and regeneration of coolant and it is, therefore, incomplete in relation to systems that imply external refrigerants. By contrast, Deng et al. [126] investigate three realistic composition scenarios encountered in captured streams from the industry and power sectors and emphasised that the presence of contaminants can result in higher liquefaction costs of up to 34% compared to pure CO_2 scenarios when external refrigeration systems implying ammonia are considered. The highest cost was encountered in a pre-combustion Rectisol stream from coal fired power plants, which contain methanol, hydrogen, carbon monoxide and hydrogen sulphide as well as nitrogen and water [126]. On the other hand, a modest increase in liquefaction cost was found in the post-combustion stream from a cement plant which mainly contains water and a minimal amount of nitrogen. Delivery pressures below 3 MPa appeared to be greatly affected by the presence of different impurities. It was moreover noted that purity constraint of the liquefied stream, mainly due to process safety considerations, can impact the cost of the process. This work provides a good outline of the conditioning and liquefaction requirements of several emitters by targeting a range of potential storage conditions; however, it lacks a comparative analysis of different liquefaction processes relative to the different delivery pressures and composition scenarios [126]. Engel and Kather [95] noted that the energy requirement of an external refrigeration system with high-pressure pipeline as inlet stream also increases with the presence of impurities, with the oxy-fuel scenario being the most significant. This trend is maintained even where more refrigeration stages are added to the process.

2.8.2 Storage

Upon liquefaction, liquid carbon dioxide must be intermediately stored at its bubble point before being loaded onto batch shipping; inside the tank, both liquid and gaseous phases coexist at the same pressure and temperature. Storage tanks can be filled to a maximum loading level of 72-98% depending on the selected pressure, thus intentionally leaving part of the volume for the gaseous phase to prevent operational issues caused by heat ingress, and rapid transient pressure spikes which may result in catastrophic vessel failure [64]. The design of appropriate intermediate storage is key to facilitate an efficient shipping schedule and optimally discharge continuous liquid CO_2 flow from the liquefaction plant [39,52]. Table 2-18 summarises the existing literature on intermediate storage tanks in relation to several projects. The intermediate storage tanks are required to comply with the relevant regulations such as BS5500 PD code [44]. Lower-pressure conditions require more energetic processes in the land liquefaction plant, though they favour storage due to enhanced density of liquid CO_2 near the triple point and reduced thickness of the vessel. Seo et al. [14] found that the overall costs of storage tanks increased linearly with storage pressure, in contrast to Nam et al. [59] as highlighted in Figure 2-15.

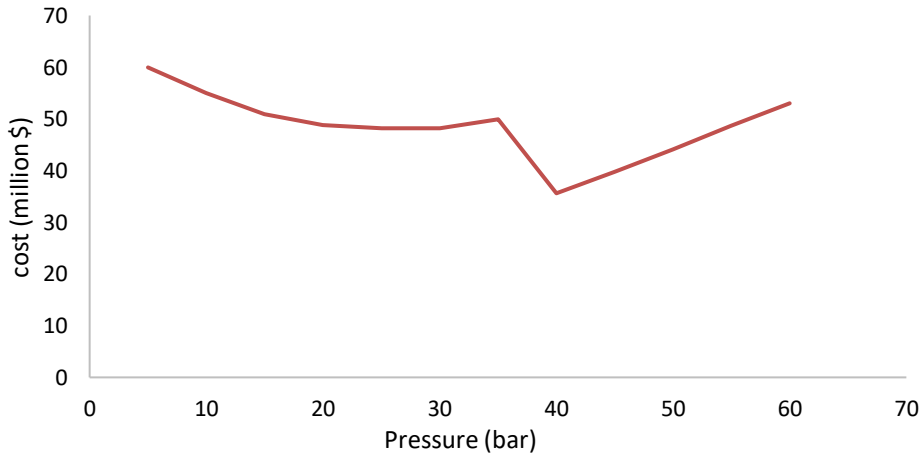

Figure 2-15: Capital expenditure costs for onshore storage segment for 150,000m^3 [59]

Table 2-18: Summary of intermediate storage variables indicated in the literature.

Source	Type of storage tanks	Size or capacity	Material	Conditions	Discharge amount	Distance	Remarks
Decarre et al. [44]	Cylindrical or bi-lobate	14x 4,500 m^3	3.5%, 5% and 9% Ni Stainless steel 304L and 316L Aluminium 1050	1.5 MPa, 243 K	2.5 Mt CO_2/year	1,000 km	• M$8 or 8% of total project cost • Choice of material is dependent on temperature. • Design to comply with BS5500 PD code. • Account for increased pressure due to boil-off gas production. • 10 mm thick casing
Haugen et al. [132]	Cylindrical	3,000 t	Steel	1.5 MPa, 245 K	670 kt CO_2/year	NA	Design of storage facility is flexible with regards to geographical location and discharge amount
Aspelund et al. [57]	Semi-pressurised cylindrical tanks	10 x 3,000 m^3	Steel	0.65 MPa, 221 K	1 Mt CO_2/year	1,500 km	Semi-pressurised vessels are indicated Cumulative storage capacity to be 150% the ship capacity
Vermeulen [39]	Bullet type tanks	10,000 m^3	P335NL2	0.7 MPa, 223 K	1.5 Mt CO_2/year 2.7 Mt CO_2/year 4.7 Mt CO_2/year 6 Mt CO_2/year	220-400 km	Final sizing of storage design is dependent on liquefied amount
Seo et al. [14]	Cylindrical	5,000 m^3	Carbon Steel	0.6 MPa, 221 K 1.5 MPa, 246 K 2.5 MPa, 261 K 3.5 MPa, 273 K 4.5 MPa, 283 K 5.5 MPa, 292 K 6.5 MPa, 298 K	1 Mt CO_2 /year	300 – 700 km	Costs of the tanks increase with liquefaction pressure.

Source	Type of storage tanks	Size or capacity	Material	Conditions	Discharge amount	Distance	Remarks
Kokubun and Ozaki [85]	Cylindrical bilobe	2 x 1,500 m^3	Carbon Steel	2.65 MPa, 263 K	1 Mt CO_2/year	200 – 800 km	Design of storage tanks is based on LPG experience.
	Cylindrical tanks	91 x 1,000 m^3	Carbon manganese steel	0.7 MPa, 223 K	10 – 20 Mt CO_2/year	180-750 km	Design is based on ASME code (2010) and IGC Code (2000) Vertical and horizontal orientation considered.
Mitsubishi Heavy Industries [52]	Spherical tanks	20,000 m^3 each	High tensile steel	1 – 10 MPa	7.3 Mt CO_2/year	200 - 12,000 km	

The literature suggests that the appropriate intermediate storage to cargo ship vessel size ratio should be in the order of 1.5-2 to enhance the flexibility of operations in the chain [8,9,57] with the exception of ZEP [34] which indicates a ratio of 1:1 to be sufficient. Intermediate CO_2 storage cylindrical vertical tanks capable of holding 3,000 t of carbon dioxide are currently utilised in commercial-grade projects by Yara Praxair [132]. Different design options such as cylindrical, bi-lobate or spherical semi-pressurised tanks have also been investigated in the literature, as they are currently applicable to other industrial applications [39,57,125,127]. Spherical tanks are reported by manufacturers to have marginally lower cumulative installation costs despite construction being more challenging; moreover, suitable construction materials include carbon steel, aluminium 1050 or 304L/316L stainless steel [127]. The maximum size and wall thickness of cylindrical storage tanks differ depending on the selected pressure; larger ships generally require lower wall thicknesses due to lower dynamic pressure resulting from the smaller ship acceleration. According to Decarre et al. [44] the optimal storage tank solution for projects discharging 0.8-5.6 Mt CO_2/year is a tank of cylindrical shape, made of 9% Ni steel, with a 10 mm thickness and a volume of 4,500 m^3;Lee et al. [133] favour 20,000 m^3 spherical carbon steel tanks instead. Conversely, Seo et al. [134] analysis is based on LCC, including the economic implication of unavailability of temporary storage, to determine optimum volume of tanks. LCC was found to be closely related to the storage capacity, and this resulted to be most economically viable when carrier capacity and intermediate storage capacity are equal. Factors such as size and number of carriers, CO_2 trade cost and distance did not appear to affect the optimal storage volume significantly. However, a limitation of this study lies in the fact that it offers primarily an economic approach to determine optimum parameters of a complex CO_2-handling terminal. The impact of inappropriate storage unavailability was calculated considering carbon credits in this study, however this can lead to mass CO_2 emissions in a real scenario, potentially harmful to both the environment and any humans present. Experience in other industries indicates, a more comprehensive and realistic approach must take into account environmental issues and process safety in addition to focussing just on costs [135]. Seo et al. [136] assert that selection of materials for storage vessels is mainly dependant on liquefaction pressure and

corresponding liquid temperature; the authors suggest the choice of A517 steel – with a low-temperature rating of 228 K – when operating pressures are comprised between 1.5 – 6.5 MPa, conversely suggesting the choice of A547-grade and specifying that the choice of materials used in temporary storage and cargo tanks is the same.

Interestingly, Vermeulen [39] and Kokubun et al. [85] regard the choice and design of tanks to be case sensitive and significantly dependent on the expected increase of pressure of the cargo due to heat leaks. Storage and the unloading system are estimated to represent 12% of the total costs according to Aspelund et al. [57], and this was also quantified by ZEP [34] to be equivalent to $1,123/m3 – while the GCCSI [80] estimates the cost to be $16 million (£1=$1.32 as of March 2019) for a tank capable of holding 10,000 t, made of high-tensile-strength steel; manufacturing costs represent 45% of the total storage tank costs [52]. Wherever land availability is an issue for onshore storage, liquid carbon dioxide tanks could be stored on floating barges. Yoo et al. [53] found that when small volumes of up to 28,000 m^3 are considered, storage tanks can be laid horizontally on the barge, whilst larger capacities would favour vertical orientation. An innovative alternative to new onshore infrastructure for tropical waters such as offshore of Brazil is the floating logistics terminal (FLT), which is an economical and environmentally friendly method to carry all infrastructure for CO_2 shipping terminal. Yamamoto et al. [137] introduce the concept of a FLT composed by several floating bodies. The advantages of the FLT are flexibility, fast installation, and cost effectiveness if such systems are derived from recycled hull from large bulk carriers. The concept of floating logistics could particularly benefit countries such as Japan where the propensity for earthquakes is significant, and generally increase the value of flexibility in the shipping chain.

2.8.3 Loading

Technical application of loading operations benefits from experience in the LNG and LPG industries. Storage tanks are loaded with a continuous stream of liquefied CO_2 from the liquefaction plant, through a loading system that makes use of high-pressure low-temperature pumps. Liu et al. [138] suggested that cargo tanks should be filled with pressurised gas phase carbon dioxide to avoid contamination with air and formation of dry ice; and

that articulated rigid loading arms designed for cryogenic liquids are to be preferred [39,44] over flexible cryogenic hoses due to lower likelihood for mechanical failure and leakage. However, both systems are in use for loading of liquid CO_2 [132]. When loading takes place, the level within the vessel builds up; in order to prevent over-pressurisation of the vessel, this vapour stream must be continuously removed and re-directed back to the liquefaction unit during the length of the operations using a second parallel arm for the CO_2 vapour 'return line' [39,44,139]. Minimising loading time improves delivery efficiency, reduces the number of ships required to discharge a given amount, and requires high flow rates; however, the resulting pressure drop must be taken into account [140]. Flowrates of 2870-3530 t/h [39,72] appear to be appropriate and would enable the loading of a 30,000 m^3 ship in 12 h [34,39,70]; such flowrates would, however, require an adequate Emergency Release System (ERS) to avert outflow of CO_2 in case of failure of the loading arm or unplanned disconnection from the ship [39,41]. During this operation the pressure within the tank will drop, and to avoid freezing, the vapour generated during the voyage in the cargo ship must be recycled back to the storage tank during the operation; this also mitigates against pressure increase in the cargo tank. Formation of dry ice, induced by rapid depressurisation of the system, can be avoided by ensuring appropriate safety margins, however there is no consensus on what they should be. Standard boil-off-gas mitigation measures such as the application of insulation must be performed around the whole loading system as a higher proportion of boil-off gas is generated in comparison with storage [72].

The specific energy requirement for the loading component is given by Aspelund et al. [57] as 0.2 kWh/t CO_2 or 1% of the specific energy requirement in the liquefaction as reported in the same work; costs, including CAPEX, are found to be negligible in relation to the full shipping chain by Decarre et al. [44]. However, such comparative economic assessment appears to be in disagreement with Kokubun et al. [85], who emphasised that loading- related CAPEX represents 37% of the capital expenditure of a two-tankers carrier over a 200 km distance, and 24% of a four-tankers carrier with 400 – 800 km transport distance. This estimation moreover highlights the fact that expenditure of carrier-loading-system is not related to size of the ship. The

significant discrepancy exhibited in the two studies can be mainly attributed to the different project boundaries adopted by the authors; as Kokubun et al. [85] clearly indicates CO_2 liquefaction facilities to be out of the scope of the study, Decarre et al. [44] includes conditioning costs and infrastructure in the economic estimation. Moreover, there is a difference in the transport distances – 200 km and 400 – 800 km in the former work and 1000 km in the latter – which change the proportional cost of loading facilities. Lastly, the choice of different cargo condition of 223 K, 0.7 MPa for Decarre et al. [44] and 263 K, 2.65 MPa for Kokubun et al. [85] also impacts on the cost of loading facilities as higher pressures require components with higher wall thickness.

2.8.4 Offloading and injection

After sea transport, carbon dioxide can be unloaded either onshore at a port before being transported by pipeline– in case of port-to-port scenarios – or offshore prior to being directed to the final storage destination. While the former option covering port-to-port shipping is well established through the extensive experience matured in large-scale shipping of similar gases such as LNG and LPG and currently applied in the food, beverage and ammonia industries, offshore unloading is still unproven and still poses some technical challenges related to its implementation [39,63]. Selection of the appropriate offloading solution and related infrastructure still sees no clear consensus and is expected to have a significant impact on the design of vessels, process equipment and costing.

Transfer systems to the wellhead include auxiliary platforms that allow instalment of equipment or direct injection from the ship. The former option allows one to generate a continuous flow into the reservoir, offering a temporary storage to mitigate adverse weather conditions; the nature of continuous operations reduces the risk of cyclical thermal and pressure loading on casings and polymeric materials [106]. The drawback associated with these systems is the higher capital expenditure required for their implementation [63]. Conversely, offloading to a flexible riser via a buoy for direct injection to the well implies that, conditioning, pressurisation and heating of carbon dioxide must take place on the ship. In order to achieve this, the stream must be pumped to the appropriate pipeline pressure of 5-40 MPa [14,39] and consequently heated to 258-293 K – depending on the site - by means of pre-warmed seawater or waste heat available from the ship. Weather variations and thus seawater temperature fluctuations

may compromise the safety of operations in view of the requirement of specific temperature and pressure conditions of the stream in order to avoid hydrate. Direct injection from the ship is found to be achievable for several wells with the integration of compression and heating equipment on board. Brownsort et al. [69] undertook a thorough investigation of offshore offloading technologies and highlighted that selection of single point systems is case-sensitive and related to several factors such as location, stream condition, availability of suitable flexible hoses and design of the ship. Similarly, Vermeulen [39] identified four different Single-Point Mooring (SML) systems that can be implemented to connect the ship with the wellhead, each one exhibiting differences in terms of water depth application and accessibility in relation to conditions of the sea. Offshore discharge is considered a novel procedure in the CO_2 shipping chain, and advanced technology is, therefore, required to mitigate the formation of dry ice during unloading and achieve a consensus on the preferred system [48].

The principal limitation is the limited understanding of the impact of impurities on the phase boundary to ensure that the safety margin from the triple point is maintained during operations [34]. Additionally, sudden stops of injection operations must be avoided at all times to mitigate the risk of dry ice formation [39]. Aspelund and Jordal [51] highlighted optimum injection temperatures to be around 288 K to mitigate against formation of hydrates during operations. When maximum storage capacity is achieved in a particular field, near-well installations have the adaptability to be relocated for injection to another field, thus, adding flexibility to the network and the opportunity to expand a shared transport web within Europe. Direct injection from the carrier is assessed as being feasible for a number of large-scale injection wells, with the exception of shallow depleted reservoirs, and pre-injection conditioning can be achieved through appropriate installations on the ship, where the heating source for injection is provided by seawater or excess heat from the engines [34]. According to Neele et al. [48] injection from the ship increases the costs by 10-25% compared to injection from a temporary platform. By contrast, Ozaki et al. [40] and the IEAGHG [63] found that direct injection from ships can potentially reduce the costs of the project as large-scale offshore installations are omitted, albeit technical and safety aspects require further optimisation.

Pre-offloading conditioning consists of heating the carbon dioxide to 273 K and compressing it to ~20-30 MPa, so appropriate heating and compression equipment must be installed on board the vessel. Heat from seawater and the ship's engines

can provide the thermal and electrical power required to inject the stream [61]. In scenarios where large volumes are transported for long distances by means of several ships, implementation of a seabed pipeline as a heat exchanger may be a favourable solution [34]. Most studies assume that offshore unloading will be performed in 12-36 h [34,48,53], with lack of temporary offshore storage increasing the injection time to 30-50 h.

2.9 Technical challenges and process safety

2.9.1 Selection of materials

The level of dehydration in the stream affects the choice of the type of metal throughout the system. Carbon steel, carbon manganese steel and stainless steel are suitable under low-, medium- and high-pressure carbon dioxide conditions with appropriate foam or vacuum insulation; carbon steel can be used for compressor piping when low water content is achieved, otherwise, stainless steel is required around the compressor in order to prevent corrosion [14,53]. Table 2-19 summarises the material selection in a CO_2 terminal. The decision on whether to make the whole pipeline and other components (scrubbers, coolers) of stainless steel rather than alternating it with carbon steel is purely based on economics. Despite the absence of water, hydrogen sulphide impurities can still react with the carbon steel, forming a thin film of iron sulphide which tends to coat the inside surface and decrease the rate of heat transfer [42].

Table 2-19 Material selection in CO_2 terminal [39]

System	Component	Media	Temperature range (K)	Pressure (MPa)	Material
CO_2 Terminal	Liquefaction	Liquefied CO_2	223 - 373	8	SS300
	Heat exchangers	Liquefied CO_2	223 - 373	8	Al
	Storage	Liquefied CO_2	223	0.7	P335NL2
	Pumps	Liquefied CO_2	223	1	316L
	Ship loading	Liquefied CO_2	223	1	316L
	HP Compression	Dry CO_2	278 – 308	8-15	CS,4140

Material selection must also account for operational temperature range: liquid carbon dioxide must be handled and transported at temperatures between 223 K and 261 K,

depending on preferred pressure conditions, though the eventuality of rapid depressurisation due to sudden shut-down in the system can potentially drop the temperature to as low as 195 K. This creates a hazard from low-temperature effects, particularly in terms of the suitability of materials to ensure the integrity of vessels, pipes and fittings that needs to be addressed in the specific operational risk assessment. Some low-temperature-grade carbon steel variations can operate at temperatures down to 227 K [73], although Omata et al. [58] suggested that heat treatment is required to enable the carbon steel to withstand temperatures below 263 K. However, using materials such as 9% Ni steel, 5% Ni steel or aluminium alloy 5083-0 increase costs by 4-6 times compared to carbon steel. Seo et al. [14] suggest the implementation of A517-grade steel in scenarios where stream's liquefaction temperature is above 228 K, with a recommendation to switch to A537 for conditions that require a liquefied temperature in the range of 213 – 228 K.

When considering polymeric or elastomer components, IEAGHG [141] suggested a range of polymers, such as EPDM, HNBR, PTFE and FKM (Viton®) are appropriate for liquid CO_2 environments. They also suggest that, to avoid issues with the performance of elastomers, it is important to consult the supplier prior to specific applications.

The suitability of elastomers that are frequently applied to the hydrocarbon industry has been questioned [13,142], and it has been noted that cracking of seals is an issue with materials such as nitrile, polyethylene, fluoro-elastomers, chloroprene and ethylene-propylene compounds during rapid depressurisation. The high diffusivity of carbon dioxide inside the molecular structure during pressure cycles, combined with expansion during rapid gas depressurisation, make these compounds unsuitable for decompression cycles that are likely to be encountered during real operations. In response, a number of standards have been developed across the industry to assess suitability or failure of seals and gaskets undergoing ageing and explosive decompression cycles in CO_2-rich environments, though a dearth of experimental findings is apparent in relation to the presence of impurities at different conditions and at different concentrations [143]; Ansaloni et al. [106] notes that little experience exists in relation to measurements of elastomer properties at temperature close to the CO_2 triple point (219 K) which will make it difficult to assess the suitability of materials in relation to conditions typical of sea vessel transport. These authors also suggest that

the impact of pressure and temperature cycling and propensity for RGD damage due to fluid absorption at such conditions should be explored to assess the impact on the elastomers' mechanical stability and lifetime of the materials. Qualification of elastomers in low-cryogenic carbon dioxide environments is therefore under-investigated by several groups [106,144]. These considerations are particularly relevant to shipping due to the batch-like nature of its operation, where continuity of loading and offloading scenarios poses a risk from thermal and pressure cycling effects on selected metallic and non- metallic materials. Prolonged exposure of materials also needs to be explored in relation to the low-temperature CO_2 environment, although the shipping distance is not specifically expected to have a profound impact, due to the fact that sea vessels and their components need to be designed for a project life of 10 -15 years in the first place.

2.9.2 Boil-off gas generation

When handling liquid CO_2 during real operations, a variable amount of boil-off gas can be generated. The boil-off gas is the vapour produced during sea transport due to the effect of waves' motion on sloshing of the cargo content or caused by ambient heat penetration into the system due to temperature difference during the chain's operations. The rate of boil-off gas is also affected by the distance travelled, level of impurities in the cargo tank, tank pressure design, and operational modes [145]. The rate of boil-off gas per day for LNG carriers is assumed to be 0.1-0.15 %, which over a 21-d voyage produces undesirable large quantity of such gas [146]. There are no exact range of values stated in literature predicting the boil-off rate per day for CO_2 carriers, but 0.15% has been inferred as a suitable value by comparison with some of the physical properties with LNG carriers [147]. Chu et al. [148] considered 0.12% of the full cargo content to be the boil-off rate per day for CO_2 carriers. A summary of the factors contributing to the generation of boil-off gas during static operations is provided in Table 2-20; Zahid et al and Vermeulen [39,72] performed some modelling sensitivities to study these phenomenon; boil-off-gas generation during loading and unloading operations is estimated to be 8-10 times higher than during hold-up conditions [72]. The minimisation of LNG BOG can be regarded to be similar to CO_2 except for differences that exist in storage conditions [44,125].

Table 2-20 Factors affecting CO_2 boil-off gas [39,72].

Factor	Desirability	Remarks
Ambient temperature	Low	Lower ambient temperature results in lower heat influx and, hence, boil-off gas
Thermal resistivity and thickness of insulation	High	Results in lower BOG. Thickness is a trade-off between material cost and resulting reduction of boil-off
CO_2 level in the tank	High	Low filling level in the tank leads to a higher evaporation rate of the liquid
Capacity of the storage tank	Low	Assuming the same absolute filling amount, smaller tanks exhibit a lower the rate of pressure build-up due to BOG within the vessel

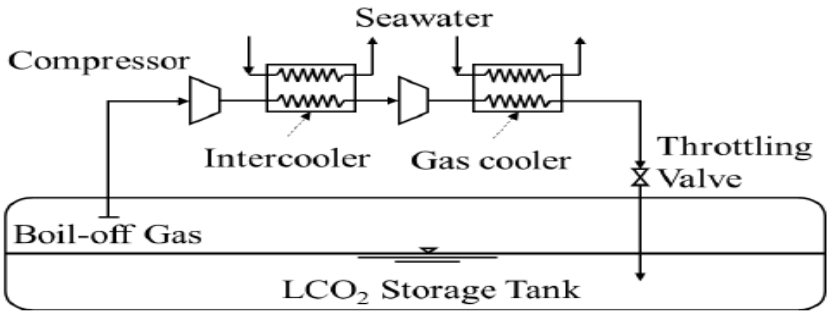

Figure 2-16: Open cycle re-liquefaction for LCO_2 transport [147]

Commercial designs for BOG re-liquefaction for gas carriers exist for LNG and LPG and can be applied to a CO_2 carrier [146,149,150]. Figure 2-16 shows a schematic representation of a potential re-liquefaction system. A study was carried out by Gómez et al. [151] on the different technologies applied for re-liquefaction of BOG on LNG carriers. The Brayton cooling cycle, an external refrigeration method, is normally used for on-board re-liquefaction [151]. The efficiency of the process is considered secondary owing to the importance of other factors such as having a minimal space constraint, displaying stability at sea conditions, easy installation, quick start-up, minimal quantity of equipment [151]. Moreover, a process that utilises the cold energy in the LNG fuel as a refrigerant and as a chilling fluid to re-liquefy

the BOG has been considered to be a viable way to deal with boil-off gas by saving cost on purchase of additional equipment and fuel consumed [116]. It was estimated that for the BOG re-liquefaction cycle for both HFO- and LNG-fuelled CO_2 ships, ammonia can be used as an external refrigerant. This is providing the capture system installed on-board uses ammonia solvent for scrubbing emissions [152,153], thereby better utilising ship storage space. Taking into consideration the lower power consumption required by ammonia compared to other refrigerants [125] and its advantages as an absorbent [154], aqueous ammonia would be a reasonable choice as a solvent because no extra solvent storage tank will be needed on the ship. The ammonia content in the ammonia storage tank for the refrigerants could also then be used for the emission absorption process.

2.9.3 Blockages due to hydrates formation

Water solubility in CO_2-rich fluids determines the propensity for slug formation, hydrates formation and corrosion and, hence, dehydration requirements in shipping transport systems. Free water in the stream can create hydrates both in liquid and gaseous states. In order to form, they require adequate amounts of free water (host), a suitable “guest” and the CO_2-rich fluid. Hydrates can lead to blockages in the conditioning systems, particularly within the compression train and, in order to mitigate them, it will be necessary to use chemical inhibitors or operate out of the hydrate-stability zones; the hydrate-water equilibrium is dictated by physical equilibrium as a function of pressure and temperature.

As can be seen in Figure 2-17 and Figure 2-18 conditions typical of carbon dioxide shipping near the triple point are within the hydrates-stability zone in both pure saturated and 250 ppmv water-carbon dioxide systems, though the hydrate-stability envelope is wider in the saturated water environment. Li et al. [155] indicated that, when shipping transport conditions are considered, a water content of 100 ppmv lies on the liquid-hydrate equilibrium line, albeit limited experimental data are available to validate existing models; nonetheless hydrates can still form in those regions at 50 ppm concentrations [91].

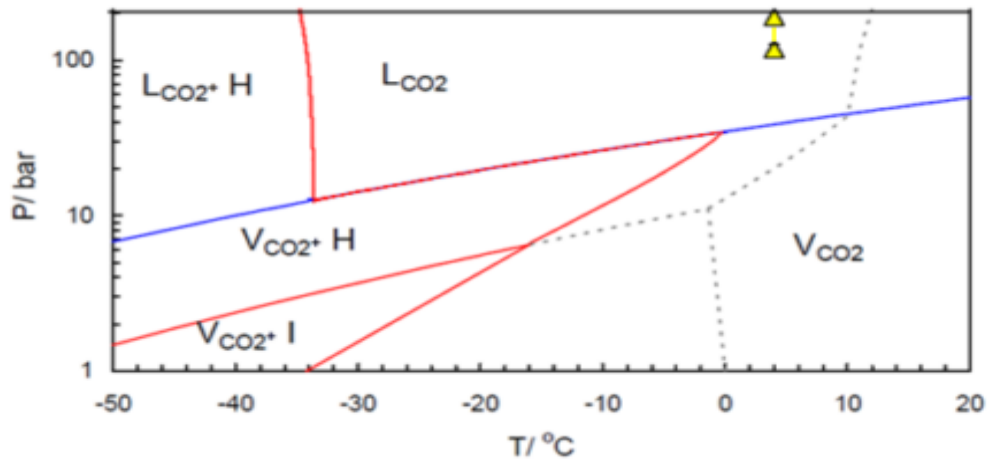

Figure 2-17: Hydrate formation in saturated carbon dioxide with 250 ppmv water system [156]; 'L' = liquid-rich zone; 'V' = vapour-rich zone; 'I' = dry-ice region; 'H' = hydrate-stability zone; yellow triangles represent CO_2 pipeline condition.

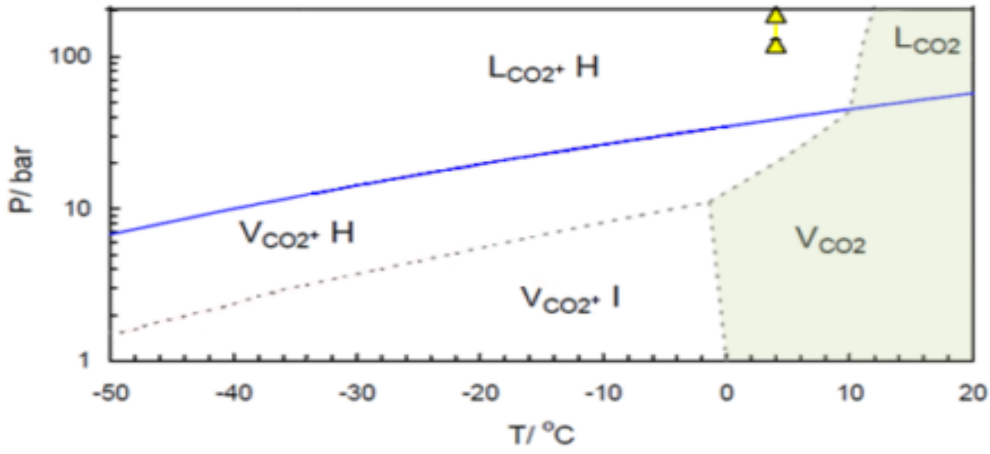

Figure 2-18: Figure 18: Hydrate formation in pure saturated carbon dioxide system [156] ; 'L' = liquid-rich zone; 'V' = vapour-rich zone; 'I' = dry-ice region; 'H' = hydrate-stability zone; yellow triangles represent CO_2 pipeline condition.

The presence of moderate quantities of N_2 and O_2 (~2 mol%, each) shifts the hydrate-stability zone to higher temperatures, while other impurities – especially sulphur-related ones such as SO_2 and H_2S – can have a reverse effect. The presence of H_2 increases the liquefaction pressure of the mixture, meaning that during a rapid depressurisation water will be the first impurity to vaporise and bond with the CO_2 to form hydrates, which are potentially dangerous to the system. As such, maintaining a constant operating pressure is essential to prevent two-phase flow and hydrates. Alternatively, controlling the presence of contaminants and a low level of water can prevent the formation of hydrates. In order to assess the predisposition of solid dry ice during depressurisation

of the system, a number of equilibria models of carbon dioxide and solids have been generated, albeit that there are some deficiencies in terms of a lack of useful thermodynamic data [157]. Impurities reduce the freezing point of the CO_2-rich mixture. Overall, more extensive investigations on more complex tertiary mixtures are required to cover realistic scenarios [86,88]. A suitable safety margin must also be applied as depressurisation below the triple point equilibrium can result in formation of dry ice [57]. This is one of the current challenges related to operation near the triple point. Here, however, removal of volatile impurities to a maximum allowable 0.2-0.5 mol% in the stream can mitigate solid formation near the triple point during liquefaction and transport.

2.9.4 Process safety, dispersion of inventory and boiling liquid expanding vapour explosions

Health and process safety is a critical aspect of industrial processes, and the CO_2 terminal is no exception [156]. While pipelines are characterised by a constant throughput of high-pressure, liquid or supercritical CO_2 transported at pressures comprised between 10 and 15 MPa [47], CO_2 shipping involves a range of operations required to incorporate the continuous liquefaction of carbon dioxide at the port terminal with the batch-like nature of carrier transport at conditions of 0.6 – 2.5 MPa pressure and refrigerated temperatures (220 – 260 K) [14]. The main risks associated with pipeline systems relate to the high transport pressures required, which imply a requirement for emergency planning zones (EPZ) in case of releases and leaks [158]. This has clear safety implications as the scale of the thermal cooling envelope from supercritical carbon dioxide can create structural integrity damage such as brittle to ductile transitions and abrupt cooling of structural members. Other than this, the toxic contaminations caused by impurities present in the supercritical CO_2 stream pose a threat to personnel, people and the environment, particularly in densely populated areas. Conversely, CO_2 shipping involves lower transport pressures (0.6 – 2.5 MPa) and temperatures (223 – 253 K) which extend the challenges related to material selection to mitigate the risk of embrittlement of steels and metals [107].Particular attention needs to be paid to the selection of appropriate materials that can sustain the operational pressures and temperatures and exhibit compatibility with carbon dioxide and the impurities present in the stream. However, the main process safety concern is the selection of appropriate safety margins from the triple point to avoid formation of dry ice blockages induced by pressure drops when handling CO_2 across the terminal [72]. This

scenario also has structural and integrity issues, as the formation of solid blockages can lead to over pressurisation of the system, and ultimately loss of containment. In particular, a safe and reliable strategy needs to be implemented to integrate the batch-like nature of shipping operations with the continuous processes of CO_2 capture and liquefaction. In both transportation systems, the risk of uncontrolled release ultimately poses a significant threat to people surrounding the facilities [158]; a study on concentration against time consequence for carbon dioxide inhalation performed by the HSE Executive, highlighted that specified level of toxicity limit (SLOT) of CO_2 ranges from 6.3% concentration in air by volume for 60 minute to 10.5% for 1 minute [158]. The UK's Health and Safety Executive produced a comprehensive analysis of the danger potential of carbon dioxide systems [158] with specific reference to the CCUS chain. Considerations of engineering aspects such as formation of dry ice, emergency protocols and integrity issues related to structural integrity are suggested as research topics in the area of CO_2 transport, especially in relation to liquid, cryogenic systems. Moreover, hazards resulting from loss of inventory from large CO_2 vessels must be investigated, and implementation of stringent risk assessments is recommended to reduce such hazards. In order to protect people and limit the impact to the plant and the surroundings, Zahid et al. [72] emphasised that terminals should include emergency shutdown (ESD) system. Such systems close the flow between the carrier and terminal in case of an unplanned emergency, similarly to what happens in hydrocarbon terminals. An ESD system normally includes fast-response valves, loading arms coupled with emergency release systems and it will be operating automatically in relation to some key operational parameters. For instance, initiation can be caused by an atypical tank pressure, level or a leakage at the terminal or ship. An ESD should always employ appropriate safety protocols. As previously noted, low-pressure shipping systems near the triple point are associated with high uncertainty and propensity for dry-ice and hydrate formations in case of depressurisation of the system, and thus maintaining a robust safety margin from the triple point is recommended. Accordingly, Noh et al. [159] undertook a preliminary hazard analysis (PHA) in the CO_2 shipping chain and identified the unloading system and storage tanks as the highest-risk components in the storage terminal. With reference to the unloading system, they found that the extensive implementation of ESD systems throughout the terminal, coupled with low- or high-pressure alarms can successfully reduce the risk of low-temperature gas and solid phase leak caused by failure of the unloading arms and recirculation line. An ERS could

mitigate the risk of CO_2 leakage in case of rupture or mechanical failure of the unloading arm or recirculation line; and for the CO_2 storage tanks, the integration of process safety valves, level gauges and alarms can aid in minimising the damage caused by CO_2 leakage in case of rupture or overpressure of intermediate storage vessels. The study can be considered a point of reference to generate a safe CO_2 transportation infrastructure in future commercialisation of CCUS technology.

The rate of incidents relating to large-scale CO_2 carriers cannot be determined due to lack of commercial implementation; experience with CO_2 pipelines systems suggests that failures are mostly related to third-party interference, corrosion or material defects. However, similarly to pipeline applications, current empirical data on operations are insufficient to establish the failure probability of a system with the same accuracy as for hydrocarbon systems [135]. The rate of incidents for different types of carriers was investigated by Doctor et al. [37] as showed in Table 2-21.

Table 2-21: Rate of incidents for different types of carriers [37]

Ship type	Number of ships (2000)	Serious incidents (1978-2000)	Frequency (incidents/ship year)
LPG tankers	982	20	0.00091
LNG tankers	121	1	0.00037
Oil tankers	9678	314	0.00144
Cargo/bulk carriers	21407	1203	0.00250

One advantage of CO_2 transport is that it exhibits lower risk from fire in comparison to LPG/LNG tankers. CCUS infrastructure is considered to be at lower risk from fire due to the fact that carbon dioxide is non-flammable, though the risk of hypercapnia and hypercarbia and even asphyxiation during collision and related tank rupture cannot be ruled out. This risk can however be reduced by applying rigorous standards of construction and operation in LPG to carbon dioxide shipping [37].

According to De Visser et al. and Det Norske Veritas [107,160], potential impurities such as CO, amines, NO_x and glycol should also be considered when making health and safety assessments, with H_2S and SO_2 implying significant additional measures. Managing the presence of such impurities is possible through more sophisticated emergency response and training which inevitably result in higher capital and operational expenditures. The Health and Safety Executive [158] found that the hazard distance for an unplanned discharge from a vessel may be up to 400 m when large,

cold, liquid phase stored inventory is considered. However, there is considerable uncertainty in the models of releases of liquid, cryogenic CO_2; this implies the need for experimental investigations.

In case of a carrier accident the liquid CO_2 tanker would release the fluid onto the water surface, and despite the fact that interactions with the environment are not completely understood at this stage, potential formation of dry ice and hydrates are expected. Release of liquid-phase CO_2 inventory into the atmosphere is followed by a phase transition as the media releases; Vermeulen [39] indicated that the release rate of liquid CO_2 will be regulated by the differential pressure between the tank and the environment, the size of the crack, and the nature of the vessel's failure as well as the receiving medium. A greater pressure differential leads to a greater release velocity such quick dispersion will result in a high-speed, cryogenic stream that can result in cryogenic burns and impact injuries to personnel caught in the jet of gas and/or a 195 K solid phase [161]. Additional considerations on material selection must be made in order to maintain process integrity. Carbon dioxide tends to pool and in case of strong winds, this could cause asphyxiation or affect engine performance rupture or failure of a vessel will result in an expansion of the inventory to ambient pressure, which has a remarkably high initial momentum due to loss in expansion energy. Upon release, the liquid phase will gradually make a transition to a two-phase gas and solid mixture.

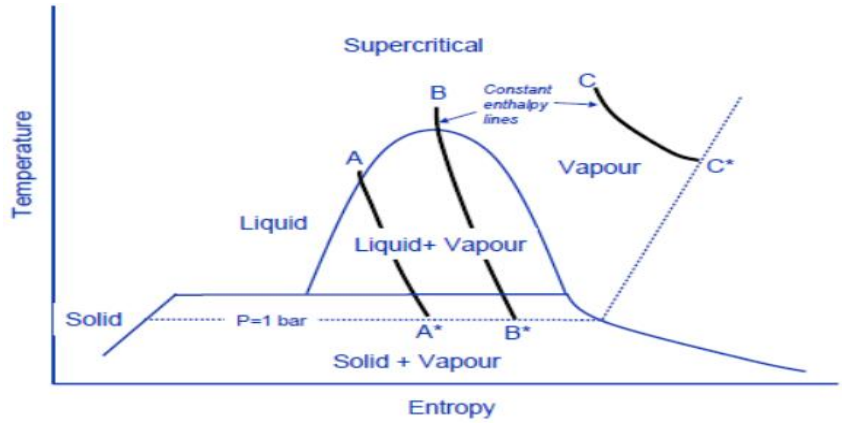

Figure 2-19: Thermodynamic path of CO_2 release [39]

As illustrated in Figure 2-19, during releases with liquid phase starting points (A and B), solids will form depending on the rate of enthalpy change: the closer this

intersection to the vapour line, the lower the proportion of CO_2 solids. Prediction of potential solid CO_2-accumulation regions is important to develop appropriate safety protocols and dispersion behaviour will be strongly affected by ambient conditions, including wind speed. Experimental investigations are still required to comment on the reliability of these prediction models in real scenarios. Han et al. [162] undertook experimental work on the behaviour of liquid inventory during loss of mechanical integrity of a CO_2 container. Here the focus of this work was the investigation of flow characteristics in CO_2 carriers, and it was found the liquid inventory must be promptly discharged to avoid operational issues by applying a 'jettisoning' process. During this operation, the liquid carbon dioxide undergoes two distinct phase transitions – the first one from liquid to liquid + vapour and the second from liquid + vapour to solid + vapour. These phase changes dictate the dispersion behaviour as the phase transition into solid and vapour takes place irrespective of the length of the experimental pipe. Moreover, the magnitude of pressure change is related to the friction pressure drop rather than due to the momentum pressure drop. An experimental validation of liquid CO_2 release at pressures of 4-5.5 MPa was performed by Pursell [163]; however, this work did not consider leakage and discharge behaviour of liquid carbon dioxide relevant to CO_2 shipping near the triple point, such as 0.7-1 MPa and 220 K to 226 K. Wetenhall et al. [91] found that dispersion behaviour in the case of a release in both pipeline and ship systems can be affected by the presence of impurities, although no further assessment was made in their work.

In some instances, the high evaporation rate of carbon dioxide into ambient air can cause a BLEVE that ruptures the containment vessel [164]. An empirical study focusing on the rapid decompression of liquid CO_2 in a vertical tube found that for a pressure of 3.5 MPa and 5.5 MPa, a velocity of 20-30 m/s for the liquid-vapour occurs [165], though thermodynamic-related properties could not be obtained due to lack of temperature and pressure measurements. Experimental work has also been performed by Van der Voort [166] using liquid CO_2 bottles of 40 L capacity in order to determine the temperature dependence of BLEVE occurrence; a homogenous nucleation temperature of 271 K was determined, although even below such temperature the risk of BLEVE only decreases, but does not completely disappear. Low-pressure CO_2 shipping, both for the storage

at terminal and shipping cargo conditions of 223 K and 0.7 MPa, is considered to be subject to low risk of BLEVE as there is little potential superheat available. However, the risk of BLEVE cannot be dismissed when medium- and high-pressure CO_2 shipping (1.5 MPa, 248 K and 4.5 MPa, 283 K, respectively) are considered.

The non-flammable nature of CO_2 prevents the ignition and acceleration of boil-off gases in generating further BOG, and as a result, a CO_2 BLEVE is also known as a 'cold BLEVE' [67]. Large-scale experiments are required to validate available models and develop appropriate risk assessments [167]. A preliminary assessment finds liquid CO_2 releases to have a significantly less stringent long-term impact on the environment in comparison to oil spills, although interactions with marine environment can lead to pH changes and generation of hydrates. Dispersion of the release due to effect of the wind may result in failure of the ship's engine [37].

2.10 Conclusions

As CCUS builds momentum in industry and establishes its role as a significant carbon reduction technology, CO_2 shipping will likely have a key role in supporting its execution in the UK and worldwide. Despite some technical and operational gaps, the implementation of carbon dioxide shipping can facilitate early de-carbonisation in numerous countries and industries. No major drawbacks have been highlighted in the literature in relation to the implementation of this technology, although demonstrational projects are necessary to build confidence in the supply chain and demonstrate continuous operations. Moreover, the use of flexible carrier ships can turn CO_2 transport and storage into a profitable industry for countries which have significantly higher storage capacities than they require, particularly after the abolishment of the constraints previously posed by the London Protocol. Carbon dioxide shipping often has lower costs than the equivalent pipeline project, depending on size, location and duration of the project, as well as transport distances and pressure specifications, with ship and liquefaction dominating the costs. However, it is characterised by high operational expenditures and fuel costs and, therefore, carbon dioxide shipping exhibits its cost-effective potential relative to pipelines when short duration projects characterised by low flowrates and longer distances are considered.

The key challenges to be addressed are mainly operational, and include amendment of existing regulations, mainly the London Protocol - and the establishment of a viable business model. However, due to the lack of experience with carbon dioxide shipping at the required scale, demonstration projects will be required to meet port restrictions in preparation for the implementation of any dedicated infrastructure in the longer term. It is expected that government incentives and economic strategies will be essential to build momentum in the CO_2 shipping industry, especially because, unlike the LNG and LPG fields, carbon dioxide is perceived as a waste rather than a valuable product.

CO_2 shipping has the potential to extend de-carbonisation to those countries and industries where CCUS is essentially infeasible due to geographical or infrastructural reasons and reduce the cost of early projects through its sink-source matching, low up-front capital expenditure requirement and high degree of flexibility. With countries such as Japan, Norway and the UK now actively seeking to commercialise large scale CO_2 shipping as part of their decarbonisation strategies, near-future developments appear to be promising.

References

[1] Quéré C, Andrew R, Friedlingstein P, Sitch S, Hauck J, Pongratz J, et al. Global Carbon Budget 2018. Earth Syst Sci Data 2018;10:2141–94.

[2] Logan J, Venezia J, Larsen K, McQuale C. Opportunities and challenges for carbon capture and storage. WRI Issue Br Carbon Capture Sequestration 2007:1–8. https://www.wri.org/publication/opportunities-and-challenges-carbon-capture-and-sequestration

[3] Bui M, Adjiman CS, Bardow A, Anthony EJ, Boston A, Brown S, et al. Carbon capture and storage (CCS): The way forward. Energy Environ Sci 2018; 11:1062–176.

[4] IEA. Energy Technology Perspectives 2020 - Special Report on Carbon Capture Utilisation and Storage, CCUS in clean energy transitions, OECD Publishing, Paris, France: 2020. https://doi.org/10.1787/208b66f4-en. International Energy Agency

[5] IPCC. Climate Change 2014: Synthesis Report. Contribution of Working Groups I, II and III to the Fifth Assessment Report of the Intergovernmental Panel on Climate Change. https://www.ipcc.ch/site/assets/uploads/2018/05/SYR_AR5_FINAL_full_wcover.pdf

[6] IPCC. Summary for Policymakers: Global warming of 1.5°C. An IPCC Special Report on the impacts of global warming. 2018. International Panel of Climate Change. https://www.ipcc.ch/site/assets/uploads/sites/2/2019/05/SR15_SPM_version_report_LR.pdf

[7] Global CCS Institute. Global Status of CCS 2020. https://www.globalccsinstitute.com/resources/global-status-report/

[8] Neele F, Haugen HA, Skagestad R. Ship transport of CO_2 - Breaking the CO_2-EOR deadlock. Energy Procedia 2014; 63:2638–44.

[9] Hegerland G, Jørgensen T, Pande JO. Liquefaction and handling of large amounts of CO_2 for EOR. Greenh. Gas Control Technol., 2005, 2541–4.

[10] Zhang Z, Pan S, Li H, Cai J, Ghani A, John E, et al. Recent advances in carbon dioxide utilization. Renew Sustain Energy Rev 2020; 125:109799.

[11] IEA. IEA Energy technology perspectives 2010-scenarios and strategies to 2050, OECD Publishing. Paris, France: 2010. https://doi.org/10.1787/energy_tech-2010-en.

[12] Coussy P, Roussanaly S, Bureau–Cauchois G, Wildenborg T. Economic CO_2 network optimization model COCATE European Project (2010-2013). Ghgt-11 2013; 37:2923–31.

[13] DNV. Report Activity 5: CO_2 transport. 2012. Report No./DNV Reg No.: 2012-0076/ 13REPT4-2 - Det Norske Veritas.

[14] Seo Y, Huh C, Lee S, Chang D. Comparison of CO_2 liquefaction pressures for ship-based carbon capture and storage (CCS) chain. Int J Greenh Gas Control 2016; 52:1–12.

[15] Emma N. Major banks set new lending standards for shipping industry to cut CO_2 emissions. CNBC 2019. https://www.cnbc.com/2019/06/17/major-banks-set-new-lending-standards-for-shipping-industry-to-cut-co2-emissions.html (accessed July 3, 2019).

[16] Smith T, Jalkanen JP, Anderson BA, Corbett JJ, Faber J, Hanayama S., et al. Third IMO GHG Study 2014. International Maritime Organisation. https://www.imo.org/en/OurWork/Environment/Pages/Greenhouse-Gas-Studies-2014.aspx

[17] IMO. Fourth IMO GHG Study 2020. International Maritime Organisation https://safety4sea.com/wp-content/uploads/2020/08/MEPC-75-7-15-Fourth-IMO-GHG-Study-2020-Final-report-Secretariat.pdf

[18] Andersson K, Brynolf S, Lindgren J., Wilewska-Bien M. Shipping and its Environment-Improving Environmental Performance in Marine Transportation. Springer; Berlin, Heidelberg; 2016. https://doi.org/10.1007/978-3-662-49045-7

[19] Tournadre J. Anthropogenic pressure on the open ocean: The growth of ship traffic revealed by altimeter data analysis. Geophys Res Lett 2014; 41:7924–32.

[20] MAN B&W. Emission Control MAN B & W Two-stroke Diesel Engines. Copenhagen, Denmark: 1997. https://www.flamemarine.com/files/MANBW.pdf

[21] Balcombe P, Brierley J, Lewis C, Skatvedt L, Speirs J, Hawkes A, et al. How to decarbonise international shipping: Options for fuels, technologies and policies. Energy Convers Manag 2019; 182:72–88.

[22] Wang H, Zhou P, Wang Z. Reviews on Current Carbon Emission Reduction Technologies and Projects and their Feasibilities on Ships. J Mar Sci Appl 2017:129–36.

[23] Liang HL. What you need to know: The 2020 IMO fuel sulphur regulation. Seatrade Maritime News. Available at: www.seatrade-maritime.com; Accessed 16th April 2020.

[24] IMO. IMO. Prevention of Air Pollution from Ships. Int Marit Organ London 2017. http://www.imo.org/en/OurWork/Environment/PollutionPrevention/AirPollution/%0APages/Air-Pollution.aspx (accessed April 20, 2020).

[25] Lloyd's Register. Understanding exhaust gas treatment systems. Guidance for ship owners and operators. 2012. https://www.alfalaval.com.au/globalassets/documents/microsites/puresox/understanding_exhaust_gas_treatment_systems.pdf

[26] Svensson R, Odenberger M, Johnsson F, Strömberg L. Transportation systems for CO_2 - Application to carbon capture and storage. Energy Convers Manag 2004; 45:2343–53.

[27] Roussanaly S, Skaugen G, Aasen A, Jakobsen J, Vesely L. Techno-economic evaluation of CO_2 transport from a lignite-fired IGCC plant in the Czech Republic. Int J Greenh Gas Control 2017; 65:235–50.

[28] GCCSI. Strategic Analysis of the Global Status of Carbon Capture and Storage – Economic Assessment of Carbon Capture and Storage Technologies; 2009. Global Carbon Capture and Storage Institute.

[29] WorleyParsons. CCS learning from the LNG sector - A report for the Global CCS Institute. 2013. Report number: 401010-01060 – 00-PM-REP-0001. Global Carbon Capture and Storage Institute.

[30] Element Energy. CCS deployment at dispersed industrial sites; 2020. Department for Business Energy and Industrial Strategy; Research paper number 2020/030.

[31] Roussanaly S, Hognes ES, Jakobsen JP. Multi-criteria analysis of two CO_2 transport technologies. Energy Procedia 2013; 37:2981–8.

[32] Knoope MMJ, Ramírez A, Faaij APC. Investing in CO_2 transport infrastructure under uncertainty: A comparison between ships and pipelines. Int J Greenh Gas Control 2015; 41:174–93.

[33] Weihs GAF, Kumar K, Wiley DE. Understanding the economic feasibility of ship transport of CO_2 within the CCS chain. Energy Procedia, 2014;63:2630–7.

[34] ZEP. The Costs of CO_2 Transport Post-demonstration CCS in the EU; 2011. European Technology Platform for Zero Emission Fossil Fuel Power Plants, Zero Emissions Platform. Available at https://www.globalccsinstitute.com/resources/publications-reports-research/the-costs-of-co2-transport-post-demonstration-ccs-in-the-eu/

[35] Patchigolla K, Oakey JE. Design Overview of High-Pressure Dense Phase CO_2 Pipeline Transport in Flow Mode. Energy Procedia 2013; 37:3123–30.

[36] Prah B. Review of State of Art of Captured CO_2 pipeline Transportation Review of State of Art of Captured CO_2 pipeline Transportation 2016:1–3.

[37] Doctor R, Palmer A, Coleman D, Davison J, Hendriks C, Kaarstad O, et al. Chapter 4: Transport of CO_2. IPCC Spec Rep Carbon Dioxide Capture Storage; 2005:179–94.

[38] Ministry of Petroleum and Energy Norway, Gassco, Gassnova. Feasibility study for full-scale CCS in Norway. 2016. Available at: https://ccsnorway.com/wp-content/uploads/sites/6/2019/09/feasibilitystudy_fullscale_ccs_norway_2016.pdf

[39] Vermeulen TN. Knowledge sharing report – CO_2 Liquid Logistics Shipping Concept (LLSC): Overall Supply Chain Optimization 2011:143. Available at:

https://www.globalccsinstitute.com/resources/publications-reports-research/knowledge-sharing-report-co2-liquid-logistics-shipping-concept-business-model/

[40] Ozaki M, Ohsumi T, Kajiyama R. Ship-based Offshore CCS Featuring CO_2 Shuttle Ships Equipped with Injection Facilities. Energy Procedia 2013; 37:3184–90.

[41] Element Energy, TNO, Engineering Brevik, SINTEF, Polarkonsult. Shipping UK Cost Estimation Study; 2018. Available at: https://assets.publishing.service.gov.uk/government/uploads/system/uploads/attachment_data/file/761762/BEIS_Shipping_CO2.pdf

[42] Wong S. CO_2 Compression & Transportation to Storage Reservoir. In: Building Capacity for CO_2 Capture and Storage in the APEC Region, APEC Energy Working Group Project EWG 03/2004T, APEC Secretariat, Singapore, May, 2005.

[43] IPCC. IPCC special report on carbon dioxide capture and storage, prepared by Working Group III of the International Panel on Climate Change. 2005.

[44] Decarre S, Berthiaud J, Butin N, Guillaume-Combecave JL. CO_2 maritime transportation. Int J Greenh Gas Control 2010; 4:857–64.

[45] Roussanaly S, Jakobsen JP, Hognes EH, Brunsvold AL. Benchmarking of CO_2 transport technologies: Part I—Onshore pipeline and shipping between two onshore areas. Int J Greenh Gas Control 2013;19:584–94.

[46] Roussanaly S, Brunsvold AL, Hognes ES. Benchmarking of CO_2 transport technologies: Part II - Offshore pipeline and shipping to an offshore site. Int J Greenh Gas Control 2014.

[47] Onyebuchi VE, Kolios A, Hanak DP, Biliyok C, Manovic V. A systematic review of key challenges of CO_2 transport via pipelines. Renew Sustain Energy Rev 2017:1–21.

[48] Neele F, De Kler R, Nienoord M, Brownsort P, Koornneef J, Belfroid S, et al. CO_2 Transport by Ship: The Way Forward in Europe. Energy Procedia 2017; 114:6824–34.

[49] Svensson R, Odenberger M, Johnsson F, Strömberg L. Transportation infrastructure for CCS -Experiences and expected development. Greenh Gas Control Technol 2005:2531–4.

[50] Scottish Carbon Capture & Storage. CO_2 storage and Enhanced Oil Recover in the North Sea: Securing a low-carbon future for the UK. 2015. https://www.sccs.org.uk/images/expertise/reports/co2-eor-jip/SCCS-CO2-EOR-JIP-Report-SUMMARY.pdf

[51] Aspelund A, Jordal K. Gas conditioning—The interface between CO_2 capture and transport. Int J Greenh Gas Control 2007; 1:343–54.

[52] Mitsubishi Heavy Industries. Report on Ship Transport of CO_2. 2004; IEA Greenhouse Gas R&D Programme. https://ieaghg.org/docs/General_Docs/Reports/PH4-30%20Ship%20Transport.pdf

[53] Yoo BY, Choi DK, Kim HJ, Moon YS, Na HS, Lee SG. Development of CO_2 terminal and CO_2 carrier for future commercialized CCS market. Int J Greenh Gas Control 2013; 12:323–32.

[54] Brownsort P. Ship transport of CO_2 for Enhanced Oil Recovery – Literature Survey 2015;44. http://www.sccs.org.uk/images/expertise/reports/co2-eor-jip/SCCS-CO2-EOR-JIP-WP15-Shipping.pdf

[55] Jung JY, Huh C, Kang SG, Seo Y, Chang D. CO_2 transport strategy and its cost estimation for the offshore CCS in Korea. Energy Procedia 2013; 111:1054–60.

[56] Skagestad R, Eldrup N, Richard H, Belfroid S, Mathisen A, Lach A, et al. Ship transport of CO_2 - Status and Technology Gaps. Tel-Tek Report No. 2214090; Report prepared for Gassnova by Tel-Tek; 2014, 1-52.

[57] Aspelund A, Mølnvik MJ, De Koeijer G. Ship Transport of CO_2- Technical Solutions and Analysis of Costs, Energy Utilization, Exergy Efficiency and CO_2 Emissions. Chem Eng Res Des 2006; 84:847–55.

[58] Chiyoda Corporation, Global CCS Institute. Preliminary feasibility study on CO_2 carrier for ship-based CCS. 2011; Chiyoda:91048/GCCSI: CON163.

[59] Nam H, Lee T, Lee J, Lee J, Chung H. Design of carrier-based offshore CCS system: Plant location and fleet assignment. Int J Greenh Gas Control 2013; 12:220–30.

[60] Ozaki M, Ohsumi T. CCS from multiple sources to offshore storage site complex via ship transport. Energy Procedia 2011;4:2992–9.

[61] De Kler R, Neele F, Nienoord M, Brownsort P, Koornneef J, Belfroid S, et al. Transportation and unloading of CO_2 by ship - a comparative assessment WP9 Final Report. 2016.

[62] ZEP. Role of CCUS in a below 2 degrees scenario 2018:1–30. https://zeroemissionsplatform.eu/wp-content/uploads/ZEP-Role-of-CCUS-in-below-2c-report.pdf

[63] IEAGHG. The Status and Challenges of CO_2 Shipping Infrastructures. 2020; IEAGHG Technical Report 2020-10.

[64] Yara, Larvik Shipping, Polarkonsult. CO_2 ship transport study in support of full-scale CCS Chain evaluation in Norway. 2016.

[65] GCCSI. Preliminary Feasibility Study on CO_2 Carrier for Ship-based CCS （Phase-2 unmanned offshore facility. 2012; https://www.globalccsinstitute.com/resources/publications-reports-research/preliminary-feasibility-study-on-co2-carrier-for-ship-based-ccs-phase-2-unmanned-offshore-facility/.

[66] Department of Energy and Climate Change. CCS Roadmap. Supporting deployment of Carbon Capture and Storage in the UK; 2012.

[67] Koers P, Maarten de Looij. Safety Study for Liquid Logistics Shipping Concept. 2011;. Rotterdam, Det Norske Veritas BV. Report number: 12TUIBY-3.

[68] Roussanaly S, Bureau-cauchois G, Husebye J. Costs benchmark of CO_2 transport technologies for a group of various size industries. Int J Greenh Gas Control 2013; 12:341–50.

[69] Brownsort P. Offshore offloading of CO_2 - Review of single mooring types and sustainability. 2015; https://era.ed.ac.uk/bitstream/handle/1842/15712/SCCS-CO2-EOR-JIP-Offshore-offloading.pdf?sequence=1&isAllowed=y

[70] Aspelund A, Gundersen T. A liquefied energy chain for transport and utilization of natural gas for power production with CO_2 capture and storage - Part 1. Appl Energy 2009; 86:781–92.

[71] Brevik P. The full scale CCS-project at Norcem Brevik Can it be realised? In: Powerpoint presentation, HeidelbergCement; 2017; https://www.sintef.no/globalassets/sintef-energi/cemcap/11_full-scale_ccs-project_norcem_brevik.pdf

[72] Zahid U, An J, Lee CJ, Lee U, Han C. Design and operation strategy of CO_2 terminal. Ind Eng Chem Res 2015; 54:2353–65.

[73] Energy Institute. General Properties and Uses of Carbon Dioxide, Good Plant Design and Operation for Onshore Carbon Capture Installations and Onshore Pipelines - A Recommended Practice Guidance Document. 2010; https://www.globalccsinstitute.com/archive/hub/publications/7276/good-plant-design-and-operation-onshore-carbon-capture-installations-and-onshore-pipelines.pdf

[74] Scottish Development International, Scottish Enterprise. Carbon Capture and Storage - CO_2 transport options for Scotland. 2011; https://www.sccs.org.uk/images/expertise/misc/CO2-Transport-Options-for-Scotland.pdf

[75] Polarkonsult, Praxair, Larvik Shipping. Concept study of CO_2 transport by ship, as part of the Norwegian CCS Demonstration Project. 2017.

[76] Haugen HA, Eldrup N, Bernstone C, Liljemark S, Pettersson H, Noer M, et al. Options for transporting CO_2 from coal fired power plants Case Denmark. Energy Procedia 2009; 1:1665–72.

[77] European Commission. GATEWAY Report Summary – Developing a Pilot Case aimed at establishing a European infrastructure project for CO_2 transport. Project ID: 657263. 2016.

[78] Global CCS Institute. The Global Status of CCS. 2018.

[79] Morbee J, Serpa J, Tzimas E. Optimal planning of CO_2 transmission infrastructure: The JRC InfraCCS tool. Energy Procedia 2011; 4:2772–7.

[80] GCCSI. Transport & Storage Economics of CCS Networks in the Netherlands. 2013. Global Carbon Capture and Storage Institute; https://www.globalccsinstitute.com/archive/hub/publications/101121/transport-storage-economics-ccs-networks-netherlands.pdf

[81] Skagestad R, Mathisen A, Eldrup NH, Haugen HA. CO_2 transport from sources to storage in the Skagerrak/Kattegat region. Energy Procedia 2011; 4:3016–23.

[82] Kjärstad J, Skagestad R, Eldrup NH, Johnsson F. Ship transport—A low cost and low risk CO_2 transport option in the Nordic countries. Int J Greenh Gas Control 2016; 54:168–84.

[83] Equinor, Shell, Total. Northern Lights Project Description; 2020. Available at: https://northernlightsccs.com/en/about Accessed 19th Novemeber 2020.

[84] Pale Blue Dot Energy. Acorn CO2 SAPLING Transport and Infrastructure Project Flyer 2018.

[85] Kokubun N, Ko K, Ozaki M. Cargo conditions of CO_2 in shuttle transport by ship. Energy Procedia 2013; 37:3160–7.

[86] Al-Siyabi I. Effect of impurities on CO_2 stream Properties. PhD Thesis, Department of Petroleum Engineering, Heriot-Watt University, 2013.

[87] Wang J, Ryan D, Anthony EJ, Wildgust N, Aiken T. Effects of impurities on CO_2 transport, injection and storage. Energy Procedia 2011; 4:3071–8.

[88] Munkejord ST, Hammer M, Løvseth SW. CO_2 transport: Data and models - A review. Appl Energy 2016; 169:499–523.

[89] Austegard A, Solbraa E, De Koeijer G, Mølnvik MJ. Thermodynamic Models for Calculating Mutual Solubilities in H_2O–CO_2–CH_4 Mixtures. Chem Eng Res Des 2006; 84:781–94.

[90] Chapoy A, Burgass R, Tohidi B. Effect of Common Impurities on the Phase Behavior of Carbon-Dioxide-Rich Systems: Minimizing the Risk of Hydrate Formation and Two-Phase Flow. SPE J 2011:921–30.

[91] Wetenhall B, Aghajani H, Chalmers H, Benson SD, Ferrari MC, Li J, et al. Impact of CO_2 impurity on CO_2 compression, liquefaction and transportation. Energy Procedia 2014; 63:2764-78.

[92] Span R, Gernert J, Jäger A. Accurate thermodynamic-property models for CO_2-rich mixtures. Energy Procedia 2013; 37:2914–22.

[93] Lovseth SW, Skaugen G, Jacob Stang HG, Jakobsen JP, Wilhelmsen Ø, Span R, et al. CO_2 Mix project: Experimental determination of thermo physical properties of CO_2-rich mixtures. Energy Procedia 2013; 37:2888–96.

[94] Li H, Jakobsen JP, Wilhemsen O, Yan J. PVTxy properties of CO_2 mixtures relevant for CO_2 capture, transport and storage: Review of available experimental data and theoretical models. Appl Energy 2011; 88:3567–79.

[95] Engel F, Kather A. Conditioning of a Pipeline CO_2 Stream for Ship Transport from Various CO_2 Sources. Energy Procedia 2017; 114:6741–51.

[96] Stouffer CE, Kellerman SJ, Hall KR, Holste JC, Gammon BE, Marsh KN. Densities of carbon dioxide + hydrogen sulfide mixtures from 220 K to 450 K at pressures up to 25 MPa. J Chem Eng Data 2001; 46:1309–18.

[97] Rivas C, Blanco ST, Fernández J, Artal M, Velasco I. Influence of methane and carbon monoxide in the volumetric behaviour of the anthropogenic CO_2: Experimental data and modelling in the critical region. Int J Greenh Gas Control 2013; 18:264–76

[98] Blanco ST, Rivas C, Bravo R, Fernández J, Artal M, Velasco I. Discussion of the influence of CO and CH_4 in CO_2 transport, injection, and storage for CCS technology. Environ Sci Technol 2014; 48:10984–92.

[99] Ahmad M, Gersen S. Water solubility in CO_2 mixtures: Experimental and modelling investigation. Energy Procedia 2014; 63:2402–11.

[100] Chapoy A, Mohammadi AH, Chareton A, Tohidi B, Richon D. Measurement and Modeling of Gas Solubility and Literature Review of the Properties for the Carbon Dioxide−Water System. Ind Eng Chem Res 2004; 43:1794–802.

[101] Song KY, Kobayashi R. Water Content of CO_2 in Equilibrium with Liquid Water and/or Hydrates. SPE Form Eval 1987; 2:500–8.

[102] Heggum G, Weydahl T, Mo R, Mølnvik M, Austegaard A. CO2 Conditioning and Transportation. Carbon Dioxide Capture Storage Deep Geol. Form., 2005, 925–36.

[103] Seiersten M. Materials Selection for Separation, Transportation and Disposal of CO_2. Corrosion 2001, NACE International, Houston, Texas.

[104] Luís Manuel Cravo Pereira, Kapateh M, Chapoy A. Impact of impurities on thermophysical properties and dehydration requirements of CO_2 -rich systems in CCS. UKCCSRC Biannual Meetiing Cambridge Univ 2014:2–3.

[105] SNC-Lavin Inc. Impact of impurities on CO2 capture, transport and storage. 2004; Report number PH4/32; IEA Greenhouse Gas R&D Programme.

[106] Ansaloni L, Alcock B, Peters TA. Effects of CO_2 on polymeric materials in the CO_2 transport chain: A review. Int J Greenh Gas Control 2020; 94:102930.

[107] De Visser E, Hendriks C, de Koeijer G, Barrio M, Liljemark S, Austegard A, et al. DYNAMIS CO_2 quality recommendations. 2007; Dynamics; Project no: 019672.

[108] Lilliestrale A, Mølnvik MJ, Tangen G, Jakobsen JP, Munkejord ST, Morin A, et al. The IMPACTS project: The impact of the quality of CO_2 on transport and storage behaviour. Energy Procedia 2013; 51:402–10.

[109] Brown S, Martynov S, Mahgerefteh H, Fairweather M, Woolley RM, Wareing CJ, et al. CO2QUEST: Techno-economic assessment of CO_2 quality effect on its storage and transport. Energy Procedia 2014; 63:2622–9.

[110] NETL. Quality guidelines for energy system studies - CO2 Impurity Design Parameters; 2012. National Energy Technology Laboratory. Available at: https://www.osti.gov/biblio/1566771-quality-guidelines-energy-system-studies-co2-impurity-design-parameters

[111] Engel F, Kather A. Improvements on the liquefaction of a pipeline CO_2 stream for ship transport. Int J Greenh Gas Control 2018; 72:214–21.

[112] SE. Carbon Capture and Storage - CO2 transport options for Scotland; 2011. Scottish Enterprise. Available at: https://www.sccs.org.uk/images/expertise/misc/CO2-Transport-Options-for-Scotland.pdf

[113] Kang K, Seo Y, Chang D, Kang SG, Huh C. Estimation of CO_2 transport costs in South Korea using a techno-economic model. Energies 2015; 8:2176–96.

[114] Jakobsen J, Roussanaly S, Anantharaman R. A techno-economic case study of CO_2 capture, transport and storage chain from a cement plant in Norway. J Clean Prod 2017;144.

[115] Yoo BY, Lee SG, Rhee KP, Na HS, Park JM. New CCS system integration with CO_2 carrier and liquefaction process. Energy Procedia 2011; 4:2308–14.

[116] Yoo B. The development and comparison of CO_2 BOG re-liquefaction processes for LNG fueled CO_2 carriers. Energy 2017; 127:186–97.

[117] Zahid U, An J, Lee C, Lee U, Han C. Design and Operation Strategy of CO_2 Terminal. Ind Eng Chem Res 2015; 54:2353–65.

[118] MHI. Ship transport of CO_2; 2004. Mitsubishi Heavy Industries – IEA Greenhouse Gas R&D Programme. https://ieaghg.org/docs/General_Docs/Reports/PH4-30%20Ship%20Transport.pdf

[119] Roussanaly S, Bureau-cauchois G, Husebye J. International Journal of Greenhouse Gas Control Costs benchmark of CO_2 transport technologies for a group of various size industries. Int J Greenh Gas Control 2013; 12:341–50.

[120] Haugen HA, Eldrup N, Bernstone C, Liljemark S, Pettersson H, Noer M, et al. Options for transporting CO_2 from coal fired power plants Case Denmark. Energy Procedia 2009; 1:1665–72.

[121] Kemper J, Sutherland L, Watt J, Santos S. Evaluation and analysis of the performance of dehydration units for CO_2 capture. Energy Procedia 2014; 63:7568–84.

[122] Øi LE, Fazlagic M. Glycol dehydration of Capture Carbon Dioxide Using Aspen Hysys Simulation 2014; Telemark Univerisry College, Department of Process, Energy and Environmental Technology

[123] Seo Y, You H, Lee S, Huh C, Chang D. Evaluation of CO_2 liquefaction processes for ship-based carbon capture and storage (CCS) in terms of life cycle cost (LCC) considering availability. Int J Greenh Gas Control 2015; 35:1–12.

[124] Øi LE, Eldrup N, Adhikari U, Bentsen MH, Badalge JL, Yang S. Simulation and cost comparison of CO_2 liquefaction. Energy Procedia 2016; 86:500–10.

[125] Alabdulkarem A, Hwang Y, Radermacher R. Development of CO_2 liquefaction cycles for CO_2 sequestration. Appl Therm Eng 2012;33–34:144–56.

[126] Deng H, Roussanaly S, Skaugen G. Techno-economic analyses of CO_2 liquefaction: Impact of product pressure and impurities. Int J Refrig 2019; 103:301–15.

[127] Lee U, Lim Y, Lee S, Jung J, Han C. CO_2 storage terminal for ship transportation. Ind Eng Chem Res 2012;51:389–97.

[128] Aspelund A, Sandvik TE, Krogstad H, De Koeijer G. Liquefaction of captured CO_2 for ship-based transport. Greenh. Gas Control Technol., 2005, 2545–9.

[129] Deng H, Roussanaly S, Skaugen G. Better understanding of CO2 liquefaction (Towards identifying optimal transport conditions for ship-based

CCS). SINTEF Blog 2019. https://blog.sintef.com/sintefenergy/co2-liquefaction-transport-conditions-ship-based-ccs/ (Accessed Sept 13th 2019)

[130] Lee SG, Choi GB, Lee JM. Optimal Design and Operating Conditions of the CO_2 Liquefaction Process, Considering Variations in Cooling Water Temperature. Ind Eng Chem Res 2015; 54:12855–66.

[131] Engel F, Kather A. Improvements on the liquefaction of a pipeline CO_2 stream for ship transport. Int J Greenh Gas Control 2018; 72:214–21.

[132] Haugen HA, Eldrup NH, Fatnes AM, Leren E. Commercial Capture and Transport of CO_2 from Production of Ammonia. Energy Procedia 2017; 114:6133–40.

[133] Lee U, Lim Y, Lee S, Jung J, Han C. CO_2 storage terminal for ship transportation. Ind Eng Chem Res 2012; 51:389–97.

[134] Seo Y, Lee S yeob, Kim J, Huh C, Chang D. Determination of optimal volume of temporary storage tanks in a ship-based carbon capture and storage (CCS) chain using life cycle cost (LCC) including unavailability cost. Int J Greenh Gas Control 2017; 64:11–22.

[135] Koornneef J, Ramírez A, Turkenburg W, Faaij A. The environmental impact and risk assessment of CO_2 capture, transport and storage - An evaluation of the knowledge base. Prog Energy Combust Sci 2012; 38:62–86.

[136] Seo Y, Huh C, Lee S, Chang D. Comparison of CO_2 liquefaction pressures for ship-based carbon capture and storage (CCS) chain. Int J Greenh Gas Control 2016; 52:1–12.

[137] Yamamoto M, Wada R, Kamizawa K, Takagi K. The Concept of FLT. Mar Syst Ocean Technol 2017; 12:104–16.

[138] Liu Y, Ye Q, Shen M, Shi J, Chen J, Pan H, et al. Carbon dioxide capture by functionalized solid amine sorbents with simulated flue gas conditions. Environ Sci Technol 2011; 45:5710–6.

[139] Skagestad R, Eldrup N, Richard H, Belfroid S, Mathisen A, Lach A, et al. Ship transport of CO_2 – Status and Technology Gaps; 2014. Gassnova, TelTek report no. [2214090].

[140] Witkowski A, Majkut M. General Physical Properties of CO_2 in Compression and Transportation Processes. In: Advances in Carbon Dioxide Compression and Pipeline Transportation Processes. SpringerBriefs in Applied Sciences and Technology. Springer, Cham 2015.

[141] Liane S, Billingham M, Barraclough C, Lee C-H, Milanovic D, Peralta-Solario D, et al. Corrosion and Selection of Materials for Carbon Capture and Storage. 2010. IEAGHG Report: 2010/03.

[142] Choi Y-S, Nesic S. Determining the corrosive potential of CO_2 transport pipeline in high pCO_2 – water environments. Int J Greenh Gas Control 2011; 5:788–97.

[143] Norsok. Qualification of non-metallic sealing materials and manufacturers. 1994; Report number: M-CR-710

[144] Ho E. Elastomeric seals for rapid gas decompression applications in high - pressure services. Heal Saf Exec BHR Gr Limited, Res Rep No 485 2006:1–74.

[145] Hasan MMF, Zheng AM, Karimi IA. Minimizing boil-off losses in liquefied natural gas transportation. Ind Eng Chem Res 2009; 48:9571–80.

[146] Gerdsmeyer K-D, Isalski W. On-board reliquefaction for LNG ships. 2005. Tractebel Gas Engineering

[147] Jeon SH, Choi YU, Kim MS. Review on Boil-Off Gas (BOG) Re-Liquefaction System of Liquefied CO_2 Transport Ship for Carbon Capture and Sequestration (CCS). Int J Air-Conditioning Refrig 2016; 24:1–10.

[148] Chu B, Chang D, Chung H. Optimum liquefaction fraction for boil-off gas reliquification system of semi-pressurized liquid CO_2 carriers based on economic evaluation. Int J Greenh Gas Control 2012; 10:46–55.

[149] Wartsila. Boil-Off Gas handling onboard LNG fuelled ships 2017. https://www.wartsila.com/twentyfour7/in-detail/boil-off-gas-handling-onboard-lng-fuelled-ships (accessed October 20, 2017).

[150] Hamworthy Ltd. LPG Cooling and Reliquefaction Hamworthy Brochure. Asker, Norway: 2007.

[151] Gómez JR, Gómez MR, Garcia RF, Catoira DM. On board LNG reliquefication technology: a comparative study. Polish Marit Res 2014; 21:77–88.

[152] Awoyomi A, Patchigolla K, Anthony EJ. CO_2/SO_2 emission reduction in CO2 shipping infrastructure. Int J Greenh Gas Control 2019; 88:57–70.

[153] Awoyomi A, Patchigolla K, Anthony EJ. Process and Economic Evaluation of an Onboard Capture System for LNG-Fueled CO_2 Carriers. Ind Eng Chem Res 2020; 59:6951–60.

[154] Ciferno JP, DiPietro P, Tarka T. An economic scoping study for CO_2 capture using aqueous ammonia. Final Report, Natl Energy Technol Lab US Dep Energy, Pittsburgh, PA 2005.

[155] Li H, Jakobsen JP, Stang J. Hydrate formation during CO_2 transport: Predicting water content in the fluid phase in equilibrium with the CO_2-hydrate. Int J Greenh Gas Control 2011; 5:549–54.

[156] Energy Institute. Hazard analysis for offshore carbon capture platforms and offshore pipelines. London: 2013.

[157] Martin Trusler JP. Equation of State for Solid Phase I of Carbon Dioxide Valid for Temperatures up to 800 K and Pressures up to 12 GPa. J Phys Chem Ref Data 2011;40.

[158] Harper P, Wilday J, Bilio M. Assessment of the major hazard potential of carbon dioxide. 2015; Health and Safety Executive.

[159] Noh H, Kang K, Huh C, Kang SG, Seo Y. Identification of potential hazardous events of unloading system and CO_2 storage tanks of an intermediate storage terminal for the Korea clean carbon storage project 2025. Int J Saf Secur Eng 2018; 8:258–65.

[160] DNV. Design and Operation of CO_2 Pipelines. 2010; Det Net Norske; DNV-RP-J202; https://www.ucl.ac.uk/cclp/pdf/RP-J202.pdf

[161] Brown A, Eickhoff C, Reinders JEA, Raben I, Spruijt M, Neele F. IMPACTS: Framework for Risk Assessment of CO_2 Transport and Storage Infrastructure. Energy Procedia 2017; 114:6501–13.

[162] Han SH, Chang D, Kim J, Chang W. Experimental investigation of the flow characteristics of jettisoning in a CO_2 carrier. Process Saf Environ Prot 2014; 92:60–9.

[163] Pursell M. Experimental investigation of high-pressure liquid CO_2 release. IChemE 2012; Hazard XXI:164–71.

[164] Li M, Liu Z, Zhou Y, Zhao Y, Li X, Zhang D. A small-scale experimental study on the initial burst and the heterogeneous evolution process before CO_2 BLEVE. J Hazard Mater 2018; 342:634–42.

[165] Tosse S, Vaagsaether K, Bjerketvedt D. An experimental investigation of rapid boiling of CO_2. Shock Waves 2015; 25:277–82.

[166] Van der Voort MM, van Wees RMM, Ham JM, Spruijt MPN, van den Berg AC, de Bruijn PCJ, et al. An experimental study on the temperature dependence of CO_2 explosive evaporation. J Loss Prev Process Ind 2013; 26:830–8.

[167] Bjerketvedt D, Egeberg K, Ke W, Gaathaug A, Vaagsaether K, Nilsen SH. Boiling liquid expanding vapour explosion in CO_2 small scale experiments. Energy Procedia 2011; 4:2285–92.

3 TECHNICAL QUALIFICATION OF ELASTOMER MATERIALS FOR CO_2 TRANSPORT SYSTEMS

Hisham Al Baroudi, Kumar Patchigolla, Stefano Mori, John E Oakey

School of Water, Energy and Environment (SWEE), Cranfield University, Cranfield, MK43 0AL, UK.

This has been accepted for poster presentation at the GHGT-15 conference; paper is drafted for submission to the Special Issue (GHGT-15) of the IJGGC

Statement of contributions of joint authorship

Hisham Al Baroudi proposed the characterisation methodology under pipeline conditions, performed characterisation under pipeline conditions (except for hardness measurements), conceptualised testing schedule under shipping conditions, performed the experiments under shipping conditions, characterised the generated samples, analysed the data and wrote this manuscript, "***Technical qualification of elastomer materials for CO_2 transport systems"***. Testing of elastomers under pipeline conditions was not performed by Hisham Al Baroudi. Kumar Patchigolla and John Oakey completed testing of elastomer materials under pipeline conditions, provided ongoing supervision throughout the project. Stefano Mori critically commented on the drafted manuscript before submission to peer-reviewed journal (still to be submitted)

Abstract

Carbon Capture, Utilisation and Storage has been identified as an essential technology to reduce anthropogenic greenhouse gas emissions and limit the average global temperature rise below the 2°C target. Upon capture from power and industrial emitters, CO_2 is transported to geological storage locations by means of pipeline networks or sea carriers. Considerations on the performance of transportation and conditioning materials, including propensity for corrosion, elastomers degradation and their mechanisms are some key engineering challenges to be considered for the implementation of CO_2 transport systems. Therefore, this work proposes a methodology to qualify the performance of elastomer materials undergoing prolonged (50 – 400 h) exposure to supercritical CO_2 conditions (9.5 MPa, 318 K) typical of pipelines and refrigerated, liquid CO_2 loading and offloading cycles (20 – 100) representative of shipping batch operations. Under pipeline conditions, Ethylene Propylene demonstrates

suitable performance attributed to the limited interaction with the polar fluid, suggesting a significant potential for implementation in future CO_2 pipeline projects. Neoprene and Buna exhibit signs of significant alterations to their structure and mechanical properties including shore A hardness as a result of the exposure. Conversely, Viton showed to be an unsuitable material choice due to its high propensity for rapid gas decompression damage, resulting in the formation of cracks in the scrutinised samples. Regarding CO_2 shipping testing, scrutinised Ethylene Propylene Diene Monomer displays satisfactory performance, manifested as excellent resistance to rapid gas decompression cycles, low Compression Set and moderate alterations to mechanical properties as a result of the performed CO_2 loading cycles

3.1 Introduction

In recent years, Carbon Capture, Utilisation and Storage (CCUS) has been widely recognised as an essential technology to reduce CO_2 emissions in the atmosphere by existing power and industrial emitters that would otherwise continue releasing 8 Gt CO_2 in 2050 [1]. CCUS consists in the capture of carbon emissions from sources such as power and industrial plants, and transmission for either utilisation or permanent storage in offshore geological formations. Upon continuous capture at emitting sources, carbon dioxide is required to be transmitted to sinks for permanent storage [2]. Selection of appropriate transport options for the captured CO_2 is dependent on a number of techno-economic and geographical considerations and considerably influenced by factors such as project location, sink-source distance and scale of the project [3]. When the economy of scale does not justify the construction of a pipeline infrastructure – characterised by a high capital expenditure and linear dependency with transport distance – ships represent the viable alternative [4]. Ships are characterised by a greater flexibility in sink-source matching, requiring relatively lower capital investments albeit higher operational costs [5]. Pipelines are considered optimal to transmit large volumes over relatively short distances - typically in the dense phase or supercritical state at ~8.4 MPa and 304 K [6] – and are particularly indicated when a constant throughput of inventory is guaranteed by the project; conversely, ships enable decarbonisation of scattered and relatively smaller emitters over long transport distances [3,5]. Operating conditions of sea vessels are found to be cost-effective under either low pressure and temperature (0.6 – 1 MPa, 218 - 233 K) [4,7,8] or at medium pressure and temperature conditions (1.6 – 2.1 MPa, 243 – 253 K) [8,9]. Both the indicated condition boundaries are found to

have a profound impact on the supply chain of CO_2 shipping projects, including selection of appropriate materials, safety protocols and assessment of operational complexity [8]. The supply chain of sea carriers is of intermittent nature and combines continuous processes - namely stream liquefaction, direct injection - with batch wise operations (storage, loading, ship transport) as summarised in Figure 3-1.

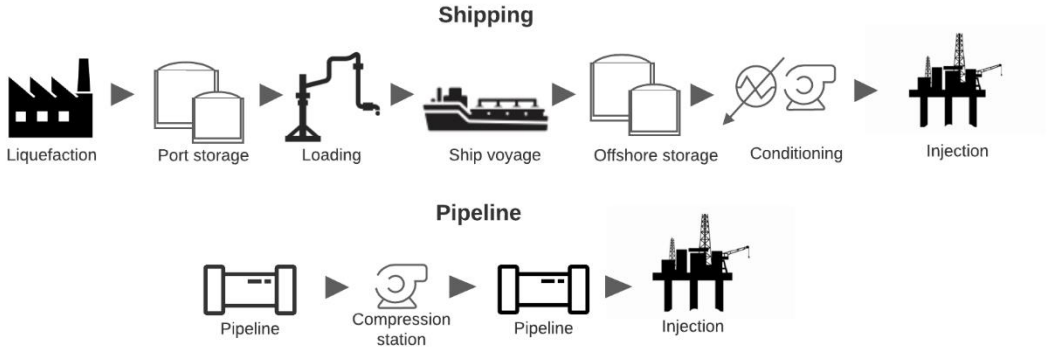

Figure 3-1: Schematic overview of the CO_2 transport chain

Conversely, pipeline transport is represented by a constant and continuous flow of dense phase CO_2 from source to sink, through periodic pumping stations [10]. Process safety exerts a crucial role in the implementation of transport solution, and integrity of the system and avoidance of loss of containment due to components failure is essential to preserve the captured capacity all the way to the storage sites. In these regards, selection of appropriate materials throughout the chain is crucial, particularly given the range of operational conditions and compatibility requirements that materials must have with the CO_2-rich environment [11]. Whilst relatively more attention has been dedicated to characterising the performance of metallic components and their propensity for corrosion and degradation [12], there is still a high degree of uncertainty around the interaction between polymeric and elastomer materials and CO_2-rich mixtures across the chain [11,13]. Moreover, depending on the source of CO_2 emission and the implemented carbon capture technology the CO_2-rich stream can be expected to be 90 – 99 vol% carbon dioxide, with the remainder being made up of other contaminants as established in the DYNAMIS project [14]. The project summarised typical concentration of impurities encountered in CCUS projects and the associated technical limitations Table 3-1.

Table 3-1: Stream composition specifications as described by DYNAMIS project [14]

Component	Concentration	Limitation
H_2O	500 ppm	Lower than solubility range of H_2O in CO_2
H_2S	100-200 ppm	Health and Safety evaluation
CO	1200-2000 ppm	Health and Safety evaluation
O_2	Aquifer < 4 vol% E.O.R. 100-1,000 ppm	Due to absence of experimental findings on effect of oxygen underground
CH_4	Aquifer < 4 vol% E.O.R. < 2 vol%	Based on previous projects
N_2	< 4 vol%	Based on previous project
Ar	< 4 vol%	Based on previous project
H_2	< 4 vol%	Limits the energy requirement in the chain
SOx	100 ppm	Health and Safety evaluation
NOx	100-200 ppm	Health and Safety evaluation
CO_2	>95.5%	

Therefore, particular attention should be committed in the selection of valve and other seals susceptible to operations in CO_2 transport systems. Elastomers are thereby used throughout the transport chain as seals, flexible hoses or valve sleeves due to their elastic nature and soft, incompressible properties [13]. Their exposure to environments typical of CO_2 transport can lead to chemical degradation and structural changes that can alter their performance and suitability [13]. The Energy Institute [11] reported that elastomers such as nitrile rubber, chloroprene and fluorocarbon are inadequate for CO_2 application due to excessive swell in use and loss of mass by extraction. Conversely, ethylene propylene diene monomer (EPDM) and ethylene propylene (EP) compounds are deemed suitable and associated with modest levels of swelling and mass loss. Menon et al. [15] investigated the compatibility of several polymers including Buna, Viton, polytetrafluoroethylene (PTFE), Neoprene and EPDM at conditions typical of sCO_2 for power generation (373 K and 25 MPa). The study highlighted the presence of physical and chemical effects on the materials as a result of the exposure. Fluorine-based elastomers showed a slower diffusion of CO_2 throughout the free volume, while EPDM and copolymers showed little interaction with the fluid due to their non-polar nature. Conversely, thermoplastics exhibited the least molecular changes, swelling and shift in glass transition temperature. Generally, Viton reports high levels of swelling in CO_2 due to chemical affinity with fluorine, complemented with a permanent degradation of mechanical properties [11,13,16] but a satisfactory performance with respect to

impurities such as H_2S and SO_2 [13]. Buna is implemented in the oil and gas industry and tends to be associated with moderate volumetric uptake in carbon dioxide environments; however, long-term change in mechanical properties can be encountered during the exposure.

As a general consideration, Neoprene reportedly presents low levels of swelling in CO_2-rich environments albeit high susceptibility to SOx interaction [13,15]. Hertz III [17] investigated the swelling behaviour of different type of elastomers – namely several types of EPDM, and FKM - in pressurised CO_2 at 5 MPa and found that EPDM exhibited the least amount of swelling, while Viton and FKM showed the highest amount. It is found that the addition of parts per hundred rubber (PHR) of carbon black significantly decreases the amount of swelling caused by exposure to CO_2 during post rapid gas decompression (RGD) conditions. In a different work [18], the author explored the performance of hydrogenated nitrile rubber (HNBR) in CO_2 at 5 MPa and found that the amount of curative additives inside the material and the level of acrylonitrile content can greatly reduce the propensity for swelling consequent to RGD. Lainé et al. [19] scrutinised the effect of high-pressure CO_2 (2-6 MPa) at variable temperatures (333 – 403 K) on the mechanical properties of FKM and HNBR materials and found the latter to be performing better, showing limited degradation of the material's mechanical properties. Accordingly, Ho [20] found that high concentrations of CO_2 can remarkably alter the mechanical properties of FKM elastomers at temperatures up to 353 K. One of the main failure mechanisms for elastomers in CO_2-rich environment arises from RGD damage [13,16,20] which can cause the formation of cracks and blisters on the cross sections of the material as a result of uncontrolled depressurisation, causing the seal to fail. Ho [20] reported that propensity for seal failure due to RGD is greatly dependent on type of material and enhanced by increasing operating pressures and temperatures. Generally, the suitability of elastomer materials that show potential to be implemented in the CO_2 transmission chain - such as EPDM - is largely derived from the experience matured in the oil and gas industry and lacks application-specific scrutiny relative to CCUS [13]. The compounds are characterised by a low level of volume uptake in carbon dioxide and a remarkable resistance to CO_2-related RGD [13,21] but specific scrutiny in a range of CO_2 transport conditions is still required. There appears to be limited knowledge on the influence of contaminants typical of real capture scenarios on the performance and reliability of elastomer materials in dense or liquid phase CO_2; this

makes it therefore essential to consider the effect and impact that such impurities can have on the performance and integrity of elastomer materials in the chain. Water in itself isn't anticipated to have a significant impact on the performance of polymers [13]; however, significant presence of free water can combine with carbon dioxide to generate carbonic acid, which can in turn combine with other contaminants – such as SO_x and NO_X - generating nitric and sulphuric acids that can weaken the material's structure. At concentrations below 2000 ppm, the majority of elastomer materials are deemed to be relatively stable with H_2S [13], although it is asserted that the presence of this compound can reduce the polymer's degradation temperature leading to chemical ageing and modification of the permeation [20].

Generally, limited studies in the literature focus on the performance of materials at temperatures in proximity of carbon dioxide triple point (~216 K) typical of sea vessel transport. The impact of pressure and temperature cycling during CO_2 loading and offloading operations - representative of the batch-wise nature of shipping chain - is not well understood in relation to the mechanical stability and propensity for RGD of polymers [13]. In response to these knowledge gaps, this work presents a characterisation methodology for the qualification of elastomer materials for CO_2 transport systems. In the first part of the work, four types of elastomers – namely Buna, Neoprene, EP and Viton – previously undergoing prolonged exposure (up to 400 h) to supercritical CO_2 (~9 MPa, 318 K) and contaminants (saturated H_2O, 500 ppm of H_2S/SO_2), are characterised with the aim of assessing their suitability in a CO_2 pipeline environment. In the second part, EPDM seals are selected for a series (20 – 100) compression and decompression cycles under CO_2 shipping conditions and characterised using the previously developed methodology with the aim of assessing the material's mechanical stability and propensity for RGD during real shipping operations. Findings from this work are intended to advise the designer on the performance and suitability of elastomer materials for CO_2 transport systems.

3.2 Materials and methods

For the CO_2 pipeline tests, a set from a Swagelok R3A pressure relief valve comprising two O-rings with different internal diameter and thickness, and PTFE-sprayed quadratic seals with coating applied to confer low-friction non-stick properties were selected for the experimental campaign. Viton, also known as Fluorocarbon FKM, is a type of fluoroelastomer characterised by strong bonding among the carbon and fluorine atoms

and a saturated, single-bond carbon backbone structure. Buna, also known as Nitrile Butadiene Rubber, is a synthetic rubber copolymer of acrylonitrile (ACN) and butadiene. Properties such as glass transition temperature, CO_2 diffusion and solubility in NBR are greatly dependant on the ACN content; resistance to nonpolar solvents improves with higher acrylonitrile content, although a lower ACN content results in a lower glass transition temperature, enabling flexibility at low temperatures [21]. Neoprene belongs to the family of chloroprene polymers, and it is synthetic compound generated through the polymerisation of chloroprene. CO_2 shipping testing in this work considered the selection of EPDM as candidate testing elastomer; the choice was primarily based on the satisfactory performance exhibited by EP under pipeline conditions and the promising chemical compatibility of the material in CO_2-rich environments [11,13,15,16]. In addition, the improved low temperature range of the material - which has a glass transition temperature in the range of CO_2 – makes it a potentially relevant to be implemented throughout the CO_2 shipping chain where operating temperatures can be as low as 221 K [8]. O-rings with thickness of 5 mm were selected to permit the performance of Compression Set testing during the experimental campaign amongst the others. EP and EPDM are copolymers of ethylene and propylene – with added diene monomer in case of EPDM - suitable in low-temperature applications due to flexibility and low glass-transition temperatures [15]. Specifications and summary of the selected elastomers and geometries for both tests is summarised in Table 3-2.

Table 3-2: Summary of type and geometry of selected elastomer seals for CO_2 pipeline and shipping tests

Tests	Materials	Geometry	Thickness (mm)	Internal diameter (mm)
CO_2 pipeline	Buna	O-ring	1.8	14
	Viton		2.7	4.4
	Neoprene EP	Quad seal*	2.3*	4.6*
CO_2 shipping	EPDM	O-ring	5	6

*** PTFE-sprayed quadratic seal**

Figure 3-2 provides an overview of the workflow and boundaries of this work; as highlighted, a material characterisation methodology is implemented to qualify both previously exposed materials under CO_2 pipeline and newly tested samples under CO_2 shipping conditions.

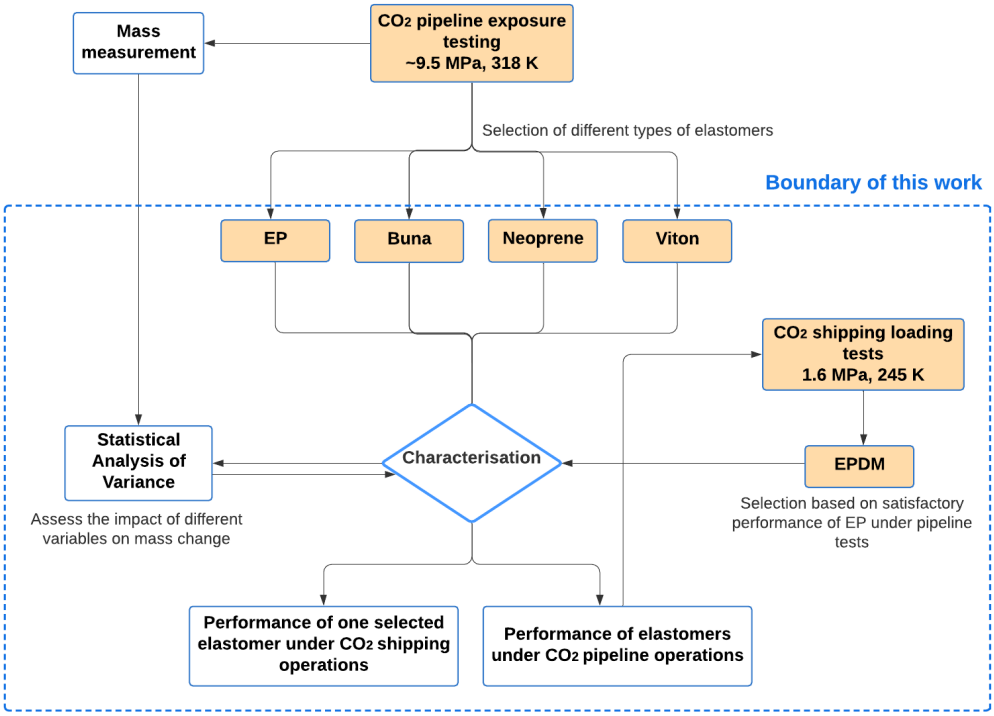

Figure 3-2: Overview of workflow and boundary of this work

Testing environments considered in this work for both pipeline and shipping tests reflect typical operating conditions encountered in real transport systems. With regards to CO_2 pipeline testing, samples were considered for prolonged exposure in a dense phase loop capacity rig which operates at conditions of ~ 9.5 MPa and 318 K in flow mode (~50 g/min) as part of the previous MATTRAN project. Testing conditions are summarised in Table 3-3. At each indicated exposure time, the complete geometry set of each selected material for CO_2 pipeline tests (described in Table 3-2) were exposed to three carbon dioxide-rich environments with varying sets of impurities – namely CO_2 and saturated H_2O (environment 1) and addition of 500 ppm of H_2S (environment 2) or SO_2 (environment 3) for a period of up to 400 h or ~17 days. H_2S was selected as a contaminant due to its chemically aggressive nature, prone to attacking elastomers causing degradation of the seals, embrittlement and cracking [20, 22]. SO_2 was considered alongside water due to the potential for the two compounds to form corrosive acids. In particular, the effect of sulphuric acids has been identified as an issue for several types of elastomers [13].Such tests were performed as part of a previous project; further details on the experimental apparatus and implemented procedures can be found in previous publications from the research team [6,22]. In order to achieve testing of

materials representative of real CO_2 shipping operations, a series of compression and decompression cycles – typical of the batch-wise nature of CO_2 loading and offloading operations (Figure 3-1) – were considered in this work.

Table 3-3: Summary of testing schedule under CO_2 pipeline conditions

Exposure time (h)	P (MPa)	T (K)	Decompression cycles*	Flowrate (g/min)	H_2S/SO_2 level (ppm)
50	9.5	318	1	50	500
150			2		
200			3		
300			4		
400			5		

***Under each exposure time, start-up and shutdown of the rig implied exposing the fitted samples to a number of compression and decompression cycles as part of MATTRAN project [6,22].**

The specific aim of these tests was to investigate the performance of the material and propensity for alteration of mechanical and structural properties and RGD damage in refrigerated, liquid carbon dioxide at conditions of 1.6 MPa and 245 K, extensively indicated for future CO_2 shipping projects for CCUS [8,9]. Summary of the performed tests is presented in Table 3-4.

Table 3-4: Summary of testing schedule under CO_2 shipping conditions

CO_2 loading cycles	Thermal cycles*	Liquid CO_2 loading cycles
20	1	1.6 MPa, 245 K
40	2	
60	3	
80	4	
100	5	

***apparatus heated to ambient temperature to permit the removal of constrained (25% compression) samples**

The experimental system comprises a copper cylindrical test vessel – 67 mm length and 55 mm inner diameter – complemented with 5 x copper plates, each able to accommodate 3 replicate samples in compressed mode; compressed samples were therefore inserted inside the copper vessel. Figure 3-3 provides a representation of compressed plate fixture implemented in this work. Temperature conditioning was attained through a Grant R5 chiller with heater, operated with silicone oil and capable of achieving low temperatures of 226 K. Compression of the samples to 75% of their original thickness was achieved using compression pates, steel spacers and a clamping device – provided by nuts (3.75 mm) and bolts. O-rings were compressed by 25% of their original thickness in order to simulate operating conditions in the pressure-relief valve seat during standard use. The compressed O-ring gives elastomer-to-metal seal for positive shutoff at the seat. Moreover, such compression value has also been selected in line with ASTM D395 in order to enable measurement of Compression Set properties. Such pre-compression is estimated to correspond to a compressive load value between 0.35 – 0.5 kN/m for an O-ring having a 5.33 mm cross section according to the supplier of the seals. Prior to their insertion inside the test vessel, samples were subjected of pre-test measurement of mass, hardness and thickness; methods are given in this section of the work.

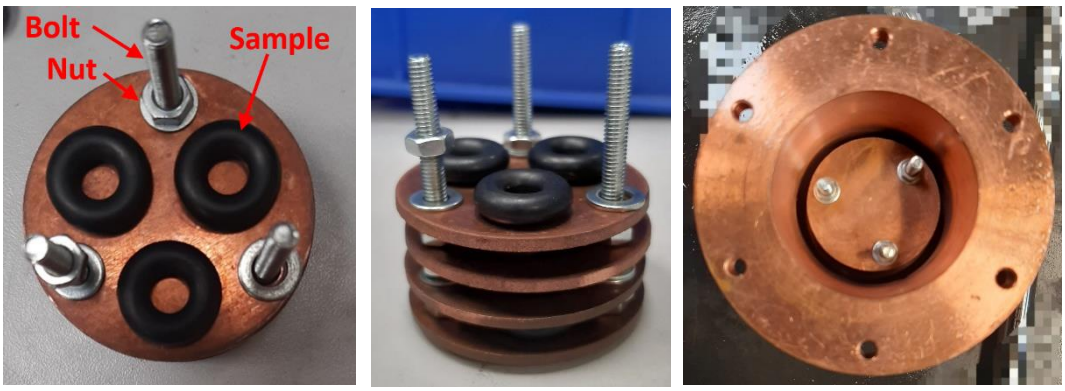

Figure 3-3: Representation of the compressed plate assembly and insertion inside the copper vessel

The copper vessel was connected to a liquid withdrawal bottle - serving as liquid, industrial grade CO_2 supply (99.8% purity, conforming to BS 4105 part 1) – by means of a pipe section with 3 mm nozzle diameter equipped with a metering valve to enable control of downstream injection pressure; the test section was fitted with an A-10 Wika pressure transmitter (0 - 2.6 MPa measuring range; accuracy ±0.03 MPa) on the discharge line and a RS components k-type thermocouple (120 – 520 K range, ± 1.5 K

accuracy) placed inside the vessel, approximately 10 mm below the top lid of the copper vessel. The response time of the pressure transmitter is 0.01 s, while the thermocouple has a response time of 0.5 s .Pressure and temperature measuring devices were connected to NI 9205 and 9213 modules respectively to enable real time monitoring and acquisition of the experimental data via NI DAQ Express software at a frequency of 10 Hz. Moreover, the test vessel was fixed on a handheld weight balance (50 kg capacity, ± 0.001 kg accuracy), implemented to monitor the level of liquid CO_2 during the experiments and ensure complete filling of the vessel.

Figure 3-4 provides a schematic overview of the experimental rig. The following test procedure was followed rigorously. Initially, the copper vessel was immersed in the reservoir of the chiller tank (~6 L volume) to allow it to refrigerate and achieve the pre-set temperature of 233 K. Consequently, injection of liquid CO_2 was initiated by regulating the metering valve fitted downstream the carbon dioxide supply to permit withdrawal of the fluid at the required pressure. As the carbon dioxide loaded into the system, the constrained samples would undergo a compression cycle. Upon filling of the complete vessel's volume with liquid carbon dioxide – as indicated from the weight balance measurement – test conditions were achieved, and supply of fluid was shut. The ball valve on the discharge line was therefore opened, resulting in the rapid discharge of the CO_2 from the test section (decompression stage). Figure 3-5 provides with a typical plot of the performed loading cycles. After completion of each set of CO_2 loading cycles –summarised in Table 3-3 – the apparatus was brought to a temperature of 293 K to allow the removal of three duplicate O-ring samples from the test section. Samples were therefore stored in the desiccator for a period of 24 h prior to characterisation.

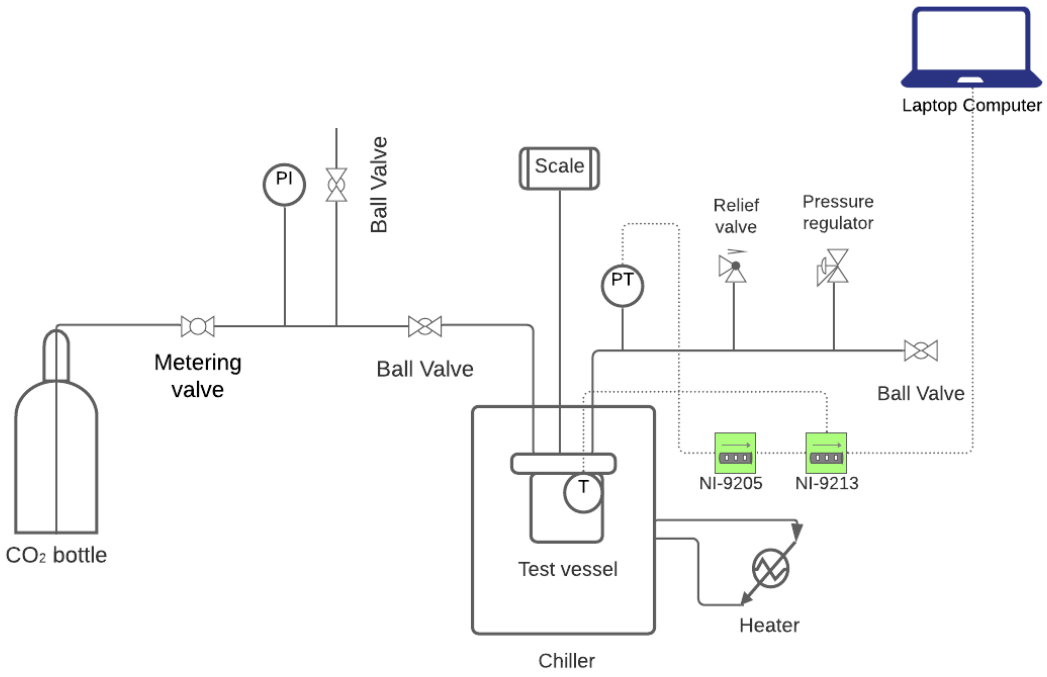

Figure 3-4: Schematic diagram of the experimental set-up

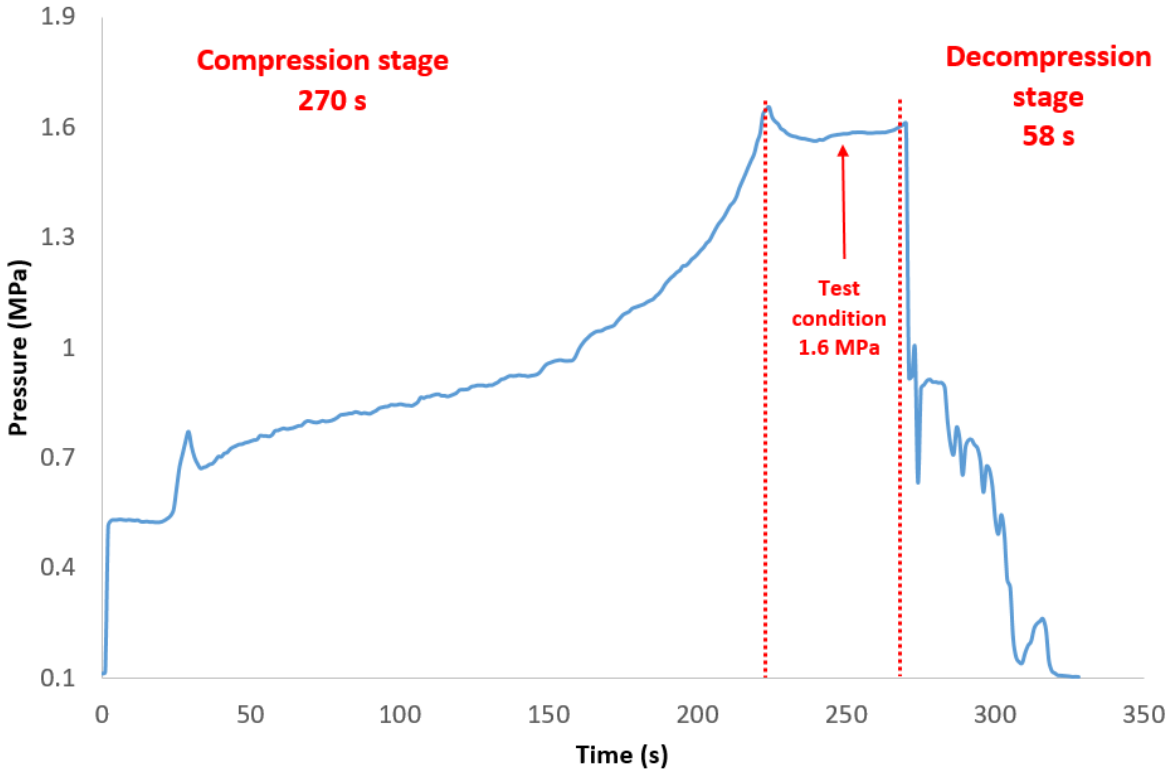

Figure 3-5: Typical CO_2 loading compression and decompression cycle

3.2.1 Samples characterisation

A characterisation methodology has been developed in this work to qualify the elastomers and assess the effect of exposure on the degradation of properties. Table 3-5 summaries the investigated elastomer properties and relative characterisation method.

Table 3-5: Summary of elastomer characterisation methodology applied in this work

Elastomer property	Characterisation method	CO_2 pipeline tests	CO_2 shipping tests
Post-exposure mass	Precision scale (± 0.00001 g)	✓	✓
Compression Set	ASTM D395 - micrometre (± 0.001 mm)	X	✓
Internal voids and RGD damage	NORSOK RGD Standard – rapid rating	✓	✓
Hardness	Digital hardness durometer (Shore A) ±0.5 HA	✓	✓
Glass transition temperature (T_g)	Differential Scanning Calorimetry (DSC)	✓	✓

Mass measurements of the exposed samples was acquired to investigate the compatibility between the elastomer and the environment and assess any related loss of material. Hardness is a mechanical property dictated by the chemical structure of the material, therefore its measurement in this work was aimed at verifying the occurrence of any structural alterations as a result of the exposure. In this work, hardness was measured in this work using a shore A durometer (0-100 HA, ±0.5); similarly, determination of glass transition temperature (Tg) by means of DSC aimed to investigate whether potential ageing and structural modification of the material resulted in a shift of its glass transition temperature. The value was taken as midpoint of the glass transition curve of a DSC plot, and obtained through TA Universal Analysis software; DSC scans were performed at 10 K/min heating and cooling rate. Inspection of the cross-section surfaces of samples for internal damage was performed following the NORSOK standard for explosive decompression damage [23] through a digital microscope (up to 300x magnification). Compression SetSet measurement on samples tested in CO_2

shipping conditions was derived from method B of the ASTM D395 standard. The cross-section of the samples was measured by means of a micrometer (± 0.001 mm accuracy) and used to determine CCompression SetSet value using the following equation:

$$CS = \frac{h_0 - h_2}{h_0 - h_1} \times 100\% \qquad \text{Equation 3-1}$$

Where h_0 represents the initial sample thickness, h_1 is the compressed height and h_2 is the measured recovered thickness of the samples. The ASTM D395 standard indicates a 30 min recovery of the sample upon removal of constraint prior to measurement of the thickness; however, implementing this timescale was impractical in this work, due to the fact that conditioning of the apparatus to ambient temperature and disassembling of the plates took several minutes. The values measured at 30 min would therefore contain considerable inaccuracies in the time scale, and therefore a 24 h recovery period was instead considered in this work and applied to all samples. The determined value of Compression Set at 24 h measurement indicates potential permanent set occurring as a result of CO_2 loading cycles [24].

The statistical method of Analysis Of Variance (ANOVA) was moreover implemented in this work to further scrutinize findings generated in CO_2 pipeline conditions and derive some statistically significant trends, given the large number of generated samples and variables considered – namely type of material, geometry and presence of impurities; ANOVA was performed using JMP 14 Pro software.

3.3 Results and Discussion

3.3.1 Mass change

Compatibility between an elastomer and a fluid is inherent to the chemical structure of the material, free volume among the chains, and presence of plasticisers [21]. Moderate resistance implies elastomer swelling in the fluid, while a low degree of chemical compatibility results in a dissolution of the material by the fluid, causing leak from the O-ring material. When CO_2 is absorbed into the molecular structure it starts acting as a plasticiser by reducing the interaction between the polymer chains and allowing a more fluid, reciprocal movement of the chains. After the process of fluid extraction, the net mass change becomes a combination of irreversible swelling and extraction or chemical reaction between the material and the environment [25]. Owing to the large number of

generated samples and variables scrutinised under CO_2 pipeline tests, statistical ANOVA was thereby applied in this work to interpret the mass change measurements and detect significant trends in relation to type of material, geometry and environment. A summary of the different analyses performed in this work is provided in Table 3-6 and Figure 3-6.

Table 3-6: Summary of findings on one-way analysis of mass change by type of material under CO_2 pipeline conditions

Material	Mean change (%)	Standard error	Lower 95%	Upper 95%
Buna	-6.0	0.7	-7.3	-4.7
Viton	1.9	0.7	0.6	3.2
Neoprene	-4.1	0.7	-5.4	-2.8
EP	-4.9	0.7	-6.2	-3.6

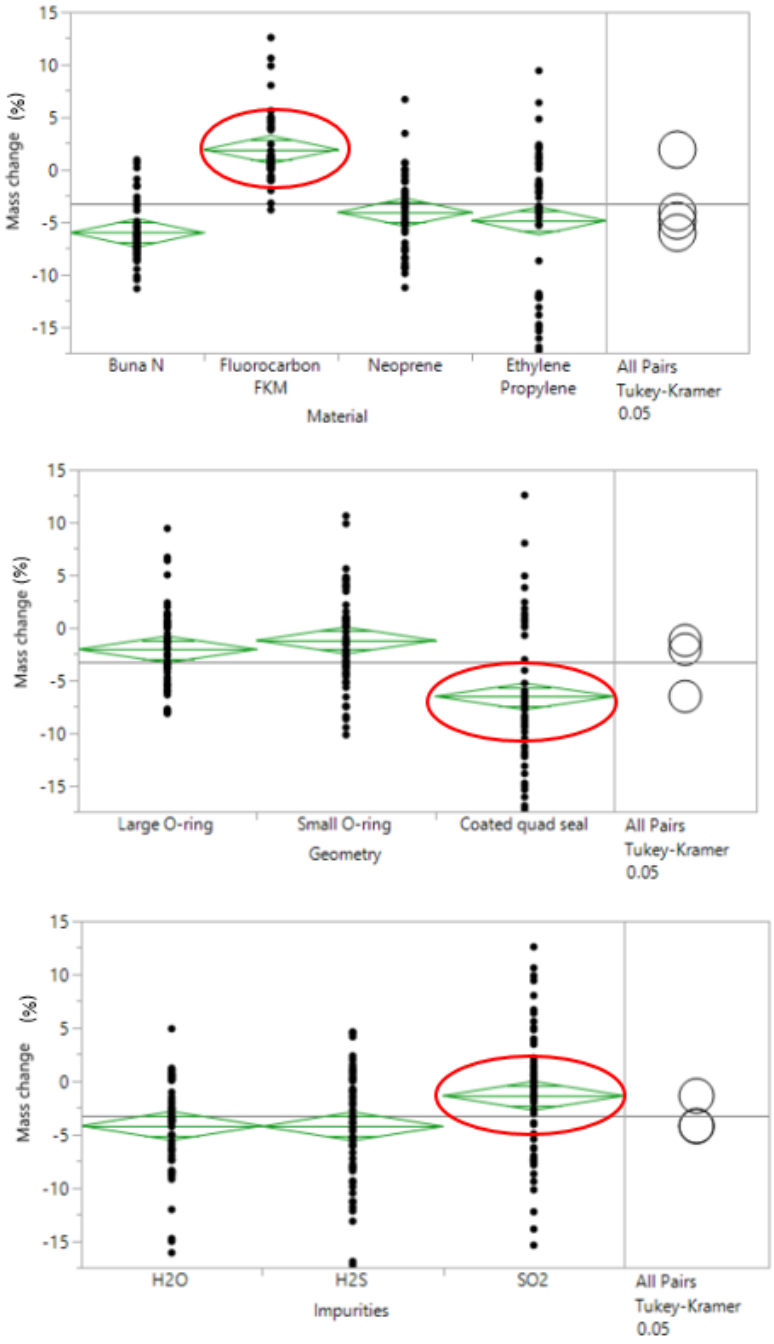

Figure 3-6: One-way analysis of mass change of samples tested in CO_2 pipeline conditions(318 K, 9.5 MPa) by (top-to-bottom): type of material, geometry and contaminants present in the environment. Circled sections represent factors with statistically significant differences

The one-way between subjects ANOVA conducted to compare the effect of selection of type of material on the % mass change showed the presence of significant difference ($F = (3, 179) = 27.5$, $p < 0.0001$). Post-hoc analysis clarified that Viton exhibited significantly different mass change compared to other materials ($p < 0.0001$). On the other hand, the reciprocal behaviour of Buna, Viton and EP does not show any

significant statistical difference, indicating that these materials behaved similarly during CO_2 pipeline tests. The one-way ANOVA conducted to compare the effect of different geometries on the mass change showed the presence a significant difference ((F = (2, 179) = 20.1, p < 0.0001); post-hoc analysis concluded that coated quad seals lost a significantly higher amount of mass (-6.5%, standard error 0.63) than non-coated samples – namely large (-2%, standard error 0.63) and small ID O-rings with a p < 0.0001, implying that the PTFE-sprayed coating applied to confer resistance to abrasion degraded during the exposure. One-way ANOVA performed to evaluate the impact of the different impurities on the mass change showed the presence a significant difference (F = (2, 44) = 5.7, p < 0.001) in relation to the environment containing CO_2 saturated water and 500 ppm SO_2. It is however important to highlight that the specific scrutiny on statistical significance of this trend has only been confirmed in relation to Neoprene (F = (2, 44) = 5.4, p = 0.0082) and Viton (F = (2, 44) = 7, p = 0.0024); conversely, Buna and EP do not exhibit any significant mass variation relative to the presence of contaminants. This trend – in line with other investigations in the literature [26] – could potentially indicate the formation of sulphurous acid (H_2SO_3) in the presence of water, which can as a result oxidise in the presence of O_2 to form sulphuric acid (H_2SO_4). The minimum required presence of water to promote formation of both the aforementioned compounds in not well known, although Dugstad et al. [26] found that presence of a mere 100 – 344 ppmv of SO_2, combined with 488 – 1222 ppmv of H_2O promotes considerable corrosion propensity of API 5L X65 Steel. In the case of elastomer testing, the presence appears to be inducing a higher amount of mass absorption (Viton) and lower degree of mass loss (Neoprene); this thus indicates the propensity for these compounds to irreversibly swell the elastomer compounds. Finally, analysis of variance performed to scrutinise the impact of exposure time on the mass change of the samples highlighted the absence of any significant difference, implying that within the exposure cycles of 50 – 400 h considered in this work, no trends were observed relative to mass change of the samples with exposure time.

Chloroprene elastomer – or Neoprene – exhibits affinity with CO_2 due to the polar Cl atom contained in its backbone structure, which implies an enhanced diffusion and solubility of the compound within the structure upon interaction [15]. One-way ANOVA performed to assess the impact of the different impurities on Neoprene samples revealed that exposure to CO_2, saturated water and 500 ppm SO_2 resulted in a

significantly lower degree of mass loss ($F = (2, 44) = 5.4$, $p < 0.001$) in comparison to the other two considered environments (CO_2 and saturated water and CO_2 and 500 ppm of H_2S). This finding indicates that presence of SO_2 results in some interaction with Neoprene's chemical structure, implying signs of adverse chemical compatibility; this is in line with the reported compatibility of the elastomer with SO_2 in the literature [13], and indicates that even modest concentrations of 500 ppm are found to have an effect. Buna exhibits affinity with CO_2 due to the presence of the ACN group contained in its backbone structure. The material also shows a trend of mass loss during the exposure. Similarly, to Neoprene, net mass loss does not imply lack of diffusion of carbon dioxide into the material's structure as the mass change can be a combination of both phenomena.

Despite being indicated as an unsuitable material with H_2S and SO_2, as they are found to predominantly attack the ACN groups [13,20], in this work Buna appears to be stable in their presence at the scrutinised concentration showing no significant mass change. Viton seals show no signs of loss of mass during the exposure, which could potentially indicate no dissolution of plasticisers. The material shows high levels of CO_2 swelling in use, caused by chemical affinity of carbon dioxide to fluorine as a higher degree of fluorination of the material can increase the solubility of the polymer in CO_2 [15]. Findings from this work show the swelling effect to be to a large extent reversible, as after the extraction process of the fluid the mass gain maintains within a value of 1% in the CO_2 + H_2O and H_2S environments. A different trend is observed in the presence of SO_2 as a contaminant, where the material shows a statistically significant mass increase (~4.3%) which indicate some particular interaction promoted by the compound. Similarly, to what reported for Neoprene, SO_2 demonstrates some interaction with Viton, although this is not reflected in the compatibility charts provided by manufacturers [13]. As previously discussed, this trend could indicate the formation of sulphurous/sulphuric acid in the presence of water. Moreover, no mass loss is encountered in the coated quad seals, meaning that the protective layer has not degraded as a result of the exposure. This is an exception amongst all the other materials, and it could be related to a degree of bonding between the material and coating – both fluorinated materials - on the basis of their structural affinity.

Ethylene Propylene and Ethylene Propylene Diene Monomer are non-polar materials that display a low-degree of diffusion and interaction with CO_2 – a polar fluid - within its

structure. In this work, EP shows the tendency to lose mass – 4.9% on average (standard error = 0.67) - upon exposure. A one-way ANOVA performed on EP samples to assess the impact of different geometries on the mass change showed the presence of a statistically significant difference ($F = (2, 44) = 66.02$, $p < 0.001$). Large and small ID O-rings were found to lose, respectively, 0.18% (standard error = 0.88) and 1.2% (standard error = 0.88) of their mass; conversely, PTFE-coated quad seals exhibited an average mass loss of 13% (standard error = 0.88), attributable to degradation of the sprayed coating as a result of the exposure. Therefore, this indicates that in uncoated EP large and small ID O-rings, mass loss during exposure to CO_2 pipeline conditions can considered to be negligible (~1% of the initial mass measurement), demonstrating the limited interaction between the non-polar EP material and polar CO_2 fluid. Accordingly, mass change of EPDM scrutinised after CO_2 loading tests at shipping conditions also revealed that the material underwent negligible mass change (Figure 3-7) and showed no observable trend in relation to number of performed cycles.

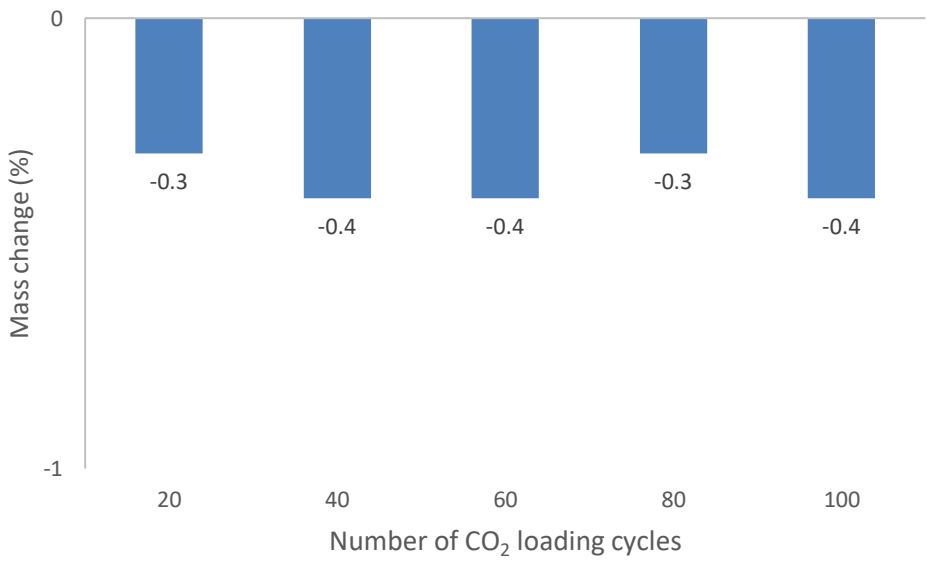

Figure 3-7: Mass change relative to loading cycles of EPDM samples at CO_2 shipping conditions (243 K, 1.5 MPa); average of three samples

Although absorption of CO_2 is enhanced at lower temperatures, mass change of EPDM in CO_2 modest albeit consistent throughout the performed loading cycles [20]. This finding strengthens the observations that both EP and EPDM perform well in CO_2-rich environments in relation to chemical compatibility. As such, it is possible to assert that the mass loss could be related to loss of plasticisers or additives added to the polymeric

structure. Later in this work, this hypothesis will be further explored given that loss of such additives typically leads to alteration of sealing and mechanical properties [21].

3.3.2 Internal inspection and RGD damage

Damage from RGD can occur during an uncontrolled release of gas trapped inside the elastomer's structure during rapid depressurisation stages. During the exposure, carbon dioxide dissolves and diffuses inside the free volume of the elastomer's structure, saturating the material; during a sudden pressure release – for instance during loading/offloading operations or emergency shutdowns - the dissolved CO_2 rapidly releases form the material, resulting in nucleation and generation of internal bubbles that can potentially cause mechanical damage. The risk of damage from RGD in the material enhances when the interaction between the elastomer and the fluid is characterised by a high solubility and a low diffusion coefficient; this is because such circumstances favour a larger amount of absorbed fluid to remain within the elastomer for a greater time during the depressurisation process [20]. Menon et al. [15] provide an approximation of diffusion and solubility coefficients of CO_2 through common elastomers, demonstrating the solubility to diffusion ratio to be considerably higher than that of other fluids such as nitrogen or methane. It is worth to note that solubility of individual gaseous species and diffusion rate of each type of elastomer vary in relation to CO_2 and presence of non-condensable components. Gases characterised by a higher solubility and low rate of diffusion in elastomers are found to produce most damage to seals during RGD. As such, in gases such as nitrogen, helium or hydrogen, solubility increments with temperature. Conversely, gases having larger molecules such as CO_2 exhibit the opposite behaviour [20]. Moreover, Menon et al. [15] reported the solubility coefficient to diffusion coefficient ratio of a range of non-condensable impurities such as helium, nitrogen and oxygen and found it to be ranging from 1 to 7. This is in contrast with CO_2, which has a solubility coefficient to diffusion coefficient ratio of 24, and thus an increased risk of RGD damage in case of sudden system decompression. Fick's First Law of diffusion given in Equation 3-2 describes that flow of fluid in any given direction is governed by the concentration slope and affected by the cross-section surface of the material:

$$Jx = -D_0 A \frac{\partial c}{\partial x}$$ Equation 3-2

Where Jx is the gas flux in the x-direction, D_0 is the diffusion coefficient, A is the cross sectional area, and c is the concentration of the media in the elastomer. Diffusion of gases inside elastomers is moreover a thermally activated phenomenon, governed by an Arrhenius equation. Therefore, diffusion processes are faster at higher temperatures [20] and the risk of RGD damage is lower. Solubility of fluids in elastomers is also dependant on temperature but, conversely to diffusion, it exhibits an inverse correlation with temperature when fluids with large molecules such as CO_2 are considered [20]. Propensity for RGD damage is not limited to absorption and diffusion phenomena between the fluid and the elastomer, but it is also related to other factors and properties, summarised in Table 3-7.

Table 3-7: Factors affecting propensity for RGD damage and their relevance to this work in industrial grade CO_2 (99.8% purity)

Factor	Remarks	CO_2 shipping tests	CO_2 pipeline tests
Pressure drop (MPa)	Higher pressures increases risk of RGD damage	1.6	9.5
Temperature (K)	Affects diffusion and solubility coefficients	245	318
Material section (mm)	Smaller is advantageous in reducing RGD risk	5	2.3
Average decompression rate (MPa/min)	Slower rate decreases RGD risk	1.6 MPa/min	0.15 MPa/min
Number of cycles	Fewer the better	20 -100	1 - 5
Hardness (Shore A)	Higher value increases RGD resistance	Buna: 70 Viton: 83 EP: 74 Neoprene: 72	EPDM: 70

Constraint	Good constraint advised 25% compression to mitigate RGD damage	None

The assessment of internal inspection and damage on elastomers from RGD performed in this work follows the rapid rating scheme proposed in the NORSOK standard [29], to establish pass or failure based on the number and size of formed cracks and blisters. For samples tested in CO_2 pipeline conditions, the assessment is performed on quad seals – which exhibit a higher thickness - given that risk of RGD damage enhances with higher cross-sectional surfaces [20]. Table 3-8 summarises findings on RGD damage assessment for quad-seals aged under CO_2 pipeline conditions. Moreover, a selection of some of the inspected samples is presented in Figure 3-8. Buna and Neoprene show a satisfying performance and indicate no internal cracks and blisters. Neoprene and Buna exhibit affinity with carbon dioxide due to the presence of, respectively, the polar Cl atom and the ACN group which promote solubility of CO_2 within the structure of the materials [15]. The mechanical properties of the materials, as well as the permeability and diffusion processes between them and CO_2 however withstand RGD under the conditions studied in this work. Although the presence of H_2S as contaminant is reported to enhance the risk and impact of RGD damage in Buna – due to it predominantly attacking ACN groups [20] - this work did not show any increased propensity for RGD damage in the material as such. EP also shows good resistance to RGD damage, with all scrutinised samples passing the inspection; it is however noteworthy that specimen exposed to 200 h and 400 h CO_2, saturated water and 500 ppm SO_2 – respectively undergoing 3 and 5 RGD cycles – reported the formation of 1-2 cracks on the cross sectional surface of the seal. EP is characterised by low solubility of CO_2 - a polar media – inside its structure due to its non-polar nature, and therefore limited degree of swelling occurs during the exposure, minimising the propensity for RGD damage. As summarised in Table 3-8, findings in this work show that Viton exhibits a poor RGD resistance as a result of the performed decompression cycles under CO_2 pipeline conditions: out of 15 inspected samples, 7 fail the inspection and 4 pass with some reservations, with only 4 samples performing satisfactorily.

Table 3-8: RGD rapid rating NORSOK Standard - quad seals exposed to pipeline conditions; Colour coding: Green = pass (rating 0-2); Orange = pass with reservations (rating 3); Red = fail (rating 4-5)

Material	50 h 1 cycle	150 h 2 cycles	200 h 3 cycles	300 h 4 cycles	400 h 5 cycles
CO_2 + saturated water					
Buna					
EP					
Neoprene					
Viton					
CO_2 + saturated water + 500 ppm H_2S					
Buna					
EP					
Neoprene					
Viton					
CO_2 + saturated water + 500 ppm SO_2					
Buna					
EP					
Neoprene					
Viton					

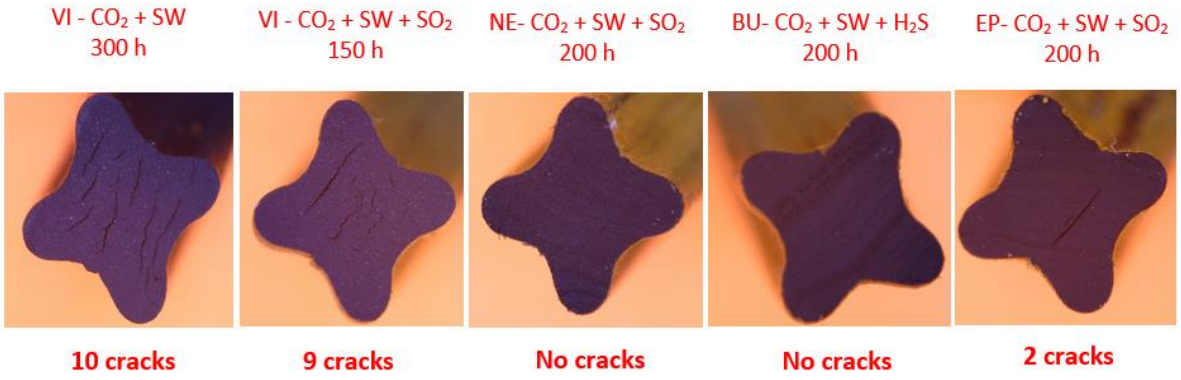

Figure 3-8: Cross-section surface of selected quad seals under pipeline tests (210X magnification); VI = Viton; NE = Neoprene; BU = Buna; SW = saturated water. Concentration of indicated impurities is 500 ppm

Here, propensity for RGD damage does not increase with number of decompression cycles, as demonstrated by the performance of specimen exposed in CO_2 with saturated H_2O and 500 ppm H_2S where 2 cycles cause the failure of the seal, and yet 5 cycles result in a satisfactory performance of the material (Table 3-8). This demonstrates that RGD is a complex function of mechanical properties and solubility, where risk increases with number of cycles but whose damage can manifest under fewer depressurisation cycles too [17]. The fluorine contained in Viton shows a high degree of chemical affinity

to carbon dioxide, implying a high degree of absorption of CO_2 in Viton during exposure as emphasised in the earlier part of this work [15]; this enhances the risk of RGD damage Interestingly, in this work Viton appears to be less prone to RGD damage and failure in the presence of 500 ppm SO_2 (Table 3-8) where samples exposed to 200 – 400 h (3-5 depressurisation cycles) perform satisfactorily exhibiting no formation of cracks on the seal's cross section. It is noteworthy that, as explained in the previous paragraph, Viton also display a statistically significant higher mass uptake with in the presence of 500 ppm SO_2 contaminant; this suggests that presence of SO_2 could be promoting a particular interaction with the material which shows propensity to increase RGD resistance as such. Similarly, diffusion rate of CO_2 out through Viton is slow due to the presence of bulky fluorine atoms, which cause the fluid to leave the structure in a progressive manner favouring local pressure build-up and explaining the formation of cracks. Findings relating to CO_2 shipping testing are summarised in Table 3-9. EPDM materials report no cracks or blisters on the cross-section surfaces of all scrutinised samples, demonstrating excellent performance and RGD damage resistance to the selected environment as show in Figure 3-9.

Table 3-9: RGD rapid rating NORSOK Standard – EPDM O-rings exposed to CO_2 shipping cycles; Colour coding: Green = pass (rating 0-2)

20 cycles	40 cycles	60 cycles	80 cycles	100 cycles

EP, Buna and Neoprene seals with 2.3 mm cross section demonstrate a satisfactory performance in CO_2 environments with saturated water and 500 ppm of SO_2/H_2S when 5 RGD cycles and an average decompression rate of 0.15 MPa/min are considered. This is particularly reassuring given that depressurisation rates above 0.1 MPa/min were deemed to represent cause for concern with regards to risk of RGD damage to elastomers in supercritical CO_2 environments [27]. Conversely, Viton – despite its higher hardness - revealed to be an unsuitable material selection due to the demonstrated considerable propensity for RGD damage, and its implementation in CO_2 transport systems is therefore strongly advised against. With regards to CO_2 shipping testing, EPDM can be considered to be a suitable material selection in this work: O-rings under 25% compression with 5 mm cross section exhibited satisfactory RGD resistance to 100 decompression cycles of refrigerated liquid CO_2 at 1.6 MPa and 245 K when a 1.6 MPa/min decompression rate was considered. The higher pressure drop range and

temperature imply more hazardous parameters relative to RGD under CO_2 pipeline tests compared to sea vessel conditions (Table 3-7); on the other hand, the enhanced fluid solubility and reduced diffusivity with the material at lower temperatures increases propensity for RGD damage at CO_2 shipping conditions. This work demonstrated that damage from RGD cannot be understated, even when single decompression cycles are considered; EP and EPDM showed to be suitable materials in relation to resistance to RGD damage at the scrutinised decompression rates and number of cycles, with the former performing satisfactorily under pipeline tests and the latter under shipping conditions.

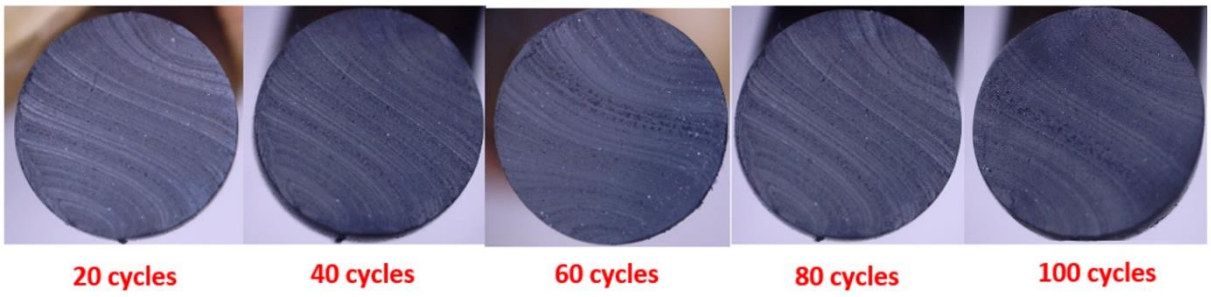

Figure 3-9: Cross-section surface of EPDM exposed to CO_2 loading cycles under shipping conditions (243 K, 1.5 MPa) taken at 210X magnification

3.3.3 Compression Set

Compression Set values (Equation 3-1) were determined in samples undergoing CO_2 shipping testing to investigate the ability of the elastomer to recover to its original shape following exposure to the sets of loading cycles. Physical changes can occur to an elastomer during exposure to the environment, particularly when elevated temperatures or temperatures in proximity of the material's glass transition temperature are considered [24]. These factors generate physical effects, and the material is characterised by a time dependant recovery of changes in chain positioning that took place upon the application of the stress. The applied stress exerts an effect on the viscoelastic nature of the elastomer: in the first instance, a rapid partial recovery of the material's thickness is promoted by its elastic nature [24]. When the material recovers from the time-dependent and reversible physical Compression Set - upon heating to ambient temperature – any residual Compression Set can be considered to be irreversible and caused by permanent structural alteration.

As shown in Figure 3-10, the measured Compression Set of EPDM O-rings (24 h after removal from the apparatus) appears to be modest and below a 3% value, which indicates an almost complete recovery of the seal to its original thickness. It is noteworthy that a tendency for Compression Set values to increase with number of CO_2 loading cycles is indicated in this work as summarised in Figure 3-10. An explanation of this trend is attempted as follows. Throughout the previous sections of this work, it has been established that interactions between EPDM and CO_2 media is limited due to the different polarity exhibited by the two; this consideration implies limited absorbance of carbon dioxide into EPDM's matrix, and chemical alterations as a result of interaction with the fluid can therefore be ruled out.

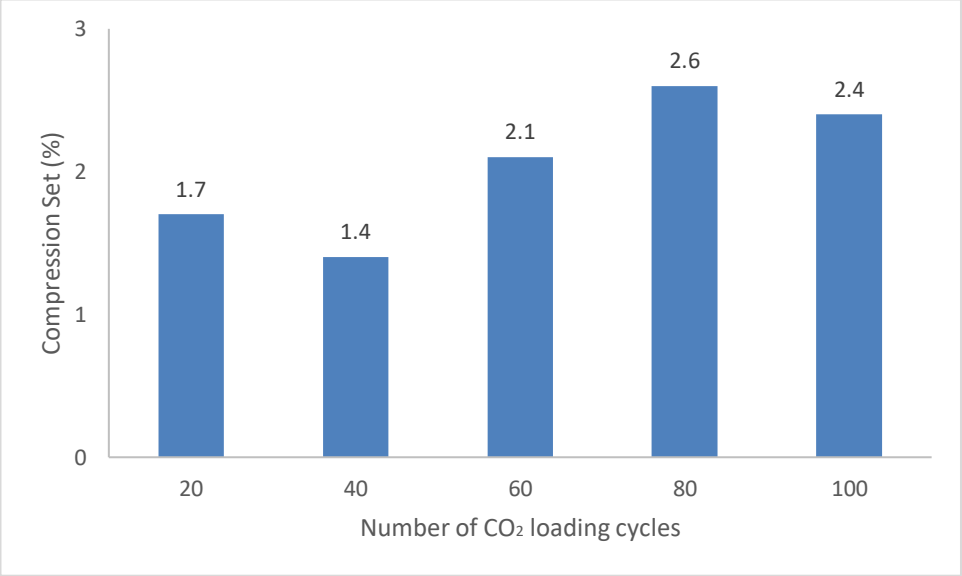

Figure 3-10: Compression Set of EPDM O-rings under CO_2 shipping tests as a function of loading cycles; values are the average of three samples

On the other hand, the imposition of stresses on the elastomer, herby represented by the force exerted by the compression plates and cyclic loading of pressurised liquid CO_2 generates deformation on the O-ring's structure, increasing the extent of stored elastic energy. In mitigating for such high amount of elastic energy, the twisted chains can slip and eventually rupture when a sufficient amount of elastic energy is concentrated in a specific segment of the elastomer. The resulting mechanical rupture of the structural bonds leads to relaxation of stresses, which manifest as an increased Compression Set value [24]. In particular, the effect may can be potentially enhanced by the multiple

number of CO_2 loading cycles performed in this work as showed by the tendency of Compression Set to increase with number of cycles.

3.3.4 Glass transition temperature (T_g)

The shift in glass transition temperature of the material implies structural alterations caused by aging effects; moreover, as the T_g of a material represents its transition from glassy brittle state as opposed to an elastic one, its shift effectively results in a change in suitable operating temperature range indicated for the material. This is because an elastomer above its T_g possesses a high amount of free volume which promotes motion of molecules; conversely, below the T_g the free volume is reduced, and the chain mobility is reduced, effectively 'freezing' the elastomer. In the CO_2 pipeline tests, DSC testing to determine T_g of the samples was performed on large ID O-rings; a one-way between subjects ANOVA was conducted to compare the effect of environment and exposure time on the T_g shift of the elastomers. The analysis highlighted that both exposure time ($F = (4,59) = 0.04$, $p = 0.99$) and presence of different contaminants ($F = (2,59) = 0.42$, $p = 0.65$) do not significantly affect the $\%T_g$ shift of the samples. Conversely, the one-way ANOVA performed to assess the impact of type of material showed that choice of different elastomers has a significant impact ($F = (3, 59) = 34.1$, $p < 0.0001$) on the change of T_g. Given the absence of statistically significant trends in relation to different impurities or exposure times, a summary of findings on glass transition temperature highlighting material performance under CO_2 pipeline conditions is provided in Table 3-10 and graphically illustrated in Figure 3-11.

Table 3-10: Summary of findings on one-way analysis of T_g shift by type of material under pipeline conditions (318 K, 9.5 MPa); large O-rings exposed to 50 – 400 h were characterised

Material	T_g of unaged sample* (°C)	Mean T_g shift (%)	Standard error mean	Lower 95%	Upper 95%
Buna	-19	-21.6	2.83	-27	-15.6
Viton	-17	-12	2.83	-17.7	-6.3
Neoprene	-42	14.8	2.74	9.3	20.3
EP	-29	5.8	2.74	-0.3	10.8

* **T_g of unaged sample determined based on the average of two unaged samples.**

Ageing and significant uptake of CO_2 can lead to plasticisation phenomena, which can result in a change of mechanical properties and decrease of the glass transition temperature [21]. Chemical degradation is enhanced by heat which accelerates the process of polymer oxidation in the presence of oxygen, leading to crosslinking or polymer chain scission [28]. Neoprene is characterised by the presence of the polar Cl functional group in the backbone structure, which implies a pronounced polar-polar interaction with CO_2; in this work the material exhibits a T_g increase of 14.8%. However, in this work it is found that this behaviour can otherwise be potentially correlated with a loss of plasticiser as indicated by the bivariate fit of T_g shift by mass change (correlation factor = -0.52, p = 0.04) shown in Figure 3-12. The graph shows potential signs of a negative correlation between mass change and glass transition temperature shift, strengthening the aforementioned hypothesis. The increase in T_g experienced by the materials and caused by cross-linking is accompanied by a reduction of free volume within the structure – which leads to higher liquid absorbance– thus reducing the amount of swelling that the material can undergo. An increased T_g decreases the free volume, which could accommodate absorbed liquid, and subsequently, reduce the degree of swelling.

Figure 3-11: Summary of average % glass transition shift of materials under CO_2 pipeline tests

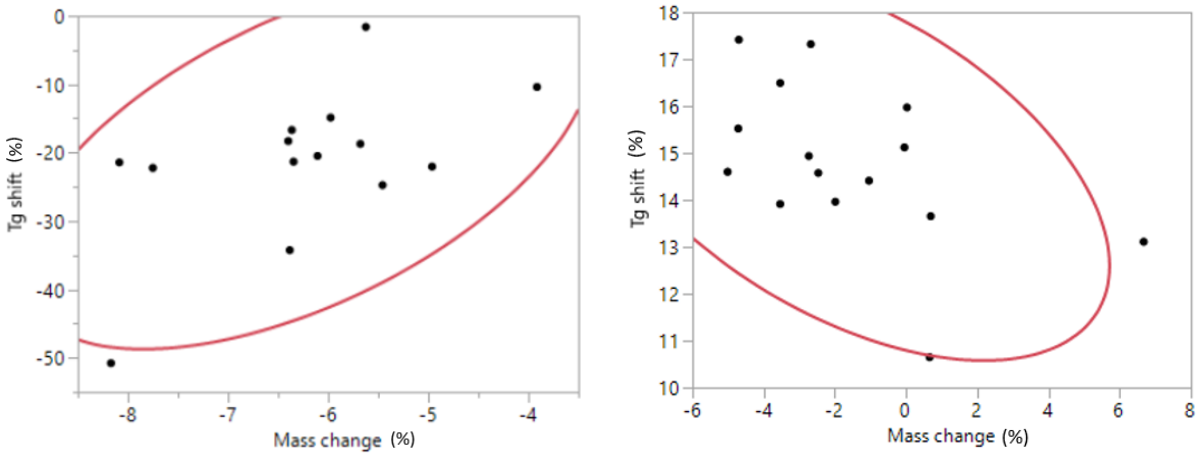

Figure 3-12: Bivariate fit of glass transition shift by mass change for Buna (left) and Neoprene (right); Bivariate Normal Ellipse p = 0.95

Buna shows a reduction of ~21.6% in Tg in this work, characteristic of the plasticisation effects of carbon dioxide on polymers [21]; this is contrasting with findings from Menon et al. [15] who reported a considerable increase of glass transition temperature as a result of 200 – 1000 h exposure to supercritical CO_2 at 20 MPa and 373 K. This behaviour was attributed to weak Van Der Waal's type interaction between molar ACN polar groups contained in Buna and CO_2, a polar media characterised by binding onto the free volume spaces; as such, the degree of interaction of Buna with CO_2 is largely dependent on ACN content. In this work, however, the considered pressure and temperature are lower (9.5 MPa, 318 K) and therefore the rate of diffusion is less prominent [29], potentially explaining a lower degree of interaction between elastomer and fluid. Maciejewska and Sowin [30] investigated the effect of different fillers on the vulcanisation processes and properties of acrylonitrile-butadiene elastomers, asserting that that their presence increased the crosslink density of the vulcanizates present in the structure. Therefore, a potential degradation of such fillers present in the backbone of Buna during CO_2 pipeline testing could be potentially reducing the crosslinking density of the material thus lowering its Tg. This supposition is supported by signs of a positive correlation encountered in the bivariate fit of Tg shift by mass change (correlation factor = 0.56, p = 0.04). Viton exhibits a ~12% reduction in glass transition temperature during CO_2 pipeline testing which can be attributed to structural alterations promoted by the high affinity between the fluorine atoms and CO_2.

Despite suggestions that presence of H_2S in the environment leads to aging of fluorocarbon by dehydrofluorinating the material by promoting scission of chains at

elevated temperatures [21] no indication of this in encountered in this work at the selected concentration. EP showed a modest increase of 5.8% of its glass transition temperature, representative of the limited interaction that the elastomer undergoes with CO_2 – a polar media - due to its non-polar nature; the modest Tg increase is thereby attributable to some degree of aging in the form of crosslinking induced by the high pressure (~9.5 MPa) of the environment. EPDM tested under CO_2 shipping conditions shows a stable glass transition temperature throughout the different cycles, comprised within a 1.5 K value in comparison to the ~218 K value of unaged sample. This modest variation indicates the absence of considerable interaction with the environment, whereby the absence of a significant shift in glass transition temperature demonstrates no significant ageing in the form of chain scission or crosslinking taking place in the material. Interestingly, in the 20 – 60 cycles samples exhibit insignificant variation of their Tg, confirming the minimal interaction with the environment. However, when considering the 80 and 100 cycles, the material shows signs of a modest reduction of glass transition temperature (Figure 3-13). This trend reflects the increased Compression Set values measured during the same cycles as shown in Figure 3-10 and can thus be potentially be attributable to signs of chain scission induced by the cyclic imposition of stresses during the loading cycles. In particular, this phenomenon appears to be promoted by the prolonged alternation of pressure cycles (liquid CO_2) at sub-zero temperatures, approaching the Tg of the material.

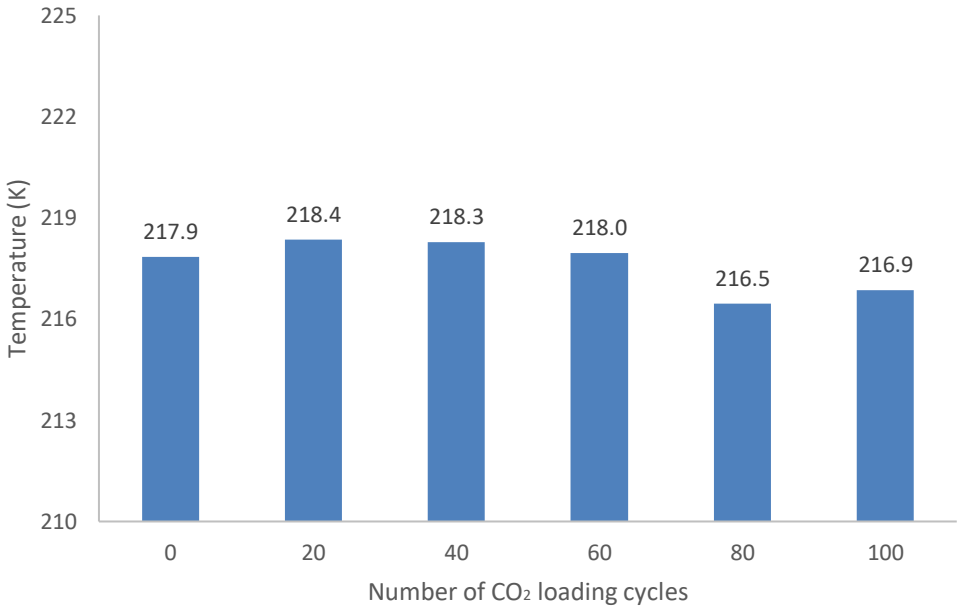

Figure 3-13: Glass Transition temperature of EPDM in relation to CO_2 shipping cycles; unaged sample tested for the 0 cycle reference

3.3.5 Hardness

For CO_2 pipeline testing, Shore A hardness testing was performed on the 2.7 mm thickness O-rings. The alteration of hardness as mechanical property provides an indication of potential structural changes that have occurred in the material as a result of the exposure. When chain scission phenomena prevail, the material softens; conversely, if the cross-linking phenomena prevail, the material stiffens and subsequently the hardness increases. Materials show a significantly different trend of hardness change ($F = (3,59) = 34.7$, $p < 0.0001$) with Buna undergoing a significantly different trend of hardness alteration compared to Viton, Neoprene and EP, which in turn do not exhibit any reciprocal significant difference as per ANOVA statistical analysis performed in this work. Indeed, this suggests that the signs of structural alteration observed through the shift of Tg of the material also implied a considerable hardening of the compound, and thus a loss of flexibility as a result of exposure. This strengthens the hypothesis that the loss of mass encountered under pipeline tests is attributed to loss of additives, given that their addition is aimed at improving low-temperature flexibility of the material compound [21].

A one-way between subjects' ANOVA was performed to assess the impact of contaminants and exposure time on change in Shore A hardness of the elastomers. The

analysis highlighted that both exposure time of (50 – 400 h) ($F = (4,59) = 0.16$, $p = 0.96$) and presence of different contaminants (500 ppm of H_2S or SO_2 in addition to saturated water) ($F = (2,59) = 0.78$, $p = 0.46$) do not significantly alter hardness change in the samples. A summary of findings on hardness change highlighting performance of each material under CO_2 pipeline conditions is provided in Table 3-11.

Table 3-11: Summary of findings on one-way analysis of hardness change by type of material

Material	Shore A hardness of unaged sample	Mean hardness change (%)	Standard error	Lower 95%	Upper 95%
Buna	70	26.6	2.1	22.4	30.8
Viton	83	4.9	2.2	0.5	9.3
Neoprene	72	-1.7	2.1	-6.0	2.5
EP	74	4.4	2.3	-0.3	9.1

Given that the impact of environment (and thus presence of different contaminants) and exposure time has been demonstrated to be statistically insignificant, Figure 3-14 presents the hardness change encountered in the different materials as a result of exposure under CO_2 pipeline conditions. As it is possible to observe, Buna undergoes a remarkable average 26.6% increase (standard error = 2.09) in hardness. This observed trend can be potentially attributed to the loss of plasticisers and additives from the material as reported in the previous sections and generally indicates sign of high degree of alteration of the mechanical property as a result of the exposure, Neoprene reports a modest 1.7% decrease in hardness (standard error = 2.09) from an initial Shore A hardness value.

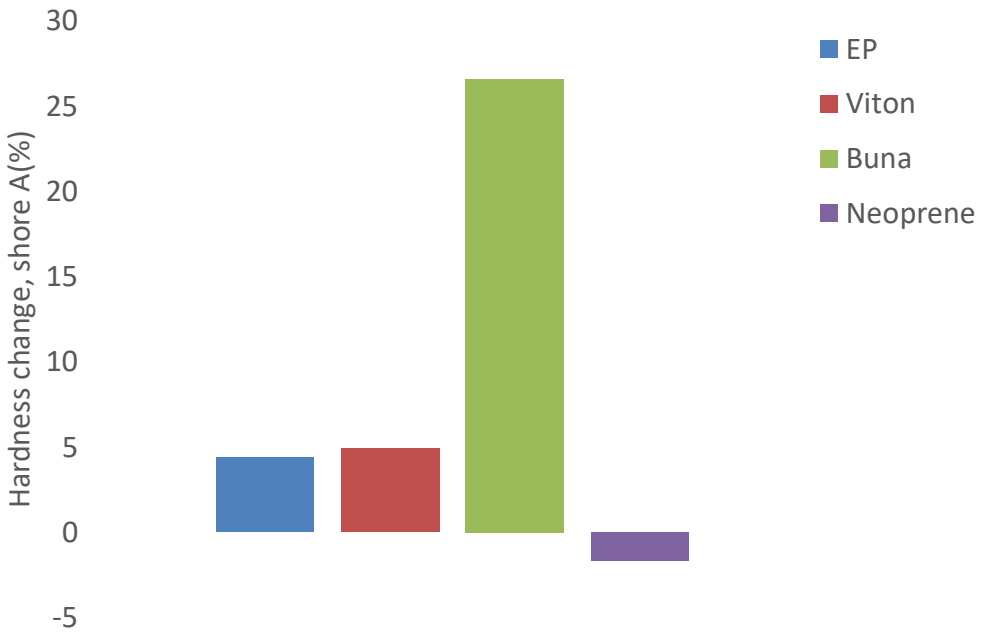

Figure 3-14: Summary of average hardness change to elastomer materials exposed to CO_2 pipeline environment

Despite the encountered mass loss of Neoprene, attributed to loss of plasticisers and supported by the signs of a linear correlation with T_g shift [21], the material would have also undergone plasticisation effects due to the interaction of CO_2 with its polar CI functional group [15]. Therefore, the arising structural changes can potentially explain the softening effect. Viton exhibits a modest 4.9% (standard error = 2.19) increase in its hardness value; as strengthened in the previous section on EP is a non-polar elastomer and does not significantly interact with carbon dioxide: therefore the modest 4.6% (standard error = 2.31) increase in hardness reflects such minimal interaction [21]. The trend encountered in EP at pipeline conditions is also common to EPDM under CO_2 shipping conditions where hardness change is limited to a mere increase of ~4.5% from the initial value of 70; interestingly, there appears to be signs of a trend in reduction of hardness change with number of CO_2 loading cycles (Figure 3-15). This behaviour can be potentially correlated with the increment of Compression Set encountered at 80 – 100 CO_2 cycles, implying an increased level of softening. As also reflected by the decrease in T_g reported in the material, the reported reduction in hardness change potentially indicates the increasing sign of chain scission phenomena with number of loading cycles considered in this work.

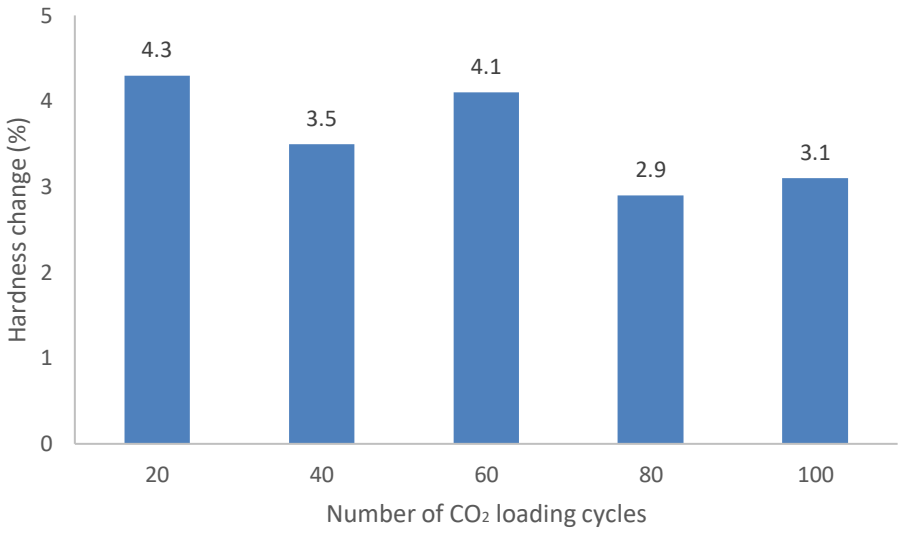

Figure 3-15: % change in shore A hardness of EPDM O-rings under CO_2 shipping tests as a function of loading cycles; values are the average of three samples

3.4 Conclusions

This work investigated and qualified the performance of different elastomer materials for CO_2 transport systems by focusing on their performance for pipeline and shipping systems. Four different types of elastomers – namely Viton, Buna, Neoprene and EP – previously considered for prolonged exposure (50 – 400 h) under supercritical CO_2 conditions, (9.5 MPa, 318 K) were characterised in this work to assess their suitability in CO_2 pipeline systems. Material testing under CO_2 shipping conditions was moreover performed in this work (1.6 MPa, 245 K), and EPDM O-rings were selected owing to the satisfactory performance of EP under pipeline conditions as well as the appropriate temperature range in the triple point region of CO_2. O-rings compressed to 75% of their thickness were exposed to 20 – 100 CO_2 loading and offloading cycles, representative of the intermittent and batch wise nature of real sea vessel transport operations.

The following findings are summarised:

- Viton showed to be an unsuitable material selection for pipeline systems due to the high level of swell promoted by interaction between the fluorine atoms with CO_2; the material demonstrates high propensity for rapid gas decompression damage even when a single cycle is considered
- Neoprene and Buna exhibited excellent resistance to RGD damage under pipeline conditions but showed signs of structural changes manifested in

significant shifts of glass transition temperature and change in hardness. Such alterations can potentially be attributed to interactions of their respective polar CI and ACN functional groups with CO_2 and loss of additives from the materials backbone.

- Due to its non-polar nature, EP demonstrated to be a stable elastomer in supercritical CO_2 environments, displaying moderate increase in glass transition temperature (~6%) and minimal hardening of its compound.
- EPDM displayed the potential to be a suitable material selection for CO_2 shipping systems, showing optimal RGD resistance (100 decompression cycles, 1.6 MPa/min decompression rate) where no cracks or blisters were found; modest is also the alteration to mechanical properties as a result of the exposure.
- EPDM displayed a moderate Compression Set (<3% at 25% compression) indicating an almost complete recovery to the original thickness as a result of the CO_2 loading cycles; a trend of increase in Compression Set with number of cycles is noticed, potentially attributed to an increased effect of the imposed stresses with loading cycles.

Findings from this work are intended to support the designer in the selection of appropriate elastomer materials for future CCUS projects.

References

[1] IEA. Energy Technology Perspectives 2020 - Special Report on Carbon Capture Utilisation and Storage, CCUS in clean energy transitions, OECD Publishing, Paris, France: 2020. https://doi.org/10.1787/208b66f4-en. International Energy Agency.

[2] ZEP. Role of CCUS in a below 2 degrees scenario 2018:1–30. https://zeroemissionsplatform.eu/wp-content/uploads/ZEP-Role-of-CCUS-in-below-2c-report.pdf

[3] ZEP. The Costs of CO_2 Transport Post-demonstration CCS in the EU; 2011. European Technology Platform for Zero Emission Fossil Fuel Power Plants, Zero Emissions Platform. Available at https://www.globalccsinstitute.com/resources/publications-reports-research/the-costs-of-co2-transport-post-demonstration-ccs-in-the-eu/

[4] Element Energy. CCS deployment at dispersed industrial sites; 2020. Department for Business Energy and Industrial Strategy; Research paper number 2020/030.

[5] Roussanaly S, Hognes ES, Jakobsen JP. Multi-criteria analysis of two CO_2 transport technologies. Energy Procedia. 2013; 37:2981–8.

[6] Patchigolla K, Oakey JE. Design Overview of High-Pressure Dense Phase CO_2 Pipeline Transport in Flow Mode. Energy Procedia. 2013; 37:3123–30.

[7] Element Energy, TNO, Engineering Brevik, SINTEF, Polarkonsult. Shipping UK Cost Estimation Study; 2018. Available at: https://assets.publishing.service.gov.uk/government/uploads/system/uploads/attachment_data/file/761762/BEIS_Shipping_CO2.pdf .

[8] IEAGHG. The Status and Challenges of CO_2 Shipping Infrastructures. 2020; IEAGHG Technical Report 2020-10.

[9] Seo Y, Huh C, Lee S, Chang D. Comparison of CO_2 liquefaction pressures for ship-based carbon capture and storage (CCS] chain. Int J Greenh Gas Control. 2016; 52:1–12.

[10] DNV. Design and Operation of CO_2 Pipelines. 2010; Det Net Norske; DNV-RP-J202; https://www.ucl.ac.uk/cclp/pdf/RP-J202.pdf

[11] Energy Institute. Hazard analysis for offshore carbon capture platforms and offshore pipelines. 2013; https://www.globalccsinstitute.com/archive/hub/publications/115563/hazard-analysis-offshore-platforms-offshore-pipelines.pdf

[12] Liane S, Billingham M, Barraclough C, Lee C-H, Milanovic D, Peralta-Solario D, et al. Corrosion and Selection of Materials for Carbon Capture and Storage. 2010.

[13] Ansaloni L, Alcock B, Peters TA. Effects of CO_2 on polymeric materials in the CO_2 transport chain: A review. Int J Greenh Gas Control. 2020; 94:102930.

[14] De Visser E, Hendriks C, , Barrio M, Mølnvik MJ, de Koeijer G, Liljemark S, Le Gallo Y. DYNAMIS CO_2 quality recommendations. International Journal of Greenhouse Gas Control. 2007.

[15] Menon N, Walker M, Anderson M, Colgan N. Compatibility of polymers in super-critical carbon dioxide for power generation systems: High level findings for low temperatures and pressure conditions. 2019; https://www.osti.gov/servlets/purl/1592964

[16] Energy Institute. General Properties and Uses of Carbon Dioxide, Good Plant Design and Operation for Onshore Carbon Capture Installations and Onshore Pipelines - A Recommended Practice Guidance Document. 2010; https://www.globalccsinstitute.com/archive/hub/publications/7276/good-plant-design-and-operation-onshore-carbon-capture-installations-and-onshore-pipelines.pdf

[17] Hertz III DL. Elastomers in CO_2. High performance Elastomers & Polymers for Oil & Gas. 2012; https://www.sealseastern.com/PDF/Elastomers-in-CO2.pdf

[18] Hertz III DL. HNBR in CO_2. High performance Elastomers & Polymers for Oil & Gas. 2014; https://www.sealseastern.com/PDF/HNBR-in-CO2.pdf

[19] Lainé E, Grandidier JC, Benoit G, Omnès B, Destaing F. Effects of sorption and desorption of CO_2 on the thermomechanical experimental behavior of HNBR and FKM O-rings - Influence of nanofiller- reinforced rubber. Polym Test. 2019; 75:298–311.

[20] Ho E. Elastomeric seals for rapid gas decompression applications in high-pressure services. Health and Safety Executive. 2006; https://www.hse.gov.uk/research/rrpdf/rr485.pdf

[21] Balassoriya Arachchige WN. Aging and long-term performance of elastomers for utilization in harsh environments (Doctoral Dissertation]. 2019; https://pure.unileoben.ac.at/portal/en/publications/aging-and-longterm-performance-of-elastomers-for-utilization-in-harsh-environments(a640a3c5-5c70-4ba9-870b-6422319a4a9e].html?customType=theses

[22] Patchigolla K, Oakey JE, Anthony EJ. Understanding dense phase CO_2 corrosion problems. Energy Procedia. 2014; 63:2493–9.

[23] NORSOK. Qualification of non-metallic sealing materials and manufacturers. M-CR-710.1994; https://www.standard.no/pagefiles/1152/m-cr-710r1.pdf

[24] Peacock D. The Effect of Geometry on the Compression Set of Elastomers (Doctoral Dissertation]. Cranfield University. 2002.

[25] Dubois J, Grau E, Tassaing T, Dumon M. On the CO_2 sorption and swelling of elastomers by supercritical CO_2 as studied by in situ high pressure FTIR microscopy. J Supercritical Fluids. 2018; 131:150–6.

[26] Dugstad A, Halseid M, Morland B. Effect of SO_2 and NO_2 on corrosion and solid formation in dense phase CO_2 pipelines. Energy Procedia. 2013;37(2]:2877–87.

[27] Paul S, Shepherd R, Woolin P. Selection of materials for high pressure CO_2 transport. In: Third International Forum on the Transportation of CO_2 by Pipeline. 2012; https://www.twi-global.com/technical-knowledge/published-papers/selection-of-materials-for-high-pressure-co2-transport

[28] Kömmling A, Jaunich M, Wolff D. Ageing of HNBR, EPDM and FKM O-rings. KGK rubberpoint 69(4]:36-42. 2016

[29] Shiladitya P, Shepherd R, Bahrami A, Woolin P. Material selection for supercritical CO_2 transport. In: The First International Forum on the transportation of CO_2 by Pipeline. 2010; https://www.twi-global.com/technical-knowledge/published-papers/material-selection-for-supercritical-co2-transport

[30] Maciejewska M, Sowin A. Thermal characterization of the effect of fillers and ionic liquids on the vulcanization and properties of acrylonitrile – butadiene elastomer. Journal of Thermal Analysis and Calorimetry 138, 4359-4373; https://doi.org/10.1007/s10973-019-08187-8

4 EXPERIMENTAL STUDY OF ACCIDENTAL LEAKAGE BEHAIVOUR OF LIQUID CO_2 UNDER SHIPPING CONDITIONS

Hisham Al Baroudi, Kumar Patchigolla, Dhinesh Thanganadar, Kranthi Jonnalagadda

Centre for Thermal Energy and Materials (CTEM), School of Water, Energy and Environment (SWEE), Cranfield University, Cranfield, Bedfordshire, MK43 0AL, U.K.

Statement of contributions of joint authorship

Hisham Al Baroudi conceptualised experimental methods and facility, conducted the experiments, generated and analysed data and wrote this manuscript, titled "***Experimental study of accidental leakage behaviour of liquid CO_2 under shipping condition".*** Kumar Patchigolla and Dhinesh Thanganadar critically commented on the manuscript before submission to peer-reviewed journal 'Process Safety and Environmental Protection'. Kranthi Jonnalagadda contributed to conceptualisation of the experimental facility.

Abstract

CO_2 shipping has been identified as a viable alternative to enable decarbonisation of scattered emitters and countries where a pipeline-based approach is impractical. However, significant lack of experience in large-scale CO_2 shipping projects implies uncertainty in the selection of optimal cargo conditions and operational safety procedures. The risk of uncontrolled releases can arise in case of mechanical rupture or cracking of storage vessels due to material failure or over pressurisation of the tank. Therefore, a thorough understanding of the discharge phenomena, including the propensity for phase changes and solid formation is necessary to implement safety protocols in the chain. A novel refrigerated experimental setup is established in this study with the aim of investigating the release phenomena of refrigerated, liquid CO_2 in under shipping conditions. The rig features a dome-ended cylindrical pressure vessel, a discharge pipe section and a liquid nitrogen refrigeration system that enables handling of carbon dioxide in proximity of the triple point - at~0.7 MPa, 223 K - and higher liquid pressures typical of vessel transport (~2.6 MPa, 263 K). Pressure, temperature and mass monitoring were considered to enable an extensive observation of the leakage behaviour profile under typical operation scenarios. Three different sets of experiments

were considered to inform the designer in the selection of optimal process conditions, with low-pressure (0.7 – 0.94 MPa, 223 – 228 K), medium pressure (1.34 – 1.67 MPa, 234 – 245 K) and high pressure tests (1.83 – 2.65 MPa, 249 – 259 K) exhibiting distinct behaviours in relation to phase transitions, leakage duration and solidification of inventory.

Keywords: GHG; CCUS; CO_2 transport; CO_2 shipping; process safety; leakage

4.1 Introduction

In response to the global warming crisis experienced as a result of anthropogenic industrial activities, carbon capture, utilisation and storage (CCUS) has been identified as a key option to reduce atmospheric emissions of CO_2 [1]. This technology consists of three principal steps – nominally capture of CO_2 from anthropogenic emitters, its transmission to the sink and storage [2]. Pipelines and sea vessels have been identified as the principal means for large-scale CO_2 transportation [3–6], each exhibiting their techno-economic feasibilities in relation to different project variables [7–9]. Generally, CO_2 shipping is deemed advantageous to discharge relatively small volumes of carbon dioxide over long distances due to its flexibility in sink-source matching and low capital investment costs [10,11]. The selection of transport conditions of future CO_2 shipping for CCUS projects is still uncertain and under debate with respect to techno-economic [12] and process safety considerations [13–15]. Refrigerated liquid conditions of CO_2 relevant to the shipping chain are broadly categorised into low-pressure and temperature conditions (0.6 – 1 MPa, 218 – 233 K), medium pressure and temperature conditions (1.5 – 1.9 MPa, 243 – 253 K) and high-pressure and temperature conditions (>1.9 MPa and 253 K) [13–15] in the literature. Process safety considerations are expected to have a profound impact on the choice of shipping conditions [16]. The propensity for operational issues such as material defects, mechanical failure which can result in cracks and loss of containment [17]. Accidental releases and leakages thus represent a hazard during sea vessel transportation of liquid CO_2 that could put humans, marine life and the carrier in danger due to oxygen displacement over a large area. A thorough understanding of leakage hazards and loss of containment scenarios of sea vessels is necessary for any successful commercial implementation of this technology and assurance of high levels of process safety and integrity throughout the chain. Releases in the liquid phase, and particularly in proximity of the triple point, are complex phenomena which involve phase transitions, dispersion of dense and gas phase

inventory, solid CO_2 formation and pressure and temperature drops in the cargo vessel [18,19]. The UK's Health and Safety Executive [20] highlighted that CO_2 releases in the refrigerated liquid state still require experimental validations of the developed discharge models to determine hazard distances and appropriate safety protocols to be adopted. Due to its density being higher than that of air, CO_2 tends to accumulate in depressed areas, creating a risk of asphyxiation to surrounding environment. Han et al. [21] investigated the implementation of a jettisoning system that could promptly discharge liquid CO_2 inventory from a defected tank in case of mechanical rupture of the vessel to mitigate the potential danger compromising the safety of the crew and integrity of the carrier. Experiments showed that high-pressure liquid CO_2 undergoes two distinct phase changes (liquid to liquid-vapour/liquid-vapour and then solid-vapour) throughout the tube that represented the jettisoning line during the discharge, with phase changes taking place at different locations throughout the pipe. In a follow-up work [22], the authors moreover found that a ventilation system to be paired with the jettisoning discharge would provide an additional level of safety to the operators involved. Speed of the ship is here deemed to be a key factor, with low speed enhancing safety for passengers inside the ship during ventilation and high speeds being safer for general public outside the carrier during jettisoning [22]. Shafiq et al. [23] performed a simulation work of CO_2 depressurisation from a high-pressure vessel (4 MPa and 233 K) in relation to orifice sizes of 4.325 mm, 6.325 mm and 8.325 mm and found that risk of solidification and blockages during the blowdown process can be drastically reduced by selecting the smallest orifice diameter. In a following work, the authors [24] performed a modelling campaign and relative experimental validation to scrutinise dry ice formation during blowdown of CO_2-CH_4 mixture from a cryogenic distillation column at initial temperature of 243 K and pressure of 4 MPa. The authors moreover derived a correlation to determine the optimal blowdown orifice size to be adopted in case of an emergency occurrence as to eliminate the risk of inventory solidification whilst also promoting the fastest discharge times. Most of the available literature concerning CO_2 accidental release for carbon dioxide transport systems focuses under pipeline conditions. Ahmad et al. [25] performed large-scale experiments on full-bore rupture of a 136 tonne pipeline containing dense phase inventory and found that the discharge produced a plume that extended over 400 m away from the rupture location. Guo et al. [26] also investigated discharges form an industrial scale pipeline of 258 m length and 233 mm of diameter from three orifice diameters of 15 mm, 50 mm and full-bore ruptures. Cao et al. [27]

worked on the same large-scale dense CO_2 system at 9.2 MPa and 288 K and investigated the temperature and phase profile in the cross-section during the release. The authors found that phase change to liquid and gas-liquid state occurred rapidly while phase transition from gas-liquid to gas was more gradual. Moreover, significant density fluctuations were observed in the initial stage of the release, attributed to the phase changes and the propagation of the decompression wave through the pipeline. CO_2 solids were found to form at a distance of more than 108 m away from the release orifice, implying the need for appropriate safety protocols. Work from Hébrard et al. [28] focused on releases of 300 kg CO_2 from a 5 m long pipeline with 50 mm internal diameter at high-pressure dense phase of approximately 5 MPa conditions; the authors found that full-bore releases result in a build-up of liquid outflow in the first transient stage, followed by a stable release and a second transient stage; following the phase transition in the section, vapour release is accompanied by a significant reduction in outflow, with the vessel dropping below the triple point and forming dry-ice in the last stage. Hulsbosch-Dam et al [29] performed vertical liquid CO_2 releases from a 1 L vessel at different pressures (6 - 18 MPa) and varying nozzle sizes - 6.4 and 12.7 mm – and found that initial pressure has a limited impact on duration of the release, with nozzle diameter exerting a larger influence. The authors highlighted that the vertical orientation of the leakage nozzle could have an impact on the amount of liquid CO_2 pushed through the opening and thus the speed of the exit jet. Pursell [30] explored liquid and gas phase releases of CO_2 at pressures between 4 – 5.5 MPa from a 60 L vessel. Xie et al. [31] explored the leakage behaviour of supercritical CO_2 releases at different pressures (5 MPa, 7 MPa and 8 MPa) and maximum temperature of 323 K in a pipeline featuring a 30 mm diameter and 23 m length. An under-expanded jet structure was observed in featuring smaller nozzle sizes (1 mm and 3 mm) with this structure disappearing with increased nozzle size of 5 mm. Discharges at higher pressures were found to exhibit lower depressurisation rates and take longer to achieve complete blowdown of the system due to the effect of chocked flow at the exit. The work showed the increase of nozzle size contributed to shorter leakage durations. Tian et al [32] experimentally investigated the release behaviour from a high-pressurised CO_2 vessel in liquid and gaseous phase in relation to different rupture sizes (1 mm, 2 mm and 3 mm) and temperatures (293 K and 323 K) and found that the different states resulted in a distinctly different decompression processes. Discharges in the dense phase resulted in an under-expanded jet flow that gradually disappeared with the decrease of the measured

pressure in the vessel; larger nozzle sizes lead to lower temperature of the fluid in the vessel during blowdown, with liquid stage releases resulting in a higher temperature drop than gas-phase discharges. As highlighted, experimental studies on CO_2 discharges and accidental releases in the literature are largely based on pipeline systems and high-pressure dense, liquid or gas conditions, with limited studies focusing on liquid CO_2 conditions typical of carbon dioxide shipping for CCUS [21,22]. Moreover, to the best of the authors' knowledge, no study has specifically investigated liquid CO_2 discharges typical of shipping systems under a refrigerated state. While the optimal conditions that future CO_2 shipping projects should adopt are still under debate, process safety considerations may well become key decisional factors. However, the nature of depressurisation behaviour in a liquid CO_2 vessel at conditions typical of sea vessel transportation remains largely unexplored, particularly in relation to the propensity for solid formations in proximity to the triple point that can largely affect safety considerations. Such dearth of knowledge is especially critical when infrastructure concerning large shipping port terminals needs to be implemented, given that liquid CO_2 under refrigerated state needs to be continuously handled throughout the liquefaction plant, storage tanks and loading terminal [18]. Therefore, to address these knowledge gaps, this work presents a novel refrigerated 2.25 L experimental set-up and relative investigation of the leakage behaviour of refrigerated liquid CO_2 at conditions relevant to shipping transportation for CCUS and with variable orifice size. The experimental campaign focuses on fifteen tests related to potential shipping conditions affiliated to low-, medium- and high-pressure boundaries in a refrigerated liquid state and scrutinises the discharge process, assessing the propensity for solid blockages on the discharge pipe, pressure and temperature profile as well as inventory solidification in the vessel.

4.2 Experimental methodology

The experimental campaign is performed through the set-up represented in Figure 4-1. The refrigerated test rig features a 2.25 L dome-ended cylindrical pressure vessel with internal diameter of 91.6 mm and 437 mm in length, made of 304L stainless steel. A coil-heat exchanger made of 6 mm copper tubing is soldered around the pressure vessel's surface and enclosed as a cylindrical shell. A vacuum pump is connected to the inlet of the shell and operated to create a layer of thermal insulation around the annulus by removing the air from the shell, thus allowing to maintain the low-temperature conditions during the conditioning stage of the test. The enclosed vessel as well as the

pipework are wrapped in ARMFLEX as thermal insulation material and the system is placed on a platform scale 0 - 150 kg capacity (± 0.05 kg accuracy) - to monitor the mass of inventory in real time throughout the test.

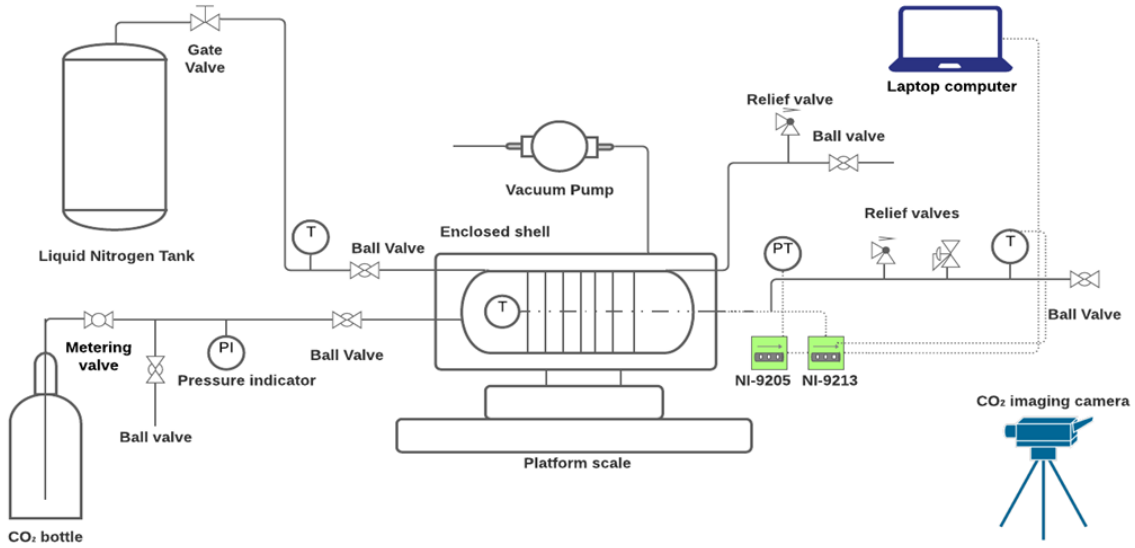

Figure 4-1: Schematic diagram of the refrigerated experimental set-up; drawing not to scale

A pressurised liquid nitrogen Dewar (120 L capacity) is connected to the inlet of the coil heat exchanger to supply the refrigerant and cool the liquid CO_2 to the required working temperature. The gate valve fitted at the source of the Dewar allows to control the flow of liquid nitrogen circulated around the system; upon circulating throughout the coil, the nitrogen is then continuously vented out to atmosphere. A liquid withdrawal bottle is implemented as industrial grade CO_2 source (99.8% purity, conforming to BS 4105 part 1); during the experiments, the bottle withdraws liquid CO_2 and is fitted with a metering valve to restrict the filling flow and thus control the downstream pressure during conditioning. The discharge line is that of a 6.4 mm outer diameter pipe with a 3.2 mm inner diameter and length of 600 mm. At the end of its length, the pipe is equipped with changeable ball valves with a variable orifice diameter. The orifices considered in this work are of 1 mm, 3.2 mm and 4.7 mm, An A-10 Wika pressure transmitter (0 - 2.6 MPa measuring range, accuracy ± 0.03 MPa) with response time of 0.01 s is installed at a distance of 100 mm downstream the pressure vessel for data acquisition purposes; additionally, a pressure-relief valve and back-pressure regulator are implemented for safety reasons. A RS components k-type thermal well (120 – 520 K range, ± 1.5 K

accuracy) is fitted inside the pressure vessel to monitor its temperature profile during the discharge, and another RS components k-type thermocouple (120 – 520 K range, ± 1.5 K accuracy) is placed just upstream of the orifice nozzle at a 550 mm length across the discharge pipe. Both thermocouples have 0.5 s response time. The pressure transmitter and thermocouples are connected to National Instruments 9205 and 9213 modules respectively to enable data acquisition via National Instrument's DAQ Express. Moreover, a FLIR GF343 Optical Gas imaging camera (60 fps) is used to visualise the CO_2 jet flow during the tests. Figure 4-2 and Figure 4-3 illustrate the experimental facility. The experimental system is designed to operate at a range of pressure and temperature conditions in the CO_2 liquid region spanning from 0.7 MPa and 223 K to 5.7 MPa and 293 K.

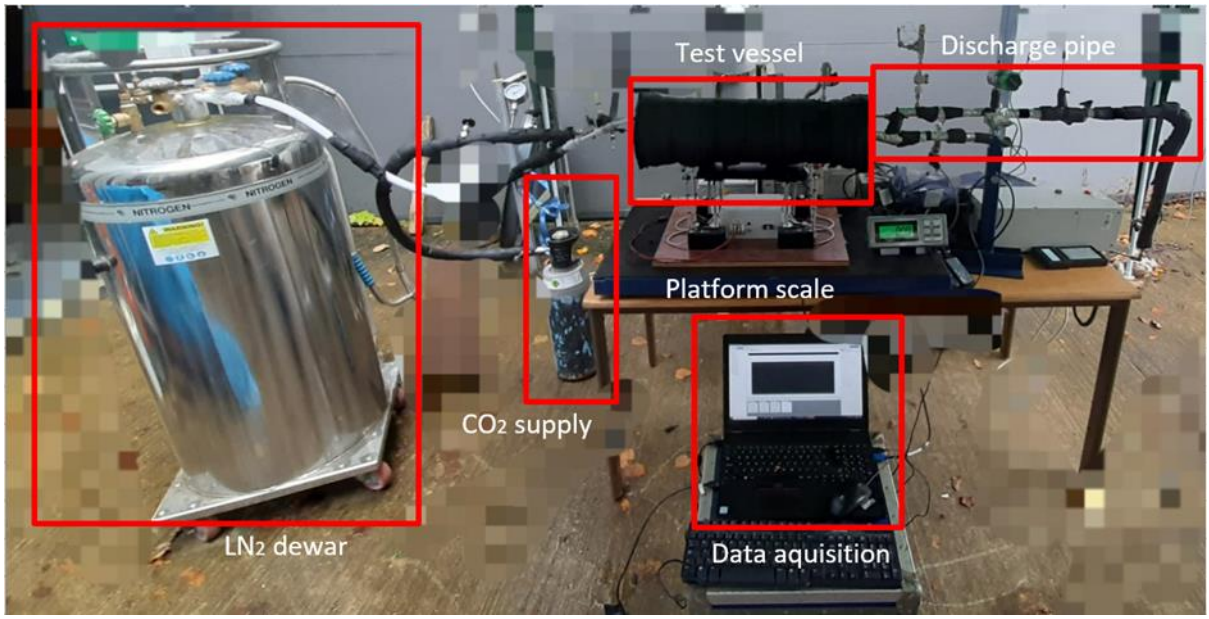

Figure 4-2: Experimental system for cryogenic liquid CO_2 leakage

Figure 4-3 : left-to-right CO_2 camera acquisition view; enclosure shell and test vessel prior to assembly

Along the length of the discharge pipe section, pressure drop is expected to occur due to momentum and friction loss. Unlike ordinary liquids, it is highlighted by Han et al. [21] that the rate of such pressure drop also continues to increase along the length of the discharge pipe. In order to describe this phenomenon, the total pressure drop (∇P_{total}) is presented through a homogeneous model correlation, applicable to both single and two-phase flows above triple point and given in Equation 4-1- Equation 4-4.

$$\nabla P_{total} = \nabla P_{momentum} + \nabla P_{friction} = -\rho_{mixture}\,\mathrm{u}\nabla\mathrm{u} - 2f\,\frac{\rho_{mixture}\,\mathrm{u}^2}{d} \qquad \text{Equation 4-1}$$

$$\mathrm{f} = \frac{0.072}{Re^{0.25}} \qquad \text{Equation 4-2}$$

$$Re = \frac{\rho_{mixture}\,\mathrm{u}d}{\mathrm{\eta}_{mixture}} \qquad \text{Equation 4-3}$$

$$\rho_{mixture} = \frac{\rho_{liquid}\,\rho_{gas}}{\alpha\rho_{liquid} + (1-\alpha)\rho_{gas}};\ \mathrm{\eta}_{mixture} = (1-\alpha)\mathrm{\eta}_{liquid} + \alpha\mathrm{\eta}_{gas} \qquad \text{Equation 4-4}$$

Where u is the flow velocity (m/s), d is the diameter of the pipe (m); Re is the Reynold Number and $\mathrm{\eta}$ is the molecular viscosity (kg/m s). Moreover, ρ denotes the density value in kg/m^3 and α represents the vapour mass fraction. As demonstrated, the variant pressure drop is promoted by both momentum change ($\nabla P_{momentum}$) and friction effects ($\nabla P_{friction}$ - given by the Blasius fanning friction factor relation f); when considering discharges scenarios where isenthalpic pressure drop also induces a change in

temperature, it is expected that the density also decreases promoting an acceleration of the flow. In this work, such correlations describe the effect of the pressure drop effects along the discharge pipe, whereby the flow is a mixture of vapour-liquid above the triple point and vapour and solid below the triple point. The temperature change encountered by the fluid when expanded through an insulated (no heat exchanged with the environment) during the discharge through the pipe restriction is described by the Joule Thomson (JT) effect. Its coefficient μ_{JT} thereby reflects the ratio of temperature change to pressure drop at constant enthalpy value, and it is expressed in Equation 4-5:

$$\mu_{JT} = \left(\frac{\partial \mathrm{T}}{\partial \mathrm{P}}\right)_H \qquad \text{Equation 4-5}$$

When the flashing fluid is initially discharged from the vessel, its state at the exit is considered to be saturated [33]. Beyond the exit plane, the jet enters in a so-called depressurisation zone, where its pressure progressively equilibrates with the atmosphere; throughout this expansion - assumed to be isenthalpic - the jet eventually equilibrates with the atmosphere and enters a two-phase vapour and solid entrainment zone [33]. An approach is proposed by the Energy Institute [33] to estimate the split vapour and solid fraction at the end of the depressurisation zone; the approach implements conservation principles and assumes that the velocity terms can be neglected. Considering p_1 and h_1 as the initial pressure and enthalpy of the stream and p_2 (= 0.101 MPa) and h_2 as the conditions at the conclusion of the depressurisation, the following relationship is thus given in Equation 4-6.

$$h_1 = h_2 = h_{s,1} + Y_{g,1} h_{sg,1} = h_{s,2} + Y_{g,2} h_{sg,2} \qquad \text{Equation 4-6}$$

Where Y_g represents the split vapour mass, $h_{sg,1}$ and $h_{sg,2}$ are the difference between solid and gaseous enthalpy at atmospheric pressure; the correlation can thus be rearranged as Equation 4-7 to give the expected solid mass fraction resulting from the release.

$$Y_s = 1 - \left(\frac{h_2 - h_s}{h_{sg}}\right) \qquad \text{Equation 4-7}$$

Shafiq et al. [24] undertook an experimental and modelling study to assess the tendency for solid formation inside a vessel containing a CO_2-CH_4 mixture during blowdown

scenarios. The approach included the generation of a frost line for the binary mixture in the phase diagram using Aspen HYSIS. In particular, it is based on the assumption that the mixture must not drop below the frost line to avoid solidification during the blowdown process. Based on the study, the authors [24] derived a correlation to determine the ideal blowdown orifice size to adopt in case of sudden emergency to mitigate the risk of inventory solidification during the unplanned release with a ranging CO_2 concentration of 20 – 80 mol% (Equation 4-8).

$$O = 0.00168 * C_{CO_2} + \frac{14.27 + 0.232 * T_i}{log(4.526 + P_i)} \quad \text{Equation 4-8}$$

Where O represents the optimum orifice size (mm), C_{CO_2} denotes the molar percentage of CO_2, and T_i and P_i represent the initial temperature (°C) and initial pressure (bar) in the vessel. This was developed through the BLOWDOWN package in Aspen HYSIS by employing the Peng-Robinson Equation of State, which was found to be the optimum package for CO_2-mixtures based on the comparison of properties with available experimental studies [24]. Such correlation is a trade-off between maximum orifice sizes to be selected to avoid solidification of the content whilst also promoting shorter leakage duration as possible. Larger orifice sizes result in faster discharge processes but increase the temperature drop and thus promote more inventory solidification. This correlation has been extended to the 100 mol% CO_2 considered in this work to explore its applicability to the leakage scenarios under shipping conditions studied in this work.

4.3 Experimental condition

The following experimental procedure was followed rigorously:

1. At the start of the test, the vacuum pump is operated for 30 minutes prior to the injection of carbon dioxide and liquid nitrogen into the apparatus to achieve thermal insulation around the vessel

2. The test vessel is purged with nitrogen gas throughout to eliminate traces of air moisture in the apparatus

3. The liquid nitrogen refrigeration supply is initiated to pre-cool the vessel to 10 K below the intended test temperature

4. Liquid CO_2 in the apparatus is initiated by regulating the metering valve to withdraw at the intended test pressure. The platform scale measurement is switched on and data acquisition is initiated

5. When the target filling of 1.8 kg of CO_2 is achieved as indicated by the platform scale, the supply of carbon dioxide to the system is shut.

6. Test conditions are held for 90 s inside the apparatus. CO_2 camera acquisition is started; the test is therefore initiated by manually opening the outlet ball (90° manual turn, taking approximately 1 s) valve to begin the discharge

7. The test is considered completed when the system's pressure stabilises to 0.1 MPa (atmospheric pressure)

Operating conditions and intended parameters estimation are summarised in Table 4-1. Nine refrigerated liquid conditions relevant to potential CO_2 shipping projects for CCUS – affiliated into low, medium and high-pressure conditions - are selected with the aim of investigating the related leakage and discharge behaviour with an orifice size of 3.2 mm. Moreover, three distinct conditions relative to low-, medium- and high-pressure conditions were considered to assess the impact of varying the orifice size (1 mm and 4.7 mm) on the leakage behaviour. Ambient temperature measurement is undertaken for all tests and found to be comprised between 283 and 287 K (± 1.5) between all the tests, eliminating its relative dependency. Figure 4-4 presents an example of the conditioning stage required to achieve experimental conditions. As it is possible to observe, a stage of pre-cooling of the apparatus and test vessel by means of liquid nitrogen is followed by the injection of liquid CO_2 to achieve the required test conditions.

As it is possible to observe in Figure 4-5, the considered initial CO_2 conditions encompass a wide range in the refrigerated state of liquid CO_2 envelope, exhibiting a close proximity to the saturation line which are favoured for shipping conditions. The experimental campaign shows the leakage behaviour to be significantly affected by the initial inventory condition.

Table 4-1: Summary of starting conditions of discharge tests

Test	Pressure (Ma)	Temperature (K)	Condition	Nozzle size (mm)	Density* (kg/m^3)	Enthalpy* (kJ/kg)
Test 1	0.7	223	Low pressure	3.2	1155	92.7
Test 2	0.83	228		3.2	1136	102.6
Test 3	0.94	225		3.2	1148	96.7
Test 4	1.34	234	Medium pressure	3.2	1114	114.7
Test 5	1.51	242		3.2	1081	131
Test 6	1.67	245		3.2	1068	137.2
Test 7	1.83	249	High-pressure	3.2	1051	145.6
Test 8	2.03	254		3.2	1028	156.3
Test 9	2.65	259		3.2	1004	167.2
Test 10	0.7	223	Low Pressure	1	1155	92.7
Test 11	1.54	244	Medium-Pressure	1	1072	135.1
Test 12	2.04	254	High-Pressure	1	1028	156.3
Test 13	0.7	223	Low-Pressure	4.7	1155	92.7
Test 14	1.52	228	Medium-Pressure	4.7	1138	102.7
Test 15	2.01	252	High-Pressure	4.7	1037	152

properties calculated in NIST REFPROP V9.5 through input of pressure and temperature values

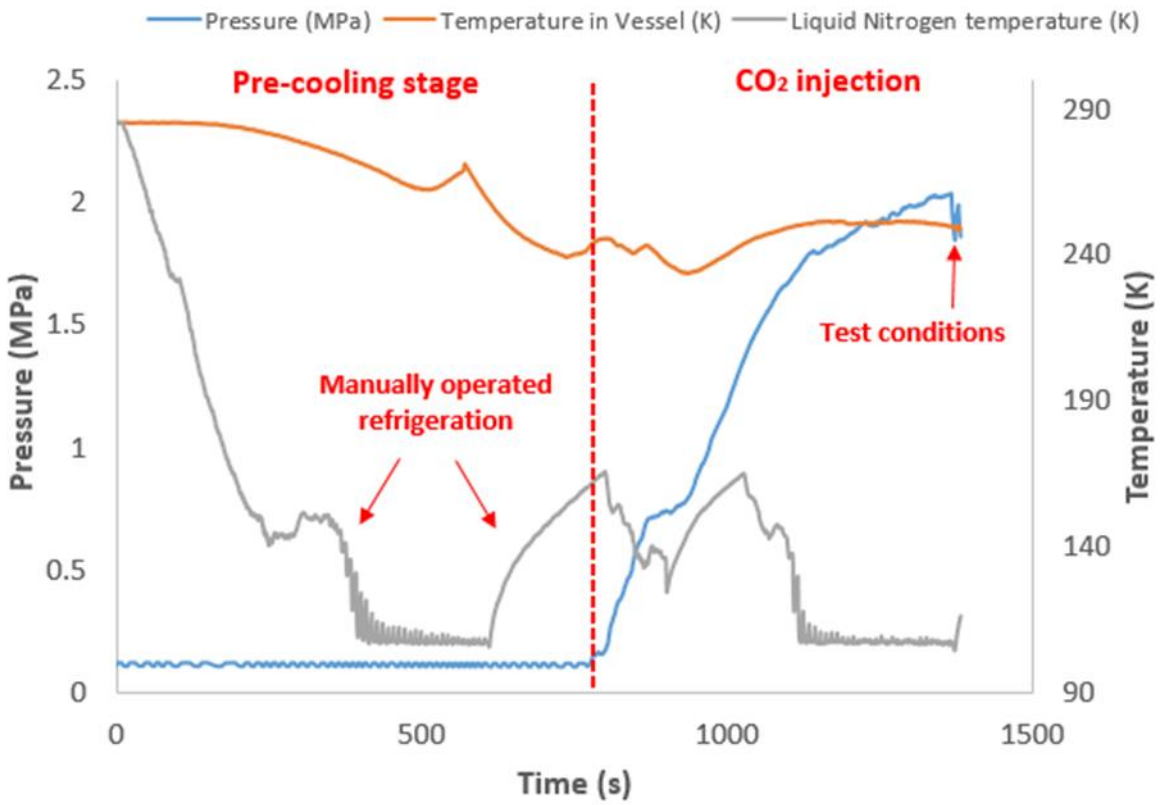

Figure 4-4: Example of test conditioning profile plot – Test 7 (1.83 MPa, 249 K)

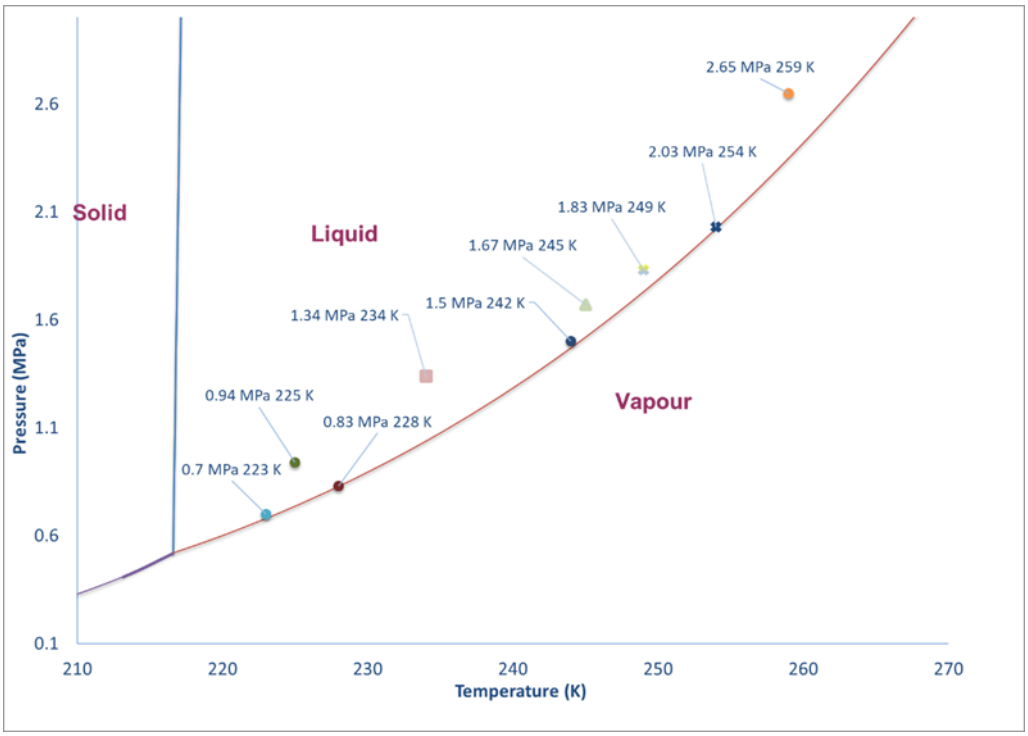

Figure 4-5: Representation of test conditions on CO_2 phase diagram

4.4 Results and Discussion

The typical structure of the initial outflow jet is shown in Figure 4-6 as captured using a FLIR GF343 optical gas imaging camera. The jet expands at the exit nozzle, and its structure is characterised by a decompression region of vapour-solid two-phase flow (initial region) and a secondary dispersion region in which the vapour CO_2 equilibrates with the atmosphere whilst entraining air and slumping to the ground [33]. A simplification can allow to state that, provided that downstream (atmospheric) conditions are unvaried, the split vapour mass fraction can be taken to be merely a function of the initial enthalpy so that $Y_g = f(h_1)$ (Equation 4-6).

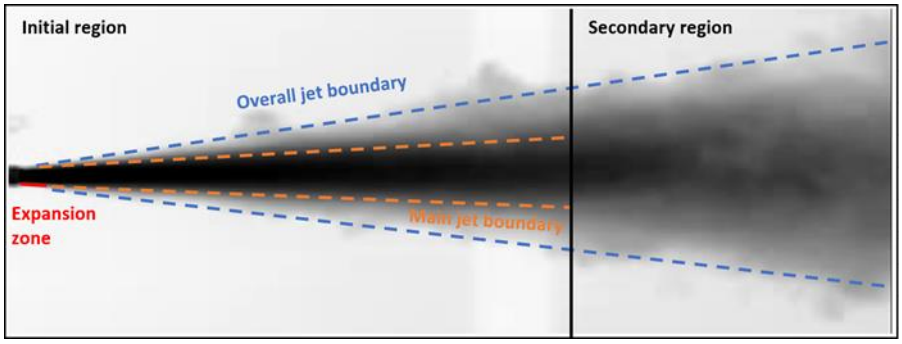

Figure 4-6: Typical jet structure of CO_2 jet flow; test 8, 3 s

As summarised in Table 4-1, enthalpy values for the different test conditions are calculated for the different test conditions. This theoretical reconstruction [33] appears to be confirmed in these tests, where the extent of downstream solid fraction produced during the expansion appears to be less remarkable with the increase of initial enthalpy values in the different tests (Figure 4-7).

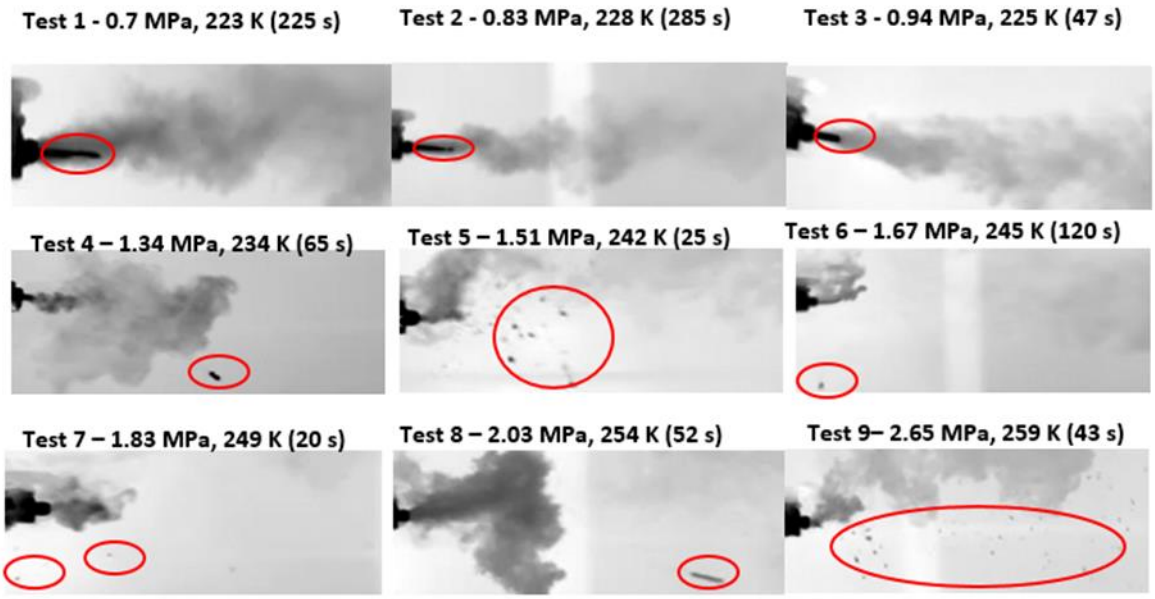

Figure 4-7: Solid formation in the outflow jet in the experimental tests with 3.2 mm orifice size; top-to-bottom: low-pressure, medium-pressure and high-pressure scenarios. Red circles represent solid particles formed in the discharge

Nonetheless, formation of carbon dioxide solids is a complex phenomenon that encompasses mere quantification of expected solid fraction; dry-ice particle begins generating because of a sudden expansion of liquid carbon dioxide throughout the depressurisation zone through a jet break up phenomenon. Size of formed particles and propensity for agglomeration and deposition is found to be accentuated at lower pressures and smaller margins of initial conditions from sublimation temperature under atmospheric pressure [34,35]. These considerations are reflected in the observation in this work, where the size and quantity of solid particles detected in the outflow cloud is considerably higher in the low-pressure discharges. In case of accidental leak scenarios, it is moreover critical to estimate the instantaneous concentration of CO_2 resulting from the dispersion cloud. CO_2 solids formation represent a critical hazard as during the process of particle sublimation, a localised risk of asphyxiation may be posed to personnel located nearby. Pursell [30] provides a simplified equation to estimate the mass of sublimed CO_2 by correlating with presence of diluting air, given as Figure 4-10;

$$m_{CO_2\ Sub} = k m_{air} \qquad \text{Equation 4-9}$$

Where $m_{CO_2\ Sub}$ represents the mass of sublimed CO_2, k is the linear correlation constant that integrated it with m_{air}, which is the mass of entrained air. Consequently, an

empirical correlation was proposed to describe the concentration of CO_2 at any given downstream distance from the leakage source and given as Figure 4-11.

$$C(x) \approx 5\ \frac{d_e C_0}{x}\left(\frac{\rho_{air}}{\rho_{mixture}}\right)^{1/2} \qquad \text{Equation 4-10}$$

Where $C(x)$ represents the CO_2 concentration (mol%) at a downstream distance x (m), C_0 is the initial carbon dioxide concentration (mol%) and d_e is the diameter of the source (m) at the atmospheric plane; ρ_{air} and $\rho_{mixture}$ are the air and gas plume density respectively (kg/m^3). As reflected in Figure 4-6, the resulting expansion of the jet at the exit plane at conditions scrutinised in this work lacks of a barrel expansion structure, which indicates a subsonic (M<1) profile at the exit nozzle. This is contrast with works on higher pressure supercritical and liquid CO_2 releases [30,31] that conversely reportedly show a barrel shock and Mack disk structure that effectively increases the dimension of d_e and thus contributes to a higher CO_2 concentration value at a given downstream distance. Low-pressure streams – possessing a lower initial specific enthalpy value (Table 4-1) - are associated with a higher mass split fraction of solid phase during isenthalpic expansion of the jet; however, the formed solid plug observed in Figure 4-7 is found to be suppressing the mass outflow from the vessel in tests 1,2 and 3 since the early stage of the release. Therefore, the risk of asphyxiation arising from CO_2 concentrations at low-pressure releases appears to be primarily associated with sublimation of localised solid particles expelled during the release.

4.4.1 Impact of initial conditions and orifice size

Upon filling of the inventory and conditioning to the required testing conditions, liquid CO_2 is contained in the pressurised, insulated vessel which enables to keep it in its liquid state. As the tests are initiated and the nozzle orifice is opened to release the CO_2 vapour in the space above the liquid, the content of the vessel begins to discharge to the atmosphere due to the pressure difference between the pressure vessel and the surroundings.

As highlighted in Figure 4-8 and Figure 4-9 – which respectively show the pressure and temperature profile of the releases - the considered tests for the low-, medium- and high pressure transport conditions exhibit a distinctively common discharge behaviour. This observation strengthens the hypothesis that selection of appropriate conditions in the refrigerated liquid state is very sensitive to the margin from the triple point. In particular,

it is interesting to observe that the modest difference initial conditions exhibited by test 6 (1.67 MPa, 245 K) and test 7 (1.83 MPa, 249 K) leads to a significantly different leakage duration. Alongside the differences, tests demonstrate common trends - namely the solidification of portion of the inventory (19- 39 wt%) that leads to the achievement of ~ 200 K temperature value in the system. As reflected by the distinct leakage duration (Figure 4-8) reported for each pressure boundary, it appears evident that propensity for solid formation in the discharge pipe is considerably more accentuated at medium pressures (1.34 – 1.67 MPa) compared to high pressure tests (1.83 – 2.65 MPa).

The low-pressure discharges show a consistent behaviour manifested in several stages (Figure 4-8 and Figure 4-9). Test 1, performed at 0.7 MPa and 223 K is considered in more detail (Figure 4-11) to describe the release at low-pressure conditions. The discharge initiates with an initial drop in pressure that could be attributed to the discharge of non-homogeneous gas phase contained in the vessel that brings the pressure to a value of 0.57 MPa [30]. At the same time, the process is characterised by the absence of inventory discharge from the early stage of the release in favour of an observed vapour-solid cloud (Figure 4-10). This is reflected by the presence of a blocked outflow form the pipe whereby no vapour-liquid flow is observed since the early stage of the release, owing to solid accumulation upstream the nozzle (Figure 4-10). As the fluid leaves the vessel and enters into the pipe section, it undergoes a rapid expansion accompanied by a loss of pressure due to momentum and friction effects; thus, the resulting temperature drop related to the Joule-Thomson effect correlated to the pressure drop in the pipe promotes the formation of dry ice particles in the two-phase (vapour-solid) as the flow condition drops below the tripe point pressure [36]. Indeed, this propensity is favoured by the close proximity of the initial fluid pressure in tests 1, 2 and 3 (0.7 – 0.94 MPa) to the triple point and thus vapour-solid envelope.

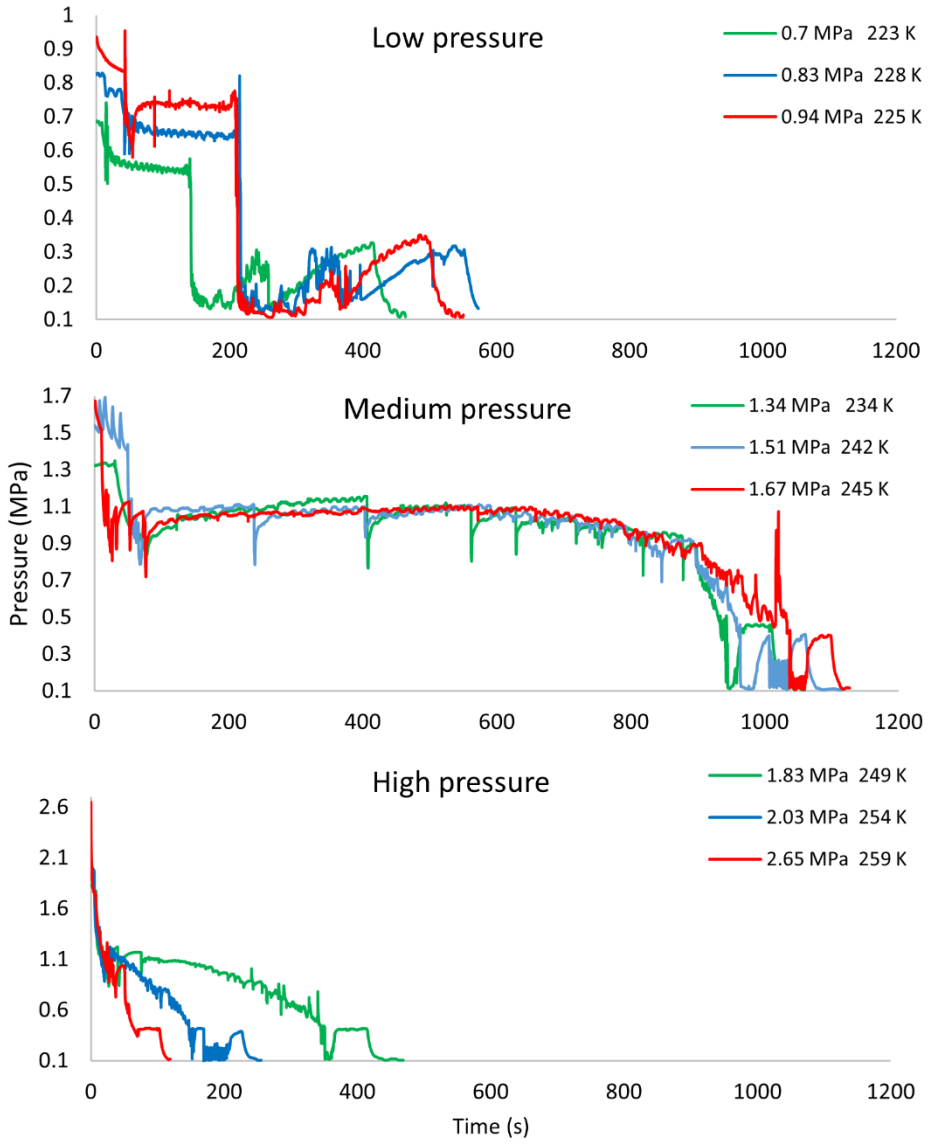

Figure 4-8: Pressure profile of the experimental tests with 3.2 mm orifice size

During this stage, the formed blockages can be considered to be located upstream of the nozzle, as reflected by the absence of flow and measured temperature profile in the discharge pipe. The recorded temperature profile (stage 1), and specifically the 30 K temperature difference between the fluid temperature in the vessel (223 K) and the measured temperature in the discharge line (255 K) confirms this observation (Figure 4-11). In such scenario the net cooling effect recorded by the thermocouple is conversely given by the accumulated solids sublimating through the pipe and thus progressively cooling the pipework. At the same time, the consistent pressure measurement of ~ 0. 57 MPa demonstrates that the aforementioned solid blockage has

generated downstream the pressure transmitter at a distance of >100 mm along the discharge pipe (where the pressure measurement is located).

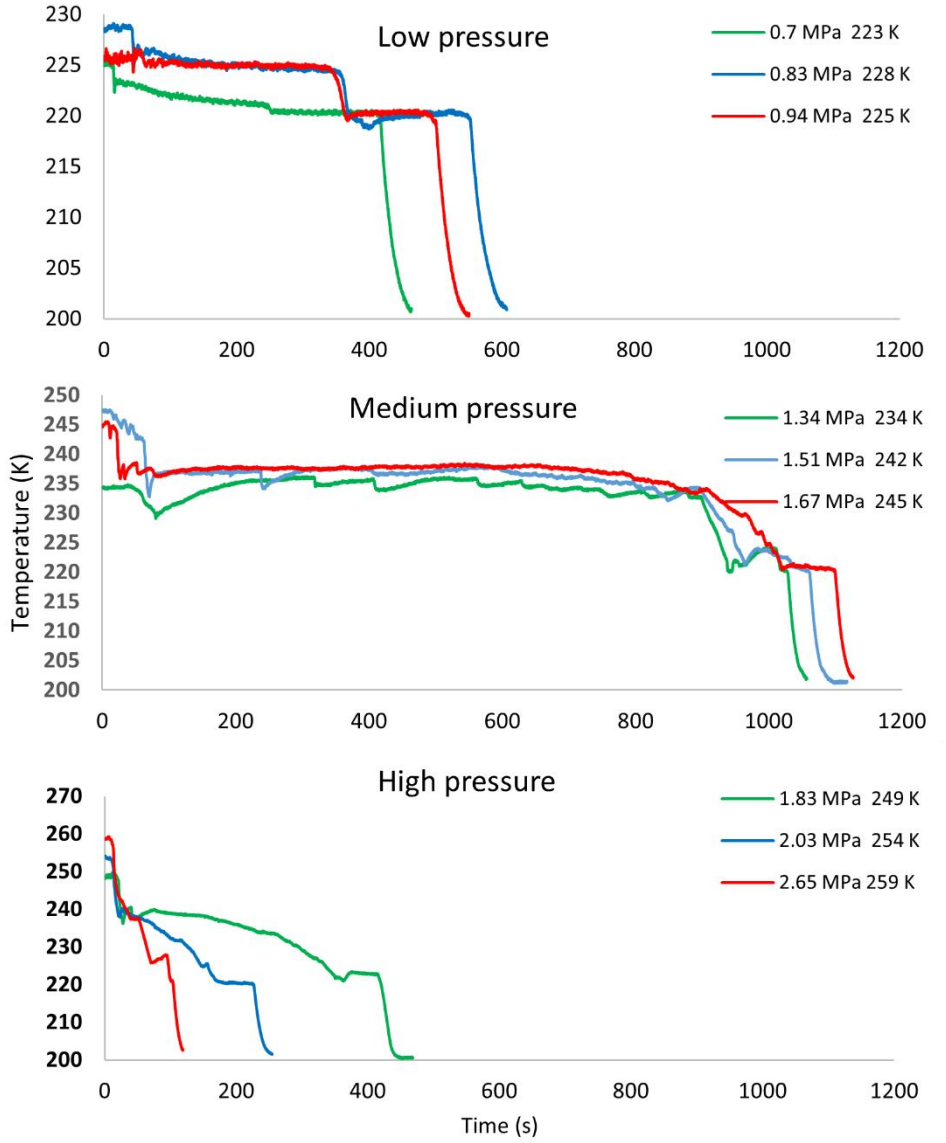

Figure 4-9: Temperature profile of the experimental tests with 3.2 mm orifice size

Throughout stage 1, measured pressure shows modest fluctuations likely caused by the intermittent flow vapour-solid flow in the pipe. At 140 s, an abrupt drop in pressure brings the measured value close to atmospheric (0.17 MPa) within 10 s. This trend is common in all performed tests under low-pressure boundaries, albeit occurring at different pressure conditions, namely at 0.64 MPa in test 2 and at 0.74 MPa in test 3; the steady temperature profile observed in the vessel alongside the fact the such pressure drop

occurs at different pressure values in tests 1, 2 and 3 allows to discard correlation of this phenomenon with a phase transition inside the vessel.

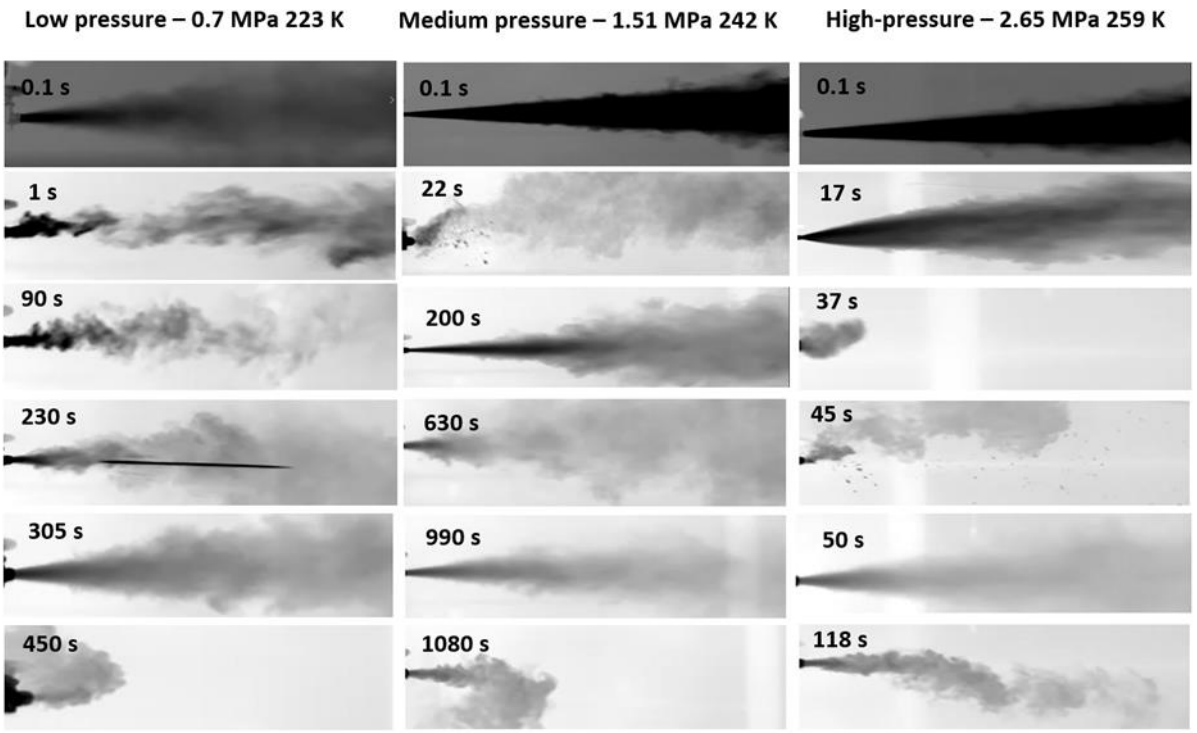

Figure 4-10: CO_2 jet flow throughout the discharge stages at different pressure conditions with 3.2 mm orifice size

The observed trend can conversely be attributed to the propagation of dry ice blockages further upstream the pressure transmitter's measurement, potentially at the exit nozzle of the vessel. As found by Teng et al. [35] and Liu et al. [36], pressure and temperature conditions of the stream largely impact the size of formed dry-ice particles: mean particle diameter is found to increase when the margin between initial temperature of CO_2 and sublimation temperature reduces, with a tendency to also reduce with the increase of pressure [35]. Agglomeration and deposition of individual solid particles takes place with particles depositing on the tube wall and entraining in the pipe resulting in a layer formation [36]. Similarly, to the solid generation phenomenon, this process is favoured at lower temperature values and modest velocity of dry-ice jet; this is because low flow velocities promote larger agglomerates sizes due to the detachment force on to the deposition stratification. Therefore, it appears clear that low-pressure conditions scrutinised in this work result in not only in the highest amount of solid generation at the triple point (as per split solid fraction generated during isenthalpic expansion, Equation

4-7) but they also have the highest propensity for formation of particles with large mean diameter during the complex discharge phenomenon (Figure 4-7).

The presence of large solid plugs that obstruct the exit nozzle of the vessel is supported by the fact that at 225 s (Figure 4-7), the recorded video profile shows the ejection of a large solid blockage having the same diameter as the discharge pipe, which can also be observed at 230 s in Figure 4-10. Such expulsion of dry-ice plug is observed in all low-pressure tests but it does not appears in any of the other tests performed at medium- and high-pressure (Figure 4-7); this demonstrates that size of formed solid particles and propensity for agglomeration and deposition is noticeably higher at low-pressure conditions. The ejection of the solid plug from the pipe section demonstrates an effect of fluid pressure on the solid blockage, potentially owing to the ongoing vaporisation process-taking place in the vessel (Figure 4-10). It is noteworthy that previous literature found that active nucleation of liquid CO_2 can delay the phase transition from liquid to liquid-vapour state [21], thereby maintaining CO_2 in a metastable state during such delay, whereby density change is limited. This suggests that vapour-liquid conditions in the vessel may have established before the encountering of this trend.

At 216 s, the pressure begins to progressively increase; this behaviour can be attributed to an increasing pressurisation occurring inside the vessel and induced by the aforementioned vaporisation process of the inventory. The vaporising CO_2 therefore starts to gradually flow into the pipe and pressure measurement hereby continues to increase until reaching a value of ~0.3 MPa at 240 s. Consequently, the pressure measurement experiences another abrupt drop to 0.15 MPa; conversely to the previously occasion, this phenomenon is hereby accompanied by a temperature reduction inside the vessel, which reaches value of ~220 K that is maintained for 196 s (Figure 4-11). This trend is also common to the other tests performed at the low temperature envelope, where the pressure drop encountered in stage 2 also occurs alongside a temperature step-change to 220 K - regardless of the initial temperature, as shown in Figure 4-9. This observation suggests that triple point conditions are established in the system in this stage and the aforementioned pressure drop represents a phase transition of liquid inventory solidifying in the vessel. At this point, the process enters into a new stage (Stage 3) lasting approximately 196 s. Achievement of near-atmospheric pressure in the vessel at the end of stage 2 – prompted by the phase change of inventory promoted at triple point conditions – indeed indicates no vapour

pressure left in the system. For this reason, the absence of vapour pressure can maintain the solids generated during the aforementioned expansion promotes a process of sublimation that starts to take place in the vessel in stage 3.

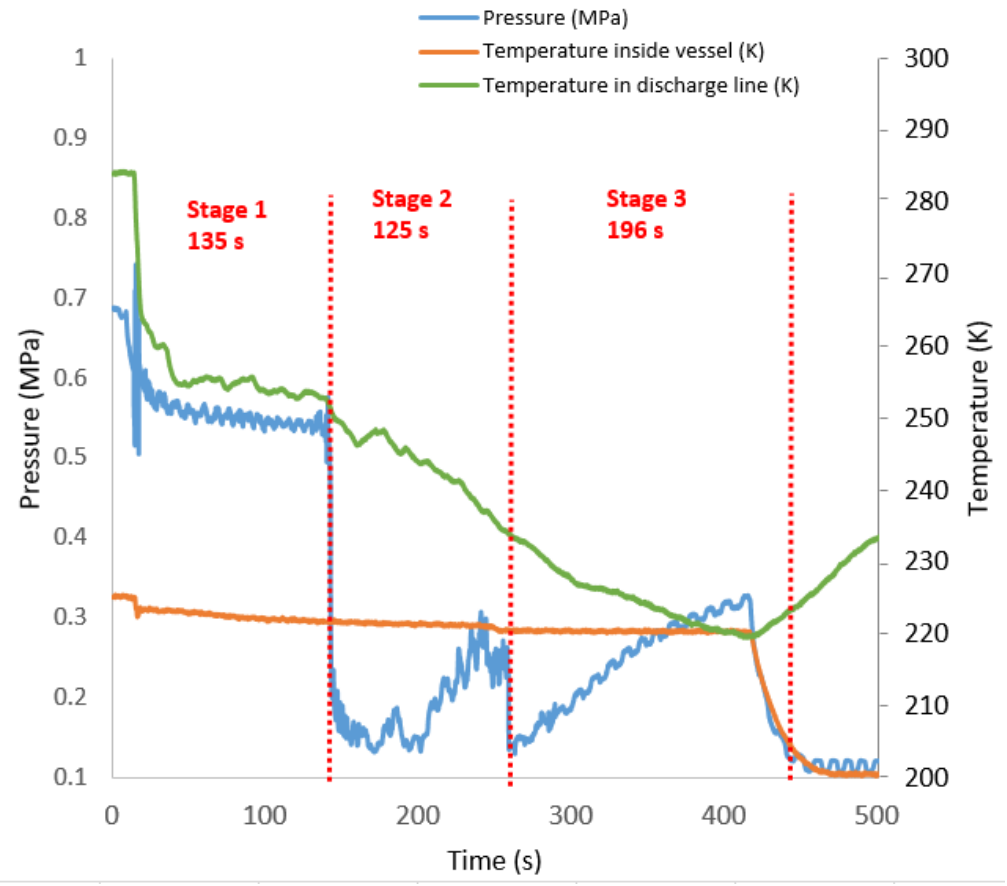

Figure 4-11: Experimental data of 0.7 MPa and 223 K release with 3.2 mm orifice size (Test 1)

As demonstrated by the tendency for pressure to increase at this stage (from 250 s onwards) – accompanied by absence of signs of blockages highlighted in the camera acquisition profile – it appears that the rate of vaporisation is higher than the outflow rate during this phase. Similarly, to the behaviour encountered throughout stage 2, the pressure increase eventually halts upon reaching the same value of ~0.3 MPa (Figure 4-11). Following this point, the pressure and temperature profile shows a steady reduction in the vessel – presumably across the sublimation line - whereby CO_2 solid phase under atmospheric pressure is thus generated in the vessel. Medium pressure conditions (tests 4, 5 and 6) also exhibit a distinctively common discharge behaviour as shown in the pressure and temperature profile in Figure 4-8 and Figure 4-9. The leakage process (Figure 4-12) begins with an initial discharge of inventory that lasts for approximately 20 s, promoting a pressure reduction inside the system; the thick jetted

cloud observed from 0.1 s (Figure 4-10) indicates the discharge of saturated inventory, in line with findings from the Energy Institutive [33].

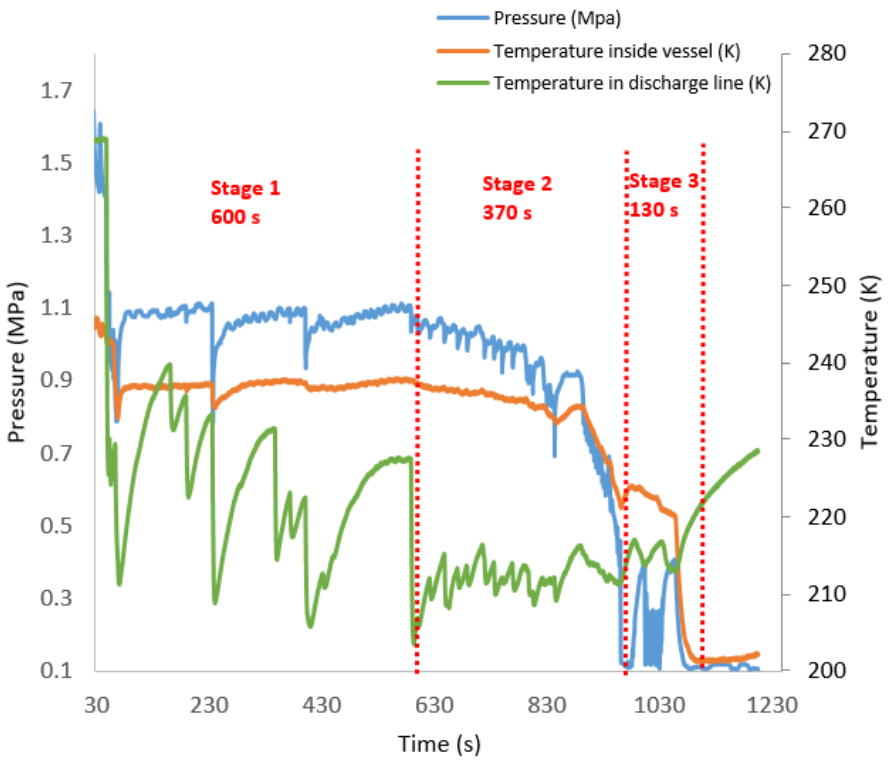

Figure 4-12: Experimental data of 1.51 MPa and 242 K (Test 4) with 3.2 mm orifice size

It is noteworthy that this initial trend is dissimilar to what encountered in the early release stage at low-pressure conditions, whereby absence of outflow was immediate, implying early formation of solid blockages in the pipe. This difference is due to the fact that the initial conditions of low-pressure tests (0.7 - 0.94 MPa) exhibit a considerably lower margin from the triple point and vapour-solid envelope compared to medium- and high-pressure releases. Eventually, the initial depressurisation stage ends at 22 s, where the system's pressure settles at 1.1 MPa. As in the previous scenario and owing to the pressure drop effects induced by momentum and friction loss in the pipe, it is possible to assert that the pressure just upstream the exit nozzle drops below the triple point pressure. The flow thus enters and thus enters in a vapour-solid phase at approximately 22 s, as demonstrated by the solid blockage formation which halts the outflow form the system. In particular, the measured temperature of 215 K at 45 s in the discharge pipe reflects the contribution of the resulting Joule Thomson cooling effect correlated with the aforementioned pressure drop, whereby the fluid flow appears to progress in the vapour-solid envelope.

From this point, the pressure and temperature profile in the system enter into a stage that lasts approximately until 600 s (Stage 1), where the profile remains steady except for sporadic discharge resumptions occurring around 230 s and 430 s (Figure 4-12). Throughout this stage, the suppressed outflow behaviour due to the solid blockage is accompanied by the absence of a significant rate of vaporisation of inventory, which is reflected absence of a pressure accumulation exerted by potential vapour phase that is not able to discharge. The plot of temperature in the discharge line in this stage show considerably large in range and cyclic fluctuations from 240 to 210 K (Figure 4-12) are reported, strengthening the observation that formation and accumulation of dry-ice solids upstream the exit nozzle was intermittently effecting the discharge of flow. Conversely to the low-pressure scenarios, at medium-pressure condition both the rate of solid formation, dry-ice particle diameter and propensity for agglomeration are found to be lower [35], owing to the higher initial pressure and temperature conditions. As such, it would be intuitive to expect shorter leakage time in the medium pressure scenario as compared to the low-pressure tests, due to the anticipated more modest impact of solid formation in the discharge pipe. The reason why this trend is not observed, and thus why medium pressure releases eventually exhibit considerably higher leakage time is related to sustained solid particles generation in the discharge pipe. As it can be observed in Figure 4-12, at 230 s the fluid flow temporarily resumes, owing to the ability of the fluid pressure to overcome the formed dry-ice blockages; this is demonstrated by the recorded pressure drop and measured temperature profile in the discharge pipe. However, it also appear evident that such high velocity flow in the vapour-solid phase (temperature in the discharge pipe 210 K) continues to promote more vapour-solid flow and thus solid formation in the pipe (measured temperature value drops again to ~215 K, Figure 4-12). Due to the thereby reformed solid particles, the discharge halts again, with this trend continuously taking place in a cyclic fashion at ~230 s and 430 s. This process continuously delays the discharge phenomena, resulting in a considerably longer leakage process. This is contrasting with the discharge behaviour displayed by low-pressure scenarios, whereby a complete absence of CO_2 flow is observed in the pipe and a pressure increase in the vessel due to CO_2 vaporisation effect leads to expulsion of the solids plug. From 600 s (Stage 2), it is possible to observe a continuous resumption of the discharge flow, attributed to the overcoming of the solid blockage in the pipe and reflected in the steadier temperature profile now exhibited in the discharge pipe. It is particularly interesting to find that the

duration of stage 2 appears to be consistent in all of the three medium pressure tests (Figure 4-8), allowing to assert that within this threshold, combination of initial liquid conditions, flow conditions in the discharge pipe creates a propensity for longer blockages that considerably delay the discharge process. The pressure and temperature within the vessel assume a parabolic decay profile lasting approximately 370 s. When dropping its pressure below the triple point, similarly to the previous set of tests, an accentuated pressure drop brings the measured pressure close to atmospheric values prior to incurring in the pressure and temperature profile described for low-pressure releases (Figure 4-12). This reflects a common trend for cyclic sublimation and deposition processes.

It is however noteworthy that duration of such stage appears to be different for the different scrutinised conditions: its duration is of 196 s at low-pressure conditions (Figure 4-11) and 130 s for medium-pressure release (Figure 4-12). High-pressure releases (test 7, 8 and 9) show a characteristically distinct discharge behaviour as show in Figure 4-8 and Figure 4-9. Under these conditions, it can be observed that leakage duration shows a more remarkable trend of inverse correlation with initial stream pressure (Figure 4-9). Therefore, having established through the previous paragraphs that formation of CO_2 solids is a significant factor in leakage duration, it is found that selecting a greater margin from the solid region demonstrates to be effective in minimising the impact of solid formation in the discharge pipe. A characteristic plot of high-pressure releases is presented in Figure 4-13; as it is possible to observe, an initial discharge (stage 1) lasting approximately 21 s brings the system's pressure to 1.1 MPa.

During this stage, the temperature in the discharge pipe also drops significantly, discharging at a ~30 K temperature margin from the temperature measurement in the vessel; similarly to the medium pressure scenario, this drop in temperature can be ascribed to the Joule-Thomson effect as of the effects as a result of the pressure drop encountered throughout the length of the pipe. The pressure profile begins to fluctuate abruptly due to solid formation in the pipe as the process enters stage 2. During this time, it is noteworthy that the rate of temperature drop in the discharge line also increments significantly; this is potentially owing to the sudden increased temperature drop in the flow promoted by the obstruction of the pipe by means of dry-ice particles. As it is possible to observe in Figure 4-10, dry-ice formation progressively leads to a blockage that can be seen from 37 to 50 s. This is reflected in the build-up of pressure

cause by a continuous evaporation inside the system that temporarily obstructs the outflow. At around 50 s, the flow is able to overcome the blockage and the discharge progresses until achieving a plateau (40 s) around the triple point region, which as previously established is associated with the solidification of part of the fluid.

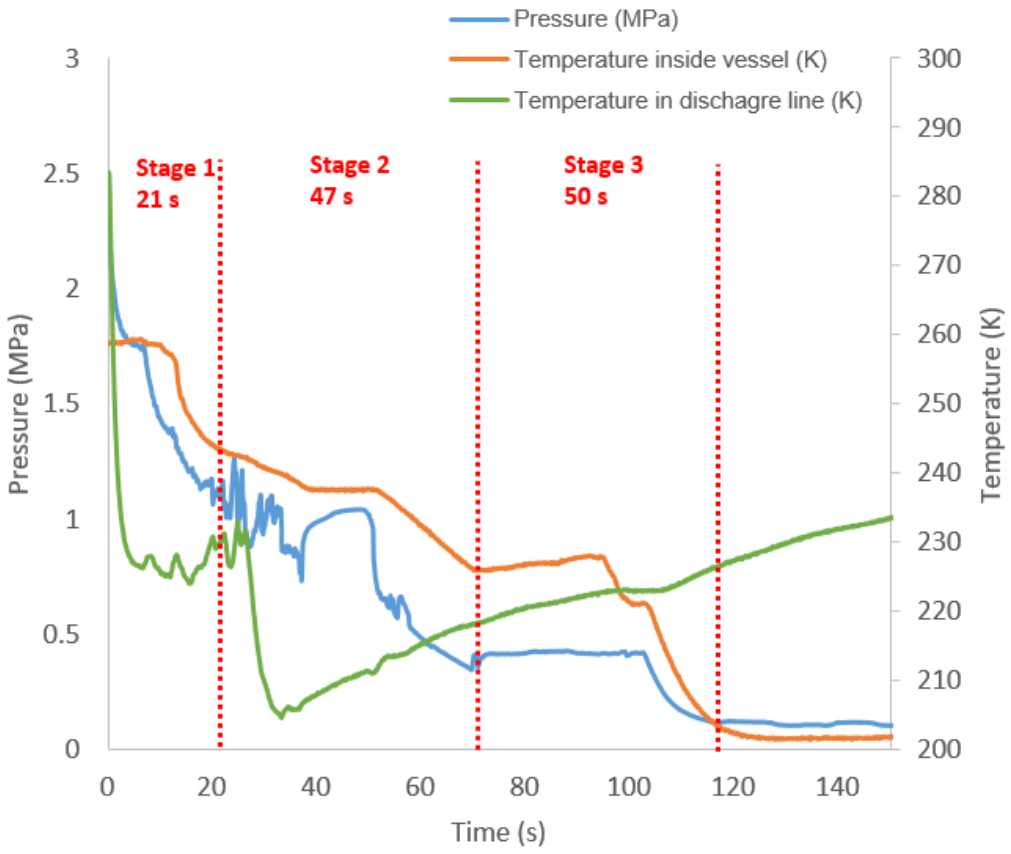

Figure 4-13: Experimental data of 2.65 MPa and 259 K release (Test 9)

Unlike medium pressure releases, the combination of flow profile through the pipe as well as the quantity and size of solid particles formed during the discharge of the flow does not imply prolonged blockages, demonstrating that the effect of solid formation is considerably more modest under these conditions.

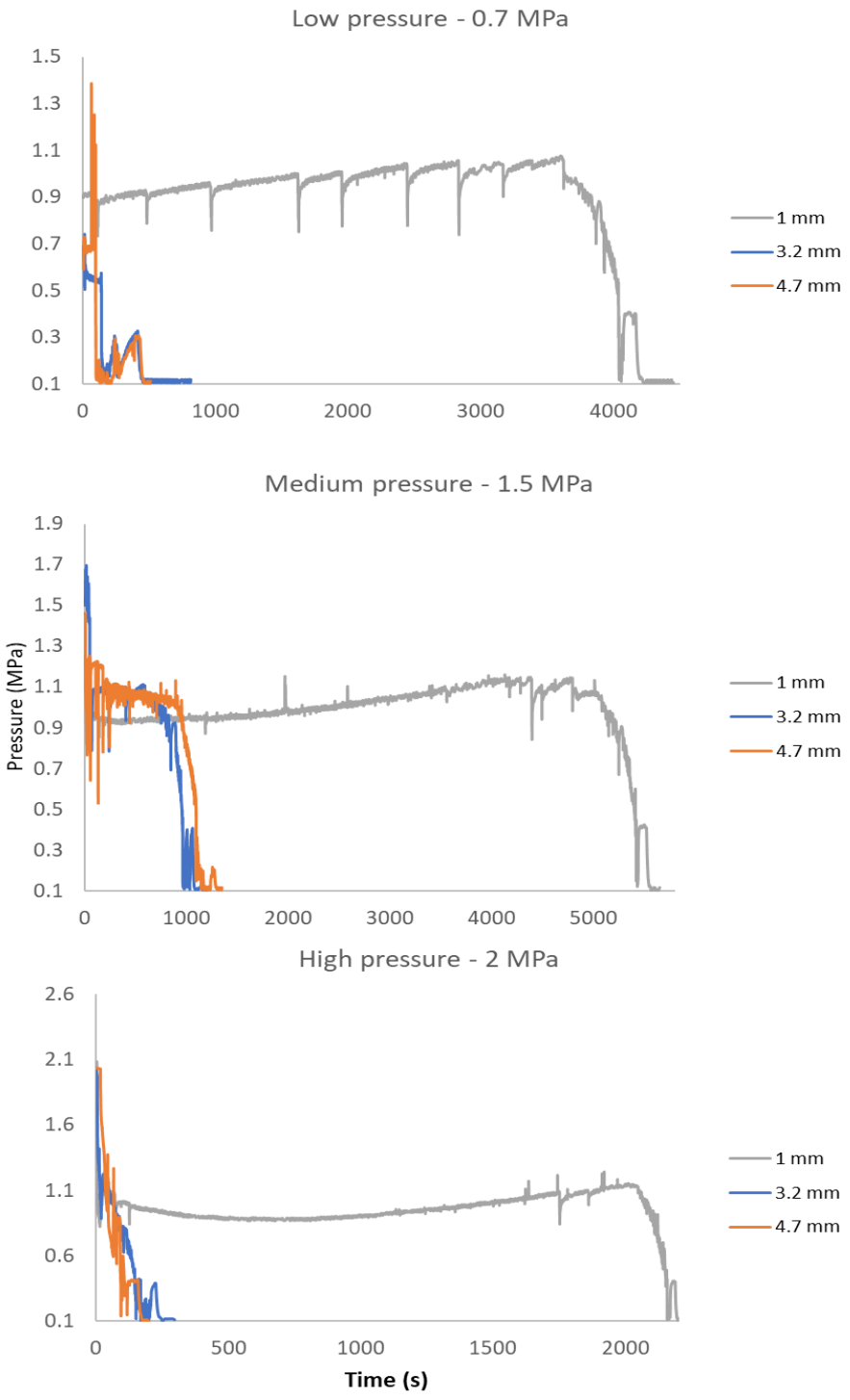

Figure 4-14 Pressure profile of the discharge under different conditions and orifice sizes

As highlighted in several studies [30,32,33] orifice size has an effect on the depressurisation behaviour of CO_2 under pipeline conditions. This study demonstrates that selection of orifice size can have a profound impact on the discharge under shipping conditions too. Figure 4-14 shows that a 1 mm orifice results in considerably longer

releases in low-, medium- and high-pressure conditions. Thus, it appears evident that leakage from 1 mm orifice generates a propensity for formation of solid CO_2 blockages which halt the discharge process and lead to a progressive increase of pressure in the system. The blockages have variable duration depending on the conditions and the resumption of the leakage process can thereby be potentially attributed to an increase in rate of vaporisation in the system that contributes to expel the blockage from the discharge pipe. In the low-pressure scenario, the flow resumes at 3700 s, after the pressure in the system reaches a value of 1.1 MPa; at 4800 s under medium-pressure conditions upon achieving a value of 1.1 MPa and at approximately 2000 s at 1.1 MPa in the high-pressure scenario. Conversely, the leakage behaviour and duration does not present any significant differences in relation to 3.2 mm and 4.7 mm orifice implying that in that range there is no significant difference in the propensity for solid blockage formation.

4.4.2 Leakage duration and solidification of inventory

The leakage duration and cargo solidification as a result of the discharge process are significantly different in relation to the different initial pressure conditions. As emphasised in Figure 4-15, releases at medium pressure conditions manifest the highest leakage duration by a significant margin; conversely high-pressure releases show the lowest, with the noticeable trend to reduce with a further increase of pressure. This trend indicates that adoption of an increased margin from the triple point in this range considerably reduces the risk and magnitude of solid formation in the discharge line and vessel system during the release, resulting in overall more linear releases.

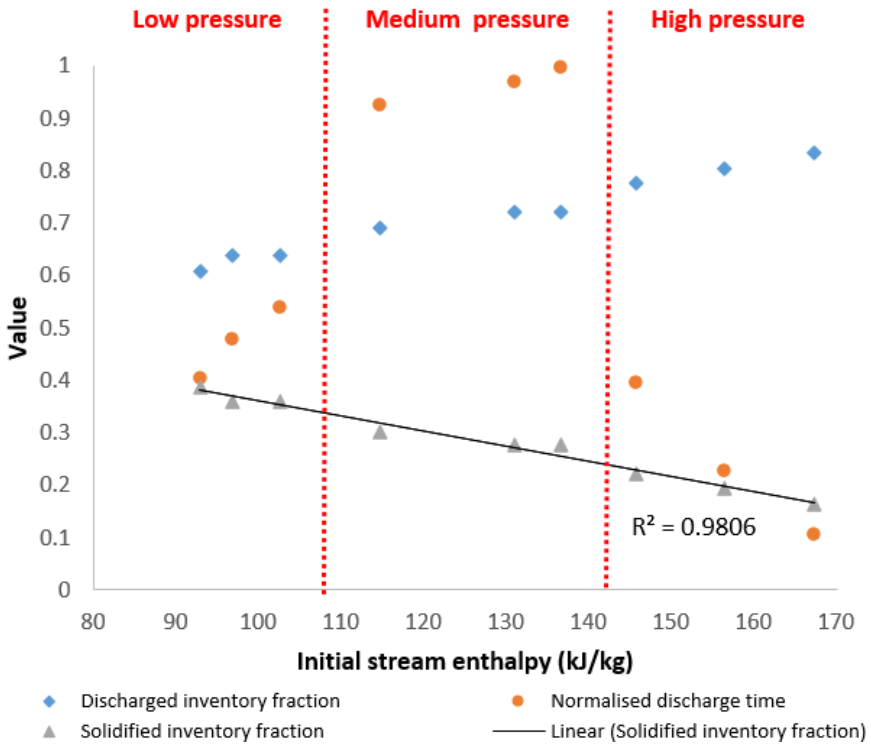

Figure 4-15: Normalised discharge time and discharged inventory fraction with respect to initial stream's enthalpy

Although low-pressure conditions exhibit a closer proximity to the triple point and thus to the solid envelope, dry-ice formation in the discharge pipe appears to be affecting medium-pressure releases to a greater extent as per duration of the leakage process (Figure 4-15). As previously explained, this tendency is promoted by the intermittent outflow from the pipe – supposedly in the vapour-solid region - which results in continuous re-formation of solid blockages in a cyclic fashion.

Conversely, the nature of the discharge process concerning low-pressure conditions is such that it results in relatively faster leakage processes albeit with a higher inventory solidification. It is particularly noteworthy that inventory outflow appears to be suppressed from the formation of solid blockages in the pipe form an early stage of the release (Figure 4-10). The significant outflow of inventory – observed in stage 3 – appears to be limited to a phase transition (sublimation) of solids generated upon achievement of triple point conditions in the vessel. Figure 4-15 shows a correlation between initial stream's enthalpy, leakage duration and discharged/solidified inventory fraction in all tests. As it is possible to observe, in the low- and medium-pressure conditions an increase of discharged inventory occurs alongside an increase in discharge time as initial stream's enthalpy increases; in high-pressure releases this

trend is reversed, with discharged amount still increasing with enthalpy, though the normalised leakage time decreases showing a negative correlation.

Table 4-2: Estimation of optimum orifice size to prevent solidification - Equation 4-8 - and measured inventory solidification in this work

Conditions	Optimum orifice size (mm)	Orifice size in this work (mm)	Actual Solidified inventory (%)
0.7 MPa, 223 K	1.3	1 – 4.7	36 - 39
1.5 MPa, 242 K	2.5	1 – 4.7	28 - 31
2 MPa, 252 K	3.2	1 – 4.7	19

Overall, the increase of the stream's initial specific enthalpy appears to promote a lower level of final inventory solidification in this experimental campaign (Figure 4-15). Table 4-2. As it can be observed in Table 2, the discharge process resulted in a variable amount of inventory solidification inside the vessel in the performed tests, ranging from 19% at high pressure to 39% at low pressure conditions. Despite also considering smaller orifice sizes (1 mm) than those indicated by Shafique et al. to avoid solid formation inside the system [25], this work demonstrated that solidification of inventory still occurred in the vessel. Moreover, varying the orifice size did not show any significant difference in rate of inventory solidification at the end of the leakage process. This finding indicates that the proposed correlation does not appear to be suitable for the refrigerated CO_2 conditions considered in this work at 100 mol% CO_2 content. This is potentially attributable to the complexity of the phenomenon and the interaction between the liquid, solid and vapour states inside the vessel. Figure 4-16 shows the plot of the two safety indicators discussed in this work in relation to all experimental tests. Values closer to zero indicate a lower level of inventory solidification at the end of the test (y-axis) and a lower leakage time (x-axis). On the other hand, a value closer to one

denotes a higher level of inventory solidification in the vessel and higher time for the leakage process to complete.

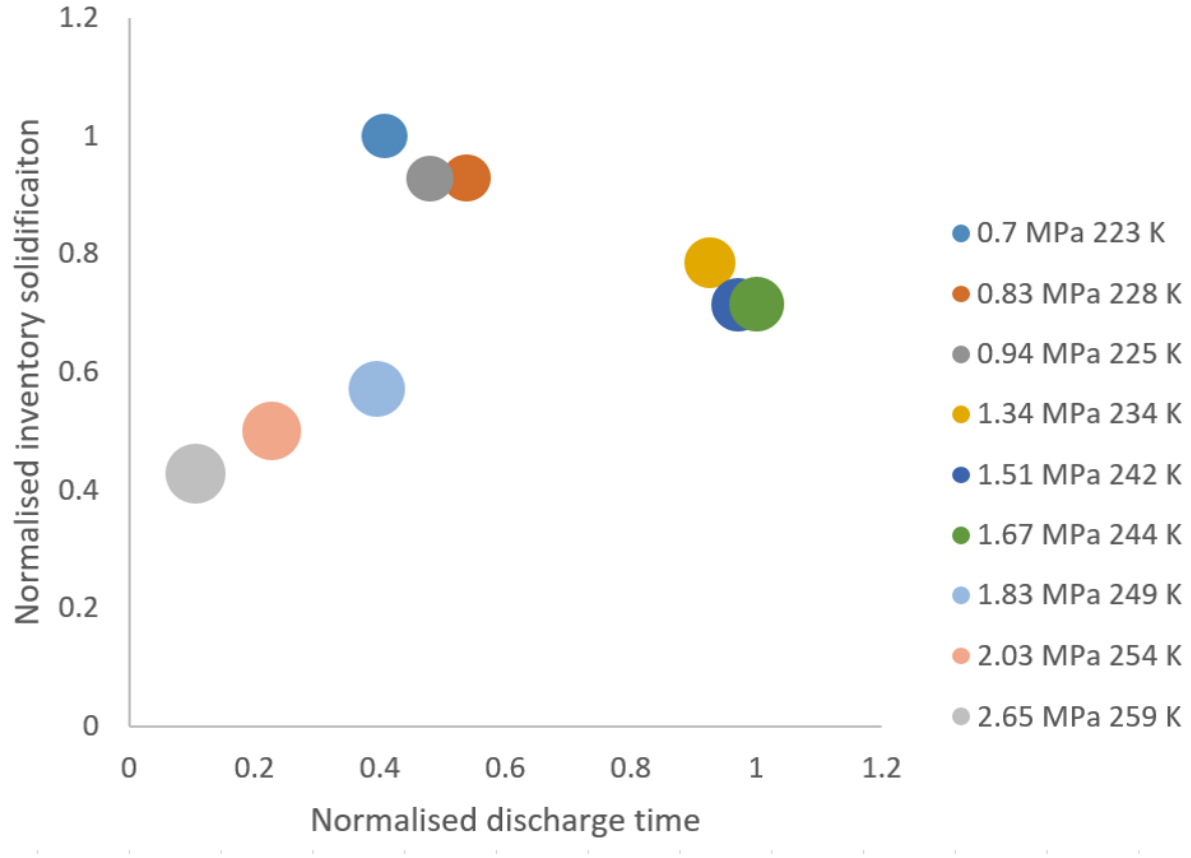

Figure 4-16: Two-factor safety assessment of liquid CO_2 discharges at shipping conditions (3.2 mm nozzle); values normalised against highest value; bubble area is relative to initial enthalpy of the stream

As shown in Figure 4-17, normalised discharge time shows a comparable behaviour in relation to both the 3.2 and 4.7 mm orifice size under all conditions. Conversely, leakage duration is significantly higher when 1 mm orifice is considered, with 1.5 MPa liquid conditions (medium pressure) exhibiting the longest duration. Such trend can be attributed to a higher propensity for longer-lasting solid blockages with smaller orifice sizes. In a real CO_2 terminal, liquefied carbon dioxide is expected to be continuously handled between the liquefaction plant, intermediate storage tanks and loading facilities [19]. In assessing the risk for potential loss of containment scenarios, previous studies provided preliminary identification of hazardous occurrences in intermediate storage terminals and sea carriers of a CO_2 port terminal [16,19].

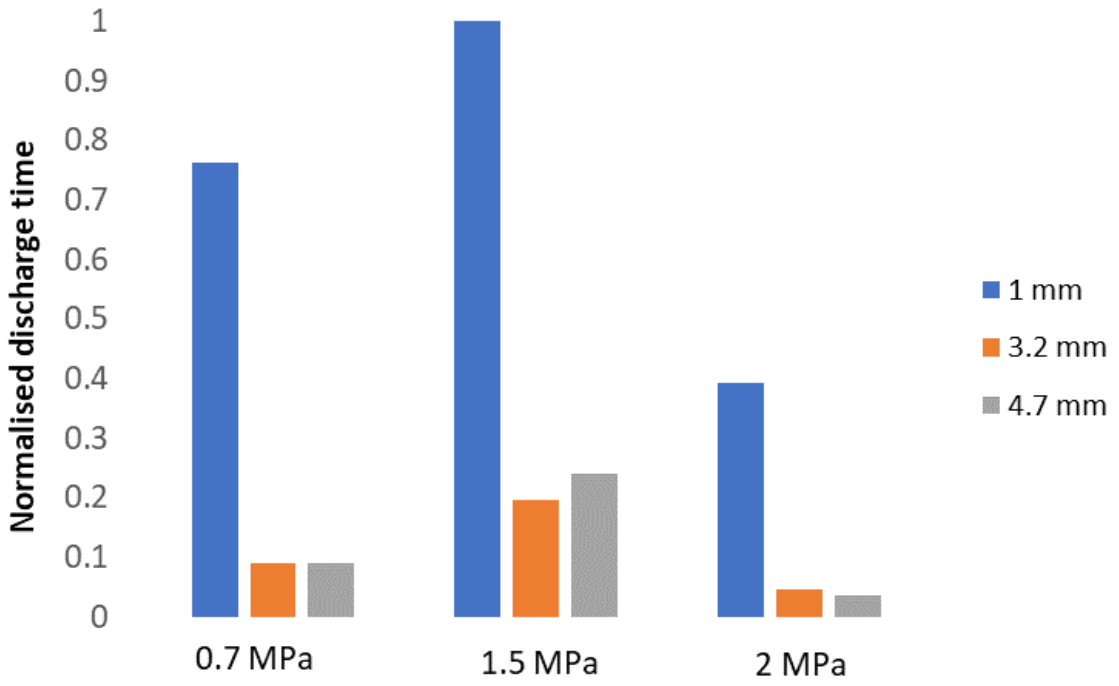

Figure 4-17 Normalised discharge time of different conditions in relation to variation of orifice diameter

Findings suggested that rupture or leakage from carbon dioxide storage tanks or transmission pipework are among the key hazardous events that need to be considered for safe and reliable operations. As such, scenarios that can pose a risk to plant, people and environment during real operations include overpressure, low pressure, or leakage due to rupture of the tank or pipe section due to mechanical failure. In particular, Koers et al. [19] performed a comprehensive operational safety study on a CO_2 terminal and found that uncontrolled release of inventory is the key hazard to be investigated, with failure modes attributed to corrosion, material failures, equipment failure or incorrect operation. Failure frequency for pressurised storage tanks is higher in a scenario where leakage initiates through a small <10 mm hole (10^{-5} per year) compared to rupture of the storage tank (10^{-7} per year) [19]. This consideration makes this study particularly relevant given its focus on leakages from small orifices. The authors [19] moreover highlight that the risk of uncontrolled release of CO_2 inventory must also be considered for scenarios where liquid CO_2 is transferred from the storage tanks to the loading terminal via piping sections, whereby the failure frequency of pipeline rupture is estimated to be 3 x 10^{-7} per year. Consequences can be disastrous, resulting in the uncontrolled release of CO_2 inventory which can lead to dangerous accidents. To reduce such risks, storage tanks and pipelines should be designed and constructed with

appropriate materials and suitable thicknesses to accommodate safety design required. In case of overpressure or overcharging, pressure-safety valves and level alarms should be implemented as mitigation measures, alongside emergency shutdown valves that halt the flow of CO_2 [16]. The latter should be fitted as close as possible to storage tanks. Additionally, the installation of low-temperature sensors around the transmissions pipeline can detect CO_2 leakages at an early stage. Moreover, the risk of low-pressure in the tanks – which promotes inventory solidification and blockages – can be reduced by feeding gaseous CO_2 through the boil-off gas return line [16]. In order to implement the appropriate risk-mitigation measures a thorough understanding of the leakage phenomena is required. In particular, this study explored such accidental leakage scenario in relation to different potential shipping conditions which can cool the walls rapidly by the evaporation of liquefied CO_2 and this might cause thermal damage to the infrastructure. This experimental campaign comes with its own set of limitations, such as the inability to assess the representative hazardous distances of the dispersion jet and its interaction with plant, people, and environment; additionally, the considered inventory amounts to a modest quantity, relevant to lab-scale apparatus, rather than that of an industrial storage tank and this is a significant difference between the laboratory environment and real-large scale transport system. Nonetheless, this work provides an understanding of the impact of selecting different CO_2 shipping conditions and orifice size on the leakage behaviour of liquid, refrigerated CO_2. Findings from this paper can moreover be used as benchmark cases for lab experiments and numerical simulations using relevant modelling software packages such as IRATE, DRIFT and PHAST [21]. As it is possible to observe, the plot shows the presence of three distinct clusters, each grouping low-, medium- and high-pressure tests. The high-pressure cluster region exhibits a relatively fast discharge process accompanied by a relatively modest level of inventory solidification inside the vessel. These performance indicators are particularly advantageous to scenarios where the rapid and complete evacuation of cargo inventory is required; for instance, in case of a CO_2 leak in a cargo vessel or storage tankthe relatively slower leakage, the defective tank must be emptied as quickly as possible through a jettisoning discharge pipe that is generally larger than the size of the crack in the tank [22]. In such instances, the high-pressure operating conditions investigated in this work appear to be the optimal choice in terms of both duration and maximum discharged amount from the vessel, and particularly at 2.65 MPa where discharge times and tank solidification have the lowest values.

The low-pressure cluster shows the maximum amount of inventory solidification (0.7 MPa, 223 K) and an intermediate range between the high and medium pressure values when it comes to leakage time. Consequently, the medium pressure cluster is the one that shows the highest discharge times – particularly in the 1.67 MPa scenario – albeit with a relatively more modest fraction of solid formation in the vessel. Indeed, this indicates that the propensity for cyclic formation of solid blockages in case of rupture of circulation pipework is highest under these conditions. This consideration implies relatively longer times for emergency response protocols compared to low- and high-pressure conditions. However, the risk of over-pressurisation cannot be ruled out similarly to pipeline conditions. Overall, both low- and medium-pressure conditions thus appear not to be optimal for an efficient jettisoning process, due to higher leakage duration and higher proportion of content leftover due to solidification. However, in different scenarios involving leaks from storage tanks located at the port terminal, slower discharge processes and lower discharged amount promote the preserving of inventory and allow longer times for emergency response and crack reparation. Low-pressure conditions are recommended when preservation of the inventory is preferred, whilst medium pressures represent the better choice if longer leak times are favoured to enable adequate emergency responses. The propensity for pressure increases in the vessel due to pipe blockage is moreover identified as a potential hazard, whereby appropriate implementation of pressure-safety valves is the suggested as a mitigation solution. In such scenario, the demonstrated propensity for large dry-ice plugs to form and progressively propagate inside the pipe at low-pressure conditions requires particular attention in optimal design and selection of suitable location of pressure-safety valves.

4.5 Conclusions

In this paper, CO_2 leakage experiments were performed to investigate the discharge behaviour under refrigerated, liquid CO_2 in a vessel. Parameters such as pressure, temperature of the fluid within the vessel and in the discharge line, and outflow jet dispersion were acquired to experimentally analyse releases of liquid CO_2 at conditions relevant to the shipping chain. The following conclusions are therefore made as part of this study:

- A distinct release behaviour is observed relative to initial condition boundaries - namely low (0.7 - 0.94 MPa) , medium (1.34 - 1.67 MPa) and high pressure (1.83 - 2.65 MPa) – demonstrating that selection of appropriate fluid conditions in the refrigerated liquid state is highly sensitive to the proximity to the triple point

- High pressure conditions (1.83 – 2.65 MPa, tests 7,8,9) showed more linear and overall smoother discharges, owing to a lower extent of solid formation in the system; this trend further accentuates with the increase of initial pressure and temperature conditions, showed the increased benefits of operating at a further margin form the triple point

- A two-factor safety assessment accounting for both inventory solidification and duration of the leakage process revealed that selection of higher pressure conditions (1.83 – 2.65 MPa) is optimal when low rate of inventory solidification and faster discharge processes are desired

- Medium pressure releases (1.34 – 1.67 MPa) show the highest leakage duration - attributed to the cyclic reformation of solid particles from the vapour-solid flow profile in the discharge pipe - and a middle ground value of inventory solidification. Such conditions therefore favour scenarios where allowing for longer response times to implement mitigation measures is prioritised

- Low pressures discharges (0.7 – 0.94 MPa) exhibit the largest fraction of inventory solidification alongside an intermediate value of leakage duration; therefore, these conditions are to be considered advantageous when preservation of inventory is the main priority.

- Reduction of orifice size from 3.2 - 4.7 mm to 1 mm demonstrated significant impact on leakage duration under low-, medium- and high-pressure conditions; conversely, variation of orifice size did not show any impact on rate of inventory solidification.

Findings from this work can be used as an overview to the safety considerations concerning different potential shipping conditions, and thus contributing to the formulation of protocols to be adopted in future sea vessel transport projects. Future work will investigate the leakage behaviour of CO_2 in binary and tertiary mixtures with

presence of contaminants such as Ar, CO, H_2 and N_2 which can be found in the CCUS chain.

References

[1] ZEP. Role of CCUS in a below 2 degrees scenario 2018:1–30. https://zeroemissionsplatform.eu/wp-content/uploads/ZEP-Role-of-CCUS-in-below-2c-report.pdf

[2] Bui M, Adjiman CS, Bardow A, Anthony EJ, Boston A, Brown S, et al. Carbon capture and storage (CCS): The way forward. Energy Environ Sci 2018;11:1062–176.

[3] DNV. Report Activity 5: CO_2 transport. 2012. Report No./DNV Reg No.: 2012-0076/ 13REPT4-2 - Det Norske Veritas.

[4] Barrio M, Aspelund A, Weydahl T, Sandvik TE, Wongraven LR, Krogstad H, et al. Ship-based transport of CO_2. Greenh. Gas Control Technol., 2005, p. 1655–60.

[5] Decarre S, Berthiaud J, Butin N, Guillaume-Combecave JL. CO_2 maritime transportation. Int J Greenh Gas Control 2010;4:857–64.

[6] Hasan MMF, First EL, Boukouvala F, Floudas CA. A multi-scale framework for CO_2 capture, utilization, and sequestration: CCUS and CCU. Comput Chem Eng 2015; 81:2–21.

[7] Roussanaly S, Hognes ES, Jakobsen JP. Multi-criteria analysis of two CO_2 transport technologies. Energy Procedia 2013; 37:2981–8.

[8] Fimbres Weihs GA, Kumar K, Wiley DE. Understanding the Economic Feasibility of Ship Transport of CO_2 within the CCS Chain. Energy Procedia 2014; 63:2630–7.

[9] ZEP. The Costs of CO_2 Transport Post-demonstration CCS in the EU; 2011. European Technology Platform for Zero Emission Fossil Fuel Power Plants, Zero Emissions Platform. Available at https://www.globalccsinstitute.com/resources/publications-reports-research/the-costs-of-co2-transport-post-demonstration-ccs-in-the-eu/

[10] Element Energy. CCS deployment at dispersed industrial sites; 2020. Department for Business Energy and Industrial Strategy; Research paper number 2020/030.

[11] Neele F, De Kler R, Nienoord M, Brownsort P, Koornneef J, Belfroid S, et al. CO_2 Transport by Ship: the way forward in Europe. Energy Procedia 2017; 114:6824–34.

[12] Seo Y, Huh C, Lee S, Chang D. Comparison of CO_2 liquefaction pressures for ship-based carbon capture and storage (CCS) chain. Int J Greenh Gas Control 2016; 52:1–12.

[13] IEAGHG. The Status and Challenges of CO_2 Shipping Infrastructures. 2020; IEAGHG Technical Report 2020-10.

[14] Element Energy, TNO, Engineering Brevik, SINTEF, Polarkonsult. Shipping UK Cost Estimation Study; 2018. Available at: https://assets.publishing.service.gov.uk/government/uploads/system/uploads/attachment_data/file/761762/BEIS_Shipping_CO2.pdf .

[15] Ministry of Petroleum and Energy N, Gassco, Gassnova. Feasibility study for full-scale CCS in Norway. 2016. Available at: https://ccsnorway.com/wp-content/uploads/sites/6/2019/09/feasibilitystudy_fullscale_ccs_norway_2016.pdf

[16] Noh H, Kang K, Huh C, Kang SG, Seo Y. Identification of potential hazardous events of unloading system and CO_2 storage tanks of an intermediate storage terminal for the Korea clean carbon storage project 2025. Int J Saf Secur Eng 2018; 8:258–65.

[17] Vermeulen TN. Knowledge sharing report – CO2 Liquid Logistics Shipping Concept (LLSC): Overall Supply Chain Optimization 2011:143. Available at: https://www.globalccsinstitute.com/resources/publications-reports-research/knowledge-sharing-report-co2-liquid-logistics-shipping-concept-business-model/ .

[18] Koers P, Looij M de. Final Public Report Safety Study for Liquid Logistics Shipping Concept. 2011; https://www.globalccsinstitute.com/archive/hub/publications/19011/co2-liquid-logistics-shipping-concept-llsc-overall-supply-chain-optimization.pdf

[19] Energy Institute. Hazard analysis for offshore carbon capture platforms and offshore pipelines. 2013; https://www.globalccsinstitute.com/archive/hub/publications/115563/hazard-analysis-offshore-platforms-offshore-pipelines.pdf

[20] Harper P, Wilday J, Bilio M. Assessment of the major hazard potential of carbon dioxide (CO_2). Health and Safety Executive. 2015.

[21] Han SH, Chang D, Kim J, Chang W. Experimental investigation of the flow characteristics of jettisoning in a CO_2 carrier. Process Saf Environ Prot 2013; 92:60–9.

[22] Han SH, Chang D. Dispersion analysis of a massive CO_2 release from a CO_2 carrier. Int J Greenh Gas Control 2014; 21:72–81.

[23] Shafiq U, Shariff AM, Babar M, Ali A. A study on blowdown of pressurized vessel containing $CO_2/N_2/H_2S$ at cryogenic conditions. IOP Conf Ser Mater Sci Eng 2018;458.

[24] Shafiq U, Shariff AM, Babar M, Azeem B, Ali A. Study of dry ice formation during blowdown of CO_2 -CH_4 from cryogenic distillation column. J Loss Prev Process Ind 2020; 64:104073.

[25] Ahmad M, Lowesmith B, De Koeijer G, Nilsen S, Tonda H, Spinelli C, et al. COSHER joint industry project: Large scale pipeline rupture tests to study CO_2 release and dispersion. Int J Greenh Gas Control 2015; 37:340–53..

[26] Guo X, Yan X, Yu J, Yang Y, Zhang Y, Chen S, et al. Pressure responses and phase transitions during the release of high-pressure CO_2 from a large-scale pipeline. Energy 2017; 118:1066–78.

[27] Cao Q, Yan X, Liu S, Yu J, Chen S, Zhang Y. Temperature and phase evolution and density distribution in cross section and sound evolution during the release of dense CO_2 from a large-scale pipeline. Int J Greenh Gas Control 2020; 96:103011.

[28] Hébrard J, Jamois D, Proust C, Spruijt M, Hulsbosch-dam CEC. Medium scale CO_2 releases. Energy Procedia 2016;86:479–88.

[29] Hulsbosch-dam C, Jong A De, Zevenbergen J, Peeters R. Vertical CO_2 release experiments from a 1 liter high pressure vessel. Energy Procedia, vol. 37, 2013, 4712–23.

[30] Pursell M. Experimental investigation of high-pressure liquid CO_2 release behaviour. Inst Chem Eng Symp Ser 2012:164–71.

[31] Xie Q, Tu R, Jiang X, Li K, Zhou X. The leakage behavior of supercritical CO_2 flow in an experimental pipeline system. Appl Energy 2014; 130:574–80.

[32] Tian G, Zhou Y, Huang Y, Wang J, Wang Y. Experimental study of accidental release behavior of high-pressurized CO_2 vessel. Process Saf Environ Prot 2021; 145:83–93.

[33] Energy Institute. Hazard analysis for offshore carbon capture platforms and offshore pipelines. 2013; https://www.globalccsinstitute.com/archive/hub/publications/115563/hazard-analysis-offshore-platforms-offshore-pipelines.pdf

[34] Hulsbosch-dam CEC, Spruijt MPN, Necci A, Cozzani V. Assessment of particle size distribution in CO_2 accidental releases. J Loss Prev Process Ind 2012; 25:254–62.

[35] Teng L, Li Y, Zhang D, Ye X, Gu S, Wang C, et al. Evolution and Size Distribution of Solid CO_2 Particles in Supercritical CO_2 Releases 2018. Ind. Eng. Chem. Res. 2018, 57, 7655 - 7663

[36] Liu Y, Calvert G, Hare C, Ghadiri M, Matsusaka S. Size measurement of dry ice particles produced from liquid carbon dioxide. J Aerosol Sci 2012; 48:1–9.

5 EXPERIMENTAL INVESTIGATION OF LIQUID CO_2 DISCHARGE FROM THE EMERGENCY RELEASE SYSTEM'S COUPLER OF A MARINE LOADING ARM

Hisham Al Baroudi[1], Ryota Wada[2], Masahiko Ozaki[2], Kumar Patchigolla[1], Makoto Iwatomi[3], Kenji Murayama[3], Toru Otaki[3]

1. Centre for Thermal Energy and Materials (CTEM), School of Water, Energy and Environment (SWEE), Cranfield University, Cranfield, Bedfordshire, MK43 0AL, U.K.

2. Dept. of Ocean Technology, Policy, and Environment, Graduate School of Frontier Sciences, The University of Tokyo, Kashiwa, 277-8561, JAPAN.

3. Nagaoka Works, Tokyo Boeki Engineering Ltd., Nagaoka, 940-0021, JAPAN.

This has been accepted for oral presentation at the GHGT-15 conference; the paper is under review for publication in the Special Issue (GHGT-15) of the IJGGC

Statement of contributions of joint authorship

Hisham Al Baroudi conceptualised experimental methods, contributed to experimental facility development, co-conducted the experiments, generated and analysed data and wrote this manuscript, titled "***Experimental investigation of liquid CO_2 discharge from the emergency release system's coupler of a marine loading arm***". Ryota Wada and Masahiko Osaki provided ongoing planning and supervision to this project and funding acquisition. Kumar Patchigolla critically commented on the manuscript before submission to peer-reviewed journal (still to be submitted). Makoto Iwatomi, Kenji Murayama, Toru Otaki contributed to this work through design and operation of pilot-scale experimental facility.

Abstract

Carbon capture, utilisation and storage has been recognised as a necessary measure to reduce greenhouse gas emissions. CO_2 shipping thereby represents a promising transportation option that offers flexible sink-source matching to enable decarbonisation at a global scale. In order to implement safe and reliable operations across the full-chain, ships carrying liquid cargo in bulk require loading systems to be integrated with an emergency release system in the event of sudden movement of the ship away from the berthing line. Therefore, in this work, a cryogenic test facility was constructed to handle

CO_2 in proximity of the triple point (~0.9 MPa – 1.7 MPa, 227 K - 239 K) and investigate liquefied CO_2 discharge from the emergency release system's coupler during an emergency shutdown. Findings show that separation of the coupler results in an abrupt discharge of the liquefied CO_2 inventory involving several phase transitions within a mere 0.6 s in all tests with peak depressurisation rates varying in relation to initial pressure of liquid inventory. Discharges at lower liquid pressures show the presence of initial 'puffs' that delay the full release, while higher liquid pressures occur more rapidly. Tests show variable generation of carbon dioxide solids inside the coupler and around the facility, with the dispersed jet assuming a 'tulip' shape that can be clearly observed from afar. The implementation of protective barriers seems to reduce the impact of the release, though the risk of asphyxiation or cryogenic burns to surrounding personnel cannot be ruled out given the magnitude of the discharge process.

Keywords

GHG; Carbon Capture, Utilisation and Storage; CO_2 transport; CO_2 shipping; marine loading arm, emergency release system

5.1 Introduction

Following the COP21 meeting in Paris, an accord to reduce the global temperature rise caused by anthropogenic emissions to below 2°C was made between the signatory states, with the European Commission declaring its intention to pursue a long-term plan to achieve net-zero emissions by 2050. Carbon Capture, Utilisation and Storage (CCUS) has been identified as a viable and promising technology that can deliver on this aim by achieving remarkable emission reductions across the power and industrial sectors [1]. The CCUS chain includes the capture of carbon dioxide from emitting sources and its transmission to a permanent storage location by means of a pipelines or sea vessels. A careful logistics design strategy to match CO_2 emitters (sources) to permanent storage sites (sinks) is a crucial issue in the implementation of CCUS at a global scale. This is especially relevant to regions where emitting sources tend to be scattered and offshore storage sites are the main available option. Sink-source matching with offshore storage sites can either be achieved by subsea pipelines or sea vessel transportation. Vessel transportation is expected to play an essential role in global decarbonisation strategies due to its lower capital expenditures, smaller impact on the coastal environment, and higher flexibility than subsea pipelines. As such, the UK is currently undertaking a

detailed study to avail of the flexibility of this technology to utilise its abundant storage capacity in the North Sea and thus become a net-importer of European emissions and early-mover in the field of CCUS [1,2]. Other countries such as Japan and Korea are also actively working towards implementation and commercialisation of CO_2 shipping for CCUS, as this approach is geographically and techno-economically optimal for their decarbonisation efforts, given the lack of hydrocarbon activity and the high-propensity for natural calamities. Literature often indicates conditions near the triple point to be the most advantageous state for sea vessel transportation [3–7] attributing this choice to the lower capital cost of the pressure vessels and enhanced cargo density at such conditions. Although often based on mere theoretical assumptions rather than in-depth techno-economical investigation, it should be noted that handling carbon dioxide near the triple point is a novel concept which will require further R&D activity and stringent safety considerations to mitigate the risk of dry-ice formations and blockages during real operations. Therefore, significant efforts are required to develop a thorough understanding of the behaviour of liquid CO_2 during real operations and thus determine the appropriate margin to adopt as to enhance safety and integrity of the systems of at all times. Conversely, shipping CO_2 at higher liquid pressures (~1.5 MPa) has also been proposed in the literature [8,9], representing a more technologically mature concept characterised by higher capital expenditure but lower operational costs. Operating at such liquid conditions would provide a higher safety margin from the triple point and a more established technological experience, given that CO_2 shipping is currently occurring in the food and brewery industries, albeit for smaller quantities [10]. Overall, no consensus has yet been achieved with regards to the optimum transportation conditions. Upon continuous capture and liquefaction of the carbon dioxide, shipping operations will need to be accurately scheduled in batches to transmit it to suitable storage locations. At the port location, loading processes are an integral and key component of the CO_2 shipping operations at the port terminal. The transfer of liquid carbon dioxide between the storage vessel and the ship's cargo tank is best performed by means of marine loading arms, which represent the most reliable and established solution in other cryogenic liquid applications such as LNG and LPG [2,11,12]. Fully Balanced Marine Arm (FBMA) represents the optimum solution for early liquid CO_2 projects for CCUS, due to its simple and fully balanced design [13]. This loading arm is suitable for relatively small applications – up to 10,000 dead weight tonnage tanker size and up to 14.5 m in length. Operations of the arm can be both manual and hydraulic

[14]. During real operations, safety considerations need to be made due to the leakage risk in the loading arms. Whenever the risk from the process or operation is deemed unacceptable as per hazard analysis, mitigation strategies must be implemented to reduce severity. Despite the non-flammable nature of carbon dioxide, the risk of asphyxiation and cold burn in case of spillage implies the requirement for rigorous safety protocols [11]. Moreover, the release of low-temperature, solid or vapour carbon dioxide as a result of a rupture or bad connection could inevitably cause fatal damage to workers and facilities [15,16].

The Energy Institute [17] suggests a list of measures to reduce released carbon dioxide during an accidental release, including the implementation crack arrestors, block valves as well as development of emergency plans. Therefore, in any incident related to cargo transfer, whether it is onshore or on ship, it is essential to halt inventory transfer by stopping the flow of pumps and isolating by means of emergency release valves. All sea carriers and large terminals implement systems for rapid emergency shut-down of cargo loading [18]. For this reason, several studies [11,19–22] found that an appropriate solution would include the installation of an emergency shutdown valve (ESDV) to isolate the compromised locations and an emergency release system (ERS) to safeguard the marine arm and limit the magnitude of the spill. The California State Lands Commission [23] reported that 10 out of 52 major LNG accidents taking place in the period between 1944 and 2006 occurred during loading and offloading operations, with significant related ship or property damage and LNG spillage taking place in all of the occurrences. The report further highlighted the importance of implementing emergency release couplings to protect the integrity of loading arms and mitigate the spillages that can result from their damage. The Society of International Gas Tankers and Terminal Operators (SIGTTO) [24] moreover set out guidelines and codes of practice for the implementation of emergency release systems in gas and liquid tankers covering the structure, standards and development of this technology. The code highlighted that in the period between 1995 and 2017, 32 spurious activations of the ERS were reported, with the majority of such occurrences being attributed to equipment failure or operational malfunctions.

ERS's are therefore extensively used for marine loading applications in the oil and gas industry [22–24], and are designed to disconnect the loading arm from the ship during operations in the event emergencies such as natural calamities, fire and strong wind or

current that causes sudden movement of the ship away from the berthing line. The system is integrated on the marine loading arm and includes two valves, one located at the loading arm's side, and the other at the ship's side. As illustrated in Figure 5-1, during an emergency the two valves will be closed simultaneously in order to avoid spillage of inventory from the loading arm and ship pipe before disconnection. The emergency release coupler, located between the two valves, decouples and discharges the loading arm from the ship instantly after the valves' closure. ERS can be operated both manually, by trained operators, or by means of an alarm sensing control system that detects anomalies in the loading operations and cuts off the supply of inventory. In the first instance, it is critical to understand the impact of liquid CO_2 discharges on the operators' health and safety in order to develop appropriate protocols and risk assessments. An interlock system is integrated to ensure that the coupler only disconnects after both valves are closed [14]. Currently, two main ERS design solutions are available, as shown in Figure 5-2. In case of ball valves, the liquid CO_2 passage through the balls inside becomes perpendicular to be closed in shutdown mode. The ball valve unit has an overall heavier and bigger structure, which requires more weight to be counterbalanced and therefore implies the need for stronger structures for the loading arm

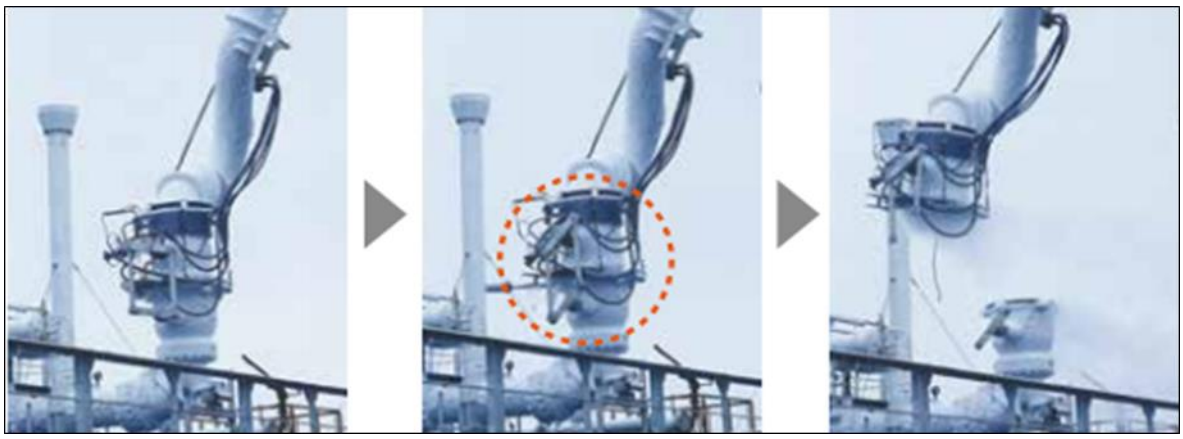

Figure 5-1: Sequence of the operation of ERS; 1) separation begins; 2) the two valves shut completely; 3) Emergency Release Coupler opens completing the separation [14].

Conversely, the butterfly valve unit is simpler, and requires a lighter structure. Butterfly valves are a quarter turn, rotary motion valves which are promptly operated on the principle of 90^{o} rotation of disk from closed to opened position. In both types, due to the distance of two valves – one located on the ship side and the other on the side of the storage tanks –, liquid CO_2 would be left as inventory at the emergency release.

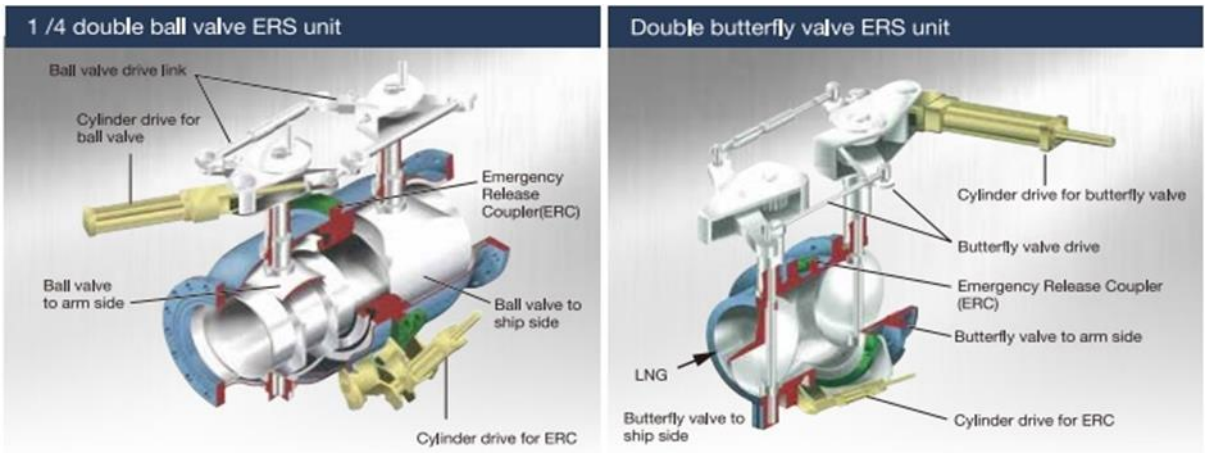

Figure 5-2: Design solutions for ERS left-to-right; double ball valve and butterfly valve [14].

Table 5-1 provides a summary of the advantages and disadvantages of the implementation of each individual ERS solution. After all, butterfly valves type is easier to install on loading arm, but the quantity of CO_2 inventory is larger. Tokyo Boeki Engineering suggests that future implementation of CO_2 shipping at large scale will need to consider the implementation of ERS systems to all manufactured marine loading arms, given that all LNG loading arms supplied domestically and internationally by the company are already fitted with an emergency release system unit. Existing experience suggests that when a ship moves away from the berthing line's pre-set limits, it does so very rapidly. This implies that the cumulative actuation time for the ERS – from valve closure to coupler's disconnection – must be designed to be short in duration to allow prompt discharge [18]. Emergency Release Systems designed by Tokyo Boeki Engineering take up to 5 s to respond to the anomaly value and a further 2 s to release and open the coupler, for a total of 7s. After the closure of the ERS valves, it is inevitable that some amount of liquid CO_2 would be left in the coupler and released into the surroundings upon the disconnection of the ERS.

Although the implementation of emergency release systems is well established within industries handling liquefied, cryogenic fluids such as LNG and LPG [18], the discharge of liquid CO_2 during emergency shutdown is expected to behave differently than any of the former applications. This implies the requirement for specific design solutions and appropriate safety protocols. The higher pressure of the contained liquid and the potential for sublimation and generation dry ice during the phenomena are features unique to carbon dioxide, which make behaviour unpredictable. For a safe and efficient

design of offloading systems, i.e. introducing protection walls, a good understanding of the phenomena is therefore necessary.

Table 5-1: Comparison of advantages and disadvantages of the different ERS types

Component	Advantages	Disadvantages
Ball-type	Lower quantity of inventory leftover in the coupler during emergency release	Heavier structure Higher costs Complicated structural changes required for retrofitting into an existing loading arm
Butterfly-type	Light weight Lower costs Installation on existing marine arms does not imply structural reinforcement of the berth	Even when fully closed, a portion of fluid is present in the valve

The risks and hazards related to the potential generation of dry-ice build-up, which can lead to equipment to become irresponsive, need to be evaluated in this scenario. The Energy Institute [17] suggested a hazard analysis procedure on onshore installations for CCUS to understand the propensity of undesirable events, their failure frequency, consequences and measures for prevention or containment of the damage. Failure frequency data relating to CO_2 shipping projects for CCUS are not currently available due to the lack of implementation. For instance, the accidental releases on a carbon dioxide transmission system will result in the release of an uncontrolled gas cloud. The ingestion of the inventory, cryogenic impact in the vicinity of the release or the effects of the physical blast may result in injury to surrounding people or adjacent equipment and structures.

The nature of failures can include small leaks and rupture of vessels or pipes, and the potential consequences may impact health of the operators. Several research projects have been delivered to explore aspects related to hazards and risks of CO_2, including CO_2PipeHaz. This project provided an assessment of failure consequence and hazard assessment for CO_2 pipeline systems [25]. Dispersion calculations to determine the hazard ranges from releases of CO_2 at 2 MPa and 243 K based on a PHAST V6.6.0 Build 406 model, show that the hazardous distance of a 50 mm leak from a 50-tonne tank can range from 28-32 m.

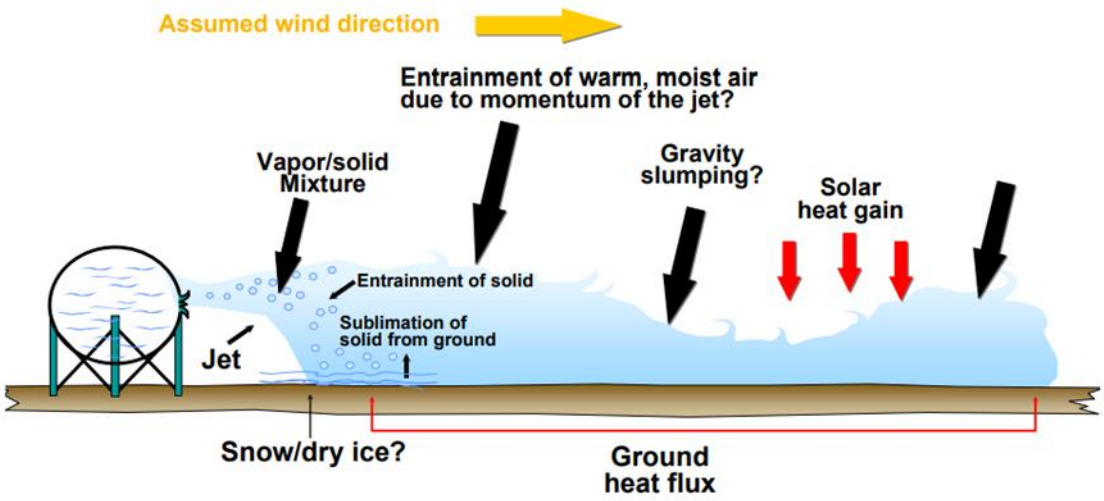

Figure 5-3: Illustration of the dispersion stage of a CO_2 release [17]

The unique feature of this experimental investigation is the nature of the release, which is more relatable to a full-bore failure or rapid instantaneous release, rather than a transient leak. The UK's Health and Safety Executive published a comprehensive assessment of the hazards posed by carbon dioxide with specific reference to the CCUS chain. Considerations of engineering aspects relating to potential accidents resulting in loss of containment (LOC) of pressurised liquid inventory highlighted several gaps related to emergency response, temporary refuge integrity issues and predictions of dry-ice formation [20,25] stated that catastrophic ruptures or instantaneous releases exhibit significantly different discharge behaviour than ordinary leaks, with factors such as phase release, initial pressure and receiving media (air, water or underground) dictating the nature of the phenomenon. Solid formation is predicted based on thermodynamic theory, although the authors highlighted that empirical investigations are still required to understand real operations. Shafiq et al. [26] found that in case of any mechanical failure, further damage can be mitigated by performing a controlled blowdown of the tank. Chances of an accident and risk of solidification can be minimised by reducing the size of the blowdown orifice and accurately controlling the operation. However, this measure is not applicable to the discharge from the release coupler of an ERS as this operation need to be performed rapidly as to allow for the prompt disconnection of the loading arm. Findings highlight that at the release point, carbon dioxide will be discharged as a high velocity, two-phase jet with some solid particles [15,20]. The momentum of the initial discharge is dependent on initial pressure, density, temperature and velocity, where the gas expands to atmospheric pressure. The cloud's initial

momentum, depending on the initial release velocity, prompts the jet to disperse from the release point. The cloud expands to atmospheric pressure at the end of its 'depressurisation zone' and air is entrained reducing the CO_2 concentration, and heat transfer begins to take place in the so-called 'dispersion area' (Figure 5-3). A portion of the solid particles entrained in the cloud of carbon dioxide can deposit on the ground and form a layer of carbon dioxide. Part of the solid sublimate in the cloud as it exchanges heat with the surrounding environment. The accumulation of solid CO_2 in proximity of the discharge point will affect the level of risk posed on personnel due to high concentrations of sublimating carbon dioxide [27].

Releases from vessels with liquid inventories are convoluted phenomena that involve several phase transitions depending on the upstream conditions [17]. Several investigations of the discharge behaviour of pressurised CO_2 are available in the literature, although they are mostly relevant to pipeline transportation systems and high pressures [28–34]. Wang et al. [34] investigated the dispersion behaviour of high pressure liquid CO_2 leaked from a pipeline at initial pressure of 5-8 MPa and temperatures of 296 – 318 K and found that temperatures can reach values as low as 245 K. Ahmad et al. [35] conducted large scale experiments on the release and dispersion of full bore rupture of a large-scale CO_2 dense phase high pressure pipeline. The rupture produced a visible jet that reached 60 m in height and extended to areas up to 400m far from the rupture location. Li et al. [36] undertook an ejection process of boiling of pressurised liquid CO_2 following vessel rupture and found that within 20 ms, the pressure peak rates prompted the start of a CO_2 Boiling Liquid Expanding Vapour Explosion (BLEVE) under studied conditions. Guo et al. [33] investigated a high-pressure CO_2 release from a 258 m long industrial scale with regards to different orifice diameters. The blowdown behaviour showed the inventory within the pipeline undergoing several phase transitions and entering into the gas-solid phase when the inventory eventually depressurises below the triple point. A study on dispersion modelling techniques for carbon dioxide pipelines by Sherpa consulting [37] analysed the nature of discharge and dispersion of dense phase throughout its stages. It was found that in scenarios with moderate upwards-directed push, the plume dips to the ground and then expands. The dispersion, throughout its distinct stages, is governed by different forces, with inertia, gravity and atmospheric turbulence being the key factors. Harper et al. [25] found that the hazards related to an instantaneous release of cold,

liquid phase may result in the highest dispersion distances, and asserted that modelling of instantaneous and continuous releases of CO_2 from storage is associated with a high level of uncertainty and that a significant amount of research is still required. Han et al. [38] undertook an experimental study to investigate the flow characteristics in the jettisoning flow line of a liquid CO_2 carrier and found that several phase changes occur along a long tube. This investigation informs on how to promptly discharge inventory from a sea vessel, in case of collision or mechanical failure of a cargo tank during voyage.

As such, process safety is a vital factor to take into considerations when scrutinising the appropriate conditions for future, commercial CCUS projects. Process safety implications may well become a decisional factor to determine viable shipping conditions and codes of practices of future projects. The literature thoroughly investigates the accidental release behaviour of dense and supercritical phase CO_2 during transport, but presented works are often merely related to pipeline systems, with limited work focusing at conditions and procedures relevant to sea vessel transportations. As a result, the majority of investigations cover transient inventory leaks rather than instantaneous releases of inventory. Emphasis is often placed in validating dispersion models via empirical investigations and numerical investigations of the leakage flow [31]. Nonetheless, there is very limited focus concerning systems and operations related to CO_2 shipping transportation, with no specific studies investigating the implementation of emergency release systems and liquid CO_2 discharge in marine loading during an emergency shutdown. A thorough understanding of the discharge behaviour of liquefied inventory is essential, and particularly in relation to different phase transitions that may occur in the process. Therefore, this work presents a real-scale investigation of the design and operation of an emergency release system during real operations. The aim is to experimentally investigate the discharge of cryogenic, liquefied carbon dioxide at different conditions from a butterfly-valve emergency release system's coupler during an emergency shutdown in order understand the impact of this phenomenon on the process safety, people and the surroundings.

5.2 Methodology

5.2.1 Experimental set-up

The cryogenic test facility is represented in Figure 5-4. The system was constructed to replicate the design of a marine loading arm's emergency release system and simulate its operation during a shutdown. The facility features a cylindrical pressure vessel, made of stainless steel and resembling the shape and dimensions of the coupler, connected to the facilities' inlet and outlet pipework to be filled with liquid CO_2 at the required conditions. The cylindrical vessel has a diameter of 250 mm and height of 130 mm, making its total internal volume ~6 L. The coupler was insulated using a polyethylene AEROFLEX and glass wool insulation to preserve the required temperatures during the conditioning stage. The feed and set pressure of the CO_2 was controlled at the source by means of pressure-reducing and flow valves fitted on the carbon dioxide supply tank and the inlet line.

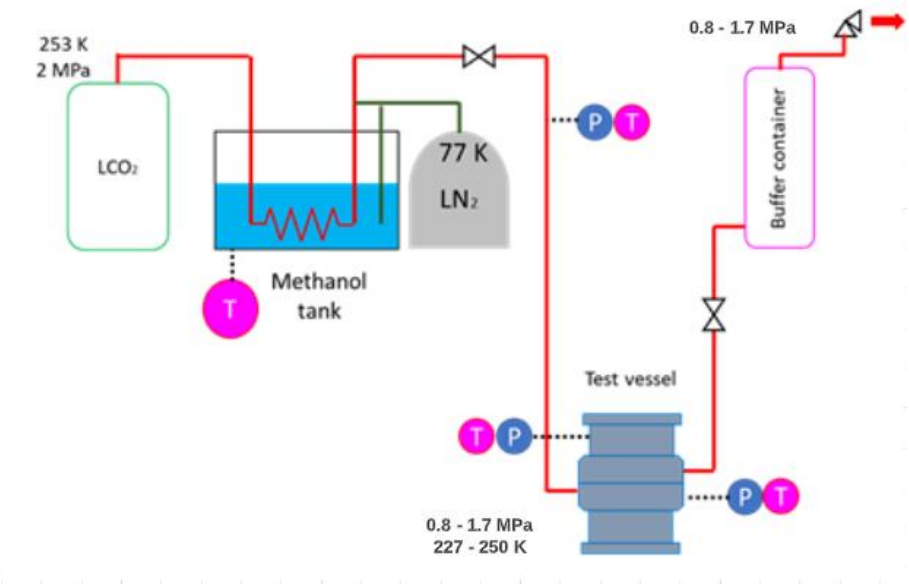

Figure 5-4: Schematic representation of the test facility

A buffer container was placed after the vessel's outlet ball valve to allow for the venting of any excess pressure from the vessel without exposing it to atmosphere, thus eliminating the risk of solid formation and blockages in the lines due to atmospheric pressure. A methanol-liquid nitrogen refrigeration tank was utilised to cool the liquid CO_2 and condition it to the required temperature prior to injecting it into the vessel. The use of such refrigeration solution enables to achieve and maintain a high level of control over

the required set temperature of the liquid carbon dioxide. Figure 5-5 shows pictures of the experimental apparatus.

Figure 5-5: Pictures of the experimental apparatus - left-to-right and top-to-bottom: vessel coupler; methanol-nitrogen refrigeration; buffer container; inlet, outlet pipework and pressurised oil system

A hydraulic cylinder was used to enable the vertical separation of the coupler required for the experimental tests. The system was operated by means of a pressurised oil reservoir, which drives the piston connected to the rod back and forth, allowing for the opening and closing of the pressure cylinder as illustrated in Figure 5-6. It is assumed that the rate of vessel's opening will be solely controlled by the hydraulic system and that the effect of pressure exerted by the fluid can be considered negligible. The hydraulic system is operated at constant flowrate and oil pressure in all the performed tests. The vessel and pipe connections were covered by a layer of insulation to maintain the carbon dioxide at the required liquid temperature. Extensive temperature and pressure measurement were applied through Hayashi Denko k-type thermocouples with 1 mm diameter (106 – 313 K range ± 0.05 K accuracy and 0.02 s response time in water) and Keyence GM-P025T pressure sensors (0 – 2.5 MPa ± 0.01 MPa with 0.01 s response time) fitted across the facility (Figure 5-4) to allow a real-time monitoring and data acquisition at a frequency of 5 Hz throughout conditioning, injection and release stages. The impact of lag in the recorded temperatures and pressures on the presented results will be discussed in the relevant section of this chapter. Experimental

observations and data acquisition also included a range of cameras to observe the phenomena both from a near and a far-view prospective and an infra-red (IR) thermal imaging camera to capture the thermal profile of the release.

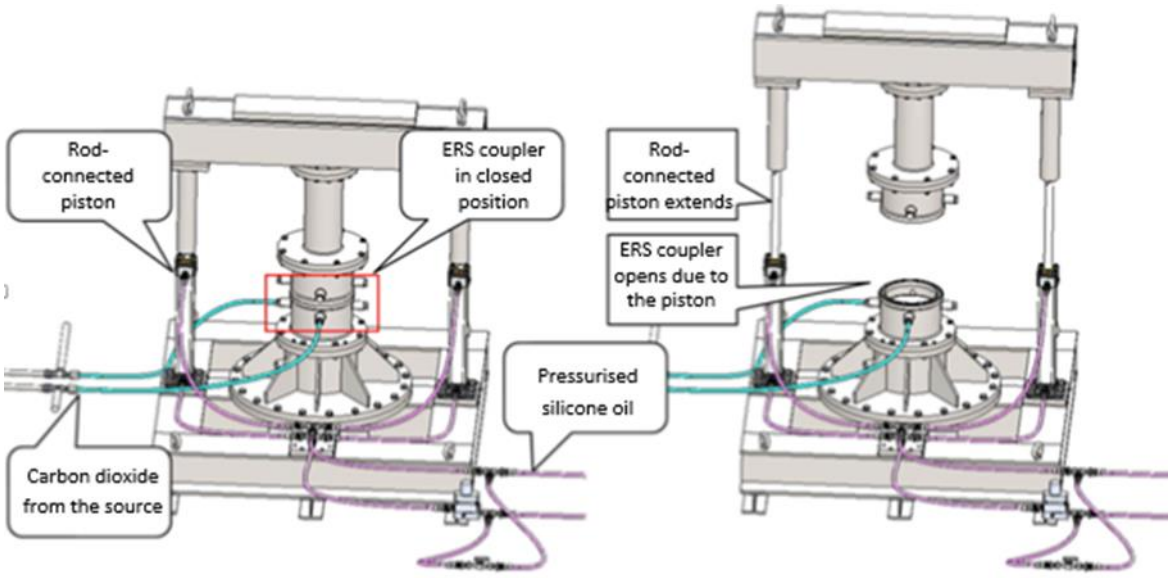

Figure 5-6: Illustration of the coupler's experimental system and its operating principles

5.2.2 Data acquisition and observations

Extensive pressure and temperature measurements were implemented across the facility including at the top and bottom of the test vessel, methanol refrigerator tank, and the inlet and outlet pipework for both data acquisition and monitoring purposes as summarised in Figure 5-4. Instantaneous release of liquid, pressurised fluid in such limited quantities is a phenomenon that is expected to occur within a few seconds, with the first stage of the discharge being of paramount importance to understand the nature and initial parameters of the phenomenon. In order to observe the discharge phenomena and the dispersion stage, several cameras were selected to permit a thorough observation. A camera with high-frame rate (240 fps) was placed at a distance of approximately 15 m away from the test facility at an elevated height to capture the dispersion of the jet and mixing with the surroundings. A GoPro camera (120 fps) was fitted on the top bracket of the test facility to allow for a top-view observation of the phenomena during the test; a high-speed camera with a capture rate of 960 fps was placed 2.5 m in front of the coupler to capture and record the discharge from the vessel in slow-motion. The captured frames are then used to determine the initial speed of the jetted flow in the first few milliseconds of the discharge. An infrared thermography AVIO R500EX with a temperature range of 233 to 773 K and video capture rate of 30 fps was

obtained to record the thermal profile of the release; the emissivity value was selected to be 0.95. The IR thermography was placed next to the high-speed camera at a distance of 2.5m from the coupler in test 1.1 and test 2.1 to promote a thorough observation of the discharge phenomena. The recording was performed through a software provided with the camera and installed on a laptop computer for video acquisition purposes. Although temperatures below a temperature of 233 K could not be directly measured, the camera would still provide an indication of the thermal profile being below such measurable threshold.

5.2.3 Experimental schedule

In this work, four distinct real-scale tests were performed to investigate the operation of the emergency release system and the discharge behaviour of industrial grade CO_2 (99.8% purity) from the coupler at two different liquid conditions. Tests 1.1 and 1.2 were performed at lower liquid pressure conditions (0.87 MPa and 0.96 MPa) which exhibit a closer proximity to the triple point and solid region; tests 2.1 and 2.2 were instead considered at higher-pressure liquid conditions and possess a wider margin from the triple point. In this work, tests 1.1 and 2.1 represent the principal experimental investigations with implementation of full experimental observation and data acquisition methodology; tests 1.2 and 2.2 were also performed to verify the trends with data acquisition as summarised in Table 5-2. The experimental campaign aims to provide an understanding of the discharge and dispersion processes in support of the development of safety protocols. Table 5-3 provides an overview of the conditions under which each experiment was performed.

Table 5-2: Summary of experimental observations and data acquisition; TC = thermocouple PT = pressure transducer

Test	Top TC and PT	Bottom TC and PT	High-speed camera	Far-view camera	Top-view - GoPro	Thermal IR camera
Test 1.1	✓	✓	✓	✓	✓	✓
Test 1.2	✓	✓	X	X	✓	✓
Test 2.1	✓	✓	✓	✓	✓	✓
Test 2.2	✓	✓	X	X	X	X

In order to provide an overview of the experimental conditioning stage and present the profile of the different streams of the facility throughout such stage, Figure 5-7 and Figure 5-8 provide summary of the conditoning stage in test 1.1 and 2.1 respecitvely. As highlighted, the figures show the overall temperature and pressure profile across the facility from beginning of the injection of CO_2 inventory to the vertical separation of the coupler. The injection process was found to take approximately 10 minutes to complete; before the loading of the carbon dioxide took place, the system underwent a pre-cooling stage by means of liquid nitrogen media, as reflected in the initial temperatures readings recorded of the coupler.

Table 5-3: Summary of the experimental campaign

Test	Pressure (MPa)	Temperature (K)	Calculated liquid density (kg/m^3)*	Calculated specific enthalpy* (kJ/kg)	Ambient temperature (K)
Test 1.1	0.87	227	1140	100.6	289
Test 1.2	0.96	231	1124	108.6	288
Test 2.1	1.65	239	1094	124.8	280
Test 2.2	1.62	240	1090	126.9	281

***calculated through NIST REFPROP V9.5 through input of pressure and temperature values**

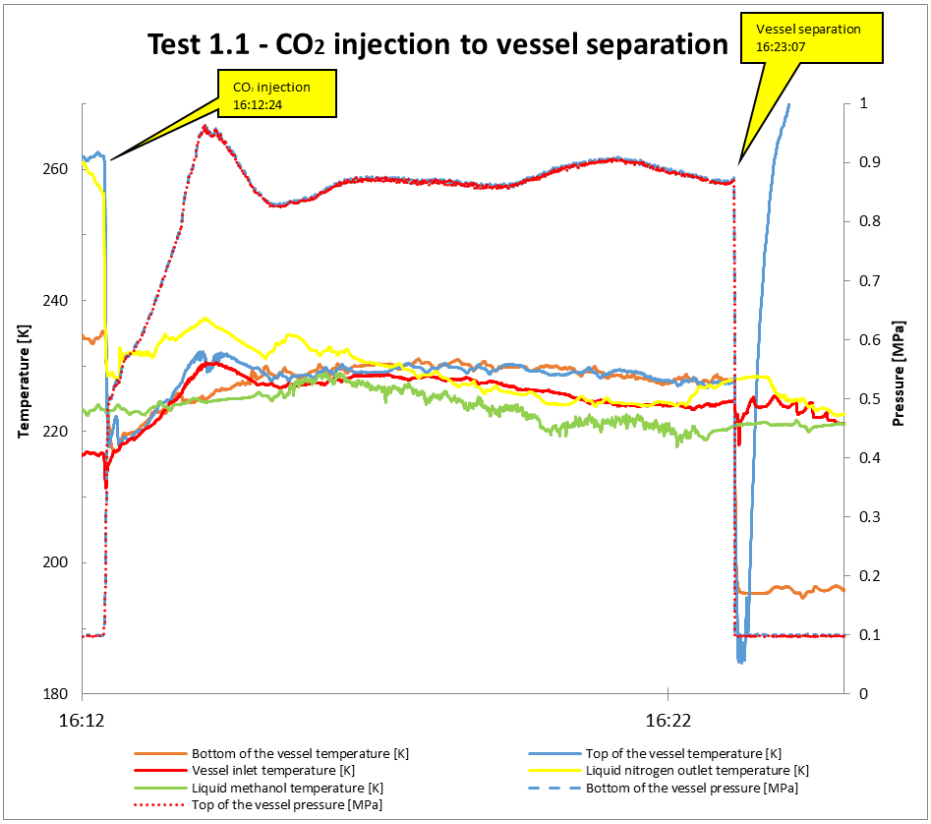

Figure 5-7: Experimental summary of 0.87 MPa, 227 K release (Test 1.1)

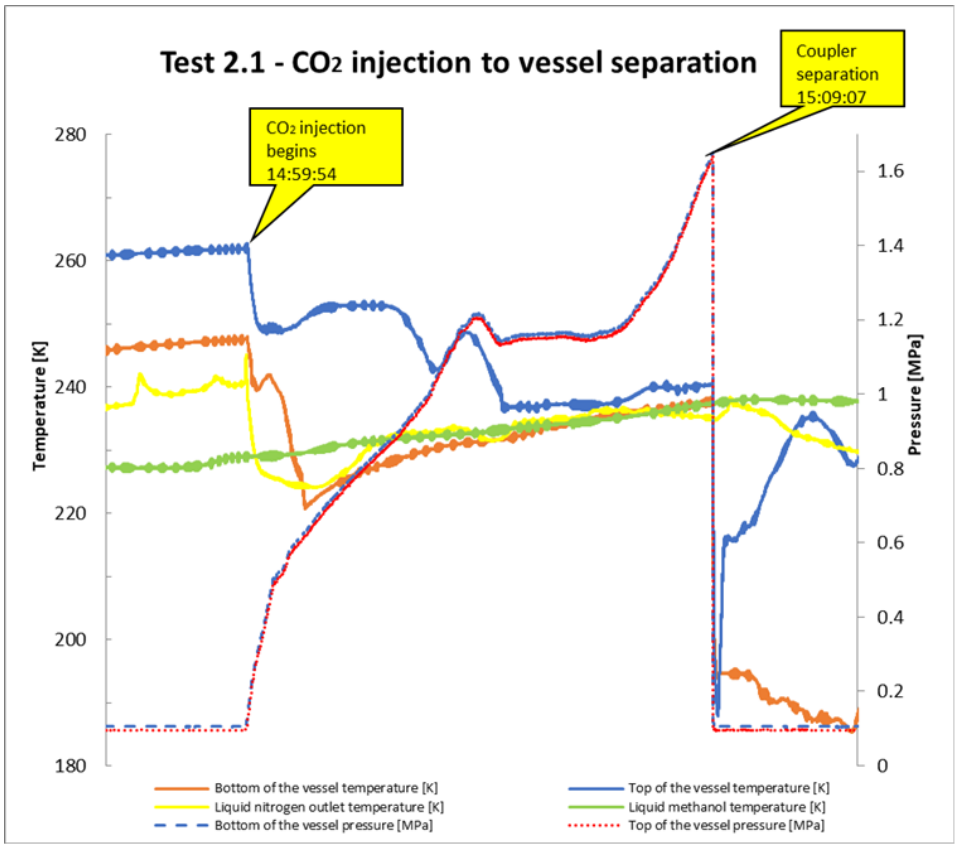

Figure 5-8: Experimental summary of 1.65 MPa, 239 K release (Test 2.1)

5.3 Results and Discussion

5.3.1 Initial discharge behaviour

At initial conditions, liquid CO_2 is contained in the insulated and pressurised cylindrical coupler with its central axis kept vertically to maintain its liquid state, above the saturated vapour pressure curve. During the vertical separation of the vessel from the middle of its height in a vertical direction, it is assumed that peripheral portions are opened from a state of airtightness. During the tests, the opening of the coupler appeared to be irregular across its circumference. Figure 5-9 shows how the release near the triple point occurs in a progressive manner and in several stages. At 4 ms into the opening, a low-momentum leak lasting 8 ms discharges from the 180° side of the opening; the vessel continues to separate vertically, and at 50 ms from the start a uniform leak discharges throughout the whole cylinder's circumference, effectively initiating the full discharge.

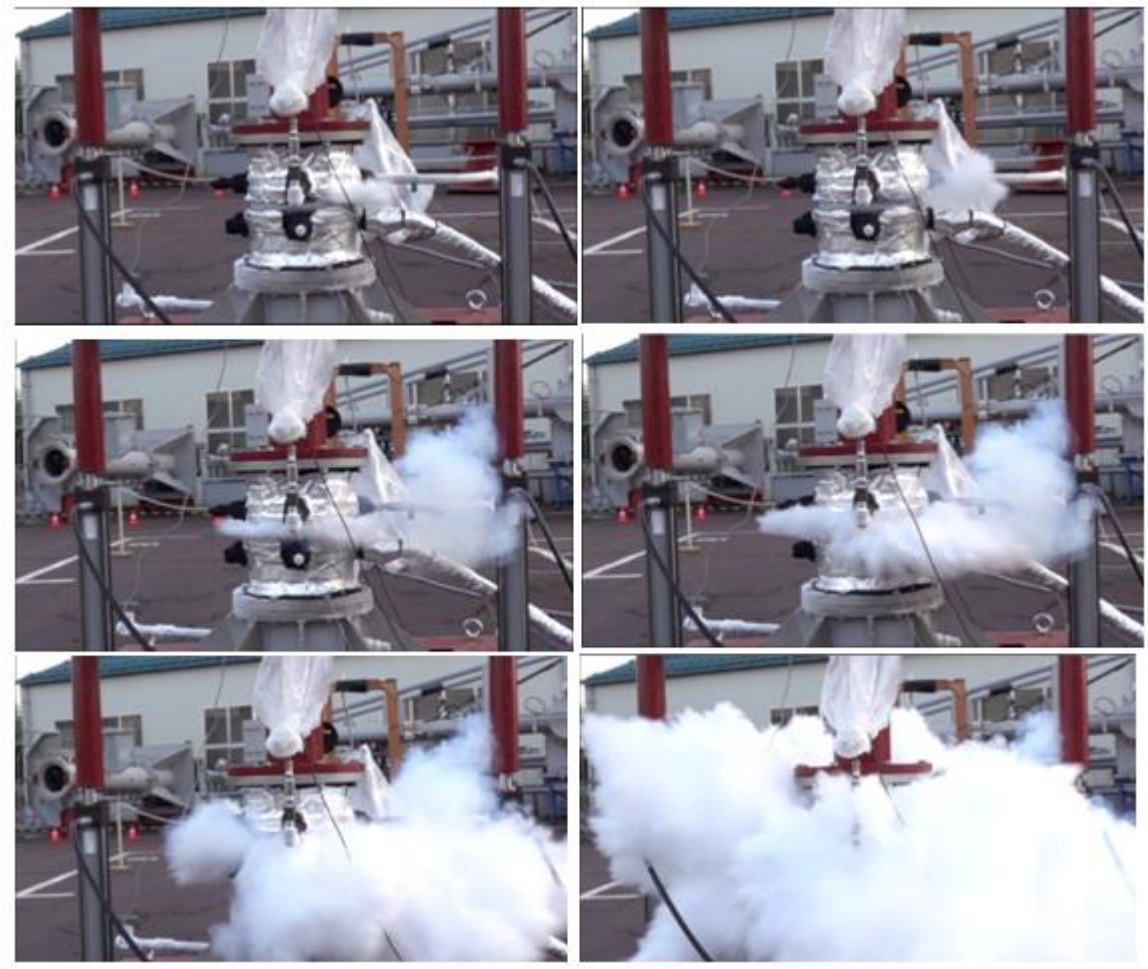

Figure 5-9: Frame sequence of high-speed release of Test 1.1; left-to-right and top-to-bottom 4 ms, 8 ms, 50 ms, 53 ms, 55 ms and 73 ms

Overall, this phenomenon delays the full-scale blast to over 55 ms from the beginning of the vertical separation. Conversely, Figure 5-10 shows that the discharge behaviour at the higher pressure is more sudden, with the fluid immediately discharging within 4 ms from the 0° side of the opening and progressively spreading across the full circumference within 8 ms. By focusing observation on the displacement of the O-ring seals from the vessel after the completion of the experiment, some interesting reconstruction of events can be performed (Figure 5-11). After Test 1.1, the O-ring was found to be shifted sideways at the bottom of the coupler, while at the completion of test 2.1 the O-ring was found to be around the outside circumference of the lower half of the vessel, as shown in Figure 5-11. An understanding of gasket operation, and related forces acting on the seals assist in the explanation of the phenomenon. As emphasised in Figure 5-12 during a flange connection assembly the gasket is under a compressive load from the faces of the flanges being under tension. Such compressive load must be significant enough to enable compression of the gasket into the surface finish of the flanges enabling the filling any potential leak paths.

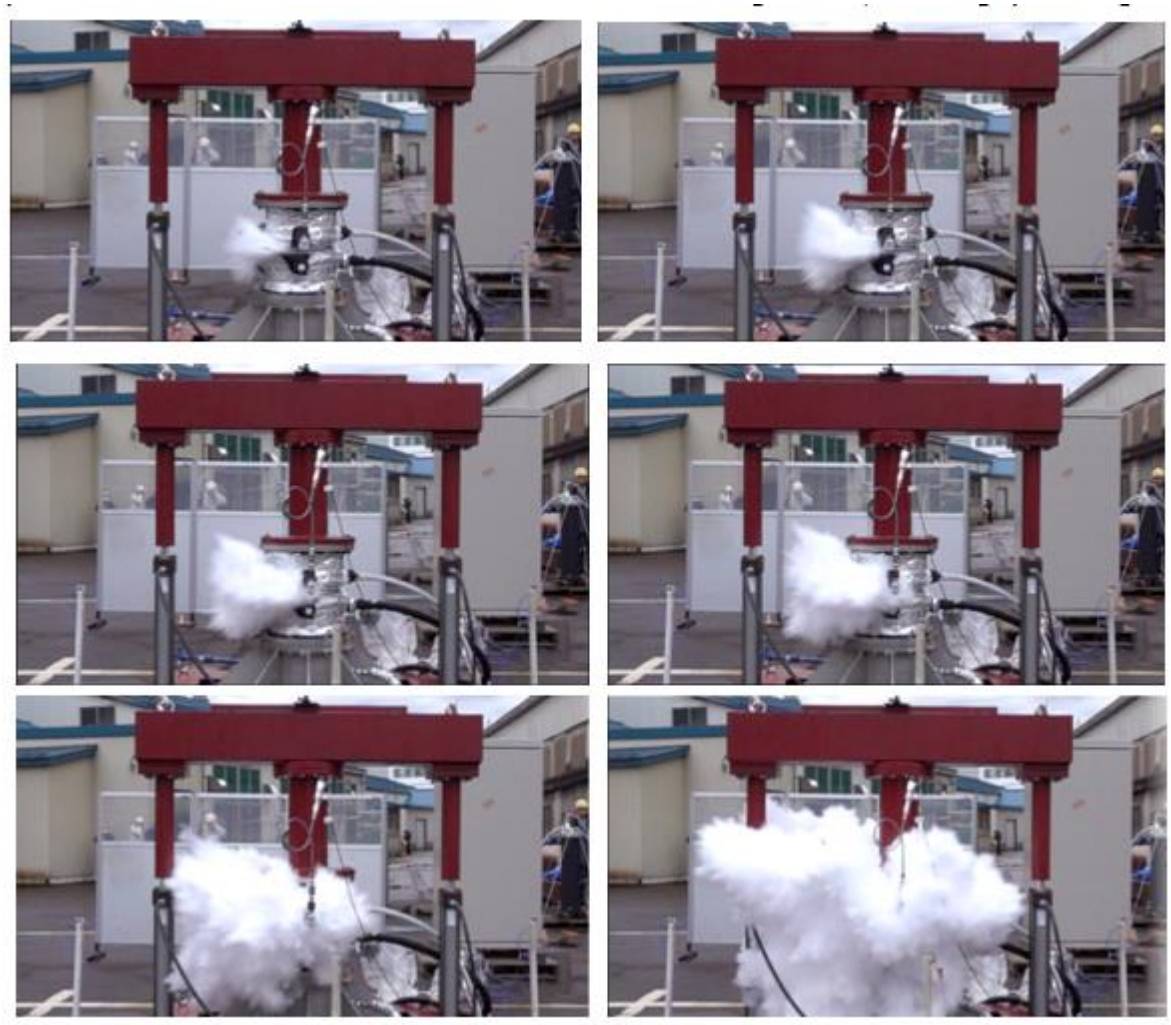

Figure 5-10: Frame sequence of high-speed release of Test 2.1; left-to-right and top-to-bottom 4 ms, 6 ms, 7 ms, 8 ms, 11 ms and 16 ms

As the pressurised liquid CO_2 gets injected into the test vessel, the fluid begins to exert its pressure to separate the flanges in an effect known as hydrostatic end load. Hereby, the compressive forces exerted on the gaskets are inevitably counterbalanced by the hydrostatic end load caused by the fluid. In order for the seal to be maintained, a continuously sufficient degree of high residual gasket load – given by the difference between the compressive and hydrostatic end load - must be maintained. Therefore, in all experimental scenarios at the initial vessel storage conditions, the hydrostatic end load acts on the seals under the effect of the pressure of the stored CO_2, while friction due to the pressing force of the vessel generates the compressive forces. Given the lower pressure of CO_2, residual gasket load is higher in test 1.1 than test 2.1, resulting in a more robust seal.

Figure 5-11: Bottom surface of the test vessel after the experiment; Test 2.1 (left), Test 1.1 (right)

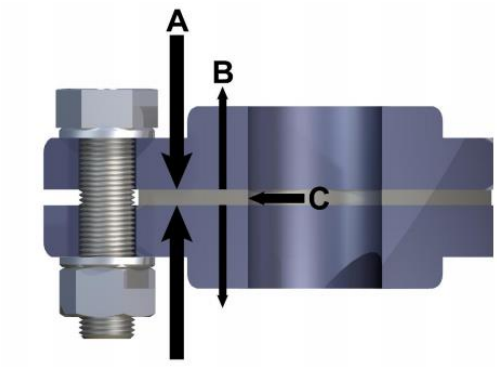

Figure 5-12: Forces acting in the flange assembly - A = flange load; B = hydrostatic end load; C = internal pressure

In test 2.1, as the vessel begins vertical separation, the friction and compression force between the flanges is suddenly reduced, causing the residual gasket load to rapidly become insufficient to guarantee the seal; the O-ring spreads at a stretch under the effect of the hydrostatic load end, causing CO_2 to violently leak from the circumference. On the other hand, in test 1.1, the hydrostatic end load and residual gasket load are, respectively, lower and higher than in the former scenario. Therefore, as the vessel begins vertical separation, the equilibrium between the two forces involved in the flange assembly results in a slower and uneven spread of the seal explained by the final position of the O-ring. This phenomenon most likely causes an initial partial leakage and subsequent clogging with dry ice generation, creating a time lag between the first ‘puff’

and the remainder of the inventory release; this is reflected in the irregular speed measurements encountered in test 1.1 at 0.87 MPa (

Figure 5-19) which will be later discussed in this work. In both tests and experimental conditions, the discharge can be observed to initiate from one particular side of the opening, subsequently spreading throughout the full circumference. This can be attributed to an irregular slip initiation of the O-ring seals between the flanges. In accordance with this discharge behaviour, the depressurisation rate measured in the tests also reflect this dissimilarity. In test 1.1 and 1.2 (Figure 5-13), the depressurisation rate occurs in a progressive fashion, achieving its peak rate at 0.4 s after a lower initial value shown at 0.2 s. By contrast, the depressurisation rate in test 2.1 and 2.2 shows a strong blast and peak depressurisation rate in its first stage, which then decreases with time Figure 5-14. Therefore, the pressure profile and depressurisation behaviour of the discharge from the coupler appears to be remarkably different in relation to the liquid pressure condition; in test 1.1 and 1.2, the pressure at the bottom of the vessel equilibrates with the atmosphere after 0.6 s, and a significant difference in depressurisation rate is observed between the top and bottom of the vessel as shown in Figure 5-13. Conversely, the discharge at higher liquid pressure observed in tests 2.1 and 2.2 shows a more consistent depressurisation rate between the top and the bottom of the coupler, with both parts equilibrating with the atmosphere after 0.4 s as shown in Figure 5-14. It is noteworthy that the peak depressurisation rate achieved during test 2.1 and 2.2 is considerably higher (5-6 MPa/s, top of the vessel) than that attained in tests 1.1 and 1.2 (2.8-3.5 MPa/s, top of the vessel); as such, it is clear that the peak depressurisation rate is found to increase with initial pressure of the fluid in this work, implying a significantly more abrupt outflow behaviour of inventory at higher refrigerated liquid pressures.

This reconstruction is further strengthened by the top-view camera observation in Figure 5-15 shows that in test 1.1 an initial puff delays the full discharge phenomena; conversely, the outflow behaviour in test 2.1 appears to be sudden and uniform. The lower depressurisation rate in the initial stage of test 1.1 is therefore the consequence of the previously discussed equilibria between the forces acting on the flange assembly. The mass conservation equation ascribed to this transient blowdown process [39] is described in Equation 5-1

$$V\frac{d\rho}{dt} = -W$$ Equation 5-1

Where V (m^3) is the coupler's volume, ρ is the density (kg/m^3), t is the time (s) and W is the mass flowrate (kg/s). Here, V is considered to remain constant in the initial phase of the vessel's separation and W assumes a negative value due to the outflow of mass from the system to the surroundings.

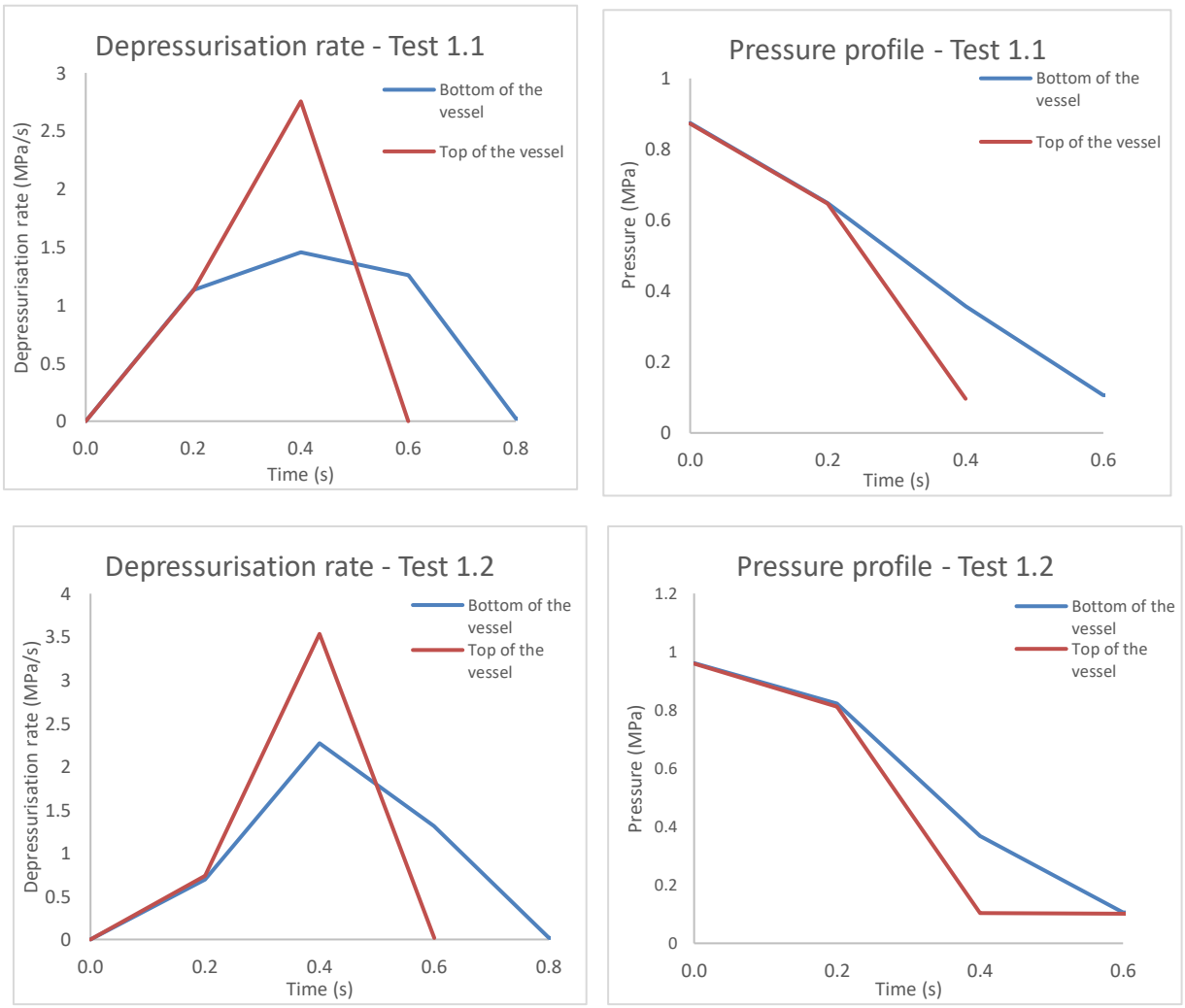

Figure 5-13: Pressure profile and depressurisation rate in the tests 1.1 and 1.2

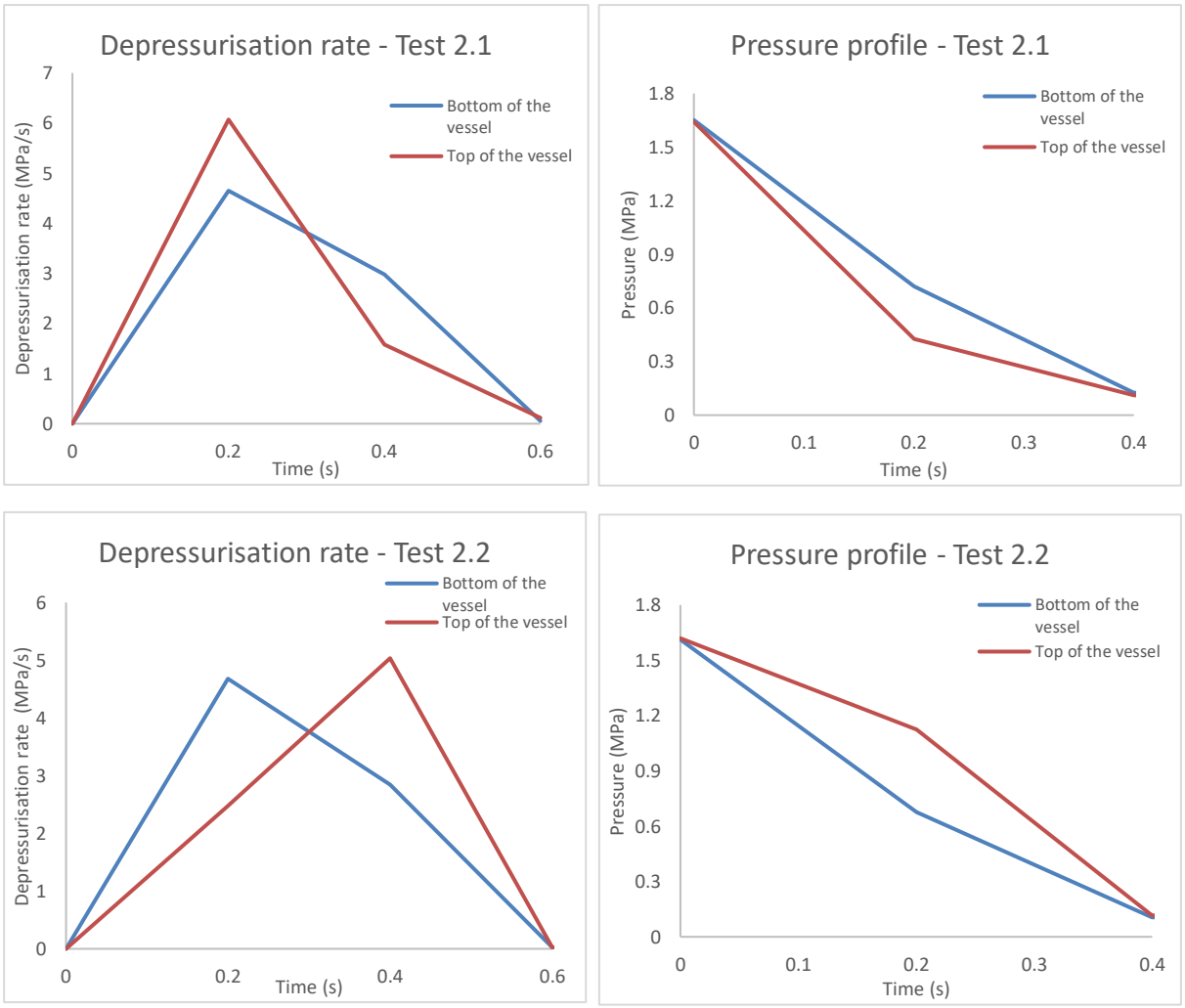

Figure 5-14: Pressure profile and depressurisation rate in tests 2.1 and 2.2

Figure 5-15: Top view of the release of Test 1.1 (left) and Test 2.1 (right) in the initial phase of the discharge

With the modest mass outflow rate caused by the higher residual gasket load and lower hydrostatic end load in the flange assembly, the density only drops minimally during the

volume expansion of the inventory in this process resulting in the modest initial pressure drop. This trend does not occur in test 2.1, where the hydrostatic end load associated with the higher stagnation pressure is more significant and the reduction of the compressive force between the flanges as a result of the coupler's opening implies a more severe and uniform blast. As the pressure of the liquid CO_2 rapidly drops below the saturation line, active nucleation takes place, and, upon that, bumping begins to occur on the inner wall of the coupler - which is expected to be at a slightly higher temperature due to heat transfer limitations and roughness on the surface.

Bumping leads to bubble formation and growth, and this results in an increase of liquid carbon dioxide discharge rate from the opening. As the liquid's temperature rises above its boiling point, it turns into the superheated phase. Once a bubble has formed, it rapidly grows, turning into a large vapour bubble that rises, expelling the inventory out of the test vessels at such high speeds. This rapid expulsion of boiling liquid represents a potential hazard to people located around the facility. High-speed observations in test 1.1 and test 2.1 show an interval of 4-6 ms between the noticeable start of the vessel's vertical separation - in the form of the extension of the pistons on the frame - and the discharge of the carbon dioxide. At the beginning of the vessel's decoupling, the discharge flow is limited by the pressure resistance in the gap and the leakage of the CO_2 is suppressed. As such, the rapidly boiling of liquid CO_2 generated in the process is forced to travel to the top of the vessel and cannot discharge from the coupler to the atmosphere. As the vessel continues to open and the gap increases, the resistance is less likely to increase and the pressure in the coupler quickly reduces, with the remaining CO_2 continuing to vaporise at the surface, resulting in a sudden gas expansion that releases the full CO_2 inventory in a short time. Throughout this process, the observed depressurisation rate from the top of the vessel appears to be remarkably higher than that at the bottom, as reflected in Figure 5-13 and Figure 5-14 . The behaviour is potentially attributed to mass transfer and diffusion phenomena of the CO_2 from the vessel to the surroundings. Fick's Law describes that the flux J travels from areas of high concentration to areas of low concentration with a driving force that is relative to the diffusion coefficient and concentration gradient. Shewmon et al. [40] suggested that in scenarios where a pressure gradient is present, the equation can also be considered as Equation 5-2:

$$J = -D\left(\frac{dP}{dx}\right)$$ Equation 5-2

Where J is the flux $\left(\frac{MPa}{m^2\,s}\right)$, D is the diffusivity value $\left(\frac{m^2}{s}\right)$, *dP* (MPa) is the pressure gradient between the vessel and the surroundings and dx (m) is the one-dimensional distance to the exit plane. Given the consistent initial conditions recorded at the top and bottom parts - nominally temperature and pressure and a comparable discharge distance i.e. length from the bottom and top sections to the opening, $\left(\frac{dP}{dx}\right)$ can be neglected in the interest of the comparison, giving:

$$J = f(-D)$$ Equation 5-3

Molecular diffusion occurs as a result of thermal motion between the molecules, with gases exhibiting a higher diffusion coefficient than liquids due to the larger kinetic force present between particles. With $D_{TOP} > D_{BOTTOM}$ due to the higher gaseous phase accumulated as a result of the suppressed rapid boiling of carbon dioxide from the surface, the inventory depressurises at a higher rate at the top of the vessel, as reflected in the higher values encountered in the tests. During the discharge, a blast was produced from the shockwave generated by the expansion energy of the initial release of liquid from the vessel. This blast was limited in duration due to the shockwave travelling at a supersonic speed and faster than the release rate of CO_2 inventory. In tests 2.1, this behaviour is less obvious and the discrepancy between the top and the bottom pressure profile in the coupler is reduced, potentially owing to the absence of the low-momentum leak induced by the flange assembly and separation; this allows the inventory to discharge to the surrounding more swiftly, resulting in lower accumulation of vapour phase at the top of the coupler.

5.3.2 Temperature profile

Figure 5-16 shows the temperature profile inside the coupler's top and bottom during all the tests. As it can be observed, the temperature profile is broadly comparable in the tests, with the vessel showing temperatures of ~ 190 K within 2 - 3 s of the start of the coupler separation and following the inventory discharge. However, it is also emphasised that tests 2.1 and 2.2 performed at higher pressure undergo a peak rate of temperature drop (32 K/s and 40 K/s respectively) than tests 1.1 and 1.2 (20 K/s and 22 K/s respectively) performed at lower pressure. In such scenarios involving the transient

release of pressurised, flashing carbon dioxide, several phase transitions take place within the system boundary; these phenomena and their nature will be discussed in more details in the next paragraphs. As an overall consideration, the total temperature change in this system can be attributed to the combination of the following phenomena:

- temperature drop due to the endothermic vaporisation (liquid-to-vapour) process
- temperature increase due to the exothermic deposition (vapour-to-solid) process
- temperature drop due to Joule-Thomson (JT) effect

The latter Joule-Thomson is a thermodynamic effect that governs the behaviour of real gases, describing their temperature change correlated with an isenthalpic expansion where no heat or work is exchanged with the surroundings. Given that the JT effect is a function of pressure drop, a higher rate of temperature drop encountered in tests 2.1 and 2.2 through the higher depressurisation rate that the tests undergo during the discharge of the inventory as shown in Figure 5-13 and Figure 5-14. Figure 5-17 and Figure 5-18 show the thermal imaging profile recorded in tests 1.1 and 1.2 respectively. Due to the higher residual gasket force and initial low-momentum leak encountered in test 1.1– explained in the previous paragraphs - test 1.1 shows an overall slower discharge process, with an initial leak or puff at 0.07 s initiating the release. The jet shows the peak of its discharge between 0.2 s – 0.27 s and then progressively dissipates and warms as the jet travels away from the release point and air gets entrained. At 0.8 s and 1.33 s some localised lower temperature area can be observed near the bottom of the coupler, indicating presence of accumulated dry ice. The thermal profile of the discharge in test 2.1 conversely shows a remarkably faster release and dispersion process – reflected by the higher initial momentum of the release relating to the higher initial pressure – which starts from 0.03 s; the jetted cloud achieves its peak discharge within a mere 0.1 s - 0.17 s interval.

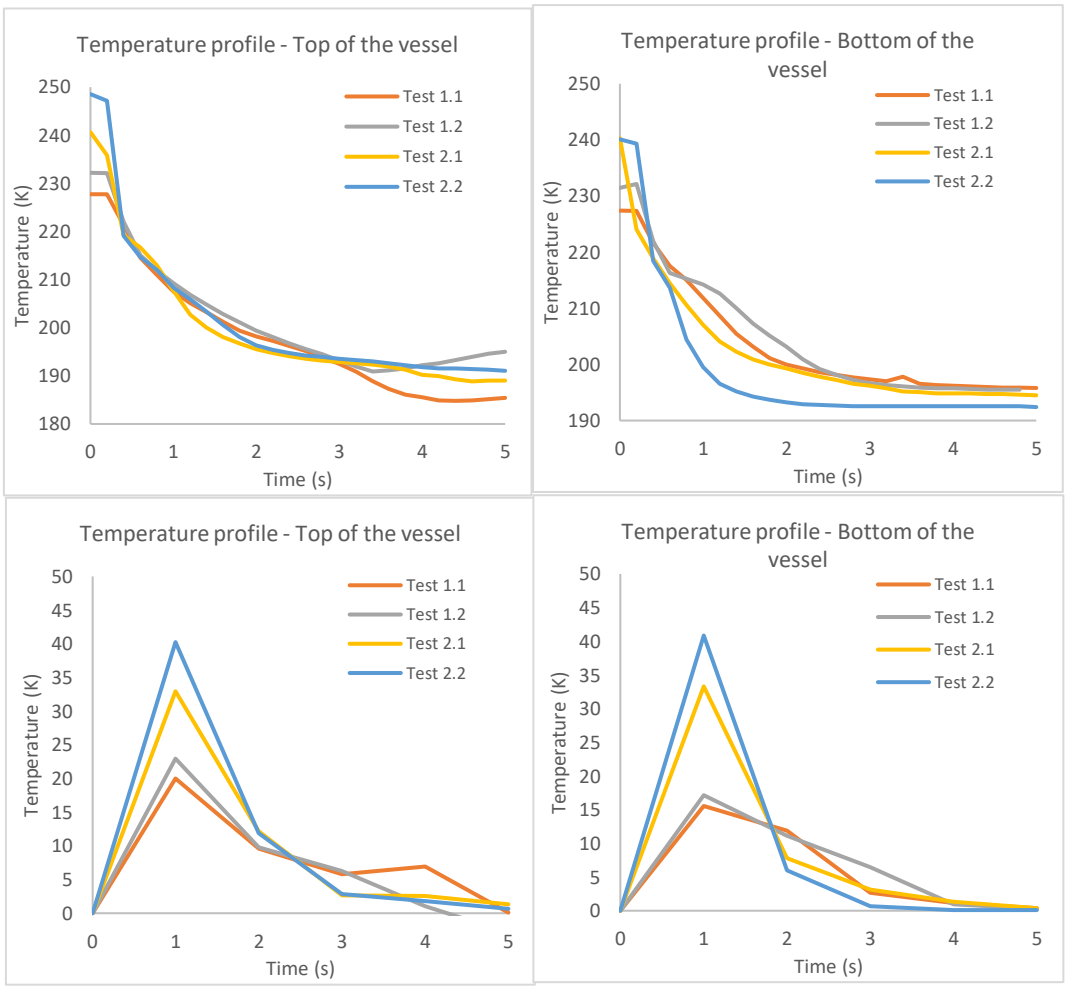

Figure 5-16: Temperature profile inside the coupler in the test

After that point, the captured thermal profile shows a progressive increase in temperature, attributed to the dispersion of the cloud and rapid air entrainment. Similarly, to what encountered in test 1.1, a localised low temperature envelope is generated at the bottom of the coupler, once again demonstrating propensity for solid carbon dioxide formation. In line with the recorded temperature profile inside the coupler shown in Figure 5-16 the temperature of the jet also found to progressively decrease with time as the inventory discharged from the coupler continues to cool down as a result of pressure drop and JT effect. The jetted cloud reaches the end of its depressurisation zone, eventually equilibrating with the atmosphere in proximity of the coupler's opening, resulting in heat transfer with the surroundings and rapid air entrainment.

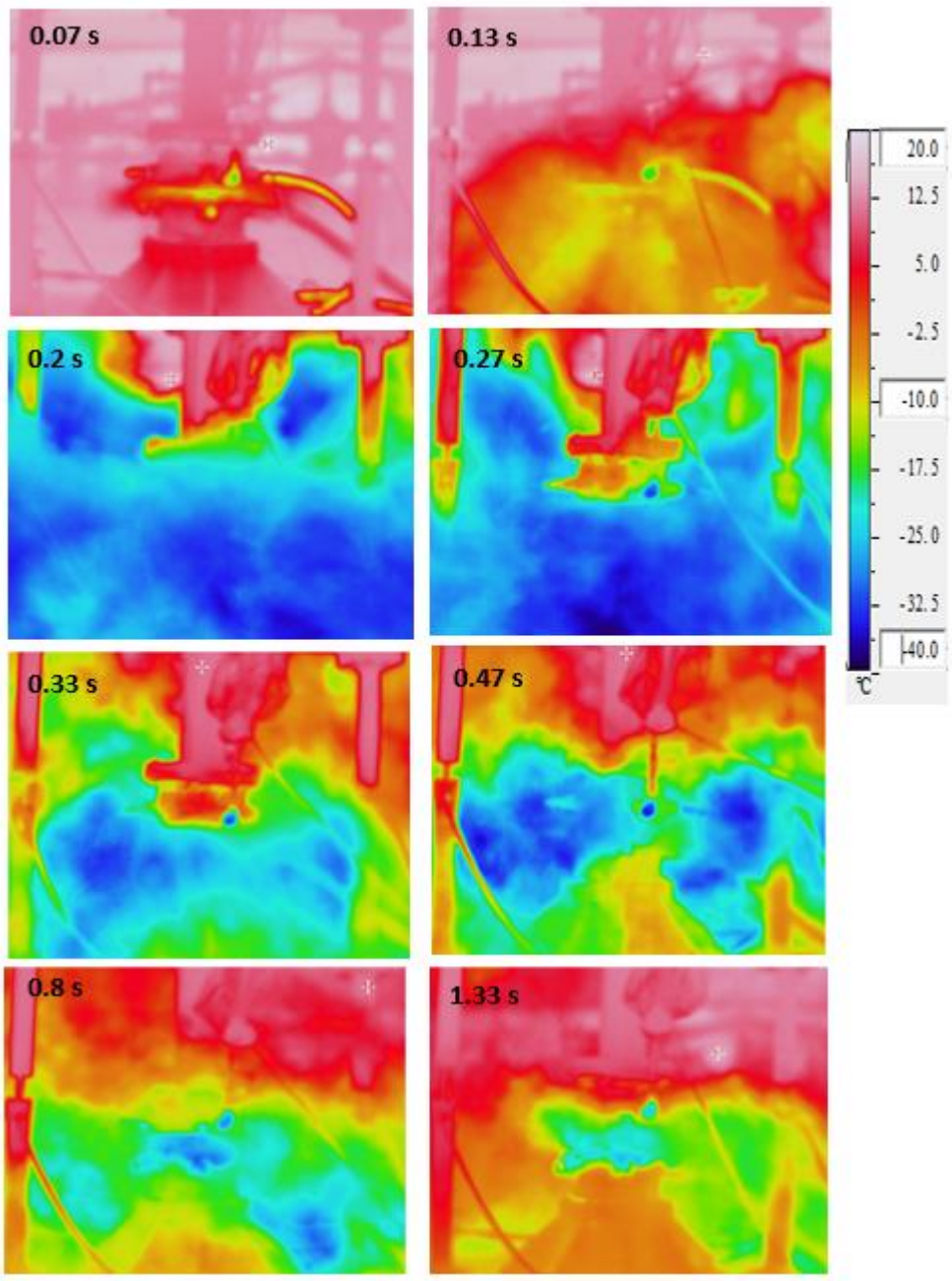

Figure 5-17: Thermal imaging profile of the discharge in Test 1.1

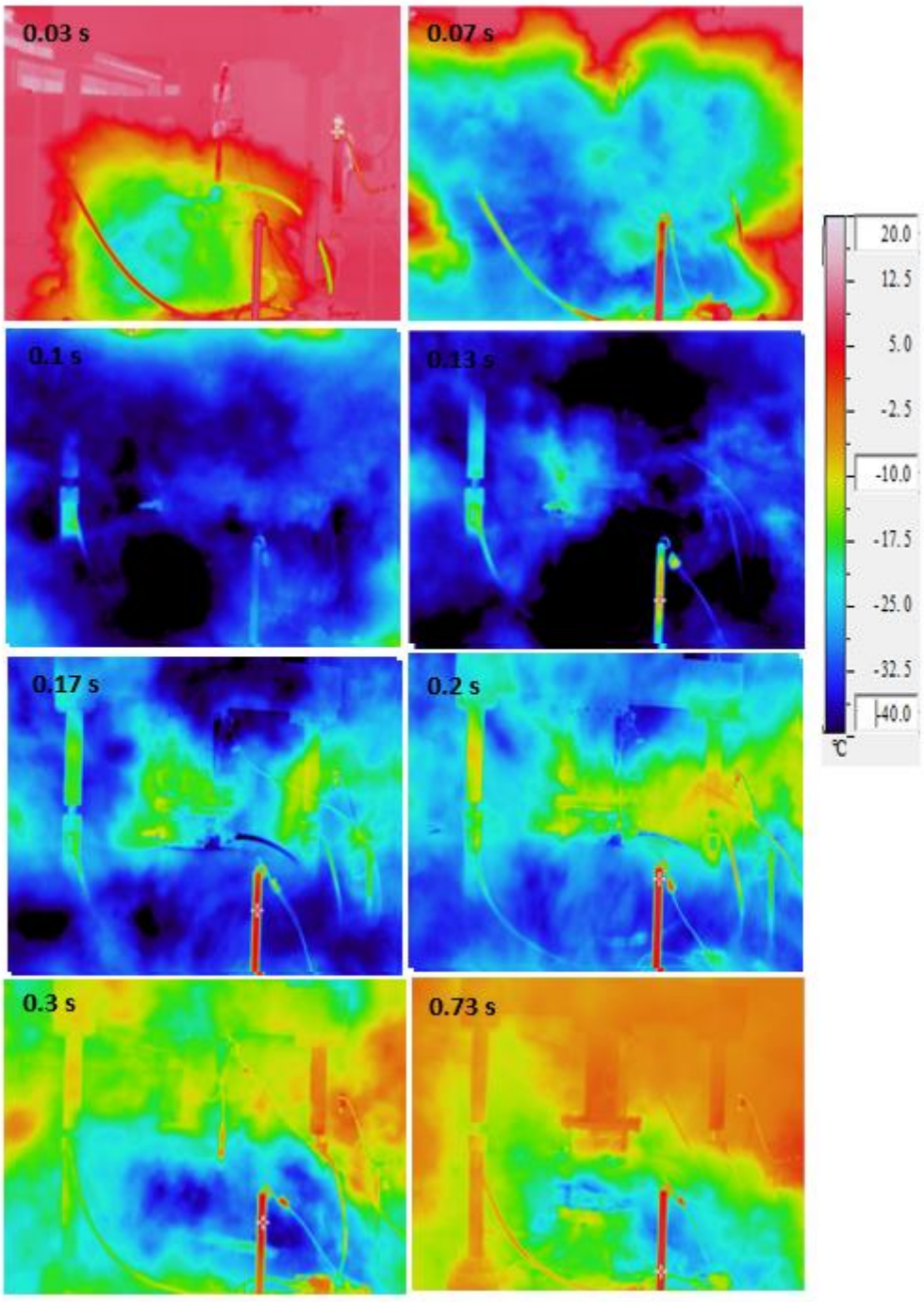

Figure 5-18: Thermal imaging profile of the discharge in Test 2.1

5.3.3 Release stage and flow characteristics

Liquid carbon dioxide expands according to its bulk modulus due to the pressure difference with the surrounding atmosphere, and the carbon dioxide leaks radially from the separated peripheral part of the coupler. As such, the inner pressure of the coupler drops by the CO_2 volume increase as a result of the leak, until reaching equilibrium with the atmosphere. The discharge behaviour is dependent on:

- Storage pressure – higher pressures result in higher release velocities and momentums
- Phase of the inventory – liquid or supercritical discharges are significantly more complex and involve several phase changes

Figure 5-19 shows the measured velocity profile of the inventory discharges in test 1.1 and test 2.1 based on high-speed camera acquisition. The velocity values were measured based on the video recording (960 fps) and they refer to the visible CO_2 cloud escaping in the radial direction with respect to time during the vertical separation of the coupler, as shown in Figure 5-9 (Test 1.1) and Figure 5-10 (Test 2.1). As indicated in Figure 5-19, these measurements were taken starting from 1 ms of the start of the release at intervals of 1 ms. It should be noted that the water vapour present in the air condenses when exposed to sub-zero temperatures. The visible cloud is therefore significantly affected by the relative humidity, and this clearly has an impact on the reliability of the velocity measurement. The relative humidity recorded during the tests ranges from 78% to 88%. As previously reported, the irregular slip initiation of the gasket seal encountered at a lower pressure leads to a lower-momentum puff prior to the full blast. The initial leak discharges from the 180^o side of the opening, exhibiting an ejection speed of approximately 34 m/s during which partial clogging of the vessel's inventory at the opening potentially takes place due to exposure to atmospheric pressure. This solid blockage is manifested in the irregular speed pattern of the discharge in test 1.1. The remainder of the inventory begins to discharge from the 0^o side of the opening at an initial speed of 115 m/s, which drops to 64 m/s at 2 ms. Conversely, the discharge at test 2.1 exhibits a more uniform profile, with no initial leaks taking place. There, the speed progressively reduces from an initial value of 149 m/s at 1 ms to a mere 60 m/s at 2 ms. The remarkable deceleration of the jetted stream is consistent to both

experimental conditions, and it indicates that the release rapidly loses momentum with respect to time as its pressure reduces equilibrating with atmosphere.

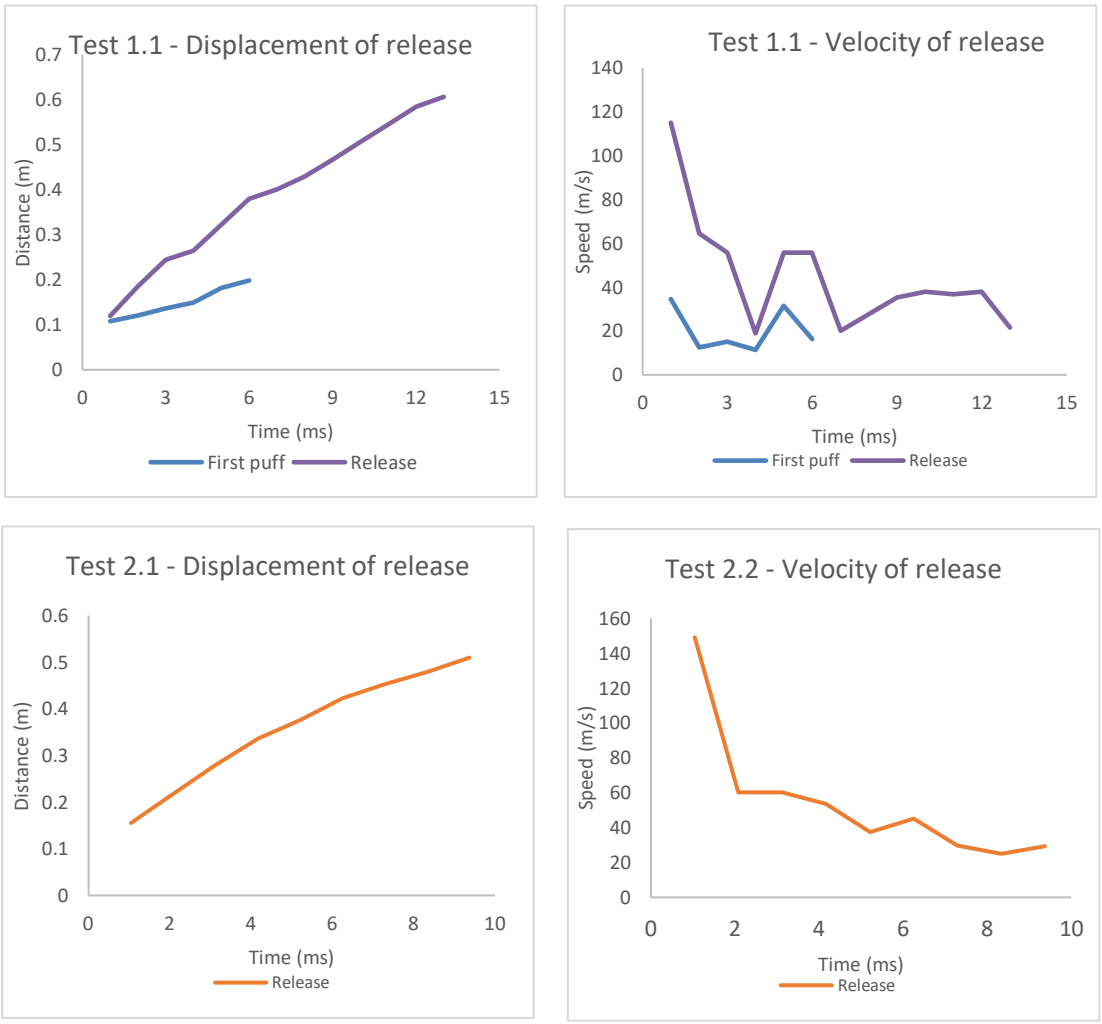

Figure 5-19: Measurement of the observed jet speed in tests 1.1 and 2.1

5.3.4 Dispersion and dry-ice formation

The pressure/temperature trajectories for test 1.1 and test 2.1 are shown in Figure 5-20 and Figure 5-21 as representation of the phase behaviour of the release at the two scrutinised conditions. As the inventory of the coupler begins to discharge from the circumferential opening as a result of the vertical separation, the pressure within the system rapidly drops below the saturated liquid pressure at the corresponding stagnation temperature – found to be 0.8 MPa for test 1.1 and 1.24 MPa for test 2.1. The CO_2 fluid discharges from the vessel at a saturated state, beyond which it starts to jet in all directions of the vessel's circumferential opening. At this point the endothermic vaporisation process promotes temperature drop of the remaining liquid CO_2 in addition to the JT effect. When the pressure eventually drops below the triple point a fraction of

the leftover inventory turns solid in an exothermic deposition process; here, assuming an isenthalpic expansion, the generated solid fraction mainly depends on upstream conditions. As the remaining CO_2 continues to discharge and the pressure in the coupler eventually equilibrates with the atmosphere, the system's boundary enters the solid phase equilibria. The solid phase envelope appears to be achieved both at the top and bottom of the vessel and maintained in the coupler upon equilibration of the coupler with atmospheric pressure.

This is demonstrated by the fact that, at the end of the experiments, a layer of dry-ice was found to be accumulated on the bottom and top surface of the coupler, as shown in Figure 5-11**.** Moreover, Figure 5-22 shows a higher amount of solid CO_2 accumulated on the insulation material in the discharge of the fluid at conditions nearer to the triple point (test 1.1) in comparison to higher liquid pressures (test 2.1). As previously discussed, the response time of the pressure sensors were reported by the manufacturer to be 0.01 s. This value is lower than the selected sampling rate of 5 Hz and therefore it does not impact the pressure measurements in the results presented. The thermocouples, having a response time of 0.02 s according to the manufacturer, show a lag of approximately 3 s in this study (Figure 5-16). However, the graphical reconstruction of the pressure and temperatures trajectories shown in Figure 5-20 and Figure 5-21 are not found to be affected by this lag. The releases show a liquid-vapour-solid transition starting from the first data point, both before and after considering the adjustment in response time.

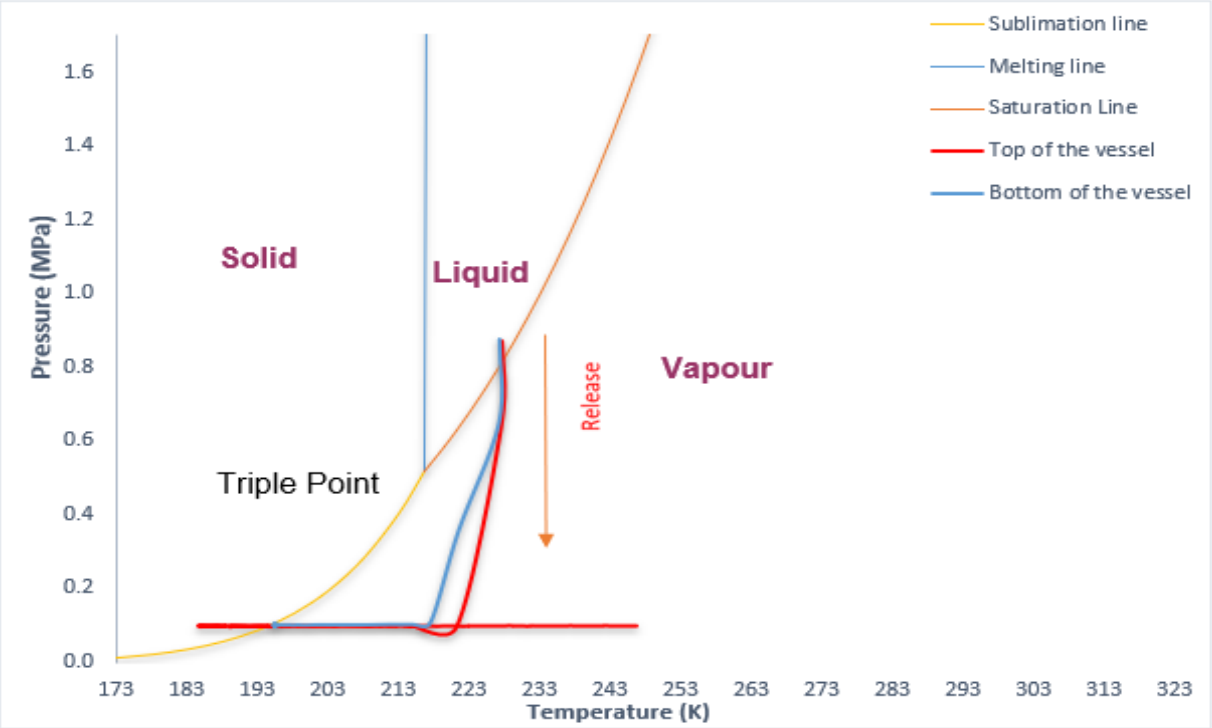

Figure 5-20: Phase diagram of the release in Test 1.1

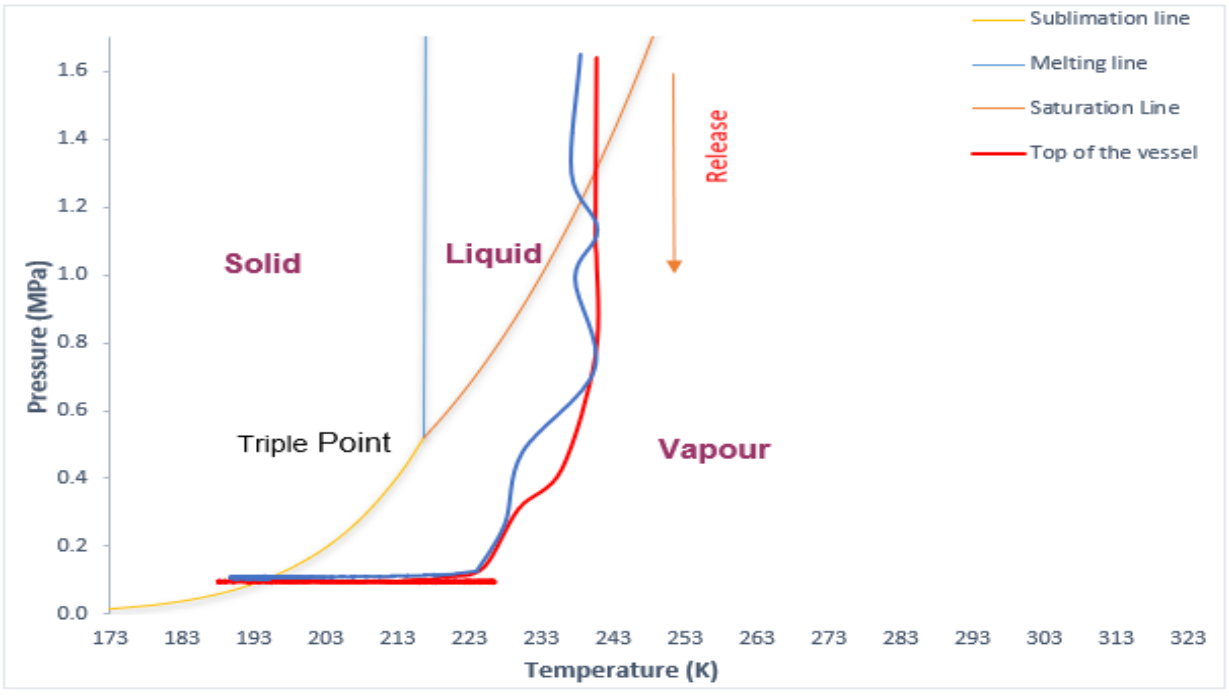

Figure 5-21: Phase diagram of the release in Test 2.1

The release behaviour in the region immediately adjacent to the exit plane is explained by the simplified method employed by Fauske and Epstein and implemented by the Energy Institute [17]. As illustrated in Figure 5-24 upon leaving the exit, the fluid

expands, and the discharge enters a depressurisation zone where no entrainment of air occurs in the jet due to pressure being higher than atmospheric value. Consequently, the jet enters a two-phase gaseous/solid entrainment zone, where pressure eventually equilibrates with atmospheric conditions and heat transfer processes begin to occur between the cloud and the surroundings.

Figure 5-22: Top view of the post-test release; Test 1.1 (left) and Test 2.1 (right)

By applying the principles of energy conservation described by the Energy Institute [17], the amount of solids generated at the end of the depressurisation zone can be estimated. The assumptions made are that the velocity terms are neglected and that the aforementioned depressurisation process is isenthalpic so that $\boldsymbol{h_2 = h_1}$. The following correlation between enthalpies and mass [40] fraction split between solid and gaseous phase is given by Equation 5-4:

$$\boldsymbol{h_1 = h_2 = h_s + Y_g h_{sg}} \qquad \text{Equation 5-4}$$

The equation can be rearranged to give the gas fraction as the subject:

$$\boldsymbol{Y_g = \begin{pmatrix} h_2 - hs \\ h_{sg} \end{pmatrix}} \qquad \text{Equation 5-5}$$

The cloud equilibrates with the atmosphere at the end of the depressurisation zone, therefore it can be assumed that $P_2 = P_{atm}$. The terms relating to solid and gaseous enthalpy in the equation (h_{sg} and h_s) are merely a function of the downstream atmospheric pressure; therefore these terms will remain constant in any given scenario where inventory discharges to the atmosphere, regardless of the upstream conditions.

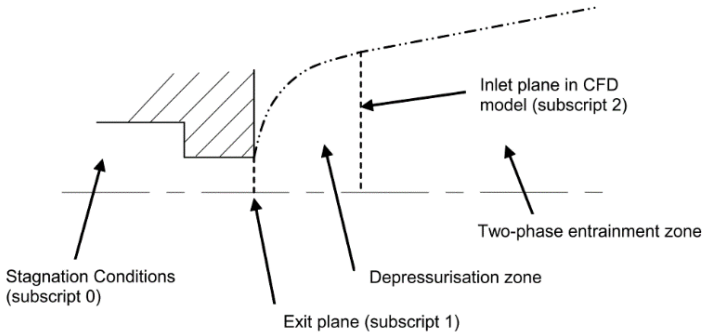

Figure 5-23: Simplified schematic of the release at the exit [17]

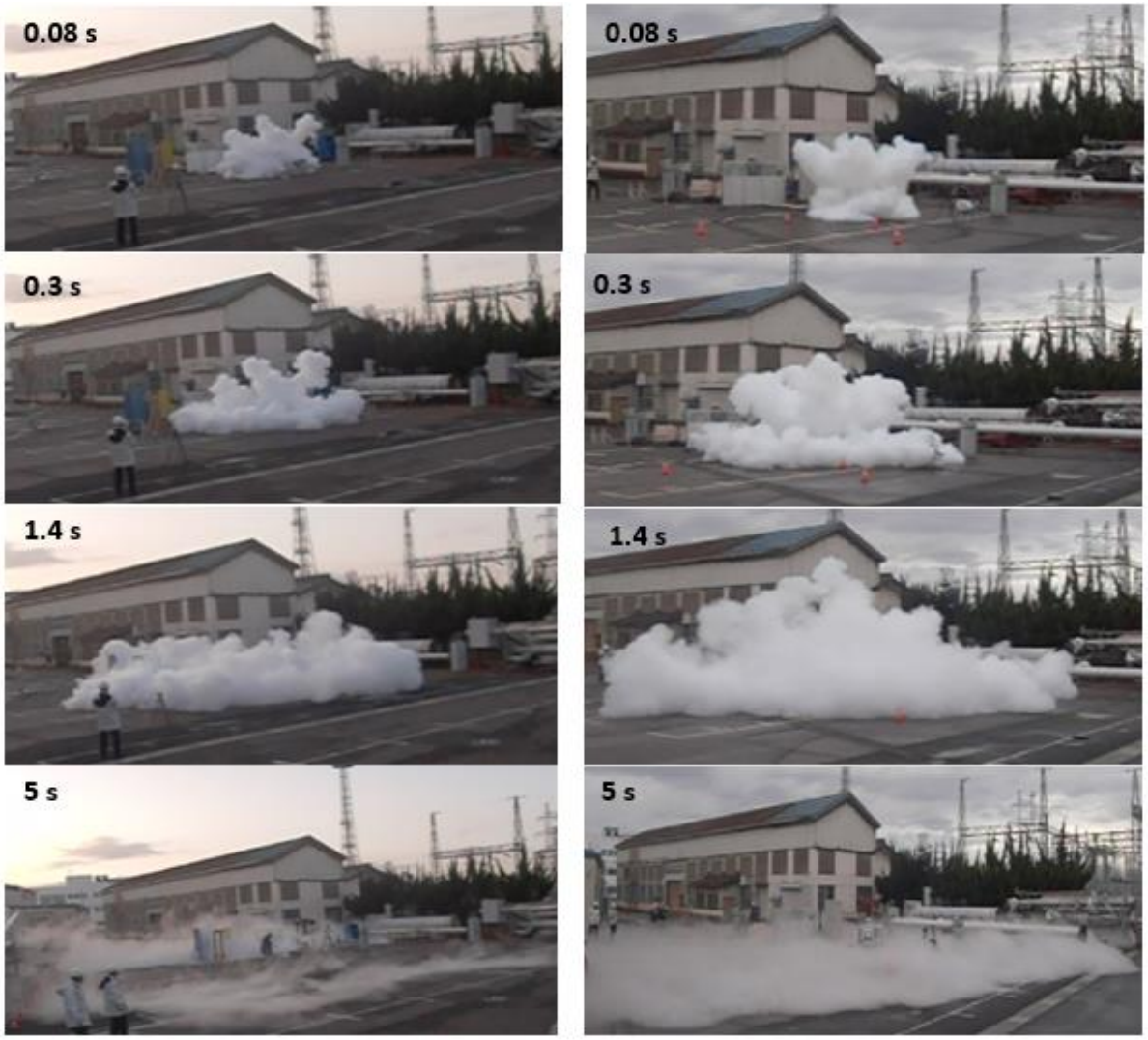

Figure 5-24: Dispersion stage of the release in Test 1.1 (left) and Test 2.1 (right)

As such, a simplistic correlation that neglects the solid and gaseous enthalpy values can be made in the interest of a comparison between the different test conditions, whereby the split vapour mass fraction becomes a function of the initial enthalpy:

$$Y_g = f(h_2)$$ Equation 5-6

As shown in Table 5-3, the stagnation enthalpy values f (h_1) were calculated to be 100.6 kJ/kg and 124.8 kJ/kg in test 1.1 and test 2.1 to be respectively. According to the aforementioned correlation, a higher upstream enthalpy results in a relatively higher vapour fraction and thus, lower solid fraction in test 2.1; this is reflected in the higher proportion of dry ice observed around the facility at the end of test 1.1. The abrupt discharge induced by the rapid separation of the coupler can be attributed to the boiling liquid expanding vapour explosion (BLEVE). During storage conditions, liquid and vapour phases inside the coupler are in proximity of thermodynamic equilibrium. As the coupler gets separated vertically, its internal pressure equilibrates with atmospheric values. The expansion of the vapour leads to cooling, condensation and freezing effects as the liquid rapidly begins to boil when depressurised. As previously demonstrated in this work, a fraction of the inventory turns into solid phase when reaching atmospheric pressure [41]. The evaporation phenomenon requires heat, which is obtained from part of the liquid. Consequently, the remaining portion of liquid continues to drop in temperature and pressure until reaching the equilibrium temperature. The rapid phase transition from liquid to vapour causes a significant volume expansion which leads to surrounding air being displaced, producing a supersonic flow and blast wave that could be heard during the tests [41].The mechanisms of BLEVE in liquid CO_2 are not well understood, particularly in relation to the metastable region. The super heat temperature is estimated to be comprised between 257 and 283 K (corresponding to saturation pressures from 2.2 to 4.5 MPa) in the literature [42], although explosive evaporation of liquid CO_2 may well be possible below the indicated homogeneous nucleation temperature range [41]. Therefore, this study indicated that the risk of BLEVE cannot be dismissed in liquid CO_2 under shipping conditions (0.8 – 1.7 MPa).

Figure 5-24 shows the dispersion stages of the inventory. In line with other empirical investigations [20,35,37] it is found that the released carbon dioxide expands in a characteristic ‘tulip’ shape (0.08 s), exhibiting the tendency to pool down on the ground in both test conditions (0.3 s) due to its density being lower than that of air. On the other hand, the jet undergoes an upwards-directed momentum, which is noticeably higher and longer-lasting at in test 2.1 and still clear at 1.4 s. In the first stage of the dispersion, the motion of the cloud is governed by inertia, and hence by its initial upstream conditions

and atmospheric flow. This potentially justifies the higher upwards-directed jet witnessed in test 2.1, where upstream pressure and initial velocity are higher. With the cloud progressively moving away from the release point, air gets rapidly entrained at an increasing rate, progressively reducing the concentration of carbon dioxide. The cloud then continues to propagate into a gravity spreading stage where it begins to slump to the ground under the effect of buoyancy. Finally, as the cloud reaches a passive dispersion stage, a higher degree of mixing with air is enhanced by atmospheric turbulence, and its movement becomes solely subject to external ambient factors such as wind speed and direction [37]. At this stage, the dispersed cloud appears to be denser with the higher initial pressure. As far as small, low-momentum releases are concerned, high wind-speeds facilitate the dispersion by enhancing mixing and transport, thus mitigating the effect of the cryogenic impact on the surroundings. However, in high-momentum discharges, CO_2 will have the tendency to rapidly accumulate on the ground level with the dispersion phenomenon being dependent on the initial momentum at the source. Under such circumstances, the effect of the wind will cause the cloud to be driven further away downstream, effectively increasing the threshold of hazardous distances. Therefore, it is expected that in such a high-momentum release, low wind-speeds are desirable to contain the cryogenic impact of the cloud.

5.4 Conclusions

This work investigated the nature of refrigerated liquid CO_2 discharge from the coupler of an emergency release system in order to support implementation of such established spillage containment technology to future CO_2 shipping for CCUS. The aim was to scrutinise the discharge behaviour and its impact on the surroundings and the facility, including the risk on personnel. Findings from this work are summarised in the following points:

- In all tests, the vertical separation of the coupler results in a violent radial leakage of the liquefied CO_2. Complete discharge occurs from the vessel within 0.6 s in all tests; the discharged CO_2 undergoes several phase transitions whilst expanding to atmospheric pressure, with large clouds arising during the dispersion stage; peak depressurisation rates recorded at the top portion of the coupler reached 3 MPa/s at 0.96 MPa and 6 MPa/s 1.65 MPa initial pressure.

- The discharge behaviour nearer to the triple point occurs more progressively with initial low-momentum leaks or ‘puffs’ from the system delaying the full-scale blast to 50 ms into the opening. Conversely, the discharge at 1.65 MPa pressure occur in a sudden and uniform manner, blasting radially from the opening.
- The inventory dispersion assumes a characteristic ‘tulip’ shape that can be clearly observed from afar. The jetted stream at 1.65 MPa shows a higher upward-pushing momentum, related to its higher initial pressure and uniform blast velocity and a higher rate of air entrainment.
- All tests are associated with the formation of carbon dioxide solids inside the test vessel and being carried over in the dispersion cloud. Propensity for solid CO_2 accumulation at the top and bottom surface of the coupler is observed in all tests.
- The dispersion clouds surrounding the coupler reach temperatures below 233 K within 0.1 s of the discharge, implying a risk for a cryogenic impact to operators.
- The selected safety distance of 2 m – where protection barriers have been placed - appears to be adequate to preserve the integrity of the data acquisition and recording equipment placed around the facility. However, this consideration may not be sufficient to guarantee the safety of personnel operating the emergency release system, particularly in relation to the risk of asphyxiation and cryogenic burns, given the magnitude of the release from the coupler.

References

[1] ZEP. Role of CCUS in a below 2 degrees scenario 2018:1–30. https://zeroemissionsplatform.eu/wp-content/uploads/ZEP-Role-of-CCUS-in-below-2c-report.pdf

[2] Element Energy, TNO, Engineering Brevik, SINTEF, Polarkonsult. Shipping UK Cost Estimation Study; 2018. Available at: https://assets.publishing.service.gov.uk/government/uploads/system/uploads/attachment_data/file/761762/BEIS_Shipping_CO2.pdf

[3] Huh C, Kang S, Park M, Lee K, Park Y, Min D, et al. Latest CO_2 Transport, Storage and Monitoring R&D Progress in Republic of Korea: Offshore Geologic Storage. Energy Procedia. 2013; 37:6520–6.

[4] Yoo BY, Choi DK, Kim HJ, Moon YS, Na HS, Lee SG. Development of CO_2 terminal and CO_2 carrier for future commercialized CCS market. Int J Greenh Gas Control. 2013; 12:323–32.

[5] Skagestad R, Eldrup N, Richard H, Belfroid S, Mathisen A, Lach A, Haugen HA. Ship transport of CO_2 - Status and Technology Gaps. Tel-Tek. 2014.

[6] Mitsubishi Heavy Industries. Report on Ship Transport of CO_2. 2004; IEA Greenhouse Gas R&D Programme. https://ieaghg.org/docs/General_Docs/Reports/PH4-30%20Ship%20Transport.pdf

[7] Jakobsen J, Roussanaly S, Anantharaman R. A techno-economic case study of CO_2 capture, transport and storage chain from a cement plant in Norway. J Clean Prod. 2017; 144:523–39.

[8] Ministry of Petroleum and Energy N, Gassco, Gassnova. Feasibility study for full-scale CCS in Norway. 2016. Available at: https://ccsnorway.com/wp-content/uploads/sites/6/2019/09/feasibilitystudy_fullscale_ccs_norway_2016.pdf

[9] Seo Y, Huh C, Lee S, Chang D. Comparison of CO_2 liquefaction pressures for ship-based carbon capture and storage [CCS] chain. Int J Greenh Gas Control. 2016; 52:1–12.

[10] IEAGHG. The Status and Challenges of CO_2 Shipping Infrastructures. 2020; IEAGHG Technical Report 2020-10.

[11] Vermeulen TN. Knowledge sharing report – CO_2 Liquid Logistics Shipping Concept [LLSC]: Overall Supply Chain Optimization 2011:143. Available at: https://www.globalccsinstitute.com/resources/publications-reports-research/knowledge-sharing-report-co2-liquid-logistics-shipping-concept-business-model/

[12] Chiyoda Corporation. Preliminary Feasibility Study on CO_2 Carrier for Ship-based CCS（Phase-2 – unmanned offshore facility). Global CCS Institute. 2012. Available at: https://www.globalccsinstitute.com/resources/publications-reports-research/preliminary-feasibility-study-on-co2-carrier-for-ship-based-ccs-phase-2-unmanned-offshore-facility/

[13] Tokyo Boeki Engineering. Private communication. Nagaoka Works, Niigata, Japan. 2019.

[14] Tokyo Boeki Engineering. Marine Loading Arms (brochure). Available at: http://www.tokyo-boeki-eng.co.jp/technology/pdf/marine%20loading%20arms_E.pdf

[15] Energy Institute. Hazard analysis for offshore carbon capture platforms and offshore pipelines. 2013. Available at: https://www.globalccsinstitute.com/archive/hub/publications/115563/hazard-analysis-offshore-platforms-offshore-pipelines.pdf

[16] Noh H, Kang K, Huh C, Kang SG, Seo Y. Identification of potential hazardous events of unloading system and CO_2 storage tanks of an intermediate storage terminal for the Korea clean carbon storage project 2025. Int J Saf Secur Eng. 2018;8[2]:258–65.

[17] Energy Institute. Technical guidance on hazard analysis for onshore carbon capture installations and onshore pipelines. 2010. Available at: https://www.globalccsinstitute.com/archive/hub/publications/7291/technical-guidance-hazard-analysis-onshore-carbon-capture-installations-and-onshore-pipelines.pdf

[18]. SIGTTO. Liquefied Gas Handling Principles On Ship and in Terminals, 4TH edition. Witherby Seamanship. ISBN: 9781856097147. 2016

[19] Worley Parsons, Schlumberger, McKenzie B&, EPRI. Strategic Analysis of the Global Status of Carbon Capture and Storage - Report 1: Status of Carbon Capture and Storage Projects Globally. Global CCS Institute. 2009. Available at: https://www.globalccsinstitute.com/archive/hub/publications/5751/report-5-synthesis-report.pdf

[20] Koers P, Maarten de Looij. Safety Study for Liquid Logistics Shipping Concept. 2011;. Rotterdam, Det Norske Veritas BV. Report number: 12TUIBY-3

[21] Zahid U, An J, Lee C, Lee U, Han C. Design and Operation Strategy of CO_2 Terminal. Ind Eng Chem Res. 2015;54[8]:2353–65.

[22] Pitblado R, Baik J, Hughes GJ, Ferro C, Shaw SJ. Consequences of LNG Marine Incidents. Det Norske Veritas (USA) Inc. CCPS Conference Orlando. 2004

[23] California State Lands Commission. Cabrillo Port Liquefied Natural Gas [LNG] Deepwater Port. 2006. Available at: https://ceqanet.opr.ca.gov/2004021107/3

[24] SIGTTO. LNG Emergency Release Systems - Recommendations, Guidelines and Best Practices. Witherby Seamanship; 2017. ISBN: 9781856097307

[25] Harper P, Wilday J, Bilio M. Assessment of the major hazard potential of carbon dioxide. 2015; Health and Safety Executive.

[26] Shafiq U, Shariff AM, Babar M, Ali A. A study on blowdown of pressurized vessel containing CO_2 /N_2/H_2S at cryogenic conditions. IOP Conf Ser Mater Sci Eng. 2018;458[1].

[27] Zheng W, Mahgerefteh H, Martynov S, Brown S. Modeling of CO_2 Decompression across the Triple Point. Ind Eng Chem Res. 2017;56[37]:10491–9.

[28] Pursell M. Experimental investigation of high-pressure liquid CO_2 release behaviour. Inst Chem Eng Symp Ser. 2012;[158]:164–71.

[29] Li K, Zhou X, Tu R, Yi J, Xie Q, Jiang X. Experimental Investigation of CO_2 Accidental Release from a Pressurised Pipeline. Energy Procedia. 2015; 75:2221–6.

[30] Xie Q, Tu R, Jiang X, Li K, Zhou X. The leakage behavior of supercritical CO_2 flow in an experimental pipeline system. Appl Energy. 2014; 130:574–80.

[31] Zhou X, Li K, Tu R, Yi J, Xie Q, Jiang X. Numerical Investigation of the Leakage Flow from a Pressurized CO_2 Pipeline. Energy Procedia. 2014; 61:151–4.

[32] Teng L, Li Y, Zhao Q, Wang W, Hu Q, Ye X, et al. Decompression characteristics of CO_2 pipelines following rupture. J Nat Gas Sci Eng. 2016; 36:213–23.

[33] Guo X, Yan X, Yu J, Yang Y, Zhang Y, Chen S, et al. Pressure responses and phase transitions during the release of high-pressure CO_2 from a large-scale pipeline. Energy. 2017; 118:1066–78.

[34] Wang C, Li Y, Teng L, Gu S, Hu Q, Zhang D, et al. Experimental study on dispersion behavior during the leakage of high-pressure CO_2 pipelines. Exp Therm Fluid Sci. 2019; 105:77–84.

[35] Ahmad M, Lowesmith B, De Koeijer G, Nilsen S, Tonda H, Spinelli C, et al. COSHER joint industry project: Large scale pipeline rupture tests to study CO_2 release and dispersion. Int J Greenh Gas Control. 2015; 37:340–53.

[36] Li M, Liu Z, Zhou Y, Zhao Y, Li X, Zhang D. A small-scale experimental study on the initial burst and the heterogeneous evolution process before CO_2 BLEVE. J Hazard Mater. 2018; 342:634–42.

[37] Sherpa Consulting. Dispersion modelling techniques for carbon dioxide pipelines in Australia. Global CCS Institute. 2015. Available at: https://www.globalccsinstitute.com/archive/hub/publications/196358/dispersion-modelling-techniques-carbon-dioxide-pipelines-australia.pdf

[38] Han SH, Chang D, Kim J, Chang W. Experimental investigation of the flow characteristics of jettisoning in a CO_2 carrier. Process Saf Environ Prot. 2014;92[1]:60–9.

[39] Yangle W, Yuan Z, Yanping H, Jingtan C, Junfeng W. Modelling of accidental release process from small rupture of pressure CO_2 vessel. Int J Greenh Gas Control. 2020; 93:1–10.

[40] Shewmon P. Diffusion in Solids. Springer International Publishing. 2016. DOI 10.1007/978-3-319-48206-4

[41] Van der Voort MM, van Wees RMM, Ham JM, Spruijt MPN, van den Berg AC, de Bruijn PCJ, et al. An experimental study on the temperature dependence of CO_2 explosive evaporation. J Loss Prev Process Ind 2013; 26:830–8.

[42] Bjerketvedt D, Egeberg K, Ke W, Gaathaug A, Vaagsaether K, Nilsen SH. Boiling liquid expanding vapour explosion in CO_2 small scale experiments. Energy Procedia 2011; 4:2285–92.

6 GENERAL DISCUSSIONS AND IMPLEMENTATION OF THE WORK

6.1 Research gap in CO_2 shipping for CCUS

CCUS has been widely identified as a key technology to reduce CO_2 emissions from anthropogenic sources in the power and industrial sectors [1,2]. Before CO_2 can be safely stored, it must be transmitted to the sink; pipelines and sea vessels thereby represent the main transportation options. CO_2 shipping exhibits a viable alternative to pipeline systems, optimal to transport smaller volumes of CO_2 over long distances. In the UK, the Department for Business, Energy and Industrial Strategy (BEIS) is thoroughly exploring the role of CO_2 shipping as part of the British decarbonisation landscape [3,4], with the opportunity for the UK to become a net importer of emissions due to the country's vast storage resources in the North Sea. CO_2 shipping is a relatively mature concept, implemented in the food and brewery industry to transport relatively small quantities of carbon dioxide for commercial projects; however the relatively small quantities – around 3 $MtCO_2$/year across Europe – and the higher-pressure conditions in the liquid form of 1.4 – 2.2 MPa and 238 – 253 K – imply that extensive considerations need to be explored in order to make this technology techno-economically relevant and reliable for the CCUS industry [5,6]. This is particularly accentuated by the fact that literature often indicates conditions near the triple point (0.7 – 0.9 MPa and 221 – 227 K) – where there is a significant lack of experience in handling liquid carbon dioxide – as optimal. It should however be noted that different shipping conditions of up to 2.2 MPa liquid pressure are also indicated in other works [5,7,8]; the choice of appropriate transport conditions is ultimately related to project variables such as discharge quantity and transport distance amongst the others. Operating at conditions close to the triple point allows to maximise cargo efficiency due to enhanced density and lowers capital expenditure of the vessel due to the reduced thickness of the tanks, but it does not allow a comfortable margin from the triple point. This consideration therefore implies a higher risk of operational issues and formation of dry-ice when handling liquid CO_2 throughout the chain [5], which can in turn undermine the system's integrity and lead to catastrophic failures as result of over-pressurisation. Although CO_2 shipping doesn't exhibit significant conceptual challenges, there are several technical gaps that need to be addressed to allow successful large-scale implementation. Technical challenges include the selection of appropriate polymeric and elastomer materials throughout the chain, as

their performance is not well understood due to dearth of investigations specific to CO_2 shipping [9]. Lack of both model-based and experimental studies on the behaviour of refrigerated, liquid CO_2 [10,11] is moreover reported, implying a high-level of uncertainty in process safety-related issues arising in case of accidental leakage from the cargo or storage tank vessel. Moreover, implementation of engineering measures that can limit the magnitude of loss of containment during real operations [12–14] requires a thorough scrutiny on the applicability of existing technologies - such as emergency release systems for marine loading operations [14,15] - to the specific application of sea vessel transport for CCUS. A detailed discussion on the future prospective for CO_2 shipping has been presented in the literature investigation as part of objective 1. Therefore, in response to the summarised technological gaps, this PhD engaged in an experimental-based approach to bridge some of the exiting knowledge gaps and contribute towards the commercialisation of this technology. In order to achieve this aim, a set of specific objectives was proposed, including: a detailed literature review, laboratory-scale experimental campaigns and real-scale investigation.

6.2 Design and commissioning of CO_2 experimental facility operating under shipping conditions

The process of experimental rig design came with its own set of technical challenges, particularly in relation to the achievement and maintenance of refrigerated conditions in the CO_2 inventory. As per the previously defined objectives of this PhD, the technical scope of the apparatus was conceived to accommodate accidental leakage behaviour of liquid CO_2 batches under shipping conditions (0.7 MPa – 2.6 MPa, 223 – 259 K) and testing of elastomer materials under real sea vessel operations at 1.6 MPa and 245 K. Thus, a versatile, multi-configuration rig with different set-ups was considered. With regards to the former experimental assessment, a 2.25 L, 304L stainless steel cylinder was implemented as test section to accommodate the liquid CO_2 in batches. The cooling of carbon dioxide was achieved by a liquid nitrogen refrigerant (77 K) supply of a pressurised Dewar (120 L capacity) through a coil-heat exchange system soldered around the test vessel surface. Regarding the set-up configuration relative to elasotmeric material testing, it soon became apparent throughout the design phase that the implementation of the aforementioned liquid nitrogen cooling system would have resulted in imprecise temperature control of inventory given the considerably smaller batch of CO_2 (~0.1 L) compared to the former set-up. Therefore, an alternative approach

was considered: this consisted in the implementation of a R5 Grant Instruments chiller (low temperature capability 226 K) operated with silicone oil.

6.3 Technical qualification of elastomer materials for CO_2 transport systems

Selection of appropriate materials is a key practice to promote integrity of transportation systems and prevent loss of containment due to component failure. A high level of uncertainty is still reported in relation to the selection of polymeric and elastomer components such as seals and gaskets [9,16] operating in CO_2-rich environments. As operating conditions in the CO_2 shipping chain range from refrigerated during CO_2 loading and port handling to supercritical during CO_2 injection into geological formations, materials will have to be suitable to withstand thermal and compression/decompression cycles, particularly in relation to the batch nature of CO_2 shipping. Previous works have demonstrated that elastomers are prone to rapid gas decompression (RGD) damage when used in CO_2-rich environments [17,18]. Several studies [17,19–21] investigated the performance of different elastomers in CO_2 and the effect of the fluid on their materials' properties. In this work, an experimental investigation was conducted to assess and technically qualify the performance of elastomer materials at conditions typical of the CCUS transport systems. In the first part of the work, O-ring sets of four different materials originating from the same production batch –namely Viton, Neoprene, Buna and Ethylene Propylene (EP) – were aged at sCO_2 conditions (9.5 MPa and 318 K) at 50 h – 400 h in the presence of different contaminants - nominally saturated water level, 500 ppm of SO_2 or H_2S – to investigate the degree of interaction with the media and degradation of mechanical properties. These samples were exposed as part of the previously delivered MATTRAN project [22,23] – focusing on materials for the next generation of CO_2 pipeline transport and exposure tests were not completed by the author of this thesis. Conversely, development and implementation of the technical qualification of elastomers was performed by the author of this thesis. In the first part of this work, a characterisation methodology was developed and applied to qualify the aged samples and assess the degradation of properties in the materials. It should be noted that, in the interest of the timescales of this PhD project, the shore. A hardness measurements of CO_2 pipeline samples was performed at the Tor Vergata University of Rome. The second part of the work focused on the performance of one material – namely Ethylene Propylene Diene Monomer (EPDM) – under CO_2 shipping conditions.

The selection was based on the satisfactory performance of EP under pipeline conditions coupled with the enhanced low-temperature suitability of EPDM (glass transition temperature ~218 K). Compressed O-rings (to 75% of the initial thickness) were subjected to 20 – 100 CO_2 loading and offloading cycles that exert pressurisation and depressurisation on the samples; exposed samples were thereby characterised using the previously developed characterisation methodology. Findings showed that EP and EPDM materials perform satisfactorily in an environment typical CO_2 transport systems. In particular EP demonstrated limited alterations of properties in supercritical CO_2 environments and EPDM exhibited high resistance to RGD damage and low Compression Set in refrigerated CO_2 conditions. Viton showed to be an unsuitable material selection for CO_2 pipeline systems, given its poor record of RGD resistance. This trend is related to the interaction of its bulky fluorine atoms with CO_2 media. Buna and Neoprene also displayed signs of structural alterations due to the more remarkably shift in glass transition temperatures encountered. Therefore, designers of CO_2 transport systems are advised to consider the selection of these materials as part of the intended infrastructure.

The novelty of this work is the qualification of the effect of contaminants on elastomers at supercritical conditions and the effect of pressurisation cycles induced by CO_2 loading and offloading under shipping conditions; findings related to both testing campaigns were reportedly lacking in the literature [9].

6.4 Lab-scale investigation: liquid CO_2 leakage behaviour under shipping conditions

Implication of unsuitable material selection throughout CO_2 transport systems can include mechanical failure of components during real operations and resulting leakage and loss of containment. Experimental studies in the literature have extensively investigated the leakage and depressurisation behaviour of pipelines and vessels at high-pressure (4 – 8 MPa) liquid or supercritical conditions, [24–31]. To the best of the author's knowledge, limited experimental investigations have primarily focused on operations typical of the shipping chain [32,33] with virtually no work in the open literature covering releases under refrigerated, liquid conditions closer to the triple point. In order to investigate the accidental release of liquid CO_2 under shipping conditions, the experimental campaign in this PhD considered three sets of tests performed at different conditions of future shipping projects [5]. Namely, these included low-pressure

(0.7 – 0.94 MPa, 223 – 228 K), medium pressure (1.34 – 1.67 MPa, 234 – 245 K) and high-pressure tests (1.83 – 2.65 MPa, 249 – 259 K). The aim was to inform the designer of the process safety considerations inherent to each condition and relative advantages or disadvantages. It was possible to implement a GF343 CO_2 detection camera to clearly visualise the outflow during the tests, allowing a more thorough investigation of the release process. A two-factor assessment emphasised that under CO_2 shipping operations, high-pressure releases represent the optimal selection to limit the amount of inventory solidification and reduce the duration of the leakage process; medium pressure conditions imply the longest release processes, while low-pressure conditions display the highest percentage of content solidification. These considerations demonstrate that selecting an increased margin from the triple point is favourable in CO_2 shipping operations to reduce the impact from accidental release occurrences that can arise during real operations.

6.5 Real-scale investigation: liquid CO_2 discharge behaviour from the emergency release coupler of a marine loading arm

The previously discussed laboratory-scale experimental campaign was successful in investigating the release behaviour of liquid CO_2 (0.7 MPa – 2.6 MPa, 223 – 259 K) with reference to small size leaks of the 3 mm ID nozzle considered. However, as highlighted by the Energy Institute [11] the behaviour of the phenomenon is highly dependent on the nature of the discharge, with instantaneous releases thereby exhibiting significant differences compared to small leaks. Therefore, the opportunity to investigate an instantaneous CO_2 release was considered through the investigation of liquid CO_2 discharge from the emergency release system during marine loading shutdown. As opposed to the accidental leakage testing previously performed, these real-scale tests focused on the instantaneous release of full inventory. Design and safety considerations in the open literature [14,34] suggest that propensity for operational issues is higher during dynamic operations throughout the chain; during CO_2 loading operations, transfer of liquefied carbon dioxide is performed by mean of marine loading arms, which represent the most established solution in liquid, refrigerated applications [4,12,13]. In case of any incident occurring during loading operations – such as adverse weather conditions or natural calamities - it is essential to shut-down the flow from the source and promptly discharge the marine loading arm to avoid its rupture and significant inventory spillages. Emergency release systems (ERS) represent the required

engineering measure to enable process safety protocols [13,14,35]. Although ERS systems are well-established in the LNG and LPG industries, their implementation is novel in relation to the liquid CO_2 shipping chain; the potential for sublimation and formation of dry-ice – which can damage equipment, causing it to become irresponsive - are unique to carbon dioxide. For a safe and reliable planning of emergency shutdown, a good understanding of CO_2 discharge phenomena from the ERS's coupler is required. Therefore, the real-scale experimental campaign in this PhD investigated the discharge of liquid carbon dioxide from the ERS of a marine loading arm during an emergency shutdown.

The experimental campaign investigated the operation of the ERS and behaviour of the liquefied CO_2 discharge during the separation of the emergency release system's coupler. After loading the pre-conditioned carbon dioxide onto the test vessel, the tests consisted in the vertical separation of the pressure vessel's top part by means of a pressurised-oil hydraulic system. The rig and its operating mechanisms replicated the implementation of emergency release systems during marine loading emergency shutdowns. Through the implementation of extensive experimental observations and data acquisition – including pressure and temperature recording, high-speed (960 fps) and far-view cameras (240 fps) to monitor the initial characteristics of the discharge and dispersion phenomena, as well as a thermal infrared camera to observe the temperature profile of the jetted flow – this study was able to gain a thorough appreciation of the phenomenon in relation to two distinct refrigerated liquid conditions – namely low pressure (0.87 – 0.9 MPa and 227 – 231 K) and medium pressure (1.62 – 1.65 MPa, 239 – 240 K) – proposed for future CO_2 shipping projects [3,5]. The effect of initial pressure was found to be significant, with a slower and more progressive discharge taking place at low-pressure conditions as opposed to the uniform blast occurring during medium-pressure conditions. The measured initial speed of the jetted flow was also higher at medium pressure (149 m/s) compared to the low-pressure counterpart (115 m/s); a higher-proportion of dry-ice was observed in the former due to closer proximity to the triple point. Overall, both discharges resulted in a characteristic tulip shape that could be observed from afar. This has clear safety implications to surrounding personnel, people and equipment with a risk of asphyxiation and cold burnt that requires further assessment and quantification.

References

[1] ZEP. Role of CCUS in a below 2 degrees scenario 2018:1–30. https://zeroemissionsplatform.eu/wp-content/uploads/ZEP-Role-of-CCUS-in-below-2c-report.pdf

[2] Bui M, Adjiman CS, Bardow A, Anthony EJ, Boston A, Brown S, et al. Carbon capture and storage [CCS]: The way forward. Energy Environ Sci 2018; 11:1062–176.

[3] Element Energy. CCS deployment at dispersed industrial sites; 2020. Department for Business Energy and Industrial Strategy; Research paper number 2020/030.

[4] Element Energy, TNO, Engineering Brevik, SINTEF, Polarkonsult. Shipping UK Cost Estimation Study; 2018. Available at: https://assets.publishing.service.gov.uk/government/uploads/system/uploads/attachment_data/file/761762/BEIS_Shipping_CO2.pdf.

[5] IEAGHG. The Status and Challenges of CO_2 Shipping Infrastructures. 2020; IEAGHG Technical Report 2020-10.

[6] Brownsort P. Ship transport of CO_2 for Enhanced Oil Recovery – Literature Survey 2015;44. http://www.sccs.org.uk/images/expertise/reports/co2-eor-jip/SCCS-CO2-EOR-JIP-WP15-Shipping.pdf

[7] Ministry of Petroleum and Energy N, Gassco, Gassnova. Feasibility study for full-scale CCS in Norway. 2016. Available at: https://ccsnorway.com/wp-content/uploads/sites/6/2019/09/feasibilitystudy_fullscale_ccs_norway_2016.pdf

[8] Seo Y, Huh C, Lee S, Chang D. Comparison of CO_2 liquefaction pressures for ship-based carbon capture and storage [CCS] chain. Int J Greenh Gas Control 2016; 52:1–12.

[9] Ansaloni L, Alcock B, Peters TA. Effects of CO_2 on polymeric materials in the CO_2 transport chain: A review. Int J Greenh Gas Control 2020; 94:102930.

[10] Harper P, Wilday J, Bilio M. Assessment of the major hazard potential of carbon dioxide (CO_2). Health and Safety Executive. 2015.

[11] Energy Institute. Hazard analysis for offshore carbon capture platforms and offshore pipelines. 2013; https://www.globalccsinstitute.com/archive/hub/publications/115563/hazard-analysis-offshore-platforms-offshore-pipelines.pdf

[12] Vermeulen TN. Knowledge sharing report – CO_2 Liquid Logistics Shipping Concept [LLSC]: Overall Supply Chain Optimization 2011:143. Available at: https://www.globalccsinstitute.com/resources/publications-reports-research/knowledge-sharing-report-co2-liquid-logistics-shipping-concept-business-model/

[13] Koers P, Maarten de Looij. Safety Study for Liquid Logistics Shipping Concept. 2011;. Rotterdam, Det Norske Veritas BV. Report number: 12TUIBY-3

[14] Noh H, Kang K, Huh C, Kang SG, Seo Y. Identification of potential hazardous events of unloading system and CO_2 storage tanks of an intermediate storage terminal for the Korea clean carbon storage project 2025. Int J Saf Secur Eng 2018; 8:258–65.

[15] Element Energy, TNO, Engineering Brevik, SINTEF, Polarkonsult. Shipping UK Cost Estimation Study; 2018. Available at: https://assets.publishing.service.gov.uk/government/uploads/system/uploads/attachment_data/file/761762/BEIS_Shipping_CO2.pdf.

[16] Energy Institute. General Properties and Uses of Carbon Dioxide, Good Plant Design and Operation for Onshore Carbon Capture Installations and Onshore Pipelines - A Recommended Practice Guidance Document. 2010; https://www.globalccsinstitute.com/archive/hub/publications/7276/good-plant-design-and-operation-onshore-carbon-capture-installations-and-onshore-pipelines.pdf

[17] Ho E. Elastomeric seals for rapid gas decompression applications in high-pressure services. Health and Safety Executive. 2006; https://www.hse.gov.uk/research/rrpdf/rr485.pdf

[18] Shiladitya P, Shepherd R, Bahrami A, Woolin P. Material selection for supercritical CO_2 transport. In: The First International Forum on the transportation of CO_2 by Pipeline. 2010; https://www.twi-global.com/technical-knowledge/published-papers/material-selection-for-supercritical-co2-transport

[19] Menon N, Walker M, Anderson M, Colgan N. Compatibility of polymers in super-critical carbon dioxide for power generation systems: High level findings for low temperatures and pressure conditions. 2019; https://www.osti.gov/servlets/purl/1592964

[20] Lainé E, Grandidier JC, Benoit G, Omnès B, Destaing F. Effects of sorption and desorption of CO_2 on the thermomechanical experimental behaviour of HNBR and FKM O-rings - Influence of nanofiller- reinforced rubber. Polym Test 2019; 75:298–311.

[21] Hertz III DL. Elastomers in CO_2. High performance Elastomers & Polymers for Oil & Gas. 2012; https://www.sealseastern.com/PDF/Elastomers-in-CO2.pdf

[22] Patchigolla K, Oakey JE. Design Overview of High-Pressure Dense Phase CO_2 Pipeline Transport in Flow Mode. Energy Procedia 2013; 37:3123–30.

[23] Patchigolla K, Oakey JE, Anthony EJ. Understanding dense phase CO_2 corrosion problems. Energy Procedia 2014; 63:2493–9.

[24] Heon S, Kim J, Chang D. An experimental investigation of liquid CO_2 release through a capillary tube. Energy Procedia 2013; 37:4724–30.

[25] Yan X, Guo X, Yu J, Chen S, Zhang Y, Mahgerefteh H, et al. Flow characteristics and dispersion during the vertical anthropogenic venting of supercritical CO_2 from an industrial scale pipeline. Energy Procedia 2018; 154:66–72.

[26] Stene J, Harper M, Witlox HWM. Modelling transient leaks from pressure vessels including effects of safety systems. DNV GL Software. IChemE. 2011. Available at: https://www.icheme.org/media/9086/paper-35-hazards24.pdf

[27] Wang C, Li Y, Teng L, Gu S, Hu Q, Zhang D, et al. Experimental study on dispersion behavior during the leakage of high-pressure CO_2 pipelines. Exp Therm Fluid Sci 2019; 105:77–84.

[28] Zhou X, Li K, Tu R, Yi J, Xie Q, Jiang X. Numerical Investigation of the Leakage Flow from a Pressurized CO_2 Pipeline. Energy Procedia 2014; 61:151–4.

[29] Ahmad M, Lowesmith B, De Koeijer G, Nilsen S, Tonda H, Spinelli C, et al. COSHER joint industry project: Large scale pipeline rupture tests to study CO_2 release and dispersion. Int J Greenh Gas Control 2015; 37:340–53.

[30] Cao Q, Yan X, Liu S, Yu J, Chen S, Zhang Y. Temperature and phase evolution and density distribution in cross section and sound evolution during the release of dense CO_2 from a large-scale pipeline. Int J Greenh Gas Control 2020; 96:103011.

[31] Teng L, Li Y, Zhao Q, Wang W, Hu Q, Ye X, et al. Decompression characteristics of CO_2 pipelines following rupture. J Nat Gas Sci Eng 2016; 36:213–23.

[32] Han SH, Chang D, Kim J, Chang W. Experimental investigation of the flow characteristics of jettisoning in a CO_2 carrier. Process Saf Environ Prot 2013; 92:60–9.

[33] Han SH, Chang D. Dispersion analysis of a massive CO_2 release from a CO_2 carrier. Int J Greenh Gas Control 2014; 21:72–81.

[34] Zahid U, An J, Lee CJ, Lee U, Han C. Design and operation strategy of CO_2 terminal. Ind Eng Chem Res 2015; 54:2353–65.

[35] SIGTTO. Liquefied Gas Handling Principles On Ship and in Terminals, 4^{TH} edition. Witherby Seamanship. ISBN: 9781856097147. 2016

7 CONCLUSIONS

This PhD focused on the increasing need to provide a safe and reliable CO_2 shipping transport chain to enable safe, efficient and reliable decarbonisation of the power and industrial sectors. The focus and approach was that of addressing key technical challenges highlighted in the open literature; in order to achieve this, an experimental apparatus capable of handling liquid, refrigerated CO_2 under shipping conditions (0.7 - 2.7 MPa, 223 - 259 K) was designed and commissioned under the scope of this PhD. The workflow of the thesis can be summarised in the following four parts: (i) extended literature review, (ii) experimental rig design and commissioning (iii) lab-scale experimental campaign on addressing technological gaps encountered in the CO_2 shipping chain (iv) scaled-up experimental study on liquid CO_2 discharge from a marine loading arm of emergency release system. The following section addresses the novelty and summary of findings in more details.

7.1 Summary of findings and novelty of this PhD

Obj. 1: Conduct a critical review on the technological status, challenges and future developments of large-scale CO_2 shipping for CCUS

The attainment of this objective represented the starting point of the research performed in this PhD. The review on large-scale CO_2 shipping for CCUS was undertaken by summarising the available literature on CO_2 shipping for CCUS. In the opening part, a techno-economic and life-cycle comparison with pipeline transportation option was performed to outline the applicability of sea vessel transport within the decarbonisation transmission options. Technological advancement in the field, from its initial conceptualisation to date, were summarised and investigated. The work moreover scrutinised potential future implementation of this technology as part of the global decarbonisation strategies, highlighting its applicability and role in facilitating CCUS implementation as a whole. In particular, its relatively modest capital requirements compared to pipeline systems and the high degree of flexibility in matching sink-source clusters, make it attractive for the early stages CCUS. The review highlighted that East Asia – particularly Japan and Korea - and northern Europe – specifically the UK, Norway and the Netherlands – represent the geographical regions where sea vessel transport will be primarily implemented. Moreover, the review discussed technical, economical and operational issues that need to be addressed to achieve successful

commercialisation of sea vessel transport. The key recommendations identified in the literature include understanding the risk and impact of operational issues and loss of containment to promote safety protocols – particularly at conditions closer to the triple point – and selection of suitable materials that can perform satisfactorily throughout the chain. Currently, the lack of pilot projects that can demonstrate full-chain operations from source to sink is deemed as a considerable drawback, particularly given the uncertainty associated with the current economic models and operational challenges associated with the batch-wise nature of the technology. Nonetheless, recent development in policies concerning CO_2 transport - including the recent amendment of the London Protocol that previously banned transnational transport of CO_2 - suggest that the deployment of this technology across the world has a promising future ahead.

Obj. 2: Design and commission an experimental facility capable of handling refrigerated liquid CO_2 (0.7 - 2.7 MPa, 223 - 259 K) to investigate accidental leakage behaviour and test the performance of elastomer materials.

Designed and commissioned a multi-functional test facility which is part of the UKCCSRC PACT facilities. This experimental facility was considered for two distinct types of tests, namely a) accidental leakage behaviour of CO_2 under shipping conditions and b) elastomer and polymer material performance and degradation under real CO_2 shipping operations. Configuration a) implemented a liquid nitrogen cooling system to allow conditioning of liquid carbon dioxide batches of up to 2.25 L to a state typical of the CO_2 shipping chain (0.7 - 2.7 MPa, 223 - 259 K); this achievement permitted accidental release testing to be performed with extensive monitoring of pressure, temperature and outflow jet observation. It is noteworthy that, although the experimental set-up has been primarily designated to allow testing with refrigerated liquid CO_2, the apparatus is capable of handling liquid carbon dioxide at ambient temperatures and corresponding saturation pressures of ~ 6.5 MPa given its design pressure of 15 MPa. Configuration b) was successfully commissioned to accommodate testing of elastomer materials at ~1.6 MPa and 243 K liquid CO_2 conditions. In this set-up, a chiller operated with silicone oil and capable of achieving low temperatures of 233 K was implemented as refrigeration method for the injected CO_2. A test vessel made of copper, where elastomer seals of different geometries can be accommodated in constraint mode, was implemented for material testing purposes. In both set-ups, implementation of National

Instruments acquisition system enabled extensive monitoring and data acquisition of selected process parameters during the tests.

Obj. 3a: Qualify the performance and degradation of elastomer materials under real CO_2 pipeline and perform testing of seals under shipping conditions through the developed liquid CO_2 rig.

The performance of several elastomer materials for CO_2 transport systems was successfully investigated under this objective. A characterisation methodology was implemented to assess the degradation of elastomer materials – namely Buna, Neoprene, EP and Viton - previously exposed to CO_2 pipeline testing (9.5 MPa, 318 K) for 50 – 400 h. Moreover, EPDM O-rings were selected for testing to 20 – 100 CO_2 loading and offloading cycles at a refrigerated, liquid state typical of sea vessel transport (1.6 MPa, 243 K) and characterised using the same characterisation methodology. Under CO_2 pipeline testing conditions (9.5 MPa, 318 K), Neoprene, Ethylene Propylene and Buna exhibited good resistance to rapid gas decompression when subjected to 1 – 5 cycles at the same rate. Conversely, Viton demonstrated to be an unsuitable elastomer selection as demonstrated by the high propensity for rapid gas decompression damage even under a single depressurisation cycle (0.18 MPa/s rate). The behaviour is attributed to a high degree of interaction between the fluorine atoms contained in its matrix and supercritical CO_2. Neoprene, Ethylene Propylene and Buna conversely exhibited good resistance to rapid gas decompression when subjected to 1 – 5 cycles at the same rate. Neoprene showed on average a 15% increase in its glass transition temperature as a result of exposure to CO_2 pipeline environment, sign that a structural alteration occurred in the material. Signs of the presence of an inverse correlation between % glass transition shift and % mass change as shown by the bivariate fit (correlation factor = -0.52, $p = 0.04$) suggest that loss of plasticisers is reflected in the reduced low temperature flexibility manifested in glass transition temperature increase. Overall, presence of different contaminants (500 pm SO_2 or H_2S) did not appear to significantly alter the hardness (shore A) and glass transition temperature shift of the materials, suggesting that at the scrutinised concentrations, contaminants do not significantly contribute to ageing of the materials. Moreover, no significant trends in mass, hardness or glass transition temperature change were observed in relation to exposure time (50 – 400 h range) implying that longer exposure times may be required to study long-term effect of the environment on the ageing of the

materials. EP demonstrated suitable performance in supercritical CO_2, attributed to limited interaction with the fluid – a polar media – given the on-molar nature of the elastomer. A mere 6% increase in glass transition temperature was attributed to cross-linking mechanisms occurring due to the high pressure of the environment. Similarly to EP under pipeline conditions, EPDM tested to 20 – 100 CO_2 loading and offloading cycles at medium pressure shipping conditions (1.6 MPa, 243 K, 1.6 MPa/s decompression rate) demonstrated a satisfactory performance, characterised by high rapid gas decompression resistance where no cracks and blisters showed on the samples. Moreover, the material exhibited low Compression Set values of ~3%, indicating that O-rings tested in compressed mode were able to almost completely recover to the original thickness, a sign of high sealing performance in real operations. High mechanical stability was demonstrated by the modest change in hardness, while no significant alteration to glass transition temperature was observed.

Obj. 3b: Experimentally Investigate the accidental leakage behaviour of liquid carbon dioxide under CO_2 shipping conditions (0.7 – 2.7 MPa, 223 - 259 K)

The experimental campaign considered three sets of tests at different refrigerated liquid conditions typical of CO_2 shipping, namely low-pressure (0.7 – 0.94 MPa, 223 – 228 K), medium-pressure (1.34 – 1.67 MPa, 234 – 245 K) and high-pressure (1.83 – 2.65 MPa, 249 – 259 K) state. The experimental campaign revealed distinct discharge phenomena relative to initial boundary conditions of the tests. Tests performed at low-pressure condition (0.7 – 0.94 MPa, 223 – 228 K), with a smaller margin from the triple point, resulted in a higher proportion of inventory solidification within the vessel (36 – 39 wt%). Discharges at such conditions were found to be particularly convoluted, given the propensity for phase changes due to the proximity to the triple point; normalised leakage time (normalised to highest value encountered at medium pressure releases) was thereby found to be 0.47 – 0.53 (value normalised against longest leakage duration at medium-pressure conditions). The release process at medium pressure conditions (1.34 – 1.67 MPa, 234 – 245 K) conversely showed a considerable propensity for continuous formation of solids in the discharge pipe, which thus increased the duration of leakage making it the highest threshold reported within this experimental campaign at a normalised leakage time of 0.97 – 1 (value normalised against longest leakage duration at medium-pressure conditions). On the other hand, a lower degree of inventory solidification in the vessel (28 – 31 wt%) was observed. Lastly, high-pressure releases

(1.83 – 2.65 MPa, 249 – 259 K) exhibited overall more linear discharge processes, demonstrating that an increased margin from the triple point implies smoother leakage phenomena; solidification of inventory was thereby found to be lower than the former two test conditions (17 – 22 wt%) and so was the leakage duration which exhibited a normalised time of 0.1 – 0.39 (value normalised to highest value encountered at medium pressure releases). Leakage duration was found to increase with initial calculated enthalpy in low- and high-pressure tests. It is noteworthy that medium pressure releases showed limited variation in relation to discharge time, suggesting that formation of solids in the discharge pipe was a dominant phenomenon whose extent made the duration of the discharge process uniform. The proportion of inventory solidification measured when the system reached atmospheric pressure was found to be inversely proportional to the initial specific enthalpy of the stream. A two-factor safety assessment suggests to the designer of CO_2 shipping systems that the studied high-pressure releases are the optimal selection to limit the amount of inventory solidification and duration of the leakage; medium pressure conditions result in the longest leakage duration, while low-pressure scenarios lead to the highest amount of inventory solidification.

Obj. 4: Undertake a real-scale investigation of the instantaneous discharge behaviour of liquid CO_2 from the of emergency release system's coupler of a marine loading arm to understand the impact on the surroundings.

Implementation of emergency release systems for marine loading arm for CO_2 shipping was successfully investigated in relation to two distinct refrigerated liquid CO_2 conditions, namely low (0.87 – 0.96 MPa, 227 – 231 K) and medium pressure scenarios (1.62 – 1.65 MPa, 239 – 240 K). All the tests showed a violent discharge of liquefied CO_2 inventory within 0.6 s of the coupler's vertical separation. Peak depressurisation rate during the release behaviour was found to be higher at the medium pressure conditions at a peak 5 – 6 MPa/s; conversely, low pressure releases showed a more modest value of 2.5 – 3.5 MPa/s. The measured temperature value inside the coupler was found to achieve 190 K within 3 s of the start of the process in all the tests. In line with the different depressurisation rate recorded at different pressure conditions, the peak rate of temperature drop at the bottom the coupler was also found to be higher at medium pressures (40 K/s) in comparison to low pressures (17 K/s), a trend attributable to the Joule Thomson effect. The measurement of initial jet velocity performed by means of high-speed camera acquisition highlighted a value of 115 m/s at 0.87 MPa and 149 m/s

at the higher pressure of 1.65 MPa. Layers of dry-ice appeared on the top and bottom surfaces of the vessel at the end of all tests, indicating solidification of part of the inventory during the discharge process. The selected safety distance of 2 m, where protection barriers had been placed appeared to preserve the integrity of the experimental equipment; however, more considerations are deemed necessary to assess the level of hazard posed to operators: this is particularly relevant as during the initial dispersion stage of the release, the jetted cloud achieved a temperature of 233 K within 0.1 – 0.2 s of the release in all the experiments, implying a risk of asphyxiation and cryogenic burn. Dispersion clouds moreover propagated assuming a characteristic “tulip shape” conferred by the initial momentum exhibited by the jet and the tendency of carbon dioxide to pool down to the ground due to its density being less than that of air.

8 RECOMMENDATIONS FOR FUTURE WORK

The research carried during the course of this PhD has contributed towards the developments of safer and more reliable operations to facilitate near-future implementation and commercialisation of CO_2 shipping for CCUS. The following section presents the limitations faced during the performance of this work, outlining some recommendations for future work that it is believed can stimulate new pathways for the development of this technology.

Accidental leakage behaviour of refrigerated liquid CO_2

- Future of experimental campaign on the leakage behaviour of liquid CO_2 under shipping conditions shall consider the presence of impurities in the stream, representative of CCUS typical stream compositions as opposed to pure CO_2. In particular, the presence of N_2, H_2, Ar and CO should be investigated due to their effect on phase equilibria and in widening the phase envelope of CO_2
- Additionally, to the scarcity of experimental data, the open literature also reported a high degree of uncertainty relative to the modelling of continuous releases of liquid CO_2 from storage vessels. Therefore, the development of new models and improvement of existing ones that can simulate the discharge behaviour at conditions typical of the shipping chain - such as DNV PHAST - is suggested as future work. A comprehensive approach which also includes experimental validation of developed models will be particularly beneficial.

Qualification of elastomer materials for CO_2 shipping systems

- Technical qualification of elastomer materials in this thesis was performed in relation to post-pressurisation performance. This approach is relevant to understand the degradation of mechanical and sealing properties of elastomers as a result of exposure. In addition to this, further work implementing in-situ measurements and monitoring of elastomers is recommended under CO_2 shipping conditions. In particular, this approach would promote understanding of the propensity for different elastomers to swell in this environment.
- Prolonged exposure of EPDM samples for hundreds or thousands of hours under CO_2 shipping conditions is suggested as future work to understand the long-term effects of on the material's mechanical stability and propensity for degradation of its properties.

- Effect of presence of impurities such as N_2, O_2 and hydrocarbons in the CO_2-rich stream on the material performance shall be scrutinised under CO_2 shipping conditions in relation to prolonged exposure and during CO_2 loading cycling. This approach would promote understanding of the impact of contaminants on the rapid gas decompression damage and selection of suitable materials throughout the chain.

Emergency release systems for CO_2 marine loading arms

- Investigation of the discharge behaviour of liquid CO_2 should be considered for ball-type emergency release systems too; in particularly this will promote comparison with the butterfly-type design investigated in this work to gain an understanding of the advantages related to the implementation of either design
- Future studies on the discharge behaviour of liquid CO_2 from an emergency release system should consider the extensive implementation of instantaneous CO_2 concentration alarms to enable real-time monitoring of CO_2 concentration at a given distance from the discharge during the dispersion stage; in particular, this will provide a specific assessment of the asphyxiation risks posed to operators.
- Experimental investigations specifically aimed at understanding the superheating of CO_2 during a BLEVE in the context of discharges from emergency couplers should be pursued to assess the risk of BLEVE during CO_2 shipping operations.